THE ROLE OF STRUCTURAL BIOPOLYMERS IN THE FUNCTIONALIZATION OF MICROALGAE FOR FOOD PROCESSING

Potential as structuring agent and implications for nutrient bioaccessibility

Tom BERNAERTS

Supervisor:

Prof. Ann Van Loey, KU Leuven

Members of the Examination Committee:

Prof. Bruno Cammue, KU Leuven - Chairman
Prof. Imogen Foubert, KU Leuven (Campus KULAK)
Prof. Paula Moldenaers, KU Leuven
Prof. Koenraad Muylaert, KU Leuven (Campus KULAK)
Dr. Joël Wallecan, Cargill R&D Centre Europe

Dissertation presented in partial fulfilment of the requirements for the degree of Doctor of Bioscience Engineering

May 2019

Doctoraatsproefschrift nr. 1575 aan de faculteit Bio-ingenieurswetenschappen van de KU Leuven.

Samenvatting

Microalgen tonen potentieel als functioneel ingrediënt dankzij hun opmerkelijke biomassasamenstelling, rijk aan verschillende (essentiële) nutriënten en gezondheidsbevorderende componenten. De functionaliteit in levensmiddelen hoeft echter niet beperkt te worden tot gezondheidsaspecten, aangezien microalgen ook een structurele rol zouden kunnen spelen in levensmiddelen. Microalgen bevatten namelijk verschillende structurele biopolymeren, zoals proteïnen, reserve-polysachariden en celwandgerelateerde polysachariden. Zo zouden microalgen dienst kunnen doen als multifunctionele ingrediënten, door combinatie van nutritionele en structurele functionaliteit, met mogelijks een verminderde nood aan additionele verdikkingsmiddelen tot gevolg. Tot op vandaag is echter zeer weinig onderzoek gebeurd naar de functionaliteit van microalgen en hun structurele biopolymeren.

Een eerste strategie voor het benutten van de structurele biopolymeren is het gebruik van geëxtraheerde celwandgerelateerde polysachariden als verdikkingsmiddelen in de voeding, zowel celwandgebonden als extracellulaire polysachariden. Hoewel polysachariden uit macroalgen reeds courant gebruikt worden als verdikkings- of geleermiddel, hebben polysachariden uit microalgen tot nog toe slechts weinig aandacht gekregen. Daarom werd in het eerste deel van deze doctoraatsthesis de moleculaire structuur van celwandgerelateerde polysachariden van tien verschillende microalgen gekarakteriseerd. Gezien de grote evolutionaire diversiteit van microalgen vertoonden de verschillende soorten een diverse celwandsamenstelling, waarbij weinig overeenkomst met conventionele verdikkingsmiddelen waargenomen werd. Op basis van de veelbelovende verdikkingseigenschappen van de extracellulaire polysachariden van *Porphyridium cruentum* beschreven in de literatuur, werden verschillende celwandfracties geïsoleerd uit deze microalg en gekarakteriseerd op vlak van moleculaire structuur en reologische eigenschappen. In tegenstelling tot de celwandgebonden polysachariden werden de extracellulaire polysachariden gekarakteriseerd als polymeren met hoog moleculair gewicht, verantwoordelijk voor hogere intrinsieke viscositeiten dan verschillende commerciële verdikkingsmiddelen. De functionaliteit van deze extracellulaire fractie is echter gelimiteerd door de co-extractie van proteïnen en mineralen, en pogingen om de polysachariden te geleren door het toevoegen van kationen en/of het aanwenden van opwarming-afkoeling cycli waren onsuccesvol.

Een tweede strategie bestaat uit het toevoegen van de volledige microalgenbiomassa aan levensmiddelen. Dit wordt namelijk beschouwd als een efficiëntere en duurzamere aanpak, aangezien nutritionele en gezondheidsbevorderende componenten eveneens geïntroduceerd worden en afvalstromen vermeden worden.

Het gebrek aan literatuurgegevens over de reologische eigenschappen van microalgensuspensies en de impact van procesvoering laten echter niet toe om het potentieel van deze toepassing in te schatten. Daarom werden de reologische eigenschappen van verschillende microalgen gekarakteriseerd, waarbij een grote diversiteit werd waargenomen, zowel voor als na procesvoering. Terwijl sommige microalgen zoals *Nannochloropsis* sp. Newtoniaans vloeigedrag vertoonden, waarbij de biomassa gebruikt zou kunnen worden zonder de reologische eigenschappen van de voedingsmatrix te verstoren, werden pseudoplastische vloei-eigenschappen en viscoelastisch gedrag waargenomen voor de andere microalgen. Het belang van mechanische en thermische procesvoering werd duidelijk aangetoond, niet alleen in het verkrijgen van verbeterde reologische eigenschappen, maar ook in het sturen van de microstructuur. Zo werden specifieke processtrategieën opgesteld voor *Chlorella vulgaris* en *Porphyridium cruentum* voor het maximaal benutten van hun structuurvormend vermogen en het creëren van verschillende microstructuren.

Het belang van deze microstructuur werd aangetoond in het laatste deel van deze doctoraatsthesis, waarbij de lipidenvertering en *in vitro* biotoegankelijkheid van carotenoïden en ω3-LC-PUFA in microalgenbiomassa onderzocht werd. Als hypothese werd namelijk vooropgesteld dat de celwand van de microalgen een fysieke barrière vormt voor de vertering en biotoegankelijkheid van intracellulaire componenten, onder de aanname dat de celwand niet afgebroken wordt door de verteringsenzymen in het gastro-intestinaal stelsel. Deze hypothese werd bevestigd, aangezien een toegenomen lipidenverteerbaarheid en biotoegankelijkheid van carotenoïden en ω3-LC-PUFA werd waargenomen voor gedisrupteerde biomassa van *Nannochloropsis* sp. ten opzichte van onbehandelde biomassa. De biotoegankelijkheid bleef echter relatief laag, wellicht te wijten aan de locatie van de carotenoïden en/of de aanwezigheid van andere macromoleculen in de biomassa, aangezien carotenoïden beduidend beter toegankelijk waren in de vorm van geëxtraheerde olie.

Deze doctoraatsthesis leverde de wetenschappelijke basis voor evaluatie van het potentieel van microalgen als structuurvormende ingrediënten in levensmiddelen. De grote diversiteit in fysicochemische eigenschappen vereist zonder twijfel een doordachte selectie van de soort microalg voor specifieke toepassingen. Het toevoegen van de volledige biomassa aan levensmiddelen wordt beschouwd als de meest beloftevolle strategie, aangezien de reologische eigenschappen doelgericht gestuurd kunnen worden door specifieke processtrategieën. Bijkomend onderzoek over de stabiliteit van de gezondheidscomponenten tijdens procesvoering en de impact op de sensorische eigenschappen is echter vereist voor het creëren van kwaliteitsvolle levensmiddelen aangerijkt met microalgen.

Abstract

Microalgae are considered promising functional food ingredients due to their balanced composition, containing various (essential) nutrients as well as health-beneficial components. However, their functionality in food products might not be limited to health aspects, as microalgae could also play a structuring role in food. Microalgae are actually rich in structural biopolymers such as proteins, storage polysaccharides, and cell wall related polysaccharides, and their presence might possibly alter the rheological properties of the enriched food product. In that case, microalgae could be considered as multifunctional food ingredients, combining nutritional enrichment of the food products with structural benefits, possibly reducing the need for additional thickening or gelling agents. However, the functionality of microalgae and their structural biopolymers has only very limitedly been studied in this context.

A first approach to benefit from these structural biopolymers consists of isolating the cell wall related polysaccharides, including cell wall bound polysaccharides and extracellular polysaccharides, for use as food hydrocolloids. While macroalgal polysaccharides have been successfully commercialized as thickening or gelling agents in food, polysaccharides of microalgae received surprisingly little attention in this context. Therefore, the first part of this doctoral thesis aimed to characterize the molecular composition of cell wall related polysaccharides of ten different microalgae species in terms of monosaccharides, uronic acids, and sulfate groups. As a result of the large evolutionary diversity of microalgae, a very diverse cell wall composition was observed for the different microalgae species, displaying little analogies with conventional food hydrocolloids. Based on the promising thickening properties reported for extracellular polysaccharides of *Porphyridium cruentum*, different cell wall fractions were isolated from this microalga and characterized in detail, in relation to their rheological properties. In contrast to the cell wall bound polysaccharides, extracellular polysaccharides were characterized by high molecular weight polymers, yielding higher intrinsic viscosities compared to several commercially used hydrocolloids. However, large amounts of co-extracted proteins and minerals limited their functionality in aqueous solutions, and attempts to induce gelation in presence of cations and/or heating-cooling cycles were unsuccessful.

A second approach to introduce structural biopolymers is the incorporation of the whole microalgal biomass into food products. This would actually be a more effective and more sustainable approach, since other nutritional and health-beneficial components are also introduced in the food product and no waste streams are generated. However, due to the lack of literature data on the rheological properties

of microalgal suspensions and the impact of processing thereon, there was an obvious need for research studies in order to evaluate the potential of this application. As expected from the variable biomass composition and physical properties of the different microalgae species, a large diversity in rheological properties was observed, with and without processing. In fact, whereas some microalgae such as *Nannochloropsis* sp. displayed Newtonian behavior, implying that their biomass could be used without disturbing the structural properties of the food matrix, other microalgae showed pseudoplastic flow properties and viscoelastic behavior. The importance of mechanical and thermal processing was clearly shown, not only in obtaining enhanced rheological properties, but also in tailoring microstructural properties. In fact, specific processing strategies were identified for suspensions of *Chlorella vulgaris* and *Porphyridium cruentum* to maximally exploit their structuring potential, resulting in different microstructural properties.

The importance of these microstructural properties was shown in the last part of this doctoral thesis, focusing on the lipid digestibility and *in vitro* bioaccessibility of carotenoids and ω3-LC-PUFA in microalgal biomass. It was actually hypothesized that the microalgal cell wall would act as a physical barrier limiting the digestibility and bioaccessibility of intracellular components, assuming that the cell wall is not degraded by the digestive enzymes in the gastrointestinal tract. This hypothesis could be confirmed, as higher values for lipid digestibility and bioaccessibility of carotenoids and ω3-LC-PUFA were observed for disrupted *Nannochloropsis* sp. biomass than for untreated biomass. However, relatively low bioaccessibility values were still observed, which were attributed to the location of the carotenoids and/or the presence of other macromolecules in the biomass, since carotenoids and ω3-LC-PUFA were significantly more bioaccessible when supplied as extracted oil.

This doctoral thesis provided the scientific knowledge base for evaluation of the potential of microalgae as structuring agents for food applications. It is obvious that the large diversity in physicochemical properties of microalgae requires a justified selection of appropriate microalgae species for specific applications. Incorporation of the whole microalgal biomass in food products is considered the most promising approach, since rheological properties can be tailored by using specific processing strategies, and nutritional and health-beneficial components are simultaneously introduced in the food product. However, additional research is required, for instance on the stability of these health-beneficial components upon processing and the impact on the sensory properties, for a complete evaluation of the design of high-quality food products enriched with microalgae.

List of notations

List of abbreviations

ω3-LC-PUFA	omega-3 long chain polyunsaturated fatty acids
CM	chloroform:methanol
CWPS	cell wall bound polysaccharides
DIC	differential interference contrast
EPA	eicosapentaenoic acid
EPMS	extracellular polymeric substances
EPS	extracellular polysaccharides
FAME	fatty acid methyl ester
FFA	free fatty acid
GC-FID	gas chromatography with flame ionization detection
HI	hexane:isopropanol
HPAEC-PAD	high performance anion exchange chromatography with pulsed amperometric detection
HPLC-DAD	high performance liquid chromatography with diode array detector
HPH	high pressure homogenization
HPSEC-MALLS-RI	high performance size exclusion chromatography with multi-angle laser light and refractive index detectors
ICP-OES	inductively coupled plasma optical emission spectrometry
MAG	monoacylglycerol
MES	2-(N-morpholino)ethanesulfonic acid
MOPS	3-(N-morpholino)propanesulfonic acid
PBS	phosphate buffered saline
PEF	pulsed electric field
SEM	scanning electron microscopy
SGF	simulated gastric fluid
SIF	simulated intestinal fluid
SPS	storage polysaccharides
TFA	trifluoroacetic acid
TLS	trilaminar sheath
TT	thermal treatment
UHPH	ultra high pressure homogenization
wiCWPS	water insoluble cell wall polysaccharides
wsCWPS	water soluble cell wall polysaccharides

List of symbols

C^*	critical overlap concentration [g/L]
G'	storage modulus [Pa]
$G"$	loss modulus [Pa]
K	consistency coefficient [Pa s^n]
n	flow behavior index [-]
γ	shear strain [%]
$\dot{\gamma}$	shear rate [s^{-1}]
δ	phase angle [°]
η	viscosity [Pa s]
η_s	serum viscosity [Pa s]
$[\eta]$	intrinsic viscosity [dL/g]
μ	dynamic viscosity [Pa s]
μ_s	dynamic serum viscosity [Pa s]
σ	shear stress [Pa]
σ_0	dynamic yield stress [Pa]
φ	phase volume [g/dL]
ω	angular frequency [rad/s]

Context and research objectives

In the context of developing food products with improved nutritional, structural, and sensory characteristics, food technologists are continuously exploring the potential of new ingredient sources. Microalgae are generally considered one of the promising sources of functional food ingredients, as they are a rich source of numerous nutrients and health-beneficial components, including vitamins, minerals, proteins with essential amino acids, polyunsaturated fatty acids, antioxidants, and dietary fiber. As a consequence, the literature on microalgae as healthy ingredients is extensively reviewed by many authors, including Buono et al. (2014), Chacón-Lee and González-Mariño (2010), Gouveia et al. (2010), Matos et al. (2017), and Plaza et al. (2009).

Beside these nutritional components, microalgae generally contain large amounts of structural biopolymers, such as proteins and carbohydrates. These structural biopolymers might possibly display interesting technological functionalities in food products, e.g. showing a potential role as texturizer, stabilizer, or emulsifier. However, apart from a limited number of fragmentary studies, this research area is still unexploited. The lack of knowledge on the functionality of microalgal cell wall related polysaccharides in particular is surprising, since cell wall polysaccharides of many taxonomically related macroalgae (e.g. carrageenans, agars, and alginates) are among the common thickening and gelling agents used in food applications.

The potential of biopolymers from microalgae as structuring food ingredients can generally be explored using two different strategies. The first strategy consists of a biorefinery based approach, in which the microalgal biopolymers are isolated as high-value products for application as food hydrocolloids. Downstream processing is obviously required to accomplish this strategy, particularly in terms of extraction, separation, and purification of the polysaccharides and/or proteins. As a consequence, microalgal biopolymers should display rather unique functionalities in order to be able to compete with conventional hydrocolloids from plants or macroalgae. The lack of studies reported on the functionality of microalgal biopolymers is related to the limited knowledge of the molecular structure of these polymers, in particular for the cell wall related polysaccharides. A thorough investigation of the molecular characteristics of microalgal cell wall related polysaccharides in relation to their functional properties (rheological properties in particular) is therefore required as a first step in evaluating their potential as food hydrocolloids.

The second strategy for introducing microalgal biopolymers in food is the incorporation of the whole microalgal biomass into food products. This might actually be a more efficient and more sustainable strategy to combine health-beneficial

components with possible structuring benefits from microalgal polymers. However, the use of food processing operations might be required to fully exploit the structuring potential of the different biopolymers. On the one hand, thermal processes might be advantageous to induce temperature-dependent reactions, such as denaturation of proteins and heat-induced gelation of polysaccharides. On the other hand, cell disruption techniques might be of interest to release intracellular biopolymers and to promote polymer interactions. However, only limited literature data are available on the rheological properties of microalgal suspensions and the impact of processing thereon.

There might however be some implications attributed to the latter strategy for introducing microalgal biopolymers in combination with nutritional compounds, in the context of nutrient bioaccessibility. Some indicative reports in literature actually suggest that the cell wall integrity would limit the bioaccessibility of intracellular components, acting as a physical barrier during gastrointestinal digestion. In that case, the use of processing, especially cell disruption techniques, might be a strategic approach to enhance the nutrient bioaccessibility. As such, cell disruption could be beneficial to create food products with enhanced nutritional value in terms of nutrient bioaccessibility. However, this research area is only very limitedly explored so far.

The main objective of this doctoral thesis is to evaluate the potential of microalgal biopolymers and/or whole microalgal biomass as food ingredients in the design of healthy food products with desired rheological properties. This work is organized in different chapters, as schematically presented in Fig. 1. An extensive review of the literature data is provided in Chapter 1, showing the current state of the art as well as identifying the research gaps in this research domain. The experimental work consists of seven chapters, starting with a characterization of the biomass composition of the different microalgae species used in this doctoral research (Chapter 2). The strategy to use cell wall related polysaccharides as food hydrocolloids will be evaluated in a first window of the experimental work, investigating the molecular composition of cell wall related polysaccharides of different microalgae (Chapter 3) in relation to their thickening and/or gelling properties (Chapter 4). The second window of the research evaluates the strategy to introduce microalgal biomass into food products. Therefore, the rheological properties are examined in aqueous model systems, and the impact of different processing operations thereon will be studied in Chapters 5 and 6. Finally, implications in the context of nutrient bioaccessibility will be evaluated, by identifying processing conditions to obtain complete cell disruption of rigid microalgae (Chapter 7) and investigating the impact of cell integrity on the bioaccessibility of omega-3 long chain polyunsaturated fatty acids (ω3-LC-PUFA) and carotenoids

(Chapter 8). As such, the research conducted in this doctoral thesis provides a broad scientific knowledge base to evaluate the potential of microalgal biopolymers and microalgal biomass as structuring ingredients in food processing.

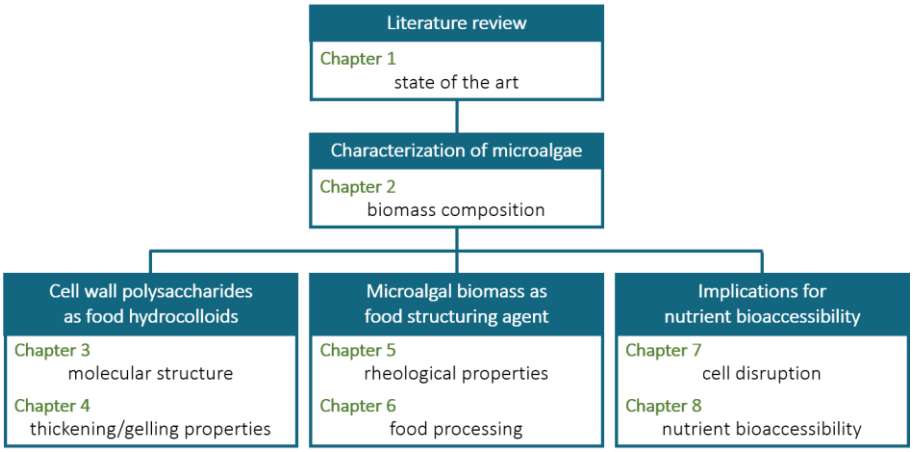

Fig. 1 Schematic overview of the work presented in this doctoral thesis.

Table of contents

LITERATURE REVIEW

CHAPTER 1

The potential of biopolymers of microalgae as structuring ingredients in food: state of the art

1.1 MICROALGAE

Due to the enormous evolutionary diversity of microalgae, a universal definition is still lacking at this moment. Nevertheless, microalgae are generally described as a very diverse group of unicellular organisms, grown in fresh water or marine environments, that are capable of performing photosynthesis. However, many heterotrophically grown species are also considered as microalgae, including several obligate heterotrophs like the marine thraustochytrids (Hu et al., 2018). While microalgae are generally referred to as eukaryotic organisms, the prokaryotic cyanobacteria are often included because of their capability of performing photosynthesis (Tomaselli, 2004). Therefore, the term microalgae used in this doctoral thesis refers to both the eukaryotic microalgae and the prokaryotic cyanobacteria.

Eukaryotic microalgae can be grown photoautotrophically, heterotrophically, or mixotrophically. Photoautotrophic microalgae only require light and inorganic compounds, such as CO_2, nitrogen, sulphur, and phosphorus, that are converted into energy using their photosynthetic pathways. Generally, microalgae are more efficient in converting solar energy into biomass (up to 3%) compared to terrestrial plants (0.2 – 2%) (Melis, 2009). Heterotrophic microalgae on the other hand require an organic carbon source and grow by fermentation in the absence of light. In fact, this heterotrophic growth is likely to be the equivalent of the dark metabolism in photosynthetic organisms (Morales-Sánchez et al., 2015). Some microalgae are mixotrophic, implying that they can perform photosynthesis and conversion of external organic carbon sources simultaneously. However, this term is often used

This chapter is based on the following paper:
Bernaerts T.M.M., Gheysen L., Foubert I., Hendrickx M.E., Van Loey A.M.
The potential of biopolymers of microalgae as structuring ingredients in food: a review.
Biotechnology Advances, under review.

incorrectly, as several species switch between photoautotrophic and heterotrophic metabolisms rather than performing those simultaneously, and these microalgae species should therefore not be referred to as truly mixotrophic organisms (Grobbelaar, 2004; Lee, 2004).

A schematic representation of the ultrastructure of a eukaryotic microalgal cell is given in Fig. 1.1. Different cell organelles are present in microalgal cells, including a nucleus, endoplasmic reticulum, ribosomes, Golgi apparatus, vacuoles, a chloroplast, and mitochondria. However, due to the high evolutionary diversity, it should be noted that some organelles are absent or differently organized in certain species (Pignolet et al., 2013). In addition, the cultivation mode might influence the presence of specific organelles. For instance, under dark and nutrient depleted conditions the chloroplast might break down to function as an internal supply of nitrogen for cell survival (Perez-Garcia et al., 2011). While lipids and storage polysaccharides (SPS) are generally associated with the cell membrane, organelle membranes, and/or the chloroplast, these storage products can also be stored in the cytoplasm as lipid bodies and SPS granules. However, these structures are generally more present when cultivated under nutrient depletion or in the late stationary phase (Wang et al., 2009). The microalgal cell is surrounded by a plasma membrane and a cell wall, although the latter is absent in a few microalgae species (Ben-Amotz and Avron, 1992). Several microalgae species also possess an extracellular layer of polysaccharides, which can be secreted into the surrounding environment such as the cultivation medium (Tomaselli, 2004). Note that the cellular structure of prokaryotic cyanobacteria is substantially different than the one represented in Fig. 1.1. A schematic representation of the ultrastructure of cyanobacteria in comparison with a microalgal cell is provided in the review paper published by Pignolet et al. (2013).

1.2 STRUCTURAL BIOPOLYMERS IN MICROALGAE

A large diversity in the biochemical composition of microalgae has been observed, resulting from the enormous evolutionary diversity of these organisms. In addition, biomass profiles can be drastically changed by adapting different cultivation conditions, including light intensity, temperature, and nutrient availability (Hu, 2004). As a consequence, largely variable literature data can be found on the composition of microalgae, with ranges of 9 – 77% proteins, 6 – 54% carbohydrates, and 4 – 74% lipids being reported. Biomass profiles of several microalgae species relevant for use as a food ingredient are compiled in Table 1.1. While some microalgae possess a low lipid content (< 20%), such as *Arthrospira platensis* (*Spirulina*), *Dunaliella* sp., and *Porphyridium cruentum*, most microalgae species have a substantial fraction of lipids (~15 – 40%), including *Haematococcus pluvialis*, *Phaeodactylum tricornutum*, and

Isochrysis galbana. Examples of lipid-rich microalgae (> 40%) are *Schizochytrium* sp. and some *Nannochloropsis* strains. Generally, the higher the lipid content of microalgal biomass, the lower the amount of structural biopolymers, i.e. proteins and carbohydrates.

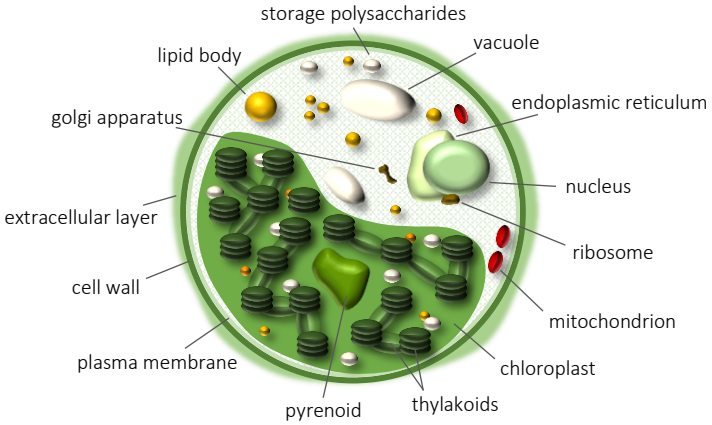

Fig. 1.1 Schematic representation of a eukaryotic microalgal cell, based on Pignolet et al. (2013), Baudelet et al. (2017), and Tomaselli (2004). Some organelles might be absent or differently organized in certain microalgae species.

1.2.1 Proteins

Proteins can be found in high amounts for all microalgae species listed in **Table 1.1**, except for the obligate heterotroph *Schizochytrium*. In fact, apart from the water soluble proteins in the cytoplasm, proteins are mainly associated with the chloroplast, i.e. the photosynthetic organelle of the microalgal cell. Examples are the Rubisco enzyme in the pyrenoid of eukaryotic microalgae and phycobiliproteins as photosynthetic accessory pigments in thylakoids of red microalgae and cyanobacteria (Arad and Yaron, 1992; Safi et al., 2014a). Even though many microalgae species can possess high protein contents, *Chlorella vulgaris* and *Arthrospira platensis* are most commonly produced as protein sources (Pulz and Gross, 2004). Their nutritional value is extensively studied, for *Arthrospira* sp. in particular, showing favorable amino acid profiles and a good digestibility (Becker, 2004). Furthermore, several reports have recently been published on their promising techno-functionalities. On the one hand, microalgal proteins could possibly display beneficial protein-surface related properties, such as foaming and emulsifying properties. For instance, Ursu et al. (2014) investigated the emulsifying capacity of *Chlorella vulgaris* proteins, and concluded them to be competitive with commercial emulsifying ingredients. The

Table 1.1 Proximate biomass composition of different microalgae species, expressed as percentage of dry biomass (%).

Microalga species	Proteins (%)	Carbohydrates (%)	Lipids (%)	References
Arthrospira platensis (*Spirulina*)	43 - 77	8 - 22	4 - 14	Becker (2004); Ciferri (1983); Gouveia and Oliveira (2009); Kent et al. (2015); Matos et al. (2016); Parages et al. (2012); Safi et al. (2013); Tibbetts et al. (2015); Tokusoglu and Unal (2003); Wild et al. (2018)
Chlorella vulgaris	38 - 53	8 - 27	5 - 28	Batista et al. (2013); Gouveia and Oliveira (2009); Kent et al. (2015); Matos et al. (2016); Rodolfi et al. (2009); Safi et al. (2013); Templeton et al. (2012); Tibbetts et al. (2015); Tokusoglu and Unal (2003); Wild et al. (2018)
Diacronema vlkianum	24 - 39	15 - 31	18 - 39	Batista et al. (2013); Fradique et al. (2013); Ponis et al. (2006)
Dunaliella sp.	27 - 57	14 - 41	6 - 22	Becker (2004); Gouveia and Oliveira (2009); Kent et al. (2015); Kim et al. (2015)
Haematococcus pluvialis	10 - 52	34	15 - 40	Batista et al. (2013); Damiani et al. (2010); Safi et al. (2013)
Isochrysis galbana	12 - 40	13 - 48	17 - 36	Batista et al. (2013); Fernández-Reiriz et al. (1989); Fradique et al. (2013); Ryckebosch et al. (2014); Sánchez et al. (2000); Tokusoglu and Unal (2003)
Nannochloropsis sp.	18 - 47	7 - 40	7 - 48	Gouveia and Oliveira (2009); Guil-Guerrero et al. (2004); Hu and Gao (2003); Huerlimann et al. (2010); Kent et al. (2015); Matos et al. (2016); Rebolloso-Fuentes et al. (2001a); Rodolfi et al. (2009); Ryckebosch et al. (2014); Safi et al. (2013); Templeton et al. (2012); Tibbetts et al. (2015); Wang and Wang (2012); Wild et al. (2018)
Odontella aurita	9 - 28	31 - 54	13 - 20	Xia et al. (2013)
Pavlova lutheri (*)	16 - 43	15 - 53	6 - 36	Fernández-Reiriz et al. (1989); Rodolfi et al. (2009)
Phaeodactylum tricornutum	13 - 40	6 - 35	14 - 39	Fernández-Reiriz et al. (1989); Guil-Guerrero et al. (2004); Matos et al. (2016); Rebolloso-Fuentes et al. (2001b); Rodolfi et al. (2009); Ryckebosch et al. (2014); Templeton et al. (2012); Tibbetts et al. (2015); Wild et al. (2018)
Porphyridium cruentum	27 - 57	12 - 39	5 - 13	Matos et al. (2016); Rebolloso Fuentes et al. (2000); Rodolfi et al. (2009); Safi et al. (2013)
Scenedesmus sp.	31 - 56	6 - 28	8 - 21	Becker (2004); Gouveia and Oliveira (2009); Ho et al. (2012); Kent et al. (2015); Rodolfi et al. (2009)
Schizochytrium sp.	11 - 14	12 - 24	46 - 74	Chen et al. (2016); Johnson and Wen (2009); Liang et al. (2010); Qu et al. (2013); Wang and Wang (2012)
Tetraselmis sp.	14 - 58	12 - 43	8 - 33	Eboibi et al. (2015); Fernández-Reiriz et al. (1989); Huerlimann et al. (2010); Rodolfi et al. (2009); Schwenzfeier et al. (2011); Suarez Garcia et al. (2018b); Tibbetts et al. (2015)

(*) taxonomically revised to *Diacronema lutheri*

same conclusion was drawn for the emulsifying and foaming properties of protein isolates from *Tetraselmis* sp. by Schwenzfeier et al. (2013a, 2013b). On the other hand, microalgal proteins might be relevant in the food industry because of their hydrodynamic properties, such as thickening or gelling properties. In this context, Chronakis (2001) studied the rheological properties of a protein isolate from *Arthrospira platensis*. An increased viscosity above 50 °C was related to the denaturation of the proteins, which resulted in elastic gels upon heating to 90 °C. Subsequent cooling resulted in an increased network elasticity. The authors concluded that *Arthrospira platensis* protein isolates showed good gelling properties at concentrations between 1.5% and 2.5% (Chronakis, 2001). Similar gelling behavior was observed for proteins extracted from *Tetraselmis suecica*, resulting in a superior gelation behavior compared to whey protein isolate (Suarez Garcia et al., 2018a).

1.2.2 Carbohydrates

Carbohydrates make up another important fraction of microalgal biomass. Even though they have been mainly determined as the total carbohydrate content, it is important to distinguish storage carbohydrates from structural carbohydrates (i.e. cell wall related polysaccharides). These two types of carbohydrates do not only exhibit different functions in the microalgal cell, they might also display different functionalities in food products.

1.2.2.1 Storage polysaccharides

Five types of SPS (starch, floridean starch, glycogen, chrysolaminarin, and paramylon) can be found in microalgae and cyanobacteria, with the type of SPS being species specific. The former three are polyglucans consisting of α-1,4 and α-1,6-linkages in different ratios, whereas chrysolaminarin polymers are composed of β-1,3 and β-1,6-linked glucose residues. In contrast, paramylon polymers are only composed of β-1,3-linked glucose residues (De Philippis et al., 1992; Myklestad, 1988; Percival, 1979; Suzuki and Suzuki, 2013). As a consequence, the different types of SPS are identified by different degrees of branching, as shown in **Fig. 1.2**. Whereas amylopectin possesses 5 – 6% of α-1,6-linkages, which is about one branch point for every 20 glucose residues (α-1,4/α-1,6 ≈ 20:1), a higher degree of branching is found in chrysolaminarin (β-1,3/β-1,6 ≈ 11:1) and in glycogen (α-1,4/α-1,6 ≈ 10:1) (Beattie et al., 1961; Buléon et al., 1998; Calder, 1991). Since floridean starch, sometimes referred to as amylopectin-rich starch, typically contains little or no amylose (0 – 5%), its granules are composed of more branched polymers compared to starch (McCracken and Cain, 1981; Percival, 1979). Moreover, the location of these types of SPS in the microalgal cell differs (**Fig. 1.1**). While starch granules are typically stored in the chloroplasts, chrysolaminarin is accumulated in the vacuoles of the cells. The

other three types (floridean starch, paramylon, and glycogen) are located as granules in the cytosol (Suzuki and Suzuki, 2013). Although starch isolated from plant sources is a commonly used thickening agent in the food industry, the diversity of microalgal SPS does not allow the prediction of the functionality of these other types of storage carbohydrates in food products. To the best of our knowledge, no studies have been reported on the functionality of microalgal starch or the four other types of SPS as a thickening agent.

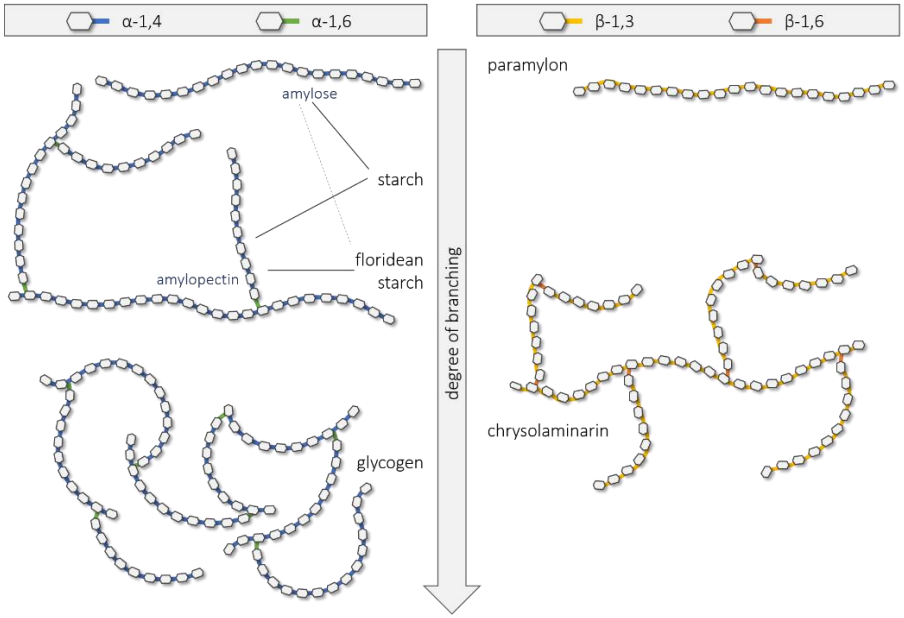

Fig. 1.2 Schematic representation of the five types of storage polysaccharides in microalgae and cyanobacteria.

1.2.2.2 Cell wall related polysaccharides

Except for a few microalgae species, the microalgal cell is surrounded by a cell wall. Microalgal cell walls are mainly composed of polysaccharides, which are referred to as cell wall bound polysaccharides (CWPS), although several other components have been identified, including proteins, resistant biopolymers, silicified or calcified structures, and so on (de Leeuw et al., 2006; Tomaselli, 2004). In addition, the cell wall of several microalgae is surrounded by an external layer of polymers. Depending on several factors such as the growth stage of the microalgae, these extracellular polymers can either remain associated to the cell surface or be released into the surrounding environment (Delattre et al., 2016). The status and the nature of these polymers is often unclear in literature, partly due to the large variety in terminology, including exopolysaccharides, extracellular polysaccharides, extracellular polymeric

substances, released polysaccharides, colloidal exopolysaccharides, capsular polysaccharides, extracellular organic matter, dissolved organic matter, and algogenic organic matter (Abdullahi et al., 2006; Delattre et al., 2016; Henderson et al., 2008; Kuhnhenn et al., 2006). For cyanobacteria in particular, terms as sheath, capsule, and slime are often used to distinguish between extracellular layers with different affinity to be released into the medium (De Philippis and Vincenzini, 1998). In this doctoral thesis, the term extracellular polysaccharides (EPS) will be used to indicate the polysaccharides in the external layer, while the term extracellular polymeric substances (EPMS) will be referred to when indicating all polymeric substances in the external layer.

Reports on the quantification of cell wall related polysaccharides are very scarce, which might be due to the difficult extractability of the total cell wall polysaccharides. Furthermore, while glucose is the dominant sugar in SPS, structural polysaccharides are generally composed of multiple monosaccharide residues. Since it is generally assumed that SPS are more sensitive to variable cultivation conditions than structural carbohydrates (González-Fernández and Ballesteros, 2012; Markou et al., 2012), it is assumed that the majority of carbohydrates as shown in Table 1.1 is probably attributed to SPS, with only a smaller fraction corresponding to cell wall related polysaccharides.

1.3 POTENTIAL OF MICROALGAL CELL WALL POLYSACCHARIDES AS FOOD HYDROCOLLOIDS

An overview on the presence of a polysaccharidic cell wall and/or an extracellular layer of polysaccharides in some microalgae species is provided in Table 1.2. The absence of a cell wall is rather unusual in microalgae. One of the few microalgae species lacking a cell wall is *Dunaliella*. The cells of this microalga do possess a mucilaginous cell coat, but this is typically considered as an extracellular layer which can be visualized with Indian ink, similar to the capsule in cyanobacteria (Ben-Amotz and Avron, 1992; De Philippis and Vincenzini, 1998). Furthermore, no consensus has been reached on the presence of a cell wall in *Isochrysis* species. The lack of a cell wall in *Isochrysis galbana* was suggested by Zhu and Lee (1997), and was related to the fragility of the cells. In contrast, Pales Espinosa et al. (2010) concluded the presence of mannose and glucose on the surface of *Isochrysis* sp. based on strong binding of fluorescently labeled lectins. However, it is unclear whether these monosaccharides are part of a structural cell wall, or only present as an extracellular layer similar to *Dunaliella* sp. cells.

Table 1.2 Presence of cell wall bound polysaccharides (CWPS) and extracellular polysaccharides (EPS) in some microalgae species (+ present; – absent; +/– only present in some subspecies or morphotypes; * no consensus on the presence of a cell wall or extracellular polysaccharides; ? unknown).

	Microalga species	CWPS	EPS	References
Cyanobacteria	*Arthrospira platensis* (*Spirulina*)	+	+	Bertocchi et al. (1990); Depraetere et al. (2015); Filali Mouhim et al. (1993); Roussel et al. (2015); Trabelsi et al. (2009)
Chlorophyta	*Chlorella* sp.	+	+	Chen et al. (2015); Cheng et al. (2011, 2015); Kaplan et al. (1987); Yalcin et al. (1994); Yang et al. (2010)
	Dunaliella salina	–	+	Ben-Amotz and Avron (1992); Mishra and Jha (2009); Mishra et al. (2011)
	Scenedesmus sp.	+	+	Halaj et al. (2018); Lombardi et al. (2005); Takeda (1996)
	Tetraselmis chuii	+	?	Becker et al. (1995); Kermanshahi-pour et al. (2014)
Haptophyta	*Isochrysis* sp.	*	*	Pales Espinosa et al. (2010); Zhu and Lee (1997)
	Pavlova lutheri (*)	+	?	Arnold et al. (2015)
Eustigmatophyta	*Nannochloropsis* sp.	+	?	Arnold et al. (2015); Scholz et al. (2014)
Diatoms	*Phaeodactylum tricornutum*	+	+/–	Abdullahi et al. (2006); Guzmán-Murillo et al. (2007); Willis et al. (2013)
Rhodophyta	*Porphyridium* sp.	+/–	+	de Jesus Raposo et al. (2014); Geresh et al. (1992, 2002); Geresh and Arad (1991); Gloaguen et al. (2004); Patel et al. (2013); Percival and Foyle (1979); Roussel et al. (2015); Soanen et al. (2015)
Labyrinthulomyceta	*Schizochytrium* sp.	+	+/–	Bahnweg and Jackle (1986); Darley et al. (1973); Lee Chang et al. (2014)

(*) taxonomically revised to *Diacronema lutheri*

The ability of microalgae to produce EPS seems to be less conserved. While EPS are typically (but not necessarily) synthesized by cyanobacteria, diatoms, green microalgae, and red microalgae, they have been less studied in other classes of microalgae (**Table 1.2**). To date, the physiological function of microalgal EPS is poorly understood, but they are thought to protect the algal cells from fluctuations in environmental conditions and/or predators. As a result, production of EPS is not only dependent on the microalga species or strain, but also on cultivation conditions (Delattre et al., 2016; Xiao and Zheng, 2016). Moreover, correct identification of microalgal EPS is challenging, since polysaccharides isolated from microalgal cultures might also originate from EPS producing bacteria which adhere to microalgal cells (Nichols et al., 2005). It was also shown that not all morphotypes within one microalgae species have the ability to synthesize EPS. For instance, while they are produced by the ovoid type of *Phaeodactylum tricornutum*, the fusiform and triradiate forms do not produce EPS (Desbois et al., 2010). Finally, it should be noted that EPS are not always easily differentiated from CWPS, as is the case for red microalgae. In fact, red microalgae are often described as cells encapsulated within a

polysaccharide complex in the form of a gel, comprised of soluble and bound polysaccharides (Arad and Levy-Ontman, 2010).

1.3.1 Molecular composition of cell wall polymers

Despite the importance of the microalgal cell wall properties towards several biotechnological applications, microalgal cell walls are poorly understood. Due to their evolutionary diversity, microalgal cell walls differ in molecular components, intra- and intermolecular linkages, and overall structure (Scholz et al., 2014). Besides, drastic variability in the composition and structure of microalgal cell walls has been reported within a genus, a species, or within a strain (Baudelet et al., 2017). Furthermore, comparison of the work in this domain that was reported in the past half-century has been challenged by recent taxonomic revisions, for instance in the organization of Chlorophyta. An extensive review on this topic was provided by Baudelet et al. (2017), clearly illustrating the diversity in the cell wall composition of green microalgae.

In general, microalgal cell walls are often described as fibrillar layers of rigid wall components that are embedded in a more plastic polymeric matrix (Gerken et al., 2013; Passos et al., 2014). While this description might be valid for the majority of microalgal cell walls, it must be noted that several species lack rigid polymers in their cell wall, and some are known for a glycoprotein-based cell wall such as *Chlamydomonas reinhardtii* and *Euglena gracilis* (Mussgnug et al., 2010). The polymeric matrix is generally defined as the fraction that is hydrolyzed under mild acid conditions such as 2 M trifluoroacetic acid (TFA), liberating different monosaccharides and uronic acids, including glucose, galactose, rhamnose, arabinose, mannose, xylose, fucose, ribose, glucuronic acid, and galacturonic acid (Gerken et al., 2013). In contrast, the rigid or fibrillar polymers are (partially) resistant to mild acids and require harsh conditions for complete hydrolysis, such as 72% sulphuric acid or 6 M hydrochloric acid. Various fibrillar polymers have been found in microalgal cell walls, such as cellulose and chitin (Baudelet et al., 2017). Finally, some microalgal cell walls contain non-hydrolyzable biopolymers that are resistant to any acid and alkaline treatment, often defined as resistant biopolymers or algaenans (de Leeuw et al., 2006).

1.3.1.1 Cell wall bound polysaccharides

Microalgal CWPS are generally heteropolymers consisting of different monosaccharides, uronic acids, and amino sugars. Table 1.3 gives an overview of the cell wall composition of different microalgae species, in which predominant monosaccharides are indicated in bold. Furthermore, microalgal CWPS are often

sulfated, but quantitative data on the amounts of sulfate esters are lacking in literature for most microalgae species.

Cell walls of the prokaryotic cyanobacteria are usually composed of peptidoglycan (also called murein), polymers of alternated N-acetylglucosamine and N-acetylmuramic acid residues connected by β-1,4-linkages. Together with cross-linked oligopeptides a three-dimensional network is formed, providing the (limited) rigidity of the cyanobacterial cell wall (Van Eykelenburg et al., 1980). Peptidoglycan is also present in *Arthrospira platensis*, despite the fact that glucosamine is not always detected as the predominant monosaccharide. Peptidoglycan actually requires harsh acid conditions for complete hydrolysis to glucosamine (Templeton et al., 2012). The structural peptidoglycan polymers are embedded in a polysaccharide matrix, mainly composed of glucose. It is suggested that peptidoglycan and matrix polysaccharides are present in equal amounts in cyanobacteria, as was previously observed for some species (Bertocchi et al., 1990). Despite the presence of a structural peptidoglycan network, *Arthrospira platensis* has a relatively fragile cell wall that is easily disrupted by mechanical forces (Safi et al., 2014b).

The cell wall composition of eukaryotic microalgae is very diverse, even within a phylum, class, or species (Table 1.3). This is illustrated by the complex cell wall composition of *Chlorella* species. Three types of cell walls have been reported for *Chlorella* sp. based on their composition: (i) glucosamine-rich cell walls, (ii) cell walls with mannose and glucose as main constituents, and (iii) cell walls rich in galactose, glucose, and rhamnose (Blumreisinger et al., 1983). Glucosamine originates from a chitin-like polysaccharide which serves as the rigid cell wall polymer in the first type of *Chlorella* species. Up to 66% of the total cell wall in *Chlorella* sp. can be made up from this rigid polymer (Baudelet et al., 2017). The other part of the cell wall corresponds to hemicellulosic material, mainly constituting rhamnose, arabinose, and galactose (Baudelet et al., 2017; Blumreisinger et al., 1983; Kapaun et al., 1992). In contrast, the occurrence of rigid polymers is not clear for the other two types of *Chlorella* sp. cell walls. Some authors suggest the presence of cellulose microfibrils to be responsible for the rigidity of these *Chlorella vulgaris* cell walls (Gille et al., 2016). Whereas Safi et al. (2015) successfully used calcofluor white for fluorescent staining of beta-glucans in the cell wall of *Chlorella vulgaris* suggesting the presence of cellulosic polymers, this could not be demonstrated by other authors, although the latter did not verify which wall-type of *Chlorella* sp. was used (Baudelet et al., 2017).

Table 1.3 Monosaccharide and uronic acid composition of cell wall bound polysaccharides (CWPS) of some microalgae species (data are not exhaustive). Predominant monosaccharides and uronic acids are indicated in bold. (Glc: glucose; Gal: galactose; Xyl: xylose; Man: mannose; Rha: rhamnose; Ara: arabinose; Fuc: fucose; Rib: ribose; GlcN: glucosamine; Kdo: 3-deoxy-manno-2-octulosonic acid; Dha: 3-deoxy-lyxo-2-heptulosaric acid; GalA: galacturonic acid; GlcA: glucuronic acid; UA: uronic acids; ? unknown).

	Microalga species	Monosaccharides and uronic acids	Sulfate esters (%)	References
Cyanobacteria	*Arthrospira platensis* (*Spirulina*)	**Glc**, **GlcN**	?	Bertocchi et al. (1990)
Chlorophyta	*Chlorella* sp. (GlcN-rich type)	**Glc**, Gal, Xyl, Man, **Rha**, Ara, Fuc, **GlcN**, UA	?	Blumreisinger et al. (1983); Cheng et al. (2011, 2015); Kapaun et al. (1992)
	Chlorella sp. (Glc-Man-rich type)	**Glc**, **Man**, Rha, GlcA	?	Loos and Meindl (1982); Shi et al. (2007)
	Chlorella sp. (Glc-Gal-Rha-rich type)	**Glc**, **Gal**, Xyl, Man, **Rha**, Ara, Fuc, Rib, GlcN, GalA, GlcA	?	Templeton et al. (2012)
	Scenedesmus sp.	**Glc**, Gal, Man, Fuc	?	Blumreisinger et al. (1983); Takeda (1996)
	Tetraselmis sp.	**Glc**, **Gal**, Xyl, Man, Rha, Ara, **Kdo**, Dha, **GalA**	6	Becker et al. (1995); Kermanshahi-pour et al. (2014); Schwenzfeier et al. (2011); Whyte (1987)
Haptophyta	*Isochrysis* sp.	**Glc**, **Gal**, Xyl, **Man**, Ara, Rib, UA	1.1 - 5.5	Y. Sun et al. (2014); Whyte (1987)
	Pavlova lutheri (*)	**Glc**, Gal, Xyl, Man, Ara	?	Arnold et al. (2015)
Eustigmatophyta	*Nannochloropsis* sp.	**Glc**, Gal, Xyl, Man, Rha, Fuc, Rib	?	Arnold et al. (2015); Scholz et al. (2014); Templeton et al. (2012); Vieler et al. (2012)
Diatoms	*Phaeodactylum tricornutum*	Glc, Gal, Xyl, **Man**, Rha, Fuc, Rib, **GlcA**	7.5 - 13.3	Ford and Percival (1965); Guzmán et al. (2003); Templeton et al. (2012)
Labyrinthulomyceta	*Schizochytrium* sp.	**Gal**	?	Bahnweg and Jackle (1986); Darley et al. (1973)

(*) taxonomically revised to *Diacronema lutheri*

Little similarity has been observed for other species of the Chlorophyta listed in Table 1.3. No glucosamine was detected in *Scenedesmus* sp. and *Tetraselmis* sp. cell walls, indicating the absence of a chitin-like rigid wall. Major amounts of glucose in the cell wall of *Scenedesmus* sp. (up to 85%) suggest the presence of cellulose (Blumreisinger et al., 1983; Takeda, 1996), however this was only verified for one strain (Bisalputra and Weier, 1963). In contrast, the rigidity of *Tetraselmis* sp. is created by mineralized scales or theca, mainly composed of acidic polysaccharides such as 3-deoxy-manno-2-octulosonic acid (Kdo), galacturonic acid (GalA), and 3-deoxy-lyxo-2-heptulosaric acid (Dha) (Becker et al., 1998).

Glucose is also the predominant monosaccharide in *Nannochloropsis* sp. (Eustigmatophyta) and in the Haptophyta *Isochrysis* sp. and *Pavlova lutheri*, although it is not attributed to the same polymers. While the majority of glucose in *Nannochloropsis* sp. and *Pavlova lutheri* was ascribed to cellulose polymers, it was suggested that no cellulose is present in *Isochrysis*. In addition, it was proven that the cellulose polymers in *Nannochloropsis* sp. exist as microfibrils resulting in a rigid cell wall layer, while *Pavlova lutheri* cells are protected by small cellulose scales (Arnold et al., 2015; Scholz et al., 2014). As a consequence, not only the presence but also the state (crystalline or amorphous) and the configuration (fibrils or scales) of cellulose polymers determine the rigidity of the cell wall layers. Scales have also been reported in the cell walls of Labyrinthulomyceta like *Schizochytrium* sp., although they are made up of non-cellulosic material (Bahnweg and Jackle, 1986; Honda et al., 1999).

The cell wall of diatoms is generally described as silica valves (called frustule) covered with hemicellulosic polymers (Gügi et al., 2015). Even though *Phaeodactylum tricornutum* is classified as a diatom, the frustule is only synthetized by the ovoid form, while the cell walls of fusiform and triradiate morphotypes contain almost exclusively organic components (Francius et al., 2008; Tesson et al., 2009). In fact, a sulfated glucuronomannan was described as the prominent polysaccharide in the cell wall of *Phaeodactylum tricornutum* (Ford and Percival, 1965). It comprises a backbone of α-1,3-linked mannose residues with side chains of mannose and glucuronic acid, resulting in a molar ratio of mannose to glucuronic acid of approximately 4:1 (Ford and Percival, 1965; Le Costaouëc et al., 2017). Because of the absence of the silicified frustule in the fusiform and triradiate forms, these morphotypes are about five times softer and will presumably be less resistant to mechanical disruption techniques than the ovoid form (Francius et al., 2008). This was evidenced by Gille et al. (2019), as the authors observed intact ovoid cells of *Phaeodactylum tricornutum* after sonication, while cells of the fusiform and triradiate morphotypes were destroyed.

In general, knowledge on the molecular characteristics of CWPS is restricted to the monosaccharide composition investigated by a limited number of researchers. To

date, detailed structural analyses to explore the architecture of microalgal CWPS are lacking in literature, except for the sulphated glucuronomannan of one *Phaeodactylum tricornutum* morphotype and the cellulose microfibrils in *Nannochloropsis* sp. (Le Costaouëc et al., 2017; Scholz et al., 2014). Hence, it is not surprising that no studies have been found on the rheological characterization of CWPS of microalgae, since detailed knowledge on the molecular structure is at the scientific basis of understanding and/or engineering the rheological properties of polysaccharide solutions.

1.3.1.2 Resistant biopolymers

In many microalgae species, the rigidity of the cell wall is caused by the presence of resistant biopolymers. These are typically defined as algaenans, aliphatic macromolecules that are resistant to any acid or alkaline chemical. However, their structure might be somewhat modified under harsh acid or alkaline conditions due to hydrolysis of associated compounds (de Leeuw et al., 2006). It is worth noting that they have been often referred to as sporopollenin, cutin- or cutan-like polymers due to their similar function and resistance to biodegradation as those polymers in spores, pollen, and plants (Tegelaar et al., 1989). However, due to essential differences in chemical structure of the microalgal biopolymers compared to the above-mentioned polymers, it is suggested to use the term algaenans for all resistant biopolymers originating from (micro)algae (Burczyk and Dworzanski, 1988; de Leeuw et al., 2006). The occurrence of algaenan polymers in several microalgae species is presented in Table 1.4. Whereas algaenans appear in various members of Chlorophyta and Eustigmatophyta, they are less common in other classes of microalgae. The resistant polymers are absent in *Arthrospira platensis*, *Porphyridium cruentum*, and *Schizochytrium* sp., and have not been detected in Haptophyta and diatoms in general (de Leeuw et al., 2006; Gelin et al., 1999; Kodner et al., 2009).

As algaenans represent a series of polymers based on their physicochemical characteristics, different types of algaenan structures have been identified. Most Chlorophyta contain algaenan structures constructed by building blocks of linear even-numbered carbon chains of 22 to 34 carbon atoms, cross-linked by ether and ester bonds. However, larger building blocks have been observed for *Botryococcus braunii* (A-Race in particular), showing an average length of 40 carbons (Baudelet et al., 2017; de Leeuw et al., 2006). In contrast, algaenans produced by Eustigmatophyta typically contain building blocks of 25 to 36 carbons, odd- and even-numbered, cross-linked by ether bonds (de Leeuw et al., 2006).

Table 1.4 Presence of algaenan in the cell wall of some microalgae species (+ present; – absent; +/– only present in some subspecies; (–) not investigated for these particular species, but typically not found in Haptophyta and diatoms).

	Microalga species	Algaenan	References
Cyanobacteria	*Arthrospira platensis* (*Spirulina*)	–	Ometto et al. (2014)
Chlorophyta	*Chlorella* sp.	+/–	de Leeuw et al. (2006)
	Dunaliella salina	–	Ben-Amotz and Avron (1992)
	Haematococcus pluvialis	+	Montsant et al. (2001)
	Scenedesmus sp.	+	Allard and Templier (2000); Burczyk and Dworzanski (1988)
	Tetraselmis chuii	–	Gelin et al. (1999)
Haptophyta	*Diacronema vlkianum*	(–)	de Leeuw et al. (2006)
	Isochrysis sp.	(–)	de Leeuw et al. (2006)
	Pavlova lutheri (*)	(–)	de Leeuw et al. (2006)
Eustigmatophyta	*Nannochloropsis* sp.	+	Gelin et al. (1999)
Diatoms	*Odontella aurita*	(–)	de Leeuw et al. (2006)
	Phaeodactylum tricornutum	(–)	de Leeuw et al. (2006)
Rhodophyta	*Porphyridium* sp.	–	Bold and Wynne (1985)
Labyrinthulomyceta	*Schizochytrium* sp.	–	Bahnweg and Jackle (1986)

(*) taxonomically revised to *Diacronema lutheri*

The presence of algaenans in microalgal cell walls is sometimes confused with the occurrence of a trilaminar sheath (TLS). Microalgal TLS are characterized by two electron-dense sublayers enclosing a third sublayer with low electron density when examined by transmission electron microscopy. Algaenans are presumably located in this inner electron-lucent sublayer. However, Allard and Templier (2000) showed that there is no direct relation between the presence of TLS and algaenan polymers, as proven for two marine microalgae. Moreover, condensation reactions initiated by certain isolation procedures might lead to artifactual non-hydrolyzable polymers, which could mistakenly be identified as algaenans. Hence, even though a TLS often creates rigidity of the cell wall, it is not necessarily composed of non-hydrolyzable algaenan polymers (Allard and Templier, 2000).

The presence of algaenan polymers in the cell wall is often related with a high rigidity and resistance to mechanical disruption techniques, such as high pressure homogenization (HPH) and bead-milling (Montalescot et al., 2015; Spiden et al., 2013b). However, cell disruption is required in case of extraction of intracellular components of the microalgae. Even though the algaenan cell walls must contain pores for exchanging compounds with the outer environment, algaenans proved to form an effective barrier for extracellular enzymes (de Leeuw et al., 2006). As a consequence, the extractability of intracellular components and CWPS might be hampered by these resistant biopolymers in the outer cell wall layer.

1.3.1.3 Extracellular polysaccharides

EPS from microalgae have received more attention than CWPS, especially for Cyanobacteria and Rhodophyta, and to a lesser extent for Chlorophyta and diatoms. To the best of our knowledge, no EPS have been reported for Haptophyta or Eustigmatophyta. The molecular structure of microalgal EPS has been previously reviewed by several authors, including De Philippis and Vincenzini (1998), De Philippis et al. (2001), Delattre et al. (2016), and Xiao and Zheng (2016). In the present work, we focus on the EPS of microalgae with high relevance for food applications, in relation to their rheological properties. The monosaccharide and uronic acid composition of these EPS are shown in Table 1.5.

Cyanobacterial EPS are typically composed of heteropolymers of six to ten different monosaccharides. They usually possess anionic characteristics because of substantial amounts of uronic acid residues and charged substituents such as sulphate and pyruvate esters (De Philippis et al., 2001). Even though glucose has been reported to be the most abundant monosaccharide in cyanobacterial EPS, this could not be stated for *Arthrospira platensis* and *Cyanospira capsulata*. In fact, a large diversity has been found for these EPS, principally composed of rhamnose (Depraetere et al., 2015), rhamnose and glucose (Roussel et al., 2015), galactose (Filali Mouhim et al., 1993), or similar ratios of five monosaccharides (Cesàro et al., 1990; Trabelsi et al., 2009; Vincenzini et al., 1993). This diversity might possibly result from variation in cultivation conditions, since EPS are typically sensitive to changes in cultivation parameters (Delattre et al., 2016; Xiao and Zheng, 2016).

Large diversity has also been reported for EPS of Chlorophyta, despite the low number of reports available. EPS of *Chlorella* sp. were characterized by large amounts of arabinose and glucuronic acid (Yalcin et al., 1994). In contrast, mannose was the predominant monosaccharide in EPS of *Scenedesmus* sp., together with fucose (Lombardi et al., 2005). While CWPS of *Chlorella* sp. have been distinguished in three major types based on their composition, it is unclear whether such classification might also be valid for EPS of this microalga species. Furthermore, diversity in composition of EPS is plausible given the taxonomic complexity of the Chlorophyta (Baudelet et al., 2017).

Table 1.5 Monosaccharide and uronic acid composition of extracellular polysaccharides of some microalgae species (data are not exhaustive). Predominant monosaccharides and uronic acids are indicated in bold. (Glc: glucose; Gal: galactose; Xyl: xylose; Man: mannose; Rha: rhamnose; Ara: arabinose; Fuc: fucose; Rib: ribose; GalA: galacturonic acid; GlcA: glucuronic acid; ? unknown).

	Microalga species	Monosaccharides and uronic acids	Sulfate esters (%)	References
Cyanobacteria	*Arthrospira platensis* (*Spirulina*)	Glc, Gal, Xyl, Man, Rha, Ara, Fuc, GalA, GlcA	1.7 - 5.0	Depraetere et al. (2015); Filali Mouhim et al. (1993); Roussel et al. (2015); Trabelsi et al. (2009)
	Cyanospira capsulata	Glc, Man, Ara, Fuc, GalA	?	Cesàro et al. (1990); Vincenzini et al. (1993)
Chlorophyta	*Chlorella* sp.	Glc, **Ara**, Fuc, **GlcA**	?	Yalcin et al. (1994)
	Scenedesmus sp.	Glc, Gal, Xyl, **Man**, Rha, Ara, **Fuc**, GalA, GlcA	?	Halaj et al. (2018); Lombardi et al. (2005)
Diatoms	*Phaeodactylum tricornutum*	Glc, Gal, Xyl, Man, Rha, Ara, Fuc, Rib	?	Abdullahi et al. (2006); Willis et al. (2013)
Rhodophyta	*Porphyridium* sp.	**Glc**, **Gal**, **Xyl**, Man, Rha, Ara, Fuc, **GlcA**	1.0 - 15.1	de Jesus Raposo et al. (2014); Geresh et al. (1992, 2002, 2009); Geresh and Arad (1991); Heaney-Kieras and Chapman (1976); Patel et al. (2013); Percival and Foyle (1979); Roussel et al. (2015); Soanen et al. (2015)

Even for diatoms, a class based on a common silicified cell wall structure, little analogies have been found in the composition of EPS (Delattre et al., 2016). For instance, the ovoid form of *Phaeodactylum tricornutum* produced EPS consisting of five different monosaccharides (Willis et al., 2013). Abdullahi et al. (2006) reported mannose and glucose as predominant monosaccharides in *Phaeodactylum tricornutum*, however, it was unclear whether these polysaccharide fractions were isolated from ovoid or fusiform morphotypes. In fact, it is generally presumed that EPS are not synthetized by the fusiform types (Desbois et al., 2010).

The molecular composition and structure of EPS of the red microalga *Porphyridium* sp. are well studied, mainly due to intensive research by the research group of Arad and colleagues (Arad and Levy-Ontman, 2010). *Porphyridium* sp. EPS are composed of xylose, glucose, galactose, and glucuronic acid, although different ratios have been reported by several authors. While xylose was the predominant monosaccharide according to most authors (Geresh et al., 2002; Geresh and Arad, 1991; Heaney-Kieras and Chapman, 1976; Percival and Foyle, 1979; Soanen et al., 2015), some studies reported galactose to be the principal monosaccharide (Patel et al., 2013; Roussel et al., 2015). Nevertheless, EPS of *Porphyridium* sp. have always been described as high molecular weight polymers, showing a weight average molar mass between 2.4×10^5 g/mol and 4×10^6 g/mol (Geresh et al., 2002; Patel et al., 2013). The polysaccharides have anionic characteristics, not only due to the presence of glucuronic acid residues, but also because of sulfate groups esterified to glucose or galactose residues in the 6- or 3-positions (Geresh and Arad, 1991). However, large diversity has been found in the percentage of ester sulfates, ranging from 1 to 15.1% (de Jesus Raposo et al., 2014; Geresh and Arad, 1991; Heaney-Kieras and Chapman, 1976; Patel et al., 2013; Percival and Foyle, 1979). The use of more advanced techniques, such as linkage analyses and NMR spectroscopy, allowed to obtain more insight in the molecular structure of the polysaccharides. Geresh and Arad (1991) established a disaccharide as a basic building block in *Porphyridium* sp. EPS, which was an aldobiouronic acid composed of glucuronic acid and galactose. This aldobiouronic acid was later shown to be part of a larger linear building block, constituting (1 → 2 or 1 → 4)-linked xylopyranosyl, (1 → 3)-linked glucopyranosyl, (1 → 3)-linked glucopyranosyluronic acid, and (1 → 3)-linked galactopyranosyl residues (Geresh et al., 2009). The use of uronic degradation of *Porphyridium* sp. EPS resulted in two other oligosaccharide fragments, also characterized by (1 → 3)-linked glucopyranosyl and galactopyranosyl residues, and (1 → 2)- as well as (1 → 4)-linked xylopyranosyl residues (Gloaguen et al., 2004). Differences in the oligosaccharide structures observed in both studies might be related to differences in microalgae strains or isolation procedures of the polysaccharides (so-called soluble polysaccharide versus bound polysaccharide) (Geresh et al., 2009; Gloaguen et al., 2004). Nevertheless, EPS

of *Porphyridium* sp. are characterized by a unique molecular structure, resulting in interesting rheological properties as discussed in next paragraphs.

1.3.2 Rheological properties of extracted microalgal polysaccharides

To evaluate the potential of microalgal polysaccharides as structuring agents for food products, two types of rheological properties are of interest. On the one hand, thickening agents are used to steer the flow behavior of the products, resulting in a desired viscosity and mouth feel. On the other hand, the use of gelling agents is more related to the texture of a food product, typically analyzed as the linear viscoelastic behavior. While most hydrocolloids display thickening properties, gel formation is restricted to a limited number of hydrocolloids with a specific molecular structure (Saha and Bhattacharya, 2010). To date, only a limited number of microalgal polysaccharides have been investigated for their rheological properties, with main focus on the flow behavior or the viscosity. Apart from some fragmentary studies of cyanobacterial EPS, the majority of the studies focused on the rheological properties of EPS of *Porphyridium*.

Geresh and Arad (1991) were among the first ones to investigate the viscosity of *Porphyridium* sp. polysaccharide solutions. They observed similar viscosities for *Porphyridium* sp. polysaccharide solutions as for xanthan gum. However, the solutions were prepared in relatively low concentrations (0.25% w/w), resulting in rather low viscosity values between 32 and 85 mPa s at a shear rate of ~40 s^{-1} (Geresh and Arad, 1991). Nevertheless, this concentration was shown to be above the critical overlap concentration (C*) of 0.6 g/L, i.e. approximately 0.06%, as determined by Patel et al. (2013). Above C*, the solution is in the semi-dilute regime in which polysaccharide entanglements take place. These entanglements are disrupted at higher shear rates, resulting in shear-thinning flow behavior, as observed by several authors for *Porphyridium* sp. EPS solutions (Eteshola et al., 1998; Geresh et al., 2002; Patel et al., 2013). Slight Newtonian plateaus were observed at very low ($\dot{\gamma} < 0.01$ s^{-1}) and very high ($\dot{\gamma} > 500$ s^{-1}) shear rates (Badel et al., 2011; Patel et al., 2013). In the shear-thinning region, i.e. at intermediate shear rates, viscosity curves frequently displayed a slope of approximately –1 in a $\log(\eta) - \log(\dot{\gamma})$ plot for polysaccharide concentrations between 0.125% and 2% (de Jesus Raposo et al., 2014; Eteshola et al., 1998; Patel et al., 2013). This was confirmed by Liberman et al. (2016), reporting low values for the flow behavior index n (below 0.2). Hence, *Porphyridium* sp. EPS solutions are characterized by a strong shear-thinning behavior, inferring the presence of multiple interactions between polysaccharide chains that break down under shear, typical of a (weak) structured medium. Some authors actually suggested that the shear-thinning behavior resulted from dissociation of hydrogen bonds under

high shear forces, similar to xanthan solutions (Eteshola et al., 1998; Ginzberg et al., 2008).

The weak gel character has been confirmed by small deformation oscillatory measurements. It was shown that *Porphyridium* sp. EPS solutions displayed a large linear viscoelastic region, with critical strains of 50% or higher (Eteshola et al., 1998). In contrast with strong gels (also called true gels), the storage modulus (G') of *Porphyridium* sp. EPS solutions was not constant, but slightly dependent on the angular frequency. While this frequency dependence was obvious at a concentration of 0.5%, it became less pronounced at a concentration of 1% with $G' \propto \omega^{0.1}$ (Eteshola et al., 1998; Ginzberg et al., 2008). The gel behavior of *Porphyridium* sp. EPS is similar to or somewhat stronger than that of xanthan gum (Rochefort and Middleman, 1987).

However, gelation of food hydrocolloids typically occurs in the presence of cations or under specific temperature conditions. Generally, three main mechanisms have been described for gelation of food hydrocolloids: (i) ionotropic gelation, typically cation-mediated gelation, (ii) cold-set gelation, and (iii) heat-set gelation (Saha and Bhattacharya, 2010). The first is common for several anionic hydrocolloids such as carrageenans, alginates, and pectins, which require either monovalent or divalent cations for successful gelation (Imeson, 1997, 2011). Even though *Porphyridium* sp. EPS have been described as anionic polymers due to the presence of glucuronic acid residues and sulfate groups, no successful gelation has been observed in the presence of different cations (Na^+, K^+, Ca^{2+}, or Zn^{2+}) (Eteshola et al., 1998; Liberman et al., 2016). X-ray diffraction studies had previously revealed that *Porphyridium* sp. polysaccharides appear as a single two-fold helical structure (Eteshola et al., 1998). It was shown by Liberman et al. (2016) that a low concentration of Zn^{2+} (250 ppm) was sufficient for screening of electrostatic repulsions of the negatively charged polysaccharide chains, but that higher concentrations did not lead to any network formation (Liberman et al., 2016). In addition, most attempts to induce gelation by using temperature were unsuccessful. Even though Eteshola et al. (1998) reported *Porphyridium* sp. EPS to have unique thermoreversible properties resulting in a strong gel upon heating, this observation could not be confirmed by other authors. In fact, different studies reported no drastic changes in storage modulus or viscosity when applying temperatures up to 80 °C, not during heating nor during cooling (de Jesus Raposo et al., 2014; Patel et al., 2013). Hence, it is likely that no three-dimensional networks are formed by cold-set gelation or heat-set gelation, and that *Porphyridium* sp. EPS only show potential as a thickening agent, not as a gelling agent.

Beside *Porphyridium* sp., other EPS investigated for their rheological properties are mostly originating from cyanobacteria. Several authors observed relatively high viscosities for EPS of *Cyanospira capsulata* in low concentrations (0.05 – 1.1%),

comparable to *Porphyridium* sp. EPS solutions and to xanthan gum (Navarini et al., 1990, 1992; Vincenzini et al., 1990). However, in comparison with EPS of *Porphyridium* sp., C* is expected to be somewhat higher, since a Newtonian-like behavior was still observed for solutions in a concentration of 0.25% w/v (Navarini et al., 1992). Similarly, the intrinsic viscosity of *Cyanospira capsulata* EPS was lower than for *Porphyridium* sp., between 20 and 30 dL/g. This is presumably related to the slightly lower average molecular weight compared to EPS of *Porphyridium* sp. (Cesàro et al., 1990). In spite of the high viscosity values, dynamic oscillatory measurements showed that *Cyanospira capsulata* polysaccharide solutions displayed a liquid-like behavior up to concentrations of 1.1% w/v, indicated by a high frequency dependence between $G' \propto \omega^{0.6}$ and $G' \propto \omega^{0.8}$. It is therefore suggested that next to polysaccharide entanglements, occasional cross-interactions between polysaccharide chains might be present, but a too high chain flexibility prevents it from forming a solid-like gel structure (Navarini et al., 1992). Similar viscosities were obtained for EPS solutions of other cyanobacteria, including *Anabaena* sp., *Nostoc* sp., and *Arthrospira platensis* (Badel et al., 2011; Bhatnagar et al., 2012; Han et al., 2014; Moreno et al., 2000).

Some fragmentary studies are available on the rheological properties of EPS of Chlorophyta. Yalcin et al. (1994) reported shear-thinning behavior for 0.5% solutions of *Chlorella* sp. EPS, but viscosities were low (below 25 mPa s). Somewhat higher values were observed for *Neochloris oleoabundans*, however still limited to 65 mPa s for a 0.5% concentration. Even though the addition of NaCl resulted in a drastic viscosity increase up to 375 mPa s, these EPS cannot compete with those of *Porphyridium* sp. or cyanobacteria, partly due to the lower average molecular weight of the polysaccharides (Wu et al., 2011). Nevertheless, no general conclusions should be drawn from this, since to date the rheological properties of EPS isolated from Chlorophyta are underexplored.

1.4 POTENTIAL OF MICROALGAL BIOMASS AS FOOD STRUCTURING AGENT

Even though microalgal polysaccharides have potential to be used as thickening agents in the food industry, the incorporation of the whole microalgal biomass into food products might be a more attractive strategy to modify the food structure, since the nutritional value of the food product is also improved due to the introduction of multiple nutritional and health-beneficial components. Moreover, the structuring potential of microalgal biomass might be extended because of the presence of other structural biopolymers, including SPS and proteins. Finally, this approach is also

considered more sustainable, since no extraction solvents are required and waste streams are avoided.

1.4.1 Rheological properties of microalgal biomass in aqueous systems

To understand the intrinsic structuring potential of microalgal biomass, the rheological behavior of microalgal biomasses of different species can be compared in simple model systems such as aqueous suspensions. Rheological properties have only been studied for a limited number of microalgae, with most studies focusing on the viscosity, whereas the linear viscoelastic behavior has been very poorly investigated. In fact, most of the experiments reported were established in the context of optimization of cultivation and down-stream processing of microalgae, resulting in a broad range of biomass concentrations. On the one hand, very dilute systems (0.004 – 0.5%) have been analyzed to simulate concentrations in raceway ponds (typically up to 0.5 g/L) or photobioreactors (typically up to 5 g/L). On the other hand, concentrations up to 25% have been studied to determine the rheological properties of algal slurries during downstream processing, which are obtained after dewatering of microalgal cultures (Yap et al., 2016; Zhang et al., 2013). Microalgal suspensions exhibit Newtonian flow behavior at low concentrations, generally associated with low viscosities, whereas non-Newtonian behavior is observed above a critical concentration (Wileman et al., 2012). The value of this critical concentration is depending on the microalga species and might be an indication of the structuring capacities of the microalgal biomass. Furthermore, a wide range of shear rates (0.01 – 1000 s^{-1}) has been applied in analyzing the viscosity of microalgal suspensions. Nevertheless, most analyses were performed between 5 and 200 s^{-1}, which are relevant shear rates for food processing operations such as mixing, stirring, pumping, and swallowing of food products (Rao, 2013).

Different strains of *Chlorella* have been investigated for their rheological properties. Wileman et al. (2012) reported Newtonian flow behavior for *Chlorella vulgaris* up to concentrations of ~4%, while substantial shear-thinning behavior was observed at higher concentrations, indicated by flow behavior indices between 0.62 and 0.78. Shear-thinning behavior was also observed for *Chlorella pyrenoidosa* at higher concentrations up to 20% w/w. However, above shear rates of 215 s^{-1} the viscosity was no longer dependent on the shear rate, reaching the infinite viscosity as predicted by the Cross model (Chen et al., 2018). The critical concentration between 4% and 6%, as concluded from the work of Wileman et al. (2012), coincides with a volume fraction of approximately 0.115. At higher volume fractions, the formation of cell aggregates occurs, which are elongated to the flow at higher shear rates, resulting in shear-thinning behavior (Cagney et al., 2017; Souliès et al., 2013). In addition, an apparent yield stress arises above a volume fraction of ~0.25 (Souliès et al., 2013).

Even though other authors have observed a yield stress behavior for *Chlorella* sp. suspensions, they emphasized that the values were rather low (Wu and Shi, 2008).

Shear-thinning flow behavior has been reported for several other microalgae species. For suspensions of *Arthrospira platensis*, deviation from Newtonian behavior was even observed at biomass concentrations of 0.5%. This was related to the filamentous morphology of *Arthrospira platensis* cells, which have stronger interactions with the medium at rest compared to spherical cells, but align to the flow when shearing forces are applied (Buchmann et al., 2018; Torzillo, 1997). In contrast, the critical concentration observed for suspensions of *Nannochloropsis* sp. was drastically higher. Schneider et al. (2016) proved that suspensions up to 15.8% behaved as a Newtonian fluid, while shear-thinning flow behavior was only reported above 17.7%. Hence, *Nannochloropsis* sp. cells do not tend to interact and require higher amounts to induce aggregation, simply based on increased volume fractions (Schneider et al., 2016). In addition, the shear-thinning region was shown to be very wide for concentrated suspensions of 24 – 25%, ranging from 0.001 s^{-1} to 1000 s^{-1} without observing the zero-shear or infinite viscosity plateaus, and no yield stress was observed (Schneider and Gerber, 2014; Yap et al., 2016). As a consequence, the occurrence of strong interactions between *Nannochloropsis* sp. cells is unlikely, possibly related to their rigid and uncharged outer cell wall, and to the absence of EPS in this microalga species.

Relatively low viscosity values were observed for *Phaeodactylum tricornutum* and *Tetraselmis chuii*. In fact, Newtonian behavior was reported for *Phaeodactylum tricornutum* suspensions up to ~8%, indicated by a flow behavior index of 1 (Wileman et al., 2012). Despite the fact that the fusiform morphotypes of *Phaeodactylum tricornutum* have a higher aspect ratio than most spherical microalgal cells, and that non-spherical particles are orienting themselves to the flow, no shear-thinning behavior has been observed (Cagney et al., 2017). It can be assumed that little intercellular interactions occur in *Phaeodactylum tricornutum*, possibly due to the absence of EPS in the fusiform morphotypes. Cagney et al. (2017) reported similar flow curves for *Phaeodactylum tricornutum* and motile *Tetraselmis chuii* in the same volume fractions.

No reports have been found on the rheological behavior of biomass suspensions of *Porphyridium cruentum*. This is surprising, since the EPS of this microalga are extensively studied for their unique rheological properties. Hence, the question arises whether these EPS still contribute to expose high viscosities in a more complex biomass suspension.

While the flow behavior or viscosity has been studied for several microalgae species, little information is available on their linear viscoelastic behavior. However, the use of small (oscillatory) deformations within the linear viscoelastic region allows to characterize the native structure of the sample, while viscosity measurements somehow disturb this structure by applying larger deformations. Hence, there is an obvious need for research studies characterizing the linear viscoelastic properties of different microalgae species.

1.4.2 Food processing operations as a tool to functionalize microalgal biomass

The use of microalgal biomass in food products requires knowledge on their behavior upon processing. Many food products actually require processing, as a functionalization step to improve the quality of the product and/or as a preservation step to guarantee the safety of the product over extended storage periods. While thermal processing is commonly used as a conventional preservation technique, it often leads to altered rheological properties of the food product. In addition, mechanical processes are often used as functionalization techniques such as HPH, e.g. for physical stabilization of milk products or for creating desired structural properties of vegetable based products. These modified physical characteristics, including the rheological properties, are generally related to microstructural changes.

To the best of our knowledge, no reports have been published on the impact of processing on the rheological properties of microalgal suspensions. However, some information is available on the microstructural changes upon processing in the context of a biorefinery approach, for increasing extraction yields by modifying the cellular integrity. HPH has mainly been studied in the context of microalgal cell disruption, and has been proven one of the most effective disruption treatments for many microalgae. Safi et al. (2014a) concluded HPH to be more efficient than manual grinding, ultrasonication, and chemical treatments for rigid cell walled species (*Nannochloropsis oculata*, *Haematococcus pluvialis*, and *Chlorella vulgaris*) as well as for microalgae with fragile cell walls (*Arthrospira platensis* and *Porphyridium cruentum*). But despite the very harsh HPH conditions that were applied in that study (2 passes at 270 MPa), the recovery yield of released proteins was limited to 41 – 53% for the microalgae with rigid cell walls (Safi et al., 2014a). However, the use of protein release as an indicator for cell disruption generally underestimates the degree of cell rupture at high disruption levels due to degradation of the metabolites (Spiden et al., 2013b). Nevertheless, *Nannochloropsis* sp. have been shown to be among the most resistant microalgae by several authors (Montalescot et al., 2015; Spiden et al., 2013b). As a consequence, the use of moderate HPH conditions that are generally

used in the food industry (typically below 100 MPa) limits the cell disruption for this microalga.

Thermal processing only indirectly enhanced microalgal cell disruption, as proven for *Chlorella* sp. and *Navicula* sp. cells. Thermal treatments actually caused weakening of the cell wall, which facilitated cell disruption by a subsequent HPH process (Spiden et al., 2015). Furthermore, thermal processing also led to solubilization of organic matter in *Scenedesmus* sp. biomass, but was largely dependent on the intensity of the thermal treatment. Whereas an intact cell wall was observed when treating the biomass at 70 °C, cell disruption took place when heated at 90 °C. Consequently, the release of intracellular material resulting in the formation of aggregates only occurred when heated at 90 °C (González-Fernández et al., 2012a). Even though it is hypothesized that such aggregate formation would result in improved rheological properties, this was not observed for thermally pretreated *Nannochloropsis* sp. suspensions. Instead, Schneider and Gerber (2014) even reported a decreased viscosity suspensions at higher concentrations (10 – 22%) due to thermal processing, which was hypothesized a result of a smaller size and altered shape of the thermally treated *Nannochloropsis* sp. cells (Schneider and Gerber, 2014; Schwede et al., 2013). However, it is unclear whether solubilization of organic matter and/or aggregation took place in that study, since no details were included on the microstructural changes induced by the thermal process.

Little knowledge is available on the microstructural changes of microalgal suspensions as affected by other food processing techniques. Microwave treatments have been shown to disrupt cell membranes and/or cell walls of microalgae, due to the heat and pressure build-up inside the cells (Günerken et al., 2015). As a result, cells are ruptured allowing intracellular material to be released, however to a lesser extent than HPH (Cho et al., 2012; Heo et al., 2017). In contrast to the previously mentioned techniques, pulsed electric field (PEF) caused permeation of the cell membrane rather than disruption of the cell wall. Carullo et al. (2018) clearly showed the shrinkage of *Chlorella vulgaris* cells after PEF treatment, indicating the partial release of intracellular compounds through the electroporated cell membranes (Carullo et al., 2018). However, since high molecular weight polymers are assumed to retain inside the cell wall, the formation of aggregates is less expected compared to HPH and possible viscosity increases are therefore supposed to be less pronounced. Finally, extrusion was shown to result in a higher lipid extractability due to cell rupture, although the microstructure was changed to a lesser extent than for HPH-treated samples (Wang et al., 2018).

There is an obvious need for research studies investigating the impact of food processing on the rheological properties of microalgal suspensions in relation to

microstructural changes. In addition, since the microstructure might be important for the digestibility and bioaccessibility of the nutritional compounds (as discussed in section 1.4.4), processing of microalgae should be optimized to combine structural and nutritional benefits of the microalgae as functional food ingredients.

1.4.3 Microalgal biomass in food matrices: impact on structure and texture

Throughout the past decade, many reports have been published on the addition of microalgal biomass to real food products, as presented in Table 1.6. A remarkable number of studies dealt with the use of *Arthrospira* sp. and *Chlorella vulgaris* biomass, although not surprising since these two microalgae are yet commercialized as healthy ingredients for human food. In contrast, not more than five reports have been found for each other microalgae species. Most studies are related to cereal based products, with main interest for enrichment of bread, cookies, and pasta, or to dairy products. Furthermore, different quality aspects have been evaluated, in particular nutritional value, color, texture, and sensory properties. In contrast, the rheological properties of fluid and semi-solid enriched food products are only limitedly studied. The next paragraphs will address the impact of microalgal biomass on the rheological properties of semi-solid food products, i.e. viscosity and/or viscoelastic behavior, based on the available studies summarized in Table 1.7.

García-Segovia et al. (2017) reported an increased viscosity of sourdoughs enriched with different microalgae species in a concentration of 1.5% w/w. However, while the viscosity was almost doubled by the addition of *Isochrysis galbana*, viscosity increases for *Nannochloropsis gaditana*, *Tetraselmis suecica*, and *Scenedesmus almeriensis* were rather limited (García-Segovia et al., 2017). The effect of *Chlorella vulgaris* enrichment on the network structure of bread dough was shown to be dependent on the added concentration. In fact, the storage moduli only increased after addition of *Chlorella vulgaris* in the wheat flour up to 3% (i.e. resulting in a final concentration in the bread dough of approximately 1.8%), due to the reinforcement of the viscoelastic protein network by the microalgae. At higher concentrations, a decreased network structure was observed due to phase separation phenomena and disruption of the gluten matrix, as shown for concentrations of 4% to 5% (i.e. final concentrations of ~2.4% and ~3.0%, respectively). Nevertheless, the rheological properties of the dough were not representative for the texture of the final bread, since the firmness was not substantially affected by any microalga concentration (Graça et al., 2018). The hardness of several other cereal based products such as cookies and pasta generally increased by the addition of various microalgae (Babuskin et al., 2014; Batista et al., 2017; De Marco et al., 2014, 2018; Fradique et al., 2010; Gouveia et al., 2007, 2008b).

Table 1.6 Research studies on the incorporation of microalgal biomass in food products.

Microalga species	Food products		References
Arthrospira sp. (*Spirulina*)	Cereal based products	Bread, cassava cake, cookies, croissants, doughnuts, extruded snacks, noodles, pasta, strudel	Abd El Baky et al. (2015); Agustini et al. (2017); Batista et al. (2017); Bolanho et al. (2014); De Marco et al. (2014); Fradique et al. (2010); Joshi et al. (2014); Khosravi-Darani et al. (2017); Lemes et al. (2012); Lucas et al. (2017, 2018); Massoud et al. (2016); Navacchi et al. (2012); Onacik-Gür et al. (2018); Pagnussatt et al. (2014); Rabelo et al. (2013); Selmo and Salas-Mellado (2014); Shahbazizadeh et al. (2015); Singh et al. (2015); Tańska et al. (2017)
	Dairy products	Fermented dairy product, feta cheese, yogurt	Barkallah et al. (2017); Beheshtipour et al. (2012); Guldas and Irkin (2010); Mazinani et al. (2016); Sengupta and Bhowal (2017); Varga et al. (2002)
	Fruit based products	Smoothies	Castillejo et al. (2018)
	Others	Gelled desserts, kiwifruit pastilles, shakes	Gouveia et al. (2008a); Khazaei Pool et al. (2016); Santos et al. (2016)
Chlorella vulgaris	Cereal based products	Bread, cookies, croissants, pasta	Batista et al. (2017); Fradique et al. (2010); Gouveia et al. (2007); Graça et al. (2018); Shalaby and Yasin (2013)
	Dairy products	Cheese analogues, yogurt	Beheshtipour et al. (2012); Mohamed et al. (2013); Shalaby and Yasin (2013)
	Fruit based products	Smoothies	Castillejo et al. (2018)
	Others	Mayonnaise, o/w-emulsions	Abd El-Razik and Mohamed (2013); Gouveia et al. (2006); Raymundo et al. (2005)
Diacronema vlkianum	Cereal based products	Pasta	Fradique et al. (2013)
	Others	Gelled desserts	Gouveia et al. (2008a)
Dunaliella salina	Cereal based products	Pasta	El-Baz et al. (2017)
Haematococcus pluvialis	Cereal based products	Cookies	Mofasser Hossain et al. (2017)
	Others	o/w-emulsions	Gouveia et al. (2006)
Isochrysis galbana	Cereal based products	Bread, chikki, cookies, pasta	Babuskin et al. (2015); Fradique et al. (2013); García-Segovia et al. (2017); Gouveia et al. (2008b)
	Others	Chewing gum	Palabiyik et al. (2018)

Table 1.6 (continued) Research studies on the incorporation of microalgal biomass in food products.

Microalga species	Food products		References
Nannochloropsis sp.	Cereal based products	Bread, chikki, cookies, pasta	Babuskin et al. (2014, 2015); De Marco et al. (2018); García-Segovia et al. (2017)
	Vegetable based products	Tomato puree	Gheysen et al. (2019b)
	Others	Chewing gum	Palabiyik et al. (2018)
Phaeodactylum tricornutum	Cereal based products	Cookies	Batista et al. (2017)
Porphyridium cruentum	Others	Chewing gum	Toker (2019)
Scenedesmus almeriensis	Cereal based products	Bread	García-Segovia et al. (2017)
Tetraselmis suecica	Cereal based products	Bread, cookies	Batista et al. (2017); García-Segovia et al. (2017)

Table 1.7 Research studies evaluating the rheological properties of food products as affected by the addition of microalgal biomass.

Microalga species	Food product	Biomass concentration (%)	Food processing	Rheology	References
Arthrospira platensis (Spirulina)	Ice cream mix	0.075 - 0.3	/	Viscosity (↘)	Malik et al. (2013)
	Yogurt	0.1 - 1.5	Incubation (24 h, 37 °C)	Viscosity (=)	Sengupta and Bhowal (2017)
Chlorella vulgaris	Bread dough	~0.6, ~1.2, ~1.8	Fermentation (1 h, 37 °C)	Viscoelastic (↗)	Graça et al. (2018)
					Graça et al. (2018)
	Bread dough	~2.4, ~3.0	Fermentation (1 h, 37 °C)	Viscoelastic (↘)	Abd El-Razik and Mohamed (2013)
	Mayonnaise	~0.5, ~1.5, ~2.5	/	Viscosity (=)	Raymundo et al. (2005)
	o/w-emulsion	2	/	Viscosity (↗)	García-Segovia et al. (2017)
				Viscoelastic (↗)	
Isochrysis galbana	Bread sourdough	1.5	Fermentation (2x 24 h, 8 °C)	Viscosity (↗)	García-Segovia et al. (2017)
Nannochloropsis gaditana	Bread sourdough	1.5	Fermentation (2x 24 h, 8 °C)	Viscosity (↗)	García-Segovia et al. (2017)
Scenedesmus almeriensis	Bread sourdough	1.5	Fermentation (2x 24 h, 8 °C)	Viscosity (↗)	García-Segovia et al. (2017)
Tetraselmis suecica	Bread sourdough	1.5	Fermentation (2x 24 h, 8 °C)	Viscosity (↗)	Malik et al. (2013)

The structuring potential of *Chlorella vulgaris* has also been proved in o/w-emulsions, representing mayonnaises and salad dressings. The presence of high amounts of proteins and carbohydrates in *Chlorella vulgaris* was evidenced to strengthen the emulsion structure through the formation of physical entanglements, resulting in an increased storage modulus and zero shear viscosity (Raymundo et al., 2005). In contrast, the addition of *Arthrospira platensis* did not result in increased viscosities of yogurt (Sengupta and Bhowal, 2017). A slight decrease in viscosity was even observed in an ice cream mix, but biomass of *Arthrospira platensis* was used to replace the commercial stabilizer sodium alginate. The authors therefore concluded that *Arthrospira platensis* can only be used to partially replace sodium alginate in ice cream, due to a lower water holding capacity of the cyanobacterial biomass (Malik et al., 2013). The type of food product might also be a determining factor in the structuring capacity of microalgae. Even though *Arthrospira platensis* did not improve the rheological properties of dairy products, addition of the cyanobacterium to a gelatin-maltodextrin gel resulted in a strong reinforcement of the gels, even more pronounced than addition of *Chlorella* sp. (Firoozmand and Rousseau, 2014). In contrast, the efficiency of structuring gels with *Arthrospira maxima* was dependent on the type of biopolymer gel, while *Haematococcus pluvialis* resulted in stronger gel systems for all tested biopolymers (Batista et al., 2011, 2012).

It should be noted that food processing in the above-mentioned studies was restricted to incubation or fermentation at relatively low temperatures (Table 1.7). Hence, the use of targeted food processing operations to functionalize the microalgal biomass should still be explored in real food matrices.

1.4.4 Implications of the use of whole biomass for nutrient bioaccessibility

The use of whole microalgal biomass in food products might have some implications for the nutritional efficacy of microalgal compounds in the human body. In this context, three important concepts should be introduced: bioaccessibility, bioavailability, and bioactivity. Bioaccessibility represents the fraction of the compound that has been released from the food matrix and has become available for absorption, and is usually evaluated by *in vitro* experiments. Bioavailability refers to the compounds that have been absorbed and have reached the systemic circulation, implying that they are available for the human body, and can be both determined by *in vitro* and *in vivo* tests. Only when a physiological response of the compound has been proved, it can be considered a bioactive compound (Carbonell-Capella et al., 2014). The extent to which a bioactive compound is released upon digestion in the gastrointestinal tract depends on several factors, including the physical entrapment in the food matrix, the physiological conditions, and the digestive enzymes in the gastrointestinal tract. The latter consist of starch-degrading enzymes (α-amylase),

proteases (pepsin, trypsin, chymotrypsin), and lipases (gastric and pancreatic lipase) (Minekus et al., 2014). However, apart from hydrolysis of α-1,4-linked glucans like starch, humans lack the ability to digest polysaccharides. Since most microalgal cell walls are composed of heteropolysaccharides or β-linked glucans (e.g. cellulose), it is assumed that microalgal cell walls will not be digested in the stomach and small intestine. In that case, the resistant cell wall presumably acts as a physical barrier for the release of nutritional and health-beneficial components that are stored inside the cells. In this context, the use of processing techniques and cell disruption steps in particular might be desired to enhance the bioaccessibility of the health-beneficial components. However, very limited research has been performed on this topic so far.

The bioaccessibility of (intracellular) components of untreated microalgae after *in vitro* digestion seems to be species-dependent (Table 1.8). Generally, low bioaccessibility values (0 – 7%) have been reported for carotenoids in *Chlorella* sp. and *Scenedesmus almeriensis*, with the exception of 26% lutein bioaccessibility in *Chlorella vulgaris* (Cha et al., 2011, 2012; Gille et al., 2016; Granado-Lorencio et al., 2009). In contrast, higher values were observed for carotenoids in *Chlamydomonas reinhardtii* (10 – 20%) and *Phaeodactylum tricornutum* (27 – 52%) (Gille et al., 2016, 2019; Kim et al., 2016). A possible explanation might be the distinct composition of the cell walls of these microalgae species. While *Scenedesmus almeriensis* and (some strains of) *Chlorella* sp. contain cellulose polymers in their cell wall, these are absent in *Chlamydomonas reinhardtii* and *Phaeodactylum tricornutum*. The cell wall of *Chlamydomonas reinhardtii* is actually composed of glycoproteins, which might be sensitive to enzymatic degradation by the proteases in the gastrointestinal tract (Gille et al., 2016). However, more research is required to conclude a direct relation between the cell wall composition and carotenoid bioaccessibility. As a matter of fact, while the fragile cell wall of *Isochrysis galbana* (even considered absent by some authors) would suggest a high bioaccessibility of intracellular compounds, low values for fatty acid bioaccessibility (8 – 13%) have been reported in this microalga. However, the authors also reported a very low degree of lipid hydrolysis after *in vitro* digestion, but it was unclear whether these low values could be attributed to the role of the cell wall as a physical barrier (Bonfanti et al., 2018).

Table 1.8 *In vitro* bioaccessibility of different bioactive compounds (carotenoids, chlorophylls, and fatty acids) in microalgae, with and without different processing techniques (= unchanged by processing; ↗ increased after processing). Bioaccessibility of lipophilic components is defined as the ratio between the amount that is incorporated in mixed micelles and the initial amount present before the digestion procedure.

Microalga species	Bioactive compound	Processing technique	Bioaccessibility without processing (%)	Bioaccessibility after processing (%)	References
Chlamydomonas reinhardtii	β-carotene	Sonication	10	= ~10	Gille et al. (2016)
	Lutein	Sonication	20	= ~20	Gille et al. (2016)
Chlorella sp.	Antheraxanthin	Microfluidization	0	= 0	Cha et al. (2012)
	β-carotene	Ball milling	/	traces	Gille et al. (2018)
		Sonication	0	↗ 13	Gille et al. (2016)
		Microfluidization	2.6	↗ 7 - 32	Cha et al. (2012)
	Chlorophylls	Pulsed electric field	77 - 84	= 73 - 80	Rego et al. (2015)
	Lutein	Ball milling	/	5 - 26	Gille et al. (2018)
		Sonication	7	↗ 18	Gille et al. (2016)
		Microfluidization	26	↗ 57 - 73	Cha et al. (2011)
	Zeaxanthin	Microfluidization	1.7	↗ 3 - 18	Cha et al. (2012)
Isochrysis galbana	Fatty acids	/	8 - 13	/	Bonfanti et al. (2018)
Phaeodactylum tricornutum	β-carotene	Ball milling	/	19	Gille et al. (2018)
		Sonication	27	↗ 76	Gille et al. (2019)
	Fucoxanthin	/	40 - 44	/	Kim et al. (2016)
		Ball milling	/	20	Gille et al. (2018)
		Sonication	52	↗ 62	Gille et al. (2019)
	Zeaxanthin	Ball milling	/	17	Gille et al. (2018)
		Sonication	29	= ~30	Gille et al. (2019)
Scenedesmus almeriensis	Lutein	Bead milling	<1	= <1	Granado-Lorencio et al. (2009)
	Zeaxanthin	Bead milling	<1	= <1	Granado-Lorencio et al. (2009)

Some fragmentary studies have been reported on the impact of processing on the carotenoid bioaccessibility of microalgal biomass, including different cell disruption techniques such as sonication, bead and ball milling, microfluidization, and PEF treatment (Table 1.8). Sonication for 15 min at 20 kHz to increase the bioaccessibility of carotenoids was species-dependent. While an increased bioaccessibility of lutein and β-carotene was observed for *Chlorella vulgaris*, no increase was observed for *Chlamydomonas reinhardtii* after sonication. The latter already showed substantial bioaccessibility values before the sonication treatment, indicating that the cell wall of this microalga had little impact on the carotenoid bioaccessibility (Gille et al., 2016). Similarly, the effect of sonication on the carotenoid bioaccessibility in *Phaeodactylum tricornutum* was rather limited, with only slight increases for fucoxanthin and zeaxanthin. The average β-carotene bioaccessibility was drastically increased to 76%, but a large standard error was observed from different repetitions of the experiments (Gille et al., 2019). Microfluidization was also considered a successful technique for improvement of the carotenoid bioaccessibility in *Chlorella* sp., but depending on the applied pressure level (Cha et al., 2011, 2012). In contrast, no improved carotenoid bioaccessibility was observed by ball milling of *Scenedesmus almeriensis*. In fact, below 1% of the initial lutein and zeaxanthin was recovered in the micellar phase. However, details on the pretreatment conditions were lacking, as well as on the cell wall integrity after ball milling (Granado-Lorencio et al., 2009). Higher values for carotenoid bioaccessibility were observed by Gille et al. (2018) for other ball milled microalgae, between 5% and 26% for *Chlorella vulgaris* and between 17% and 20% for *Phaeodactylum tricornutum*. However, as no values were available for the untreated biomasses, no conclusions can be drawn on the effect of ball milling (Gille et al., 2018). The effectiveness of bead milling has however been proven by Cavonius et al. (2016) for the rigid microalga *Nannochloropsis oculata*, as the protein digestibility increased from 3% to 32% and the free fatty acid release from 0% to 34% (Cavonius et al., 2016). Finally, the use of PEF for increasing nutrient bioaccessibility has not been successfully proven yet. Rego et al. (2015) observed no increased chlorophyll bioaccessibility for *Chlorella* sp., but high values were yet observed for untreated biomass, indicating that the cell wall does not seem to be a barrier for chlorophylls. Moreover, since PEF generally has little impact on the cell wall integrity, but mainly causes permeation of the cell membrane, no direct expectations can be established about the effect on the bioaccessibility.

It should be noted that various *in vitro* digestion models have been used in these studies. As a consequence, comparison of results obtained in distinct research studies is limited because of different simulated conditions, including sample volume, pH, ionic strength, enzyme activities, bile concentrations, and digestion times. For instance, incorporation of lipophilic compounds into mixed micelles is related to the

amount of bile salts present. Under- or overestimation of the bile salts in the simulated digestion model might mistakenly lead to conclusions on the bioaccessibility of lipophilic nutrients, such as carotenoids and ω3-LC-PUFA. The use of a standardized *in vitro* digestion protocol, like the static digestion model proposed by Minekus et al. (2014), would aid the production of more comparable data in the future. In addition, in order to verify the hypothesis of the microalgal cell wall as a barrier for nutrient bioaccessibility, design of experiments should include microstructural analyses to obtain clear evidence on the cell wall integrity of the microalgal cells.

1.5 CONCLUSIONS

The application of microalgae as potential structuring food ingredients is obviously still in its infancy. This is partly attributed to the evolutionary diversity of microalgae, involving an enormous complexity in terms of presence, composition, molecular organization, and potential functionality of structural biopolymers (cell wall related polysaccharides in particular). Although several attempts have been made to characterize the molecular structure or composition of cell wall related polysaccharides, these microalgal polymers are poorly understood. However, since the functionality of cell wall polysaccharides is generally related to the precise molecular structure of the polymers, there is an urgent need for more insights into cell wall related polysaccharides of microalgae. In fact, to successfully introduce microalgal polysaccharides as novel food hydrocolloids, characterization and targeted functionalization should be performed for polysaccharides from individual strains.

A more economic and sustainable strategy is the incorporation of the whole microalgal biomass into food products, to overcome extraction protocols and waste streams. As such, the simultaneous introduction of nutritional and health-beneficial compounds allows the creation of high-quality food products, often accompanied by quality labels and/or nutrition claims. However, the structuring capacity of intact microalgal biomass seems to be rather low, although rheological properties have only been studied for a limited number of microalgae. Therefore, food processing operations need to be considered and investigated in detail to maximally exploit the structuring capacity of microalgal biomass. The use of processing might not only be favorable for steering the rheological properties, there are indications that the use of cell disruption techniques also results in an improved bioaccessibility of intracellular components. However, there is a need for more harmonized studies investigating the effect of processing on the bioaccessibility of microalgal compounds in relation to the microstructure, for instance by using standardized *in vitro* digestion models.

EXPERIMENTAL WORK

PART I: CHARACTERIZATION OF MICROALGAL BIOMASSES

Chapter 2: Biomass composition of different microalgae

PART II: CELL WALL RELATED POLYSACCHARIDES AS FOOD HYDROCOLLOIDS

Chapter 3: Cell wall related polysaccharide composition of different microalgae

Chapter 4: Molecular and rheological characterization of cell wall fractions of *Porphyridium cruentum*

PART III: MICROALGAL BIOMASS AS STRUCTURING AGENT

Chapter 5: Rheological characterization of microalgal suspensions upon processing

Chapter 6: Impact of different processing sequences on the rheological properties of *Porphyridium cruentum* and *Chlorella vulgaris*

PART IV: IMPLICATIONS FOR NUTRIENT BIOACCESSIBILITY

Chapter 7: Effect of (ultra) high pressure homogenization on cell disruption of *Nannochloropsis* sp.

Chapter 8: The role of cell integrity in the lipid digestibility and *in vitro* bioaccessibility of carotenoids and ω3-LC-PUFA in *Nannochloropsis* sp.

PART I

CHARACTERIZATION OF MICROALGAL BIOMASSES

CHAPTER 2

Biomass composition of different microalgae

2.1 INTRODUCTION

Since the composition of microalgal biomasses is largely depending on the species, the strain, and the cultivation conditions (Hu, 2004), knowledge on the biochemical composition of a specific batch of microalgae is required in the selection of suitable microalgal biomass towards specific food applications. Even though biomass profiles of the selected microalgae species have been studied by other authors, one of the main drawbacks is the fact that quantification of microalgal polysaccharides has usually been done by analyzing the total carbohydrate content, thus including both SPS and cell wall related polysaccharides (CWPS and EPS). However, these types of polysaccharides not only exhibit different functions in the microalgal cell (Raven and Beardall, 2003), they might also display different functionalities in food products. Hence, there is an urgent demand for studies comparing microalgal biomass profiles distinguishing cell wall related polysaccharides from SPS.

The microalgae species used in this research thesis were selected for their potential as functional food ingredients: *Arthrospira platensis*, *Chlorella vulgaris*, *Diacronema lutheri*, *Tisochrysis lutea* (formerly listed as *Isochrysis galbana*), *Nannochloropsis* sp., *Odontella aurita*, *Phaeodactylum tricornutum*, *Porphyridium cruentum*, *Schizochytrium* sp., and *Tetraselmis chuii*. Most of them show interesting nutritional profiles, e.g. containing omega-3 long chain polyunsaturated fatty acids (ω3-LC-PUFA), proteins rich in essential amino acids, and antioxidants (Buono et al., 2014; Chacón-Lee and González-Mariño, 2010; Matos et al., 2017). In addition, some of these biomasses have been accepted or authorized under the European novel food

This chapter is based on the following paper:
Bernaerts T.M.M., Gheysen L., Kyomugasho C., Jamsazzadeh Kermani Z., Vandionant S., Foubert I., Hendrickx M.E., Van Loey A.M. (2018)
Comparison of microalgal biomasses as functional food ingredients: Focus on the composition of cell wall related polysaccharides.
Algal Research, 32, 150-161.
[2017 Impact Factor = 3.745; Ranked 38/161 (Q1) in Biotechnology and Applied Microbiology]

regulation, or applications are ongoing (European Commission, 2016, 2017, 2019a, 2019b). Finally, by selecting these microalgae a diverse taxonomic spectrum was obtained, composed of photoautotrophic eukaryotic species classified as Chlorophyta (*Chlorella vulgaris* and *Tetraselmis chuii*), Rhodophyta (*Porphyridium cruentum*), Haptophyta (*Diacronema lutheri* and *Tisochrysis lutea*), Eustigmatophyta (*Nannochloropsis* sp.), Bacillariophyta or diatoms (*Odontella aurita* and *Phaeodactylum tricornutum*), one heterotrophic species belonging to Labyrinthulomyceta (*Schizochytrium* sp.), and one prokaryotic cyanobacterium (*Arthrospira platensis*) (Borowitzka et al., 2016).

The objective of this chapter is to characterize the biomass composition of ten microalgae species that are of interest for use as functional food ingredients, with particular interest for specific quantification of SPS and cell wall related polysaccharides. The analyses were performed on commercially available dry biomasses with regard to the application of dried microalgal biomass as a functional ingredient in food products, as food ingredients are generally delivered in a dry form to guarantee long term storage stability.

2.2 MATERIALS AND METHODS

2.2.1 Microalgal biomass

Commercially available microalgal biomasses were obtained from different companies. Lyophilized biomasses of *Nannochloropsis* sp. and *Tisochrysis lutea* were obtained from Proviron Industries nv (Hemiksem, Belgium). *Odontella aurita* was purchased from Innovalg (Bouin, France), *Tetraselmis chuii* from Fitoplancton Marino (Cádiz, Spain), and the cyanobacterium *Arthrospira platensis* from Earthrise (Irvine, CA, USA). Lyophilized biomass of *Schizochytrium* sp. was kindly donated by Mara Renewables Corporation (Dartmouth, Canada). Spray-dried biomass of *Chlorella vulgaris* was obtained from Allmicroalgae Natural Products (Lisbon, Portugal). Biomasses of *Phaeodactylum tricornutum* and *Porphyridium cruentum* were obtained as a wet paste from Necton Phytobloom (Olhão, Portugal) and immediately lyophilized after arrival. All biomasses were stored in closed containers at -80 °C until use.

Biomass of *Diacronema lutheri* (CCAP 931/1) was produced at Laboratory of Enzyme, Fermentation and Brewing Technology (KU Leuven Odisee Technologiecampus Gent, Gent, Belgium). This species was cultured in Wright's Cryptophyte medium in 125 L pilot-scale tubular airlift photobioreactors. Prior to use, the medium was sterilized by membrane filtration (0.2 µm pore size). The photobioreactors were continuously illuminated (125 µmol photons/m^2 s) and the culture was maintained at pH 7.5 by

automated CO_2 injection. The biomass was harvested at the end of the exponential growth phase by centrifugation, lyophilized, and stored at -80 °C.

It should be noted that different batches of microalgal biomasses (supplied by the same companies) have been used in following chapters of this doctoral thesis (Chapters 4, 6, 7, and 8). The biomass composition of those batches has been analyzed using the same methods, and will be discussed in the corresponding chapters. Nevertheless, only minor changes in biomass composition have been observed within different batches.

2.2.2 Moisture

Moisture content of the biomass was determined in triplicate by vacuum drying as described by Nguyen et al. (2016). Briefly, 20 mg of microalgal biomass was dried using a vacuum oven (UNIEQUIP 1445-2, Planegg, Germany), with sequential drying steps for 1 h at 0.8, 0.6, and 0.4 bar, and for 30 min at 0.2 bar. The difference in weight before and after drying was expressed as a percentage, representing the moisture content. The average moisture content was used in the calculation of the chemical components, being expressed in percentage of total dry matter.

2.2.3 Lipids

Lipid content was determined by a chloroform:methanol (CM) extraction, according to the method optimized by Ryckebosch et al. (2012). Briefly, 4 mL methanol, 2 mL chloroform, and 0.4 mL demineralized water were added to 100 mg of dry biomass and the samples were vortexed for 30 s. Subsequently, 2 mL chloroform and 2 mL demineralized water were added and the samples were again vortexed for 30 s. After centrifugation (10 min, 750g, 25 °C), the upper aqueous layer was discarded, while the lower solvent layer was collected. The remaining pellet was re-extracted with 4 mL of chloroform:methanol (1:1 v/v), vortexed for 30 s, and centrifuged (10 min, 750g, 25 °C). The solvent phase was collected and the extraction procedure was repeated on the pellet. All solvent phases were combined and filtered through a layer of sodium sulphate to remove remaining water. The solvent was finally removed by rotary evaporation and lipids were quantified gravimetrically. Lipid content was determined in triplicate.

2.2.4 Proteins

Protein content was determined by the Dumas method. Approximately 1.5 mg of biomass was transferred to tin capsules and total nitrogen content was analyzed using an elemental analyzer (Carlo-Erba EA1108, Thermo Scientific, Waltham, MA, USA). Protein content was estimated from the total nitrogen content, multiplied by an

overall conversion factor of 4.78, as proposed by Lourenço et al. (2004). The analysis was performed in triplicate.

2.2.5 Storage polysaccharides

2.2.5.1 Starch, floridean starch, and glycogen

According to literature, starch is present in *Chlorella vulgaris*, *Tetraselmis chuii*, and *Schizochytrium* sp. (Brányiková et al., 2011; Qu et al., 2013; Yao et al., 2012), whereas *Porphyridium cruentum* contains floridean starch as SPS (Brody and Vatter, 1959). Lastly, the cyanobacterium *Arthrospira platensis* contains glycogen (De Philippis et al., 1992). Since all these SPS are polyglucans with α-1,4 and α-1,6-linkages, they were quantified using the same procedure, based on the method of Pleissner and Eriksen (2012). Briefly, 50 – 100 mg biomass was washed in MOPS buffer (3-(N-morpholino)propanesulfonic acid, 55 mM, pH 7) and cells were subsequently disrupted using ultra high pressure homogenization (UHPH) at 250 MPa (Stansted Fluid Power SPCH-10, Harlow, United Kingdom). A single pass was applied for most microalgae, except for the more rigid *Chlorella vulgaris* requiring two passes for full cell disruption. After addition of ethanol and dimethyl sulfoxide, the mixtures were boiled for 15 min at 100 °C to gelatinize (floridean) starch. Samples were then incubated with thermostable α-amylase from *Bacillus licheniformis* (519 U/mg, Sigma-Aldrich) for 10 min at 90 °C, followed by incubation with amyloglucosidase from *Aspergillus niger* (70 U/mg, Sigma-Aldrich) for 1 h at 50 °C. Both enzymes were added to achieve a ratio of 10 U/mg biomass. The mixtures were subsequently centrifuged (15 min, 5000g, 25 °C) and the glucose content in the supernatant was measured using the glucose oxidase method (McCleary et al., 1994). SPS content was finally calculated by multiplying the glucose content by 0.9, taking into account the addition of a water molecule during enzymatic hydrolysis of the polyglucans. The analysis was done in triplicate.

2.2.5.2 Chrysolaminarin

Chrysolaminarin content was determined for *Nannochloropsis* sp., *Tisochrysis lutea*, *Phaeodactylum tricornutum*, *Odontella aurita*, and *Diacronema lutheri*, using a modified version of the method described by Granum and Myklestad (2002). Dry biomass was suspended in demineralized water, after which the cells were disrupted using UHPH at 250 MPa. Whereas two passes were used for *Nannochloropsis* sp., a single pass at 250 MPa was sufficient for the other microalgae species. The disrupted microalgae were lyophilized and β-1,3-glucans were subsequently extracted with 0.05 M sulfuric acid at 60 °C for 10 min. The extract was filtered using GF/C glass fiber filters and the glucose content was determined by the phenol-sulfuric acid method

(Dubois et al., 1956). Glucose content was multiplied by 0.9 to quantify the chrysolaminarin content. Extraction and quantification of chrysolaminarin was performed in triplicate.

2.2.6 Cell wall related polysaccharides

The extraction and characterization of CWPS and EPMS is extensively described in Chapter 3 (sections 3.2.2 and 3.2.3). In short, EPMS were extracted by incubation in simulated cultivation medium, recovered by alcohol precipitation, dialyzed, and lyophilized. CWPS were obtained by performing cell disruption and subsequent removal of lipids, SPS, and proteins, after which CWPS were recovered by alcohol precipitation and dried at 40 °C. Both cell wall fractions were hydrolyzed with methanolic HCl and TFA to monosaccharides and uronic acids, which were quantified by high performance anion exchange chromatography combined with pulsed amperometric detection (HPAEC-PAD).

The total content of CWPS and EPMS was then calculated from the monosaccharide and uronic acid content using Eq. 2.2, taking into account the addition of a water molecule to the dehydrosugar in a polysaccharide chain (Eq. 2.1):

$$(dehydrosugar)_n + n \cdot H_2O \rightarrow n \cdot monosaccharide \qquad \text{(Eq. 2.1)}$$

$$PS\ (\%) = \sum \left(\frac{MM_{dehydroMS}}{MM_{MS}} \times MS\ (\%) \right) + \sum \left(\frac{MM_{dehydroUA}}{MM_{UA}} \times UA\ (\%) \right) \qquad \text{(Eq. 2.2)}$$

in which following abbreviations were used: PS polysaccharide; MM molar mass; MS monosaccharide; UA uronic acid.

2.2.7 Ash and minerals

Approximately 20 mg of biomass was ashed in a muffle furnace (Nabertherm Controller P330, Lilienthal, Germany), operating for 24 h at 550 °C. The ashes were weighed and dissolved in 10 mL of ultrapure water (organic free, 18 MΩ cm resistance). These solutions were then acidified with 0.1 mL of 65% HNO_3 and filtered through a 0.45 µm syringe filter (Chromafil® A-45/25, Macherey-Nagel, Duren, Germany). Mineral composition was determined using inductively coupled plasma optical emission spectrometry (ICP-OES, Perkin-Elmer Optima 3300 DV, Norwalk, CT, USA). Ash content and mineral composition were determined in triplicate.

2.2.8 Statistical analysis

The data obtained are presented as the average of three measurements ± standard error. Differences in biomass composition of different microalgae species were

statistically analyzed using one-way ANOVA combined with Tukey's test for multiple comparison ($P < 0.05$) with JMP statistical software (JMP Pro 12, Cary, NC, USA).

2.3 RESULTS AND DISCUSSION

The microalgal biomasses were characterized in terms of macronutrient content and mineral composition. It is worth noting that commercial biomasses have been used, eliminating control on the cultivation conditions and/or possible contamination with other microorganisms. The occurrence of contamination in the used biomasses was evaluated using DIC microscopy, by judging the visual appearance of the cells. No contamination was observed for the used microalgae species, except for *Odontella aurita*. Apart from cells of *Odontella aurita*, characterized by rectangular-shaped cells with a length of ~50 µm and a width of ~20 µm, smaller microorganisms were also observed (as shown in **Fig. 2.1**). The contamination is likely due to the cultivation of *Odontella aurita* in open raceway ponds, as it is known that these cultivation systems are more prone to contamination with other microorganisms than closed photobioreactors (Deruyck et al., 2019; McBride et al., 2016). Hence, the observed biomass composition might therefore be affected by this contamination, and might not truly represent the composition of *Odontella aurita* biomass.

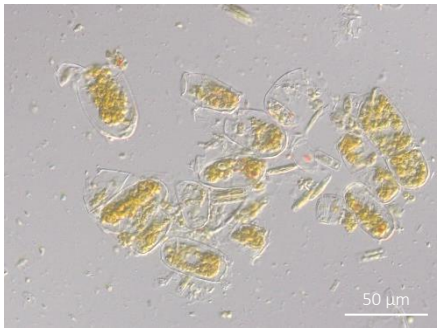

Fig. 2.1 Microscopic image of *Odontella aurita* biomass, indicating contamination with other microorganisms.

Results obtained from the biochemical characterization of the microalgal biomasses are presented in **Table 2.1**. These results are expressed as a percentage of dry matter, as they were corrected for the moisture contents (1.5 – 8.2%). Generally, substantial differences were found in the biomass composition amongst different species, with each microalga showing a distinct biomass nutrient profile. It is worth noting that only 64% to 82% of the microalgal biomasses is characterized in this study (except for *Schizochytrium* sp. biomass), determined as the sum of the different compounds presented in **Table 2.1**. First, it should be noted that some microalgal components are not included in this biomass composition. For instance, several non-polysaccharidic

cell wall compounds, such as algaenan and silica frustules, were not quantified. Nevertheless, these cell wall compounds are characteristic for specific microalgae species, and are not expected to represent more than 10% of the biomass (Gügi et al., 2015; Scholz et al., 2014). Hence, part of the incomplete characterization is possibly attributed to experimental protocols. On the one hand, the protein contents represented in Table 2.1 might be an underestimation, due to the use of an average nitrogen-to-protein conversion factor of 4.78 based on evaluation of 12 marine microalgae species (Lourenço et al., 2004). However, determination of individual conversion factors for the selected microalgae species in the current work, by evaluating the amino acid profile and non-protein nitrogen sources, would result in a more accurate quantification of the protein content. Moreover, it is known that conversion factors are depending on the growth phase of the microalgae, on average ranging from 4.33 in the mid-exponential phase to 5.06 in the late stationary phase (Lourenço et al., 2004). Since no information was available on the time of harvesting of the commercial biomasses, this might also have contributed to inaccurate quantification of the protein content. On the other hand, underestimation of the carbohydrates could have occurred, both for CWPS and SPS. In fact, during these experimental protocols, UHPH has been applied to obtain full cell disruption. However, the use of ultra high pressures might possibly have resulted in the formation of dense networks (as later observed in Chapter 7 for *Nannochloropsis* sp.), which might limit the extractability of the polysaccharides and/or the accessibility for SPS-degrading enzymes. Moreover, accurate quantification of the total cell wall related polysaccharides is a challenging task, as no acid hydrolysis conditions are available to obtain full hydrolysis of all glycosidic linkages (typically by strong acids under harsh conditions) while avoiding degradation of liberated monosaccharides of matrix polysaccharides (typically by weak acids under mild conditions).

2.3.1 Lipids

A large diversity is observed in terms of lipid content among all microalgae. *Arthrospira platensis* and *Chlorella vulgaris* presented low lipid contents, making up 5.5% and 6.6% of the biomass, respectively. Similar lipid contents were found in literature for biomasses of *Arthrospira* sp. (3.6 – 7.5%) (Batista et al., 2013; Gouveia and Oliveira, 2009; Ogbonda et al., 2007; Tokusoglu and Unal, 2003), while a wider range of fat contents was observed for *Chlorella vulgaris*. Although some authors reported similar values of 5% lipids for *Chlorella vulgaris* (Batista et al., 2013; Gouveia and Oliveira, 2009), higher lipid contents (13 – 20%) have also been found (Tokusoglu and Unal, 2003). This could be related to differences in cultivation conditions, as it is known for Chlorophyceae (and oleaginous microalgae in general) that biomass composition can be selectively modified by adapting the cultivation conditions, such

as nitrogen depletion and temperature (Ördög et al., 2016). In contrast, lipid content and composition of cyanobacteria are less affected by changes in cultivation conditions (Becker, 2004), confirming the smaller range of lipid contents found in literature for *Arthrospira* biomasses. In contrast to the former two species, *Nannochloropsis* sp., *Diacronema lutheri*, *Tisochrysis lutea*, and *Phaeodactylum tricornutum* can be considered as lipid-rich microalgae, presenting lipid contents of 17 – 32%. In fact, these microalgae species are considered among the most interesting sources of ω3-LC-PUFA, and similar values for total lipid content have been reported in literature (Ryckebosch et al., 2014a). In addition, a very high lipid content was observed for *Schizochytrium* sp., making up 74% of the dry biomass. It was microscopically confirmed that *Schizochytrium* sp. cells were completely filled with lipid bodies, as previously reported by Morita et al. (2006). Generally, lipid contents of *Schizochytrium* sp. are somewhat lower (32 – 50%) (Chen et al., 2016; Wang and Wang, 2012), although a similar content of 73% has been reported by Liang et al. (2010). Finally, intermediate lipid contents (11 – 13%) were observed for *Porphyridium cruentum*, *Tetraselmis chuii*, and *Odontella aurita*, corresponding to literature reports (Guihéneuf et al., 2010; Ryckebosch et al., 2014a).

2.3.2 Proteins

Proteins generally make up an important part of the biomass, being more than 20% for the investigated microalgae (except for *Schizochytrium* sp.). The highest protein contents were observed for *Arthrospira platensis* and *Chlorella vulgaris*, comprising 47% and 39% of the dry biomass, respectively. These two species have been commercialized as a source of proteins, containing high amounts of essential amino acids (Buono et al., 2014). Although some authors presented similar protein contents, approximately 38% for *Chlorella vulgaris* and 39 – 46% for *Arthrospira platensis* (Batista et al., 2013; Ogbonda et al., 2007), higher values (up to 70% for *Arthrospira* sp.) have also been reported (Becker, 2007; González López et al., 2010; Safi et al., 2014a; Tokusoglu and Unal, 2003). However, it should be noted that part of this variation can be ascribed to different analytical approaches, such as the use of different correction factors for non-protein nitrogen in elemental analyses (González López et al., 2010; Lourenço et al., 2004). Large amounts of proteins were also found for lipid-rich microalgae species (*Diacronema lutheri*, *Tisochrysis lutea*, *Nannochloropsis* sp., and *Phaeodactylum tricornutum*), representing 22 – 35% of the biomass. Generally, the protein values obtained are in agreement with those reported in literature (Batista et al., 2013; Fernández-Reiriz et al., 1989; González López et al., 2010; Qu et al., 2013; Rebolloso-Fuentes et al., 2001a, 2001b; Xia et al., 2014)

Table 2.1 Biochemical composition of microalgal biomasses, expressed as the average percentage of dry matter (%) ± standard error of triplicate measurements. (SPS: storage polysaccharides; CWPS: cell wall bound polysaccharides; EPS: extracellular polysaccharides; n.d.: not detected). The results were compared statistically (one-way ANOVA). Significant differences (Tukey test, $P < 0.05$) within each column are indicated with different letters (n = 3).

	Lipids	Proteins	SPS	CWPS	EPS	Ash
Porphyridium cruentum	11.5 ± 1.0 **e**	28.2 ± 1.2 **e**	2.1 ± 0.1 **e**	9.6 ± 0.3 **b**	2.6 ± 0.2 **a**	17.9 ± 0.6 **a**
Chlorella vulgaris	6.6 ± 1.5 **f**	39.4 ± 0.3 **b**	1.8 ± 0.1 **e**	9.3 ± 0.7 **b**	0.5 ± 0.1 **c**	6.7 ± 0.1 **d**
Tetraselmis chuii	11.9 ± 1.1 **e**	31.1 ± 0.3 **d**	7.8 ± 0.2 **bc**	17.0 ± 1.0 **a**	n.d.	14.5 ± 0.3 **bc**
Phaeodactylum tricornutum	17.1 ± 0.9 **d**	29.4 ± 0.4 **de**	5.2 ± 0.7 **d**	5.3 ± 0.2 **d**	n.d.	15.9 ± 0.9 **b**
Odontella aurita	12.8 ± 1.1 **e**	20.2 ± 0.1 **f**	21.7 ± 0.6 **a**	7.4 ± 0.3 **c**	1.2 ± 0.1 **b**	14.1 ± 0.6 **c**
Nannochloropsis sp.	31.7 ± 1.3 **b**	35.1 ± 0.8 **c**	5.9 ± 0.5 **cd**	3.8 ± 0.1 **e**	n.d.	6.1 ± 0.9 **d**
Schizochytrium sp.	73.9 ± 1.7 **a**	10.2 ± 0.1 **g**	6.3 ± 1.1 **bcd**	6.9 ± 0.4 **c**	n.d.	3.4 ± 0.3 **e**
Tisochrysis lutea	27.2 ± 1.6 **c**	29.8 ± 0.7 **de**	7.3 ± 0.4 **bc**	3.5 ± 0.1 **f**	n.d.	13.5 ± 0.6 **c**
Diacronema lutheri	31.5 ± 1.4 **b**	21.9 ± 0.3 **f**	7.2 ± 0.8 **bc**	10.2 ± 0.5 **b**	n.d.	13.0 ± 0.4 **c**
Arthrospira platensis	5.5 ± 0.5 **f**	47.4 ± 0.1 **a**	8.1 ± 0.6 **b**	9.7 ± 0.7 **b**	0.7 ± 0.1 **c**	4.5 ± 0.2 **e**

2.3.3 Carbohydrates

In contrast to most studies on microalgal biomass profiles, different types of carbohydrates were quantified separately in this chapter.

2.3.3.1 Storage polysaccharides

According to literature, four types of SPS are present in the selected microalgae, being either starch, floridean starch, glycogen, or chrysolaminarin. Relatively low SPS contents were observed for all microalgae species (2 – 8%), with the exception of *Odontella aurita* biomass presenting 22% of chrysolaminarin. For biomasses of *Porphyridium cruentum*, *Schizochytrium* sp., and *Arthrospira platensis*, the values obtained correspond with previously reported SPS contents (Arad et al., 1988; De Philippis et al., 1992; Qu et al., 2013). In contrast, the amount of SPS in *Chlorella vulgaris* and *Phaeodactylum tricornutum* biomass differs from those in literature (Brányiková et al., 2011; Zhu et al., 2016), although only one article was encountered for each microalga reporting SPS contents grown under standard conditions. Typically, SPS are very sensitive to cultivation conditions and time of harvesting. Whereas SPS contents are usually low in the exponential growth phase, they rapidly increase when nutrients are exhausted in the stationary phase. Similarly, cultivation in a nutrient depleted medium leads to accumulation of SPS (Myklestad, 1988; Xia et al., 2014; Yao et al., 2012). The low amounts of SPS in these commercially obtained biomasses therefore suggest that cells were harvested in the late exponential phase, preserving the nutritional quality of the biomass in terms of protein content and lipid composition. Biomass of *Odontella aurita* was cultivated in open raceway ponds and could have experienced more stress in terms of nutrient heterogeneity or competition with other organisms, possibly resulting in higher chrysolaminarin contents compared to the other microalgae species.

2.3.3.2 Extracellular polymeric substances

Two fractions of cell wall related polysaccharides were extracted from the microalgal biomass. On the one hand, EPMS were comprised of polymers on the outer layer of the cell wall, which dissolved into the medium without disruption of the microalgal cells. EPMS were only obtained for four microalgae species (*Porphyridium cruentum*, *Odontella aurita*, *Arthrospira platensis*, and *Chlorella vulgaris*), implying that the other microalgae do not have a layer of extracellular polymers. The highest content of EPMS was found in *Porphyridium cruentum*, a red microalga which is known for its sulfated EPS (Arad and Levy-Ontman, 2010; Gloaguen et al., 2004). In addition, EPMS were also obtained for *Arthrospira platensis*, *Chlorella vulgaris*, and *Odontella aurita*. While EPMS have been previously reported for *Arthrospira platensis* (Filali Mouhim et al.,

1993; Trabelsi et al., 2009) and *Chlorella vulgaris* (Morineau-Thomas et al., 2002; Xiao and Zheng, 2016), no information was found on the presence of EPMS in *Odontella aurita*. Furthermore, the absence of EPMS in *Nannochloropsis* sp., *Tisochrysis lutea*, and the fusiform type of *Phaeodactylum tricornutum* as seen in Table 2.1 was confirmed by other authors (Desbois et al., 2010; Guzman-Murillo and Ascencio, 2000). In contrast, although EPMS have been reported in literature for *Tetraselmis* sp. and *Schizochytrium* sp. (Guzman-Murillo and Ascencio, 2000; Lee Chang et al., 2014), they were not observed in the current study.

It should be noted that EPMS were extracted starting from dried biomass. Therefore, the yield obtained in this study is probably lower than when EPMS are directly extracted from the cultivation medium, due to losses of EPMS during harvesting steps. In addition, Table 2.1 shows the content of EPS, quantified as the sum of monosaccharides and uronic acids in the extracts, without considering other polymers such as proteins or co-extracted molecules like minerals and nucleic acids. However, when considering the weights of extracted EPMS, including other extracellular polymers, yields of 2.7 – 8.3% were obtained for these four microalgae species. Even though proteins were not quantified in EPMS samples (since they are accounted for in the total protein content of the biomasses), it can be inferred that they are present in all EPMS of the four microalgae species.

2.3.3.3 Cell wall bound polysaccharides

CWPS generally made up around 10% of the microalgal biomass. However, it is known that the cell wall of some microalgae contains non-polysaccharide substances, presumably resulting in a reduced amount of polysaccharides in the cell wall. For instance, several authors have reported the presence of algaenan in the *Nannochloropsis* sp. cell wall, a resistant aliphatic biopolymer composed of ether-linked long alkyl chains of esterified monomers (Gelin et al., 1999; Scholz et al., 2014). This could explain the lower CWPS content found in *Nannochloropsis* sp. compared to the other microalgae species. Similarly, the cells of diatoms are surrounded by a silicified cell wall, called a frustule, which is coated with a layer of organic material. Although *Phaeodactylum tricornutum* is classified as a diatom, the ovoid form is the only morphotype presenting true silica valves, while the other morphotypes are poor in silica (Francius et al., 2008). Thus, the lower amount of CWPS in the fusiform *Phaeodactylum tricornutum* used in the current work cannot be attributed to the presence of a frustule. The lowest amount of CWPS was found in *Tisochrysis lutea*, representing only 3.5% of the total biomass. It is known that *Isochrysis* sp. cells are easily disrupted, which is related to its weak cell wall structure (Pales Espinosa et al., 2010). Some authors even doubt the presence of a cell wall in *Isochrysis* sp., claiming that this microalga species only contains a plasma membrane around the cells (Zhu

and Lee, 1997). However, the results obtained in this chapter imply that a cell wall layer of polysaccharides is present in *Tisochrysis lutea*, but the low CWPS content suggests a rather thin cell wall layer, possibly responsible for its low resistance to mechanical disruption.

2.3.4 Ash and minerals

Even though all microalgae contained considerable amounts of minerals, clear differences were observed between marine and freshwater microalgae. Whereas most of the marine microalgae presented high ash contents due to accumulation of minerals from the cultivation medium (13 – 18% of the total biomass), the freshwater species *Chlorella vulgaris* and *Arthrospira platensis* only presented ash contents of 6.7% and 4.5%, respectively. The lowest ash content was observed for the heterotrophic *Schizochytrium* sp., representing only 3.4% of the total biomass. As L. Sun et al. (2014) stated that high lipid contents coincide with decreased ash contents in *Schizochytrium* sp., it is not surprising that a low ash content was observed in the current study. In addition, a low ash content was also observed in *Nannochloropsis* sp. biomass, even though this marine species was cultivated in a salt-rich medium. Nevertheless, similar values (6 – 10%) have been previously reported by other authors (Faeth et al., 2013; Rebolloso-Fuentes et al., 2001a). Moreover, each microalga species presented a typical mineral profile, as shown in Table 2.2.

Generally, marine microalgae were rich in the monovalent cations sodium and potassium. In fact, sodium represented more than 60% of all minerals in biomasses of *Nannochloropsis* sp., *Schizochytrium* sp., *Tisochrysis lutea*, and *Diacronema lutheri*. In contrast, the freshwater species *Chlorella vulgaris* and *Arthrospira platensis* contained low amounts of sodium, representing less than 10% of the analyzed minerals in these biomasses. From a nutritional point of view, *Phaeodactylum tricornutum* has the most interesting mineral profile, possessing very high amounts of calcium and iron. Given that iron deficiency is considered as the most prevalent single nutritional deficiency in the world (Camara et al., 2005), *Phaeodactylum tricornutum* biomass shows great potential as an iron source in the human diet. In addition, this microalga presented substantial amounts of magnesium and manganese and a relatively low amount of sodium, which was also observed by Rebolloso-Fuentes et al. (2001b). Biomasses of *Porphyridium cruentum* and *Tetraselmis chuii* also contained considerable amounts of calcium and iron, however they may be of lower interest for nutritional purposes due to higher amounts of sodium. Sodium consumption is after all associated with increased blood pressure and cardiovascular diseases, and a reduced sodium intake is recommended (Aburto et al., 2013). Nevertheless, these three microalgae species, together with the freshwater species *Arthrospira platensis* and *Chlorella vulgaris*, can be considered as good mineral source for human nutrition.

Table 2.2 Mineral composition of microalgal biomasses, expressed as the average ± standard error of triplicate measurements. The results were compared statistically (one-way ANOVA). Significant differences (Tukey test, $P < 0.05$) within each column are indicated with different letters (n = 3).

	Na (mg/g)	K (mg/g)	Ca (mg/g)	Mg (mg/g)	Fe (mg/100 g)	Zn (mg/100 g)	Mn (mg/100 g)	Cu (mg/100 g)
Porphyridium cruentum	27.1 ± 1.4 **a**	17.5 ± 2.7 **ab**	13.3 ± 0.9 **c**	9.8 ± 0.5 **a**	131.1 ± 3.3 **b**	6.9 ± 0.5 **a**	8.7 ± 0.4 **b**	0.9 ± 0.1 **ab**
Chlorella vulgaris	2.4 ± 0.2 **e**	12.2 ± 0.2 **cde**	4.1 ± 0.6 **e**	1.1 ± 0.1 **f**	11.7 ± 6.6 **ef**	1.8 ± 0.8 **de**	1.6 ± 0.8 **de**	0.6 ± 0.1 **b**
Tetraselmis chuii	10.1 ± 0.9 **cd**	11.5 ± 0.7 **cde**	17.7 ± 0.8 **b**	3.6 ± 0.2 **d**	49.0 ± 6.4 **d**	1.3 ± 0.1 **ef**	8.0 ± 1.0 **b**	0.9 ± 0.2 **ab**
Phaeodactylum tricornutum	7.1 ± 1.8 **d**	16.2 ± 1.3 **abc**	50.1 ± 3.2 **a**	3.7 ± 0.2 **d**	240.6 ± 14.0 **a**	2.9 ± 0.3 **cd**	12.0 ± 0.7 **a**	2.0 ± 1.2 **a**
Odontella aurita	18.8 ± 2.3 **b**	19.1 ± 2.8 **a**	4.4 ± 0.5 **de**	3.5 ± 0.3 **d**	19.2 ± 2.7 **e**	0.3 ± 0.01 **f**	11.9 ± 1.4 **a**	0.2 ± 0.02 **b**
Nannochloropsis sp.	12.8 ± 0.9 **c**	5.2 ± 1.1 **fg**	1.1 ± 0.2 **ef**	1.9 ± 0.2 **e**	7.3 ± 3.0 **ef**	2.3 ± 0.5 **de**	2.2 ± 0.4 **cd**	0.5 ± 0.2 **b**
Schizochytrium sp.	11.0 ± 1.0 **c**	4.3 ± 2.4 **g**	0.4 ± 0.2 **f**	0.8 ± 0.1 **a**	1.5 ± 0.7 **ef**	3.9 ± 0.01 **bc**	0.1 ± 0.02 **e**	0.1 ± 0.01 **b**
Tisochrysis lutea	29.1 ± 0.9 **a**	10.0 ± 2.1 **def**	1.4 ± 0.1 **ef**	1.9 ± 0.1 **e**	1.0 ± 0.4 **f**	4.8 ± 0.3 **b**	0.7 ± 0.5 **de**	0.1 ± 0.03 **b**
Diacronema lutheri	27.7 ± 1.7 **a**	7.6 ± 0.7 **efg**	3.7 ± 0.9 **ef**	6.1 ± 0.3 **b**	42.0 ± 5.7 **d**	1.9 ± 0.4 **de**	1.4 ± 0.3 **de**	0.4 ± 0.1 **b**
Arthrospira platensis	2.8 ± 0.2 **e**	14.0 ± 0.9 **bcd**	7.7 ± 0.3 **d**	4.6 ± 0.2 **c**	93.3 ± 6.1 **c**	1.9 ± 0.5 **de**	3.8 ± 0.1 **c**	0.5 ± 0.03 **b**

2.3.5 Microalgal composition in relation to food applications

Despite the enormous diversity in biomass composition of the investigated microalgae, it is obvious that they possess a fruitful biomass profile for food applications. All photoautotrophic microalgae showed substantial amounts of proteins, between 20% and 47% of the total biomass. Based on literature data, microalgal proteins are generally represented by favorable amino acid profiles and a good digestibility, being suitable for human consumption (Becker, 2004; Lourenço et al., 2004; Safi et al., 2013). In addition, the fraction of carbohydrates (SPS, CWPS, and EPS) generally contains substantial amounts of dietary fiber (Dvir et al., 2000; Nuño et al., 2013; Rebolloso-Fuentes et al., 2000, 2001a, 2001b). Hence, the macronutrient composition of the selected microalgae is suitable for use as part of a healthy diet.

In terms of micronutrients, the large amount of minerals is noteworthy in comparison with conventional food products. In fact, the fraction of potassium, iron, and magnesium in microalgae is approximately 10 times higher than for vegetables, cereals, and legumes. In addition, the investigated microalgae contain up to 100 times higher amounts of calcium compared to the aforementioned food matrices (Rousseau et al., 2019; Srikumar, 1993). However, one should keep in mind the excessive amounts of sodium in (marine) microalgae, being approximately 100 times higher than for vegetables, cereals, and legumes. A reduced sodium intake is after all recommended to reduce risks in terms of blood pressure increase and cardiovascular diseases (Aburto et al., 2013). In this context, the freshwater species *Arthrospira platensis* and *Chlorella vulgaris* might be of interest, possessing lower amounts of sodium compared to the marine microalgae species.

2.4 CONCLUSIONS

As expected, a large diversity in biomass composition was demonstrated, although some taxonomic similarities were observed. Microalgae belonging to the Haptophyta (*Tisochrysis lutea* and *Diacronema lutheri*) were characterized by high amounts of lipids and proteins, intermediate SPS and ash contents, and the absence of EPMS. In contrast, *Chlorella vulgaris* and *Tetraselmis chuii* (Chlorophyta) were mainly composed of proteins and CWPS, while lipids represented a smaller fraction of these biomasses. Less similarities were found among the two investigated diatoms, *Phaeodactylum tricornutum* and *Odontella aurita*, which might be ascribed to distinct cultivation conditions resulting in a high SPS content in *Odontella aurita*. Moreover, the presence of large amounts of structural biopolymers in most microalgae, such as EPS in *Porphyridium cruentum* or high protein contents in *Chlorella vulgaris* and *Arthrospira platensis*, is promising towards possible functionalities of microalgal biomasses and/or biopolymers as structuring agents for food applications.

PART II

CELL WALL RELATED POLYSACCHARIDES AS FOOD HYDROCOLLOIDS

CHAPTER 3

Cell wall related polysaccharide composition of different microalgae

3.1 INTRODUCTION

As shown in the previous chapter, the selected microalgae contain large amounts of structural biopolymers, which might possibly display interesting functionalities in food products. However, this research area is still unexplored, especially for microalgal cell wall related polysaccharides. This is surprising, since cell wall polysaccharides of several taxonomically related macroalgae have commercially been used as structuring agents for decades (Saha and Bhattacharya, 2010). In order to explore the potential of microalgal polysaccharides as food hydrocolloids, there is an urgent need for fundamental knowledge on the composition and molecular structure of microalgal cell wall related polysaccharides.

Although several authors have reported monosaccharide profiles of microalgae, the composition of the cell wall related polysaccharides of many microalgae is still unknown. On the one hand, some studies presented monosaccharide profiles after hydrolysis of the total biomass (de Souza et al., 2017; Templeton et al., 2012). However, due to possible interference of other components such as SPS and glycolipids, these results provide only limited information on the cell wall composition. On the other hand, some authors have characterized the composition of cell wall related polysaccharides, but the results were mostly concerning specific polysaccharide fractions obtained by a selective extraction procedure (Becker et al., 1995; Y. Sun et al., 2014). Studies focusing on the polysaccharide composition of the

This chapter is based on the following paper:
Bernaerts T.M.M., Gheysen L., Kyomugasho C., Jamsazzadeh Kermani Z., Vandionant S., Foubert I., Hendrickx M.E., Van Loey A.M. (2018)
Comparison of microalgal biomasses as functional food ingredients: Focus on the composition of cell wall related polysaccharides.
Algal Research, 32, 150-161.
[2017 Impact Factor = 3.745; Ranked 38/161 (Q1) in Biotechnology and Applied Microbiology]

whole cell wall are therefore very limited. Moreover, large variability in cell wall composition has been reported within a genus, a species, and even within a strain, which can be due to differences in cultivation conditions or depending on the life stage of the cell (Baudelet et al., 2017), further limiting the comparison among the studies available. Therefore, this study aims to apply a universal procedure for extraction of the total cell wall related polysaccharides of commercially available microalgae species, followed by characterization of the monosaccharide profile, uronic acid content, and sulfate content. This information would allow to identify analogies with currently used polysaccharidic texturizers, originating from macroalgae as well as from other sources, possibly resulting in a knowledge-based selection of microalgal polysaccharides with potential as food hydrocolloids.

3.2 MATERIALS AND METHODS

3.2.1 Microalgal biomass

The same microalgal biomasses as those in Chapter 2 have been used for the current study.

3.2.2 Extraction of cell wall related polysaccharides

A schematic representation of the procedure for extraction of EPMS and CWPS is shown in Fig. 3.1.

3.2.2.1 Extraction of extracellular polymeric substances

A procedure was implemented for extraction of EPMS based on methods of Hanlon et al. (2006) and Patel et al. (2013). Dry biomass (1.5 g) was suspended in 30 mL of saline solution at pH 7.5 to mimic cultivation conditions of the microalgae. All marine microalgae were suspended in 2.5% w/v NaCl, whereas the freshwater species *Chlorella vulgaris* was suspended in 0.02% w/v NaCl. All suspensions were incubated for 16 h at 25 °C, allowing the EPMS to dissolve into the medium. Subsequently, suspensions were centrifuged (10 min, 10000g, 4 °C), followed by a second centrifugation step of the supernatants (30 min, 17000g, 4 °C) to completely separate the biomass from the medium. The integrity of the cells in the residual biomass was confirmed using light microscopy (Olympus BX-51, Optical Co.Ltd, Tokyo, Japan). Cold ethanol (95% v/v) was added to the resulting supernatant to precipitate EPMS, ensuring a final ethanol concentration higher than 70% v/v. The solution was vacuum filtered using MN 615 filter paper and the insoluble residue was extensively dialyzed against demineralized water for 48 h (Spectra/Por®, MWCO 3.5 kDa, Spectrum Laboratories, CA, USA). Finally, the dialyzed EPMS extracts were lyophilized (Alpha 2-4 LSC plus, Christ, Osterode, Germany).

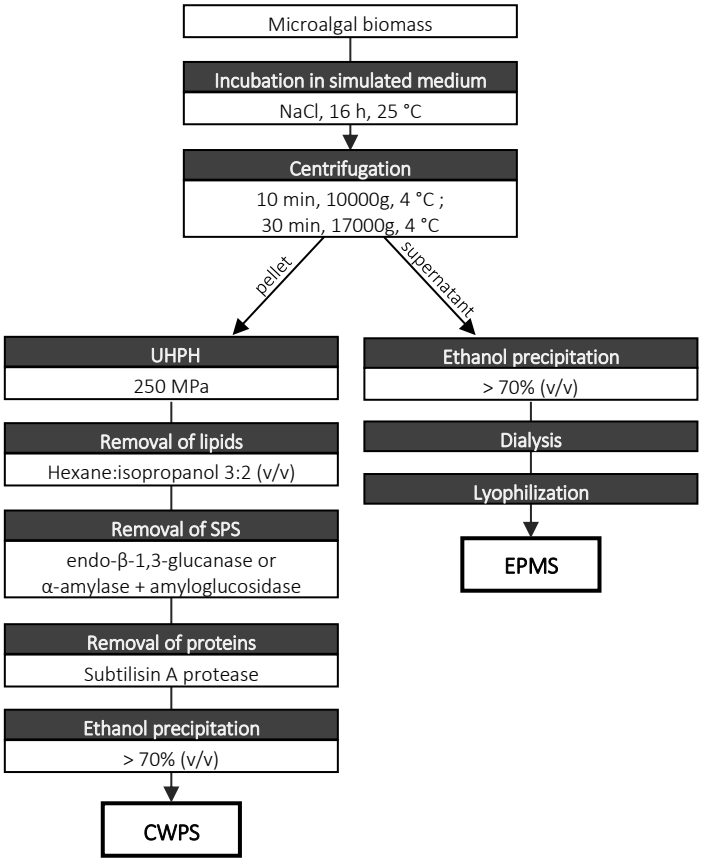

Fig. 3.1 Schematic overview of the extraction of extracellular polymeric substances (EPMS) and cell wall bound polysaccharides (CWPS).

3.2.2.2 Extraction of cell wall bound polysaccharides

CWPS were extracted by isolating an alcohol insoluble residue according to McFeeters and Armstrong (1984), with the additional removal of lipids, SPS, and proteins as demonstrated by several authors (Cheng et al., 2011; Kermanshahi-pour et al., 2014; Y. Sun et al., 2014).

The residual biomass, i.e. the pellets obtained in the two centrifugation steps in section 3.2.2.1, was resuspended in 100 mL MOPS buffer (55 mM, pH 7). Cells were disrupted using UHPH at 250 MPa, applying four passes for the rigid microalgae *Nannochloropsis* sp. and *Chlorella vulgaris*, while a single pass was used for the other microalgae species. Cold ethanol was added to the suspensions (> 70% v/v), the mixtures were centrifuged (10 min, 10000g, 4 °C), and the pellet was recovered. Lipids were removed by a hexane:isopropanol (3:2 v/v) extraction, based on the method of Ryckebosch et al. (2013). Hexane:isopropanol (3:2 v/v) was chosen as

extraction solvent instead of chloroform:methanol (1:1 v/v), as the latter solvent mixture can also remove some non-lipid substances from the microalgal biomass (Ryckebosch et al., 2014b). In short, 30 mL of hexane:isopropanol (3:2 v/v) was added to the pellet, mixed, and centrifuged (10 min, 900g, 20 °C) to remove the upper solvent layer. This lipid extraction was repeated to obtain a defatted pellet. Afterwards, SPS were enzymatically removed using either endo-β-1,3-glucanase or a combination of α-amylase and amyloglucosidase, depending on the type of SPS (Cheng et al., 2011; Milke et al., 2011). For removal of (floridean) starch or glycogen, the defatted pellet was resuspended in sodium acetate buffer (140 mM, pH 4.5) and heated for 10 min at 100 °C to gelatinize the (floridean) starch. The low pH of 4.5 was used to avoid possible degradation reactions of CWPS occurring at high temperatures, such as beta-elimination of pectic polysaccharides (Sila et al., 2009). After gelatinization, the pH was adjusted to 5.2 and α-amylase from *Bacillus* sp. (839 U/mg, Sigma-Aldrich) and amyloglucosidase from *Aspergillus niger* (300 U/mL, Sigma-Aldrich) were both added in a ratio of 1 U/mg initial biomass. The mixtures were incubated for 4 h at 60 °C. To remove chrysolaminarin, the defatted pellet was resuspended in sodium acetate buffer (100 mM, pH 4.5) and heated for 10 min at 100 °C. Afterwards, pH was adjusted to 5 and endo-β-1,3-glucanase of barley (2500 U/mL, Megazyme) was added to achieve 400 U/g initial biomass and the mixture was incubated for 4 h at 40 °C. After enzymatic incubations, cold ethanol was added to all samples (> 70% v/v), the suspensions were centrifuged (10 min, 10000g, 4 °C), and the pellets were recovered. Lastly, proteins were removed enzymatically. Therefore, pellets were resuspended in phosphate buffer (80 mM, pH 7.5) and Subtilisin A protease from *Bacillus licheniformis* (12 U/mg, Sigma-Aldrich) was added to achieve 50 U/g initial biomass. The mixtures were incubated for 1 h at 60 °C and after addition of cold ethanol (> 70% v/v), they were centrifuged (10 min, 10000g, 4 °C). The pellet was finally washed in acetone, vacuum filtered, and dried overnight at 40 °C. This residue was considered as CWPS.

3.2.3 Characterization of cell wall related polysaccharides

3.2.3.1 Quantification of monosaccharides and uronic acids

Monosaccharide and uronic acid composition of CWPS and EPMS was determined according to De Ruiter et al. (1992). Polysaccharides were first hydrolyzed using methanolysis combined with TFA hydrolysis. The resulting monosaccharides and uronic acids were then quantified by HPAEC-PAD.

Methanolysis and TFA hydrolysis was performed as described by De Ruiter et al. (1992). Briefly, sample was dissolved in ultrapure water (organic free, 18 MΩ cm resistance) in a concentration of 2 mg/mL, of which 40 µL was transferred to a pyrex

tube and dried by N_2 evaporation at 45 °C. Then, 2 mL of 2 M methanolic HCl was added to the sample and the mixtures were incubated for 16 h at 80 °C. The solvent was removed by N_2 evaporation at 30 °C. Subsequently, 2 mL of 2 M TFA was added to the tubes and incubated for 1 h at 121 °C. After removing the solvent by N_2 evaporation at 45 °C, the hydrolysate was dissolved in ultrapure water (organic free, 18 MΩ cm resistance) and filtered through a 0.45 µm syringe filter (Chromafil® A-45/25, Macherey-Nagel, Duren, Germany). The hydrolysis was performed in triplicate.

Monosaccharides and uronic acids in the hydrolysates were identified and quantified by HPAEC-PAD, as described by Jamsazzadeh Kermani et al. (2014). A Dionex system (DX600) equipped with a GS50 gradient pump, a CarboPac™ PA20 column (150 × 3 mm), a CarboPac™ PA20 guard column (30 × 3 mm), and an ED50 electrochemical detector were used (Dionex, Sunnyvale, CA, USA). The detector was equipped with a reference pH electrode (Ag/AgCl) and a gold electrode. Equilibration was performed for 10 min with 100 mM NaOH, after which 10 µL of hydrolysate was injected. First, isocratic elution of monosaccharides was performed for 20 min. In order to achieve a complete chromatographic separation of all monosaccharides analyzed, each sample was eluted using 0.5 mM NaOH as well as 15 mM NaOH in two separate runs. Secondly, uronic acids were isocratically eluted with 500 mM NaOH for 10 min. It was validated that the current HPAEC-PAD conditions resulted in accurate quantification of uronic acids, by comparison with the colorimetric method of Blumenkrantz and Asboe-Hansen (1973).

Mixtures of commercial sugar standards (D-glucose, D-galactose, D-xylose, D-mannose, L-rhamnose, L-arabinose, L-fucose, D-ribose, D-glucosamine, D-galacturonic acid and D-glucuronic acid) at varying concentrations (1 – 10 ppm) were used as external standards for identification and quantification. These standards were also subjected to the above-mentioned hydrolysis in order to correct for monosaccharide degradation during methanolysis and TFA hydrolysis.

3.2.3.2 Quantification of sulfate groups

Sulfate groups in the polysaccharide samples were quantified using the barium chloride-gelatin method of Dodgson and Price (1962). Briefly, 2 – 5 mg of sample was hydrolyzed with 1 M HCl for 5 h at 100 °C. The hydrolyzed sample was then incubated with 3% trichloroacetic acid and barium chloride-gelatin reagent for 15 min at 25 °C, and the absorbance was measured at 360 nm. A standard curve was prepared with K_2SO_4. Samples were corrected for UV-absorbing materials formed during hydrolysis, which were determined in absence of barium as described by Dodgson and Price (1962). All glassware was cleaned with HNO_3. The analysis was performed in triplicate.

3.3 RESULTS AND DISCUSSION

The monosaccharide and uronic acid profiles of CWPS of the investigated microalgae are presented in Table 3.1, in which each sugar is expressed as a percentage of the total amount of monosaccharides and uronic acids. Diverse monosaccharide profiles were observed for the different microalgae species. All microalgae species presented at least five different monosaccharides in the CWPS extracts, suggesting that their cell walls are composed of heteropolymers or multiple types of polysaccharides. Glucose, galactose, xylose, and mannose were generally the most abundant monosaccharides, while the ratio of galacturonic and glucuronic acid was strongly dependent on the microalga species. The composition of the EPMS is shown in Table 3.2 for the four microalgae *Porphyridium cruentum*, *Chlorella vulgaris*, *Odontella aurita* and *Arthrospira platensis*. As mentioned before, no EPMS could be extracted for the other microalgae species. Similar to CWPS, EPMS are considered heteropolysaccharides, containing both neutral monosaccharides and uronic acid residues. Finally, the sulfate content of both polysaccharide fractions is given in Table 3.3. All microalgae contained sulfated polysaccharides, although the degree of sulfation was generally low (0.6 – 14%). However, it should be noted that the obtained cell wall fractions were not further purified and still contained some impurities such as minerals and co-extracted proteins. As a consequence, sulfate contents of the purified cell wall related polysaccharides are likely somewhat higher than the data presented in Table 3.3.

Cells of *Porphyridium* sp. are generally encapsulated within a cell wall polysaccharide complex (Arad and Levy-Ontman, 2010). The external part easily dissolves into the cultivation medium and polymers therein are usually identified as soluble polysaccharides, corresponding to EPMS in this study. On the other hand, the part that remains bound to the cell, usually referred to as bound polysaccharides (Geresh et al., 2009), corresponds to CWPS. The proposed cell wall structure, i.e. one polysaccharide complex surrounding *Porphyridium cruentum* cells, is supported by our results, since CWPS and EPMS showed comparable monosaccharide profiles, with glucose, galactose, and xylose being the dominant sugars. This was previously reported by several authors, but with variable molar ratios of these monosaccharides (Geresh et al., 2002, 2009; Patel et al., 2013). In addition, uronic acids accounted for 8 – 9% of all monosaccharides in CWPS and EPMS, in accordance with previous studies (Geresh and Arad, 1991; Patel et al., 2013). However, whereas EPMS consisted only of glucuronic acid, CWPS presented both galacturonic and glucuronic acid. Another difference between CWPS and EPMS was the degree of sulfation, which was lower in CWPS (4.2%) than in EPMS (7.1%). These sulfate contents fall in the range reported in literature for *Porphyridium* sp. (4 – 14%) (de Jesus Raposo et al., 2015; Geresh and Arad, 1991).

Table 3.1 Monosaccharide and uronic acid composition in cell wall bound polysaccharides (CWPS) of microalgae, expressed as the average percentage of total monosaccharides and uronic acids (%) ± standard error of triplicate measurements (n = 3). (n.d.: not detected).

	Porphyridium cruentum	*Chlorella vulgaris*	*Tetraselmis chuii*	*Phaeodactylum tricornutum*	*Odontella aurita*
Glucose	30.5 ± 1.1	41.5 ± 1.8	28.9 ± 4.1	4.4 ± 2.4	11.1 ± 0.8
Galactose	22.4 ± 0.3	8.6 ± 0.2	5.7 ± 0.9	3.8 ± 0.9	35.7 ± 0.6
Xylose	27.8 ± 2.4	n.d.	5.3 ± 0.7	14.3 ± 0.1	9.3 ± 0.6
Mannose	9.3 ± 0.5	34.8 ± 7.6	41.3 ± 3.4	46.4 ± 1.3	17.1 ± 1.2
Rhamnose	n.d.	2.7 ± 0.1	1.0 ± 0.2	8.9 ± 0.8	3.2 ± 1.1
Arabinose	n.d.	n.d.	0.8 ± 0.2	n.d.	n.d.
Fucose	n.d.	n.d.	0.7 ± 0.7	2.5 ± 0.3	12.4 ± 0.6
Ribose	n.d.	1.9 ± 0.1	n.d	2.9 ± 1.2	1.3 ± 0.6
Glucosamine	1.8 ± 1.3	2.9 ± 0.1	n.d	n.d.	n.d.
Galacturonic acid	3.9 ± 0.9	3.3 ± 0.2	15.1 ± 1.3	2.9 ± 0.1	4.0 ± 2.6
Glucuronic acid	4.3 ± 0.1	4.3 ± 0.1	1.2 ± 0.2	13.9 ± 0.1	5.9 ± 1.0

	Nannochloropsis sp.	*Schizochytrium* sp.	*Tisochrysis lutea*	*Diacronema lutheri*	*Arthrospira platensis*
Glucose	75.8 ± 4.9	33.1 ± 1.6	22.7 ± 1.2	82.2 ± 3.3	49.8 ± 5.8
Galactose	6.4 ± 0.4	29.0 ± 3.5	14.8 ± 0.9	n.d.	3.8 ± 0.3
Xylose	3.5 ± 0.4	14.3 ± 0.2	9.6 ± 1.3	4.9 ± 2.7	n.d.
Mannose	4.7 ± 0.1	20.5 ± 3.4	16.4 ± 0.7	6.2 ± 0.3	29.8 ± 3.7
Rhamnose	3.0 ± 0.1	n.d.	1.3 ± 0.2	n.d.	6.7 ± 0.9
Arabinose	n.d.	n.d.	20.3 ± 0.9	3.4 ± 0.7	n.d.
Fucose	2.1 ± 0.2	n.d.	4.2 ± 0.4	0.8 ± 0.4	n.d.
Ribose	4.5 ± 0.1	n.d.	4.0 ± 0.5	1.3 ± 0.6	n.d.
Glucosamine	n.d.	3.1 ± 1.9	n.d.	n.d.	2.1 ± 0.3
Galacturonic acid	n.d.	n.d.	4.1 ± 3.3	n.d.	5.6 ± 2.9
Glucuronic acid	n.d.	n.d.	2.6 ± 0.4	1.2 ± 0.3	2.2 ± 0.3

Table 3.2 Monosaccharide and uronic acid composition in extracellular polymeric substances (EPMS) of microalgae, expressed as the average percentage of total monosaccharides and uronic acids (%) ± standard error of triplicate measurements (n = 3). (n.d.: not detected).

	Porphyridium cruentum	*Chlorella vulgaris*	*Odontella aurita*	*Arthrospira platensis*
Glucose	35.4 ± 5.6	24.2 ± 1.1	2.1 ± 0.3	11.8 ± 0.4
Galactose	21.3 ± 1.6	17.3 ± 0.5	60.8 ± 1.7	11.1 ± 0.6
Xylose	29.3 ± 1.8	6.3 ± 0.4	10.6 ± 0.2	2.7 ± 0.3
Mannose	3.8 ± 2.5	19.1 ± 0.5	3.3 ± 0.2	1.7 ± 0.1
Rhamnose	n.d.	11.0 ± 0.3	2.8 ± 0.2	29.1 ± 1.4
Arabinose	n.d.	1.9 ± 0.1	n.d.	n.d.
Fucose	1.3 ± 0.1	8.7 ± 0.1	15.9 ± 0.5	8.9 ± 0.2
Ribose	n.d.	n.d.	n.d.	25.8 ± 0.8
Glucosamine	n.d.	n.d.	n.d.	n.d.
Galacturonic acid	n.d.	3.3 ± 0.1	1.3 ± 0.1	n.d.
Glucuronic acid	8.9 ± 0.3	8.2 ± 0.4	3.2 ± 0.1	8.9 ± 0.3

Table 3.3 Sulfate content in cell wall bound polysaccharides (CWPS) and extracellular polymeric substances (EPMS) of microalgae, expressed as the average percentage of CWPS or EPMS (%) ± standard error of triplicate measurements (n = 3). (n.a.: not analyzed)

	CWPS	EPMS
Porphyridium cruentum	4.24 ± 0.12	7.05 ± 0.18
Chlorella vulgaris	1.14 ± 0.06	1.73 ± 0.21
Tetraselmis chuii	1.18 ± 0.10	n.a.
Phaeodactylum tricornutum	6.89 ± 0.17	n.a.
Odontella aurita	10.89 ± 0.61	13.93 ± 0.52
Nannochloropsis sp.	6.43 ± 0.11	n.a.
Schizochytrium sp.	2.69 ± 0.08	n.a.
Tisochrysis lutea	4.69 ± 0.20	n.a.
Diacronema lutheri	5.99 ± 0.14	n.a.
Arthrospira platensis	0.64 ± 0.11	1.34 ± 0.13

In CWPS of *Chlorella vulgaris*, glucose and mannose were the most abundant monosaccharides, suggesting the presence of glucomannans. Other authors also reported that these monosaccharides account for most of the cell wall of *Chlorella* sp. (Loos and Meindl, 1982; Shi et al., 2007), although it should be noted that two other types of CWPS can also be found in chlorococcal algae (Blumreisinger et al., 1983). However, glucomannans typically contain larger amounts of mannose than glucose, indicating that another source of glucose was present in the *Chlorella vulgaris* cell wall. For instance, glucose could also result from (partial) hydrolysis of cellulosic and

hemicellulosic polymers. Chen et al. (2013) described the cell wall of Chlorophyta consisting of an inner cell wall layer mainly composed of cellulose and hemicellulose, and an outer cell wall layer with a variable composition depending on the species. However, discrepancies in cell wall structures of *Chlorella* sp. have been described in literature. This can be partly attributed to taxonomic revisions, resulting in a new definition of the *Chlorella* genus and therefore a transfer of previously assigned species to other genera (Baudelet et al., 2017). Nevertheless, contrasting findings of several studies still result in a lack of clarity on the *Chlorella* sp. cell wall composition. Whereas some authors ascribe the rigidity of the cell wall to cellulose microfibrils (Chen et al., 2013; Gille et al., 2016), others attribute it to a chitin-like polysaccharide (Baudelet et al., 2017; Gerken et al., 2013; Kapaun et al., 1992). Given the low amount of glucosamine observed in this study, the latter statement cannot be confirmed based on our results. Moreover, even though the presence of hemicelluloses is mentioned by most authors, there is no consensus on the type of hemicelluloses in *Chlorella* sp. cell walls. In fact, the presence of either arabinomannans, arabinogalactans, glucomannans, or xyloglucans was reported in various studies (Pieper et al., 2012; Shi et al., 2007; Templeton et al., 2012). Furthermore, CWPS of *Chlorella vulgaris* contained low amounts of sulfate groups. Although some authors reported substantial amounts of sulfate esters in certain species of the *Chlorella* genus (de Jesus Raposo et al., 2015; Guzmán et al., 2003), no reports were found on *Chlorella vulgaris*. Finally, EPMS from *Chlorella vulgaris* showed a very heterogeneous composition, containing seven monosaccharides and two uronic acids, with a low degree of sulfation. Whereas the values obtained are confirmed for EPMS of *Chlorella* sp. by some authors (Delattre et al., 2016; Guzman-Murillo and Ascencio, 2000), others show contrasting results (de Jesus Raposo et al., 2015; Kaplan et al., 1987). It can thus be concluded that microalgae of the *Chlorella* genus show a very large diversity in cell wall composition, presenting different cell wall structures depending on the species and the strain.

Similar to *Chlorella vulgaris*, mannose and glucose were the main monosaccharides in the CWPS of *Tetraselmis chuii*. Several authors reported these monosaccharides in *Tetraselmis* sp., but together with high amounts of galactose (Brown, 1991; Schwenzfeier et al., 2011; Whyte, 1987). In addition, appreciable amounts of galacturonic acid in combination with minor amounts of galactose, rhamnose, arabinose, and fucose suggest the presence of pectic polysaccharides. In fact, Arora et al. (2012) have reported the presence of glucans, galactomannans, and pectins in cell walls of *Tetraselmis indica*. It should be noted that the obtained monosaccharide composition probably does not provide the full carbohydrate profile of the *Tetraselmis chuii* cell wall. In fact, *Tetraselmis* sp. cell walls are built up of thecae which contain up to 80% of acidic polysaccharides, characterized as 3-deoxy-manno-

2-octulosonic acid, 3-deoxy-5-O-methyl-manno-2-octulosonic acid, and 3-deoxy-lyxo-2-heptulosaric acid (Baudelet et al., 2017; Becker et al., 1998). However, no attempts were made to quantify these keto-sugar acids in the current study. Finally, a sulfate content of 1.2% was observed in CWPS of *Tetraselmis chuii*, somewhat lower compared to previous studies (Becker et al., 1998; Guzman-Murillo and Ascencio, 2000).

CWPS of the diatom *Phaeodactylum tricornutum* consisted mainly of mannose and glucuronic acid, representing 60% of the total sugars. Several authors have previously identified a sulfated glucuronomannan as the most prominent polysaccharide present in *Phaeodactylum tricornutum* (Brown, 1991; Ford and Percival, 1965; Le Costaouëc et al., 2017). A sulfate content of 6.9% was observed, corresponding to previous reports (Ford and Percival, 1965; Guzmán et al., 2003). In addition, minor amounts of other monosaccharides, mainly xylose, rhamnose, glucose, and galactose, suggest the presence of other hemicellulosic polymers in the cell wall of *Phaeodactylum tricornutum* (Templeton et al., 2012). Although some authors suggest that sulfated glucuronomannans are a conserved structural polymer in diatoms (Le Costaouëc et al., 2017), this was not obvious from the CWPS composition of *Odontella aurita*, another diatom. A heterogeneous monosaccharide profile was found, mainly containing galactose, mannose, fucose, and glucose. EPMS of *Odontella aurita* also presented high amounts of galactose and fucose, while mannose and glucose were only minor constituents of EPMS. Uronic acids accounted for 10% of the sugar composition in both fractions. In addition, high sulfate contents were found for CWPS and EPMS of *Odontella aurita*, being 11% and 14%, respectively. As a consequence, cell wall related polysaccharides of *Odontella aurita* possess anionic characteristics and could therefore be an interesting source in terms of several functionalities.

CWPS of *Nannochloropsis* sp. consist of 75% glucose, together with minor amounts of other monosaccharides. This large fraction of glucose was previously observed by several authors and was ascribed to cellulose polymers (Baba Hamed et al., 2016; Brown, 1991; Scholz et al., 2014). Scholz et al. (2014) described the cell wall of *Nannochloropsis gaditana* as a bilayer structure, consisting of a cellulosic inner wall representing approximately 75% of the mass balance, protected by an outer algaenan layer. The latter layer was not identified nor quantified in this study. It must be noted that microcrystalline cellulose is only partially hydrolyzed by methanolysis and TFA hydrolysis, with a recovery of only 30 to 50%. This might be another explanation for the low amount of CWPS of *Nannochloropsis* sp. presented in Table 2.1. No uronic acids were present in *Nannochloropsis* sp., while a substantial amount of sulfate groups was observed. The latter results, in combination with low amounts of other

monosaccharides, suggest the presence of sulfated polysaccharides in the *Nannochloropsis* sp. cell wall in addition to cellulose and algaenan.

Only few studies investigated the cell wall composition of *Schizochytrium* sp., describing a thin non-cellulosic cell wall with galactose as the principal monosaccharide (Bahnweg and Jackle, 1986; Darley et al., 1973). In the current study, galactose was also observed, however together with glucose, mannose, and xylose. The latter two monosaccharides have been previously reported in *Thraustochytrium* species. These fungi are phylogenetically related to *Schizochytrium* sp., based on the structure and formation of the cell wall in particular (Bahnweg and Jackle, 1986; Darley et al., 1973). Furthermore, CWPS of *Schizochytirium* sp. presented a low degree of sulfation (2.7%) and uronic acids were absent.

In CWPS of *Tisochrysis lutea*, all monosaccharides were detected in substantial amounts, except for glucosamine. The largest fraction of CWPS was composed of glucose, mannose, arabinose, and galactose. These were also the major monosaccharides observed in previous studies (Brown, 1991; Whyte, 1987), although glucose represented 76% of the total sugar composition in the study of Brown (1991). However, that study reported the overall polysaccharide composition, including the SPS chrysolaminarin. Since it was shown in the previous chapter that *Tisochrysis lutea* contained a large fraction of chrysolaminarin in comparison with the fraction of CWPS (Table 2.1), it is inferred that glucose is mainly attributed to chrysolaminarin, and only partially constituting the cell wall of *Tisochrysis lutea*. Finally, the CWPS also contained sulfated polysaccharides, with similar sulfate contents as previously reported (1.1 – 5.5%) (Y. Sun et al., 2014). Although *Diacronema lutheri* also belongs to the Haptophyta, i.e. the same class as *Tisochrysis lutea*, a different CWPS composition was observed for this microalga species. Glucose was found as the principal monosaccharide, while mannose, xylose, and arabinose were present in low amounts. Arnold et al. (2015) reported that *Diacronema lutheri* cell walls consist of small cellulose scales covered by an organic matrix of hemicellulose, mainly xyloglucans. Moreover, a sulfate content of 6% was determined for CWPS of *Diacronema lutheri*, indicating the presence of sulfated polysaccharides.

Finally, CWPS of the cyanobacterium *Arthrospira platensis* were mainly composed of glucose and mannose. In fact, these monosaccharides are typically found in the cell walls of cyanobacteria, together with minor amounts of galactose and xylose (Bertocchi et al., 1990). In addition, the observed amounts of rhamnose could result from spirulan polymers, a sulfated polysaccharide which was previously extracted from *Arthrospira platensis* (Lee et al., 1998). It should be noted that polysaccharides probably represent a small fraction of the cell wall, since cyanobacterial cells are typically covered by a peptidoglycan layer, a polymer composed of N-acetyl-

glucosamine (Bertocchi et al., 1990). Surprisingly low amounts of glucosamine were detected in the current study, which could be due to incomplete hydrolysis of peptidoglycan by methanolysis and TFA hydrolysis. In fact, some authors hypothesized that a harsher HCl hydrolysis procedure would result in a more complete hydrolysis of N-acetyl-glucosamine containing polymers (Templeton et al., 2012). Furthermore, a heterogeneous monosaccharide profile was observed for EPMS of *Arthrospira platensis*, showing substantial amounts of rhamnose, ribose, glucose, galactose, fucose, and glucuronic acid. These sugars have been previously reported for EPMS of *Arthrospira platensis*, but in different ratios (Delattre et al., 2016; Trabelsi et al., 2009). Although several bioactivities are ascribed to specific sulfated polysaccharides of *Arthrospira platensis* (Delattre et al., 2016; Lee et al., 1998), it is assumed that these polymers only make up a small fraction of the cell wall related polysaccharides, since low degrees of sulfation were observed in both CWPS and EPMS (0.6% and 1.4%).

3.4 CONCLUSIONS

Based on the data obtained in this chapter, CWPS generally make up ~10% of the microalgal biomass, while the contribution of other non-polysaccharide substances to the cell wall could not be excluded. Extraction of EPMS was only successful for four microalgae species, implying that the other microalgae do not possess extracellular polymers. Even though CWPS and EPMS of all microalgae species were sulfated, their degree of sulfation was generally low. In addition, some microalgae presented polysaccharides with substantial amounts of uronic acids and sulfate groups, providing anionic characteristics to these polymers. Nevertheless, little analogies were observed with the polysaccharide composition of conventional thickening or gelling agents, even when compared to commercial macroalgal polysaccharides. More elucidated analyses of the molecular structure, such as molecular weight determination and linkage analysis, are required for a structural comparison of the cell wall related polysaccharides of microalgae with conventional hydrocolloids.

CHAPTER 4

Molecular and rheological characterization of cell wall fractions of *Porphyridium cruentum*

4.1 INTRODUCTION

In spite of a thorough characterization of the cell wall related polysaccharide composition of various microalgae species in the previous chapter, little analogies with conventional (macroalgal) structuring agents have been observed. Nevertheless, several authors have reported promising rheological properties for EPS of *Porphyridium* sp., attributed to their unique molecular structure (Eteshola et al., 1998; Geresh and Arad, 1991). Hence, an in-depth investigation of the rheological properties of different cell wall fractions of *Porphyridium cruentum* in relation to their molecular composition is of interest to evaluate their possible use as food hydrocolloids.

Porphyridium sp. EPS are known to yield highly viscous aqueous solutions at relatively low polymer concentrations comparable to xanthan gum (Eteshola et al., 1998; Geresh and Arad, 1991). Furthermore, the rheological properties were stable in a wide range of pH values (2 – 9) and temperatures (30 – 60 °C) (Arad et al., 2006). However, contrasting observations have been reported by different authors when temperatures were further increased. Whereas Eteshola et al. (1998) observed a strong gelation at temperatures above 60 °C which was reversible upon cooling, other authors reported the rheological properties to be unaffected by temperature (Arad et al., 2006; Patel et al., 2013). However, a clear understanding of the rheological

This chapter is based on the following paper:
Bernaerts T.M.M., Kyomugasho C., Van Looveren N., Gheysen L., Foubert I., Hendrickx M.E., Van Loey A.M. (2018)
Molecular and rheological characterization of different cell wall fractions of Porphyridium cruentum.
Carbohydrate Polymers, 195, 542-550.
[2017 Impact Factor = 5.158; Ranked 2/72 (Q1) in Applied Chemistry]

behavior of *Porphyridium* sp. EPS and its temperature dependence is required for commercialization of these polysaccharides towards specific applications.

To date, the rheological properties of *Porphyridium* sp. polysaccharides are only studied for the external part of the cell wall (i.e. EPS), without any knowledge on the functionality of the CWPS. If CWPS would show similar rheological properties as EPS, the potential of *Porphyridium* sp. polysaccharides as food hydrocolloids would gain drastic interest. The polysaccharide yield would actually largely increase since CWPS make up ~10% of the biomass, as observed in Chapter 2. However, an in-depth characterization of the molecular structure of these polysaccharides is required for a targeted functionalization as food hydrocolloids.

The objective of this chapter is to provide a structural characterization of different cell wall polysaccharide fractions of *Porphyridium cruentum* in relation to their rheological behavior in aqueous polysaccharide suspensions. Four cell wall fractions were isolated from *Porphyridium cruentum*, including two extracellular fractions and two cell wall bound fractions, and were characterized in terms of purity and molecular structure of the polysaccharides. Moreover, the rheological properties were studied, including attempts to functionalize by cation addition and temperature cycles. The insights provided by this study could indicate the potential of different cell wall polysaccharide fractions of *Porphyridium* sp. as thickening or gelling agents for food applications.

4.2 MATERIALS AND METHODS

4.2.1 Microalgal biomass

Lyophilized biomass of *Porphyridium cruentum* was purchased from Necton Phytobloom (Olhão, Portugal), i.e. a different batch than the one used in previous chapters. Information on the cultivation conditions was provided by the company. In short, the microalgae were cultured in Nutribloom Plus® medium in tubular photobioreactors. The photobioreactors were placed outdoor and were subjected to natural sunlight (time of cultivation: June – July 2016). The temperature of the culture was set at 28 °C and the culture was maintained at pH 8. Biomass was harvested in the late exponential phase by centrifugation and lyophilized to obtain dry biomass. The residual moisture content was 3.36 ± 0.56%, determined by vacuum drying as described in section 2.2.2. The dry biomass was stored in closed containers at -80 °C until use.

4.2.2 Characterization of the biomass composition

Since a different batch of *Porphyridium cruentum* was used in this chapter compared to Chapters 2 and 3, the biomass composition was determined for this new batch. All analyses were performed in triplicate, as described in Chapter 2. As seen from Table 4.1, the biomass composition of the new batch of *Porphyridium cruentum* is very similar to the previously used batch.

Table 4.1 Biomass composition of different batches of *Porphyridium cruentum* used in different chapters of this doctoral thesis, expressed as percentage of dry matter (%) ± standard error (n = 3). (SPS: storage polysaccharides; CWPS: cell wall bound polysaccharides; EPS: extracellular polysaccharides).

	Chapters 2 - 3	Chapter 4
Lipids	11.5 ± 1.0	12.6 ± 0.7
Proteins	28.2 ± 1.2	28.0 ± 0.6
SPS	2.1 ± 0.1	4.4 ± 0.1
CWPS	9.6 ± 0.3	14.0 ± 0.5
EPS	2.6 ± 0.2	2.7 ± 0.1
Ash	17.9 ± 0.6	22.3 ± 0.8

4.2.3 Extraction of cell wall related polysaccharides

Different fractions of cell wall related polysaccharides were extracted as described in section 3.2.2, with some modifications to scale up the procedure. In order to gain a better understanding of the role of specific polymers in the extracellular fractions, EPMS were further purified by enzymatic removal of co-extracted proteins to obtain the EPS fraction. In addition, the cell wall bound polysaccharides were further fractionated based on the solubility of the polymers, using a hot water fractionation to obtain water soluble cell wall polysaccharides (wsCWPS) and water insoluble cell wall polysaccharides (wiCWPS). Differences in solubility might actually be related to distinct functionalities, which could also be of interest for a targeted solubilization of specific polysaccharide fractions upon processing when using the whole microalgal biomass (Chapters 5 and 6). A schematic overview of the applied extraction procedures is shown in Fig. 4.1.

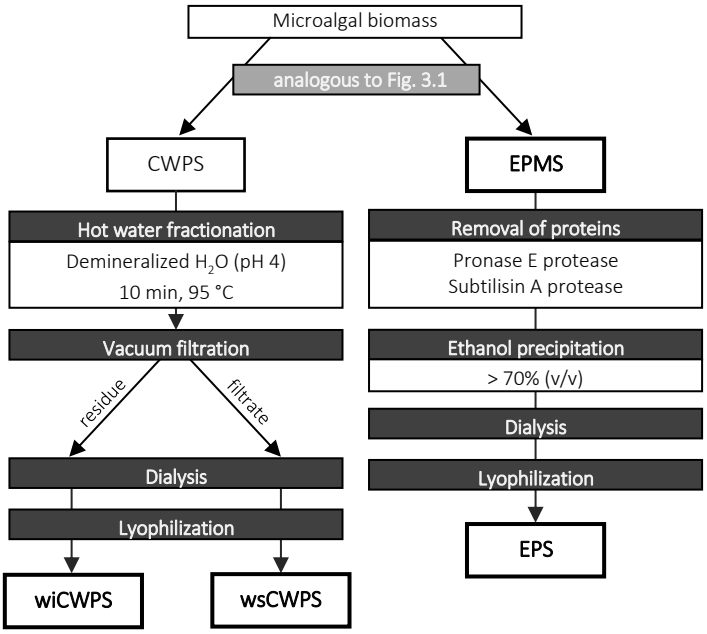

Fig. 4.1 Schematic overview of the extraction and fractionation procedure for isolating different fractions of *Porphyridium cruentum* (EPMS: extracellular polymeric substances; EPS: extracellular polysaccharides; wsCWPS: water soluble cell wall polysaccharides; wiCWPS: water insoluble cell wall polysaccharides).

4.2.2.1 Extracellular polymeric substances

Dry biomass (50 g) was suspended in 2 L of saline solution (2.5% NaCl, pH 7.5) and incubated for 16 h at 25 °C. The suspension was centrifuged (10 min, 10000g, 4 °C), the resulting supernatant was again centrifuged (30 min, 17000g, 4 °C), and cold ethanol was added to the final supernatant to obtain an ethanol concentration above 70% v/v. After vacuum filtration, the insoluble residue was dialyzed against demineralized water for 48 h (Spectra/Por®, MWCO 3.5 kDa, Spectrum Laboratories, CA, USA), lyophilized (Alpha 2-4 LSC plus, Christ, Osterode, Germany), and denoted as EPMS.

4.2.2.2 Extracellular polysaccharides

Lyophilized EPMS (4 g) was dissolved in 500 mL of sodium phosphate buffer (50 mM, pH 7.5). Pronase E of *Streptomyces* sp. (3.5 U/mg, Sigma-Aldrich) was added to achieve 100 U/g EPMS and the mixture was incubated for 24 h at 37 °C. Subtilisin A protease of *Bacillus licheniformis* (12 U/mg, Sigma-Aldrich) was subsequently added in a ratio of 100 U/g EPMS and the suspension was incubated for 24 h at 60 °C. Ethanol was added to the suspensions to achieve a final concentration above 70% v/v

and vacuum filtration was applied. The residue was resuspended in acetone and vacuum filtered. The residue was finally dialyzed and lyophilized to obtain EPS.

4.2.2.3 Cell wall bound polysaccharides

The residual biomass, i.e. the pellets obtained in the two centrifugation steps in section 4.2.2.1, was resuspended in 1.5 L demineralized water (pH 7). Cells were disrupted using HPH (Pony NS2006L, Gea Niro Soavi, Düsseldorf, Germany) for 4 passes at 100 MPa. The homogenate (mixture of disrupted cells) was lyophilized and subsequently lipids were removed by extraction with 1 L of hexane:isopropanol (3:2 v/v) for 1.5 h. The solvent was removed by vacuum filtration and this lipid extraction procedure was repeated. Floridean starch was subsequently removed by dissolving the defatted biomass in 500 mL of sodium acetate buffer (140 mM, pH 5.2), heating for 20 min at 95 °C for gelatinization, and incubating for 24 h at 60 °C with α-amylase from *Bacillus* sp. (1333 U/mg, Sigma-Aldrich) and amyloglucosidase from *Aspergillus niger* (70 U/mg, Sigma-Aldrich), each in a ratio of 100 U/g disrupted biomass. After ethanol precipitation, the residue was incubated with pronase E from *Streptomyces* sp. (3.5 U/mg, Sigma-Aldrich) for 24 h at 37 °C. Polysaccharides were subsequently precipitated with ethanol (> 70% v/v), the precipitate was washed with acetone, and the final residue was lyophilized and denoted as CWPS.

A hot water fractionation was subsequently applied based on Sila et al. (2006). CWPS (10 g) were dissolved in 1 L of demineralized water (pH 4), incubated for 10 min at 95 °C, and vacuum filtered using MN 615 filter paper. The filtrate and the residue were dialyzed and lyophilized to obtain wsCWPS and wiCWPS, respectively.

4.2.4 Molecular characterization

The obtained fractions were characterized for their molecular structure using methods described in Chapters 2 and 3. All analyses were performed in triplicate. Briefly, moisture content was determined by vacuum-drying and the average moisture content was taken into account in expressing all components as a percentage of dry matter and in the preparation of aqueous solutions in specific concentrations. Protein content was determined through nitrogen measurement by the Dumas method and estimated using a nitrogen-to-protein conversion factor of 6.25, assuming that no non-protein nitrogen sources were present in the isolated cell wall fractions. Ash content was determined gravimetrically after 24 h at 550 °C. Mineral composition was subsequently determined using ICP-OES.

Polysaccharides were hydrolyzed into monosaccharides and uronic acids using methanolysis combined with TFA hydrolysis, and subsequently analyzed by HPAEC-PAD using the exact conditions as described in section 3.2.2.3. Monosaccharide

standards were subjected to the same hydrolysis conditions in order to correct for sugar degradation during the acid hydrolysis. Sulfate groups were quantified using the barium chloride-gelatin method of Dodgson and Price (1962).

The molecular weight distribution of the polymers was determined according to Kyomugasho et al. (2015). High performance size exclusion chromatography (HPSEC) was used, equipped with multi-angle laser light scattering (MALLS, PN3621, Postnova Analytics, Landsberg am Lech, Germany), a refractive index (RI) detector (Shodex RI-101, Showa Denko K.K., Kawasaki, Japan), a diode array detector (DAD, G1316A, Agilent Technologies, Diegem, Belgium), and a viscometer (Postnova Analytics, Landsberg am Lech, Germany). MES buffer (0.1 M of 2-(N-morpholino)ethanesulfonic acid, pH 7, containing 0.1 M NaCl) was filtered through a 0.1 µm filter and used as the eluent. Samples were dissolved in the eluent (2 mg/mL) for 48 h and filtered through 0.45 µm syringe filters (Millex®-HV, Merck Millipore Ltd, Cork, Ireland) prior to analysis. Exactly 100 µL of sample was injected onto a series of Waters columns (Waters, Milford, MA, USA): Ultrahydrogel 250, 1000 and 2000 with exclusion limits of 8×10^4, 4×10^6 and 1×10^7 g/mol, respectively. Samples were eluted at 40 °C using a flow rate of 0.5 mL/min. The molecular weight was calculated using the 2nd order Debye fitting method with Nova Mals software (version 1.0.0.18, Postnova Analytics, Landsberg am Lech, Germany), using a dn/dc value of 0.146 mL/g, which is within the range of dn/dc values for polysaccharides in aqueous buffers (0.140 – 0.160 mL/g) (Harding, 2005).

4.2.5 Rheological characterization

4.2.4.1 Preparation of cell wall suspensions

Lyophilized fractions were suspended overnight in ultrapure water (organic free, 18 MΩ cm resistance) in a concentration of 2% w/w. Suspensions were then homogenized for 5 min at 8000 rpm (Ultra-Turrax T25, Janke & Kunkel GmbH, Staufen, Germany) and again stirred overnight to ensure complete hydration of the polymers. It was validated that the homogenization step did not affect the rheological properties of the samples, while it allowed the reduction of the measuring gap, since non-hydrated particles were avoided as validated by laser diffraction (data not shown). Moreover, no changes in molecular properties were expected due to the homogenization step, as it was previously shown that the molecular weight of pectin polymers was not altered by application of HPH using pressures up to 50 MPa (Shpigelman et al., 2015).

The effect of additional cations on the rheological properties was investigated for suspensions of EPS and wsCWPS. Suspensions were prepared by addition of 0.2 M

NaCl, KCl, or $CaCl_2$ to achieve a final concentration of 2% w/w and stoichiometric ratios of R ≥ 1, with $R = \frac{[Na^+ \, or \, K^+]}{[COO^-]+[SO_3{}^-]}$ for monovalent cations and $R = \frac{2[Ca^{2+}]}{[COO^-]+[SO_3{}^-]}$ for divalent cations, irrespective of the intrinsic ions present in the samples. The pH of the suspensions was between 7.3 and 7.6, ensuring that the carboxylic and sulfate groups were negatively charged.

Prior to rheological analyses, stability of the suspensions was checked using a Turbiscan MA 2000 (Formulaction, L'Union, France). Since suspensions of wiCWPS showed significant sedimentation within 30 min, no rheological analyses were performed for this fraction. All other fractions resulted in stable suspensions.

4.2.4.2 Rheological measurements

Rheological analyses were performed using a stress-controlled rheometer (MCR 302, Anton Paar, Graz, Austria). A parallel plate geometry (PP25, diameter 25 mm) was used as a measuring system for suspensions of EPMS and EPS, with a measuring gap set at 1 mm. For the low viscous wsCWPS suspensions, a double wall Couette geometry (DG26.7, internal radius 12.3 mm, external radius 13.3 mm and measuring height 40 mm) was used. Samples were presheared for 30 s at a shear rate of 20 s^{-1} followed by 300 s of rest before each measurement. To ensure reliability of the obtained data, a minimum torque limit was fixed at 0.1 µN m.

The flow behavior was studied using steady-shear measurements, by logarithmically increasing shear rate from 0.1 to 100 s^{-1} and applying each shear rate for 20 s. To determine the viscoelastic properties, strain sweep measurements were performed by increasing the shear strain logarithmically from 0.01 to 1000%, at a constant angular frequency of 10 rad/s. In frequency sweep tests, the angular frequency was decreased logarithmically from 100 to 0.1 rad/s, at a constant shear strain of 2% within the linear viscoelastic region. All measurements were performed at 25 °C.

Temperature sweeps were performed for suspensions of EPS and wsCWPS, with and without the addition of cations. For these measurements, the parallel plate geometry (PP25) was also used for wsCWPS suspensions, but with a measuring gap of 0.5 mm. Samples were heated from 20 to 80 °C at a heating rate of 2 °C/min, followed by a holding time of 10 min at 80 °C, prior to cooling to 20 °C at a rate of 2 °C/min. To prevent evaporation during the measurement, the sample surface was covered with light paraffin oil and a solvent trap was installed. Storage and loss moduli were monitored at a constant angular frequency of 10 rad/s and a constant shear strain of 5%, within the linear viscoelastic region. No correction was made for thermal expansion of the measuring system (PP25). Nevertheless, since the thermal expansion coefficient α of the stainless steel geometry was below 17.3 × 10^{-6} m/(m K), the linear

thermal expansion obtained as $dl = L_0 \cdot \alpha \cdot \Delta T$ was below 0.519 × 10^{-3} mm, resulting in a relative error of <0.1% in applied deformations.

4.2.6 Statistical analysis

The composition and molecular characterization of the cell wall fractions was determined in triplicate and the data obtained presented as the average of three measurements ± standard error. Differences were statistically analyzed using one-way ANOVA combined with Tukey's test for multiple comparison ($P < 0.05$) with JMP statistical software (JMP Pro 12, Cary, NC, USA). Frequency sweep curves were fitted to rheological models using non-linear regression with SAS statistical software (SAS 9.4, Cary, NC, USA). The estimated model parameters were statistically compared by use of 95% confidence intervals.

4.3 RESULTS AND DISCUSSION

4.3.1 Chemical composition of the cell wall fractions

Four cell wall fractions were isolated from lyophilized *Porphyridium cruentum* biomass, including two extracellular and two cell wall bound fractions. The extraction yield of the different fractions is presented in **Fig. 4.2**. First, it should be noted that the extraction procedures were performed on lyophilized biomass, implying that (part of) the extracellular polymers which were secreted into the cultivation medium have not been recovered during harvesting of the biomass. As a consequence, the yield of EPMS and EPS obtained in the current study is presumably lower than when directly extracted from wet biomass or the cultivation medium. Furthermore, the growth conditions were not optimized for polysaccharide production. Nevertheless, the presence of unsecreted extracellular layers surrounding the harvested cells was confirmed by DIC microscopy (not shown). The isolated cell wall fractions contributed for one third of the weight of the dried biomass. About 70% of the cell wall related polysaccharides remained bound to the cell wall, i.e. the sum of wsCWPS and wiCWPS, which is in agreement with previously reported values (Arad and Levy-Ontman, 2010).

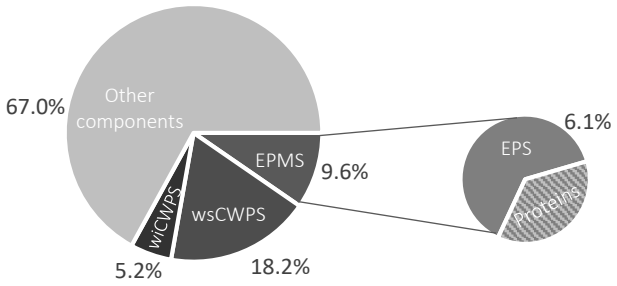

Fig. 4.2 Yield of different fractions isolated from dry biomass of *Porphyridium cruentum*, expressed as a weight percentage of dry biomass (%) (EPMS: extracellular polymeric substances; EPS: extracellular polysaccharides; wsCWPS: water soluble cell wall polysaccharides; wiCWPS: water insoluble cell wall polysaccharides).

The chemical composition of the isolated cell wall fractions is shown in **Fig. 4.3**. Polysaccharides, i.e. the combination of monosaccharides, uronic acids, and sulfate esters, presented less than half of the isolated fractions, with proteins and ash making up a large part of the fractions except for wsCWPS. It has been previously reported that the use of traditional alcohol precipitation for the extraction of *Porphyridium* sp. EPS resulted in low purified polymers with high salt content (Patel et al., 2013). Even though protease treatments and dialysis steps were included in this extraction procedure to remove proteins and minerals, respectively, substantial amounts of these components were co-extracted. Further purification of the cell wall fractions might therefore be desired, as this might improve their solubility and rheological properties (Patel et al., 2013).

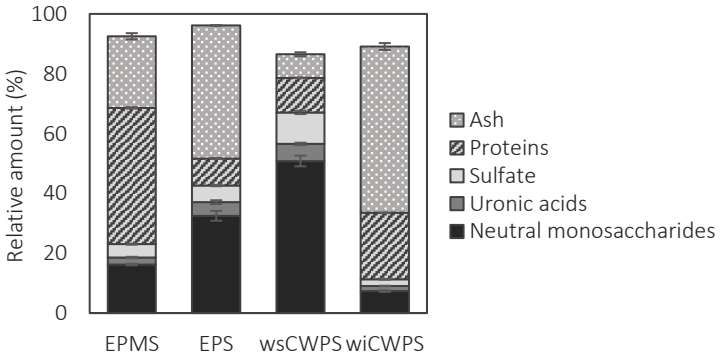

Fig. 4.3 Chemical composition of different fractions isolated from *Porphyridium cruentum* (EPMS: extracellular polymeric substances; EPS: extracellular polysaccharides; wsCWPS: water soluble cell wall polysaccharides; wiCWPS: water insoluble cell wall polysaccharides).

The use of saline solution for extraction of extracellular polymers resulted in an EPMS fraction mainly rich in proteins. Although a glycoprotein has been described in the extracellular matrix of *Porphyridium* sp., proteins generally only represent about 5% of the dry weight of the extracellular polymers (Arad and Levy-Ontman, 2010; Gloaguen et al., 2004). In the current study, the high protein content in this fraction was probably a result of co-extraction of phycobiliproteins, water-soluble pigments providing a red color to the sample. Even though these pigments are stored in the phycobilisome inside the cell, Marcati et al. (2014) reported the co-extraction of EPS and B-phycoerythrin in absence of an intense cell disruption step. The use of two broad-spectrum proteases led to the removal of 80% of the proteins, resulting in the EPS fraction. A higher contribution of ash was observed in this EPS fraction, probably resulting from buffer salts of the protease treatment which were not completely removed by dialysis. Next to the extracellular fractions, CWPS were obtained and fractionated using a hot water fractionation. Most of the CWPS were soluble in hot water, as wsCWPS accounted for 76% of the total CWPS weight. Moreover, this fraction was the purest fraction obtained, with low amounts of ash and proteins. In contrast, wiCWPS only presented 10% of polysaccharides and was mainly composed of residual proteins and ash after the extraction.

It should be noted that the reported protein contents are probably an overestimation, since the traditional nitrogen-to-protein conversion factor of 6.25 was used. This conversion factor was selected instead of 4.78, i.e. the average conversion factor for microalgal biomasses, under the assumption that the amount of non-protein nitrogen in the isolated cell wall fractions is negligible. In fact, the major sources of non-protein nitrogen in microalgae are inorganic nitrogen (e.g. nitrate, nitrite, ammonia), nucleic acids, and chlorophylls (Lourenço et al., 2004), which were assumed to be removed during the extraction protocol and dialysis steps. However, since the amount of minerals was remarkably high in these fractions, it is expected that the removal of smaller molecules during dialysis was impeded, probably due to the viscous behavior of these cell wall fractions. The incomplete removal of non-protein nitrogen sources might therefore result in an overestimation of the protein contents in all fractions.

Since substantial amounts of ash were observed in most cell wall fractions, the composition of minerals was also analyzed. The amounts of mono- and divalent cations in the different cell wall fractions are shown in **Fig. 4.4**. In fact, the presence of intrinsic minerals might influence the physicochemical properties of polysaccharide suspensions, as specific cations play an important role in the stabilization of electrostatic repulsions and in the gelation of negatively charged polysaccharides (Beckett, 2012). Both extracellular fractions mainly contained the divalent cations calcium and magnesium. Moreover, an increased sodium content was observed for

EPS, resulting from the phosphate buffers used in the protease treatment. While low mineral amounts were observed for wsCWPS, the high ash content in wiCWPS was largely due to calcium and iron, which were probably strongly bound to the polysaccharides in the wiCWPS fraction.

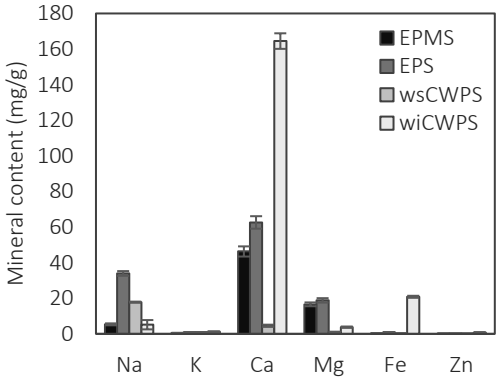

Fig. 4.4 Mineral composition of different fractions isolated from *Porphyridium cruentum* (EPMS: extracellular polymeric substances; EPS: extracellular polysaccharides; wsCWPS: water soluble cell wall polysaccharides; wiCWPS: water insoluble cell wall polysaccharides).

4.3.2 Molecular characterization of the cell wall related polysaccharides

The polysaccharides in the different fractions were characterized in terms of monosaccharide and uronic acid composition, sulfate ester content, and molecular weight distribution. The monosaccharide and uronic acid profiles are presented in **Fig. 4.5**. All fractions were mainly composed of galactose, glucose, xylose, and glucuronic acid. These sugars were previously reported by several authors as the main constituents in EPS of *Porphyridium* sp. in similar ratios (Geresh et al., 2002, 2009; Patel et al., 2013). Interestingly, wsCWPS showed exactly the same monosaccharide profile as the extracellular fractions, while a different ratio of galactose and xylose was observed in wiCWPS. This suggests that the difference in solubility of extracellular and CWPS is not related to the monosaccharide composition. Although the same monosaccharides were present in all fractions, they might be differently organized into polysaccharide chains with a distinct molecular structure, possibly resulting in different solubilities. Moreover, the solubility might be related to the sulfate ester content, as differences in sulfate ester groups were observed among the different samples. In **Fig. 4.3**, sulfate groups are presented as a weight percentage of each fraction. However, as the yield of polysaccharide largely differed for all fractions, the molar ratios of sulfate groups to monosaccharides and uronic acids might be a better comparison among the different cell wall fractions. A larger ratio was observed for EPMS (0.23) compared to wsCWPS (0.18). In other words, whereas one out of four monosaccharide residues in the extracellular fraction is sulfated, only one out of five

monosaccharides contains a sulfate group in wsCWPS. In fact, it was previously reported that as the sulfate content of *Porphyridium* sp. polysaccharides increased, their solubility in NaCl solutions increased (Geresh et al., 1992). Although sulfate contents of 4 – 14% w/w are generally found in literature for *Porphyridium* sp. EPS (de Jesus Raposo et al., 2015; Geresh and Arad, 1991), several reports did not specify the purity of the isolated fractions and might therefore underestimate the amount of sulfated sugar residues.

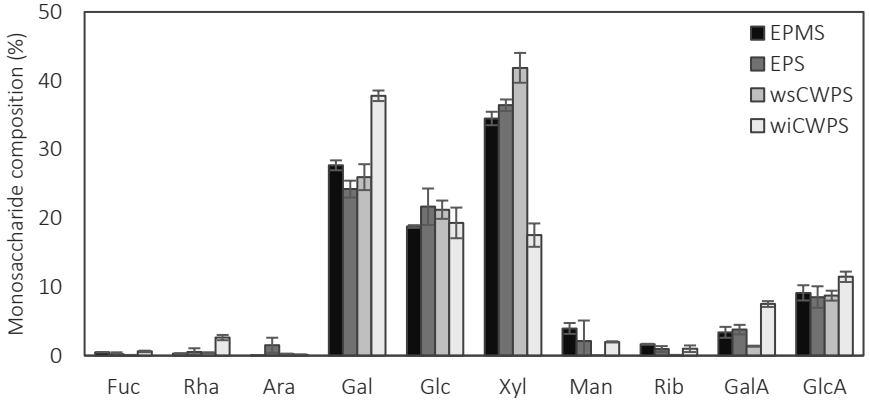

Fig. 4.5 Monosaccharide and uronic acid composition in different fractions of *Porphyridium cruentum*, expressed as a percentage of total monosaccharides and uronic acids (%). (EPMS: extracellular polymeric substances; EPS: extracellular polysaccharides; wsCWPS: water soluble cell wall polysaccharides; wiCWPS: water insoluble cell wall polysaccharides)

The molecular weight distributions of the polymers in the different cell wall fractions are presented in **Fig. 4.6**. Results of wiCWPS are not shown due to a very low recovery, since a large part of the sample was retained in the filtration step prior to HPSEC-analysis. High recoveries were obtained for the other cell wall fractions, being 75.6% for EPMS, 75.2% for EPS and 89.2% for wsCWPS. It is clear from **Fig. 4.6** that similar elution profiles were observed for the two extracellular fractions, with two populations of larger polymers eluting between 32 and 50 min with peak maxima at ~35 and 41 min, and three populations of smaller compounds eluting after 60 min. From the UV absorbance at 280 nm, it was inferred that the populations of larger polymers were only composed of polysaccharides, whereas proteins were present in the fraction eluting after 60 min. In this region, the UV absorbance was clearly lower for EPS compared to EPMS, confirming the successful removal of substantial amounts of proteins by the protease treatment. The weighted-average molecular weight was determined using data between 32 and 50 min, since compounds eluting after 60 min are not expected to be polymers (Jamsazzadeh Kermani et al., 2015). Comparable molecular weight distributions were observed for both extracellular fractions, with weighted-average molecular weights of 1.70×10^6 g/mol and 1.40×10^6 g/mol for

EPMS and EPS, respectively. These values are in the same order of magnitude as reported by Geresh et al. (2002). The molar mass profiles (slanting lines) showed a very small slope, suggesting populations of polymers with a similar molecular weight but a distinct hydrodynamic volume, as concluded from the different elution times. The same observation was made by the above-mentioned authors and they ascribed it to aggregation of polysaccharide molecules preventing size separation (Geresh et al., 2002). In general, both extracellular fractions possessed high molecular weight polysaccharides, which could give rise to interesting physicochemical properties.

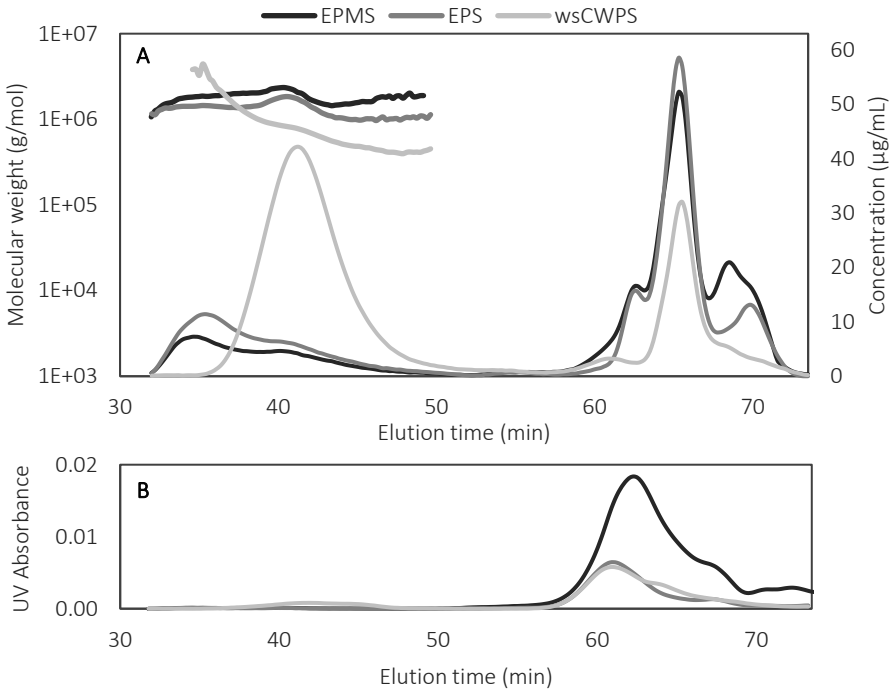

Fig. 4.6 Molecular weight distribution of polymers in different fractions isolated from *Porphyridium cruentum* (EPMS: extracellular polymeric substances; EPS: extracellular polysaccharides; wsCWPS: water soluble cell wall polysaccharides). Molecular weight (thick lines) and concentration (thin lines) **(A)** and UV absorbance at 280 nm **(B)** are presented as a function of elution time. Between 75.2% and 89.2% of the samples were recovered by HPSEC-MALLS-RI.

A different elution profile was observed for wsCWPS, showing a unimodal distribution of large polymers eluting between 36 and 50 min with peak maxima at 42 min, indicating that the hydrodynamic volume of wsCWPS polymers is smaller compared to those in the extracellular fractions. Moreover, a steady decrease in molecular weight with increasing elution time was observed for this fraction, indication that a larger hydrodynamic volume was related with a larger molecular weight. The higher

concentration of polymers eluting at 36 – 50 min can be ascribed to the higher polysaccharide purity of this fraction, as previously mentioned. The presence of proteins, although limited, was evidenced by a small UV absorbance peak in this region. A weighted-average molecular weight of 0.75×10^6 g/mol was observed for wsCWPS, being significantly smaller ($P < 0.05$) than that of the extracellular fractions. This is interesting given that the wsCWPS fraction exhibited a similar monosaccharide profile as the extracellular fractions, and suggests a distinct molecular organization of these sugars into polysaccharide chains compared to the extracellular fractions.

The use of a viscosity detector attached to the HPSEC-MALLS allowed quantification of the intrinsic viscosity of the eluting polymers. No significant differences were observed between the intrinsic viscosity of both extracellular fractions, being 46.62 ± 3.06 dL/g for EPMS and 50.62 ± 1.37 dL/g for EPS. Since the removal of proteins did not influence the intrinsic viscosity, the viscous behavior can be ascribed to the polysaccharides in these fractions. The results obtained in the current study are somewhat higher than previously reported values for EPS of *Porphyridium* sp. (20.9 – 42 dL/g) (Eteshola et al., 1996; Heaney-Kieras and Chapman, 1976). To evaluate the potential of the *Porphyridium* cell wall fractions as food hydrocolloids, the intrinsic viscosities are compared to different commercially used texturizers in **Fig. 4.7**. EPS of *Porphyridium cruentum* possessed high intrinsic viscosities in comparison with conventional thickeners, such as alginates (6 – 17.2 dL/g), locust bean gums (7.7 – 11.2 dL/g), and guar gums (0.7 – 15 dL/g), but lower than those of xanthan gums (up to 168 dL/g) (Imeson, 1997, 2011; Rao, 2010). These high intrinsic viscosities demonstrate the potential of *Porphyridium* sp. polysaccharides as a thickening agent in food products.

A lower intrinsic viscosity of 7.13 ± 0.14 dL/g was observed for wsCWPS, which is not surprising since intrinsic viscosity is directly related to the molecular weight of the polymer (Saha and Bhattacharya, 2010). Nevertheless, the value obtained is still in the range of the abovementioned thickening agents. However, it should be noted that intrinsic viscosity is not related to the ability to form gels. In fact, some of the hydrocolloids shown in **Fig. 4.7** are rather used as gelling agents than as thickening agents, like pectins and guar gum. In spite of their lower intrinsic viscosity, the use of temperature and/or cation addition results in the formation of strong gels, a property which has not yet be appointed to *Porphyridium* sp. EPS. Therefore, these functionalization steps were included in the rheological analyses of the cell wall suspensions discussed in the next paragraph.

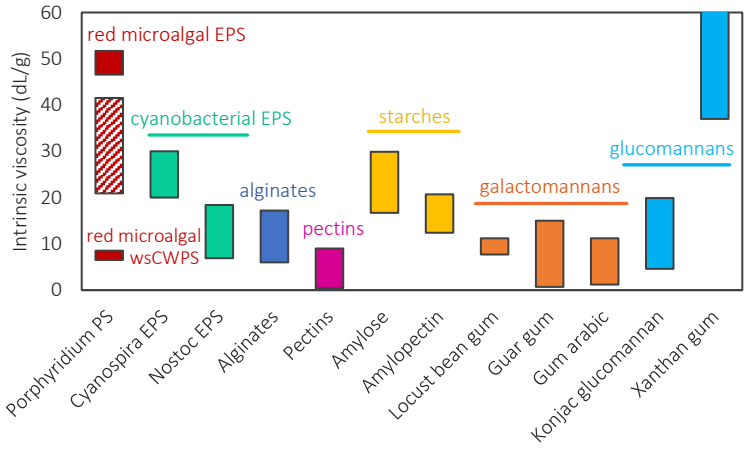

Fig. 4.7 Comparison of intrinsic viscosities of *Porphyridium cruentum* polysaccharides with those of cyanobacterial EPS and common thickening and gelling agents. Intrinsic viscosities obtained in the current chapter are shown in solid red bars for extracellular polysaccharides (EPS) and water soluble cell wall bound polysaccharides (wsCWPS), whereas values of *Porphyridium* sp. EPS found in literature are presented in dashed bars. Intrinsic viscosities of xanthan gum are not completely shown in the graph, but values up to 183 dL/g have been reported. References: BeMiller and Whistler (2009); Cesàro et al. (1990); Eteshola et al. (1996, 1998); Heaney-Kieras and Chapman (1976); Imeson (1997, 2011); Kishida et al. (1978); Parikh and Madamwar (2006); Rao (2010, 2013).

4.3.3 Rheological characterization of the suspensions

The potential of the obtained cell wall fractions as thickening or gelling agents was investigated through rheological analyses. The flow behavior of 2% w/w suspensions of the cell wall fractions is presented in **Fig. 4.8**. Both extracellular fractions (EPMS and EPS) showed shear-thinning flow behavior, i.e. the viscosity decreased with increasing shear rate. Even though the amount of polysaccharides was rather low in these fractions (**section 4.3.1**), the critical overlap concentration C* was exceeded in the 2% w/w suspensions, indicating physical entanglement of the polysaccharides (Saha and Bhattacharya, 2010). As C* is inversely related to the intrinsic viscosity, and thus to the molecular weight of the polymers, a low value of C* was indeed expected for the high molecular weight polymers in the extracellular fractions. Shear-thinning behavior was previously reported by several authors for 1% polysaccharide solutions (Eteshola et al., 1998; Geresh et al., 2002; Liberman et al., 2016). Moreover, suspensions of EPS showed a higher viscosity and a larger shear-thinning degree compared to EPMS. This indicates a higher initial degree of system entanglement (weak network) in the EPS suspension, which is lost when applying higher shear forces. In this context, removal of the proteins resulted in increased thickening

properties, indicating that the viscous behavior can be ascribed to the polysaccharides in this sample. As a consequence, increasing the purity of the extracellular fractions will probably result in a further increase of the viscosity. It is actually obvious from **Fig. 4.8B** that EPS showed a rather constant shear stress in the investigated range of shear rates, in contrast to the other cell wall fractions. Hence, it is likely that the polymer network leads to an apparent yield stress in the EPS suspension, confirming the occurrence of structuring polymer-polymer interactions in the EPS sample. Surprisingly, the suspensions of wsCWPS presented Newtonian flow behavior, implying that C* was not reached and no polymer-polymer interactions were formed in this suspension. Therefore, even though the polysaccharides in wsCWPS exhibited a relatively high weighted-average molecular weight and an appreciable intrinsic viscosity, a higher concentration of this fraction is needed to induce thickening in aqueous solutions.

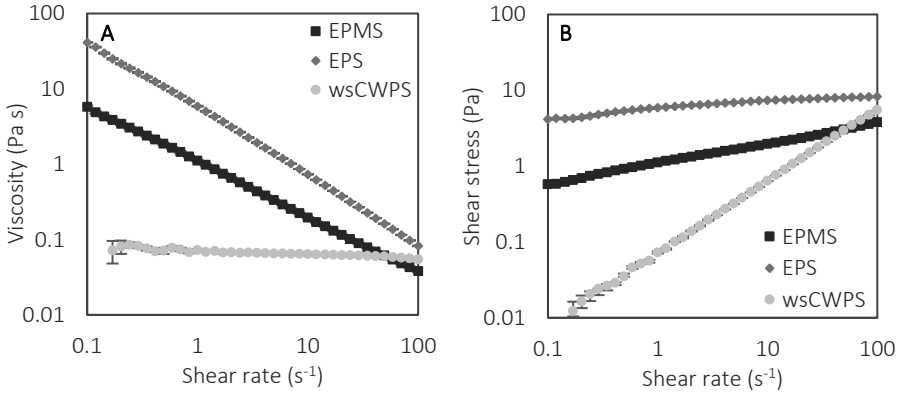

Fig. 4.8 Viscosity curves **(A)** and flow curves **(B)** of suspensions (2% w/w) of different fractions of *Porphyridium cruentum* (EPMS: extracellular polymeric substances; EPS: extracellular polysaccharides; wsCWPS: water soluble cell wall polysaccharides). Only data points with reliable torque values (> 0.1 µN m) are shown.

Dynamic oscillatory measurements were applied to gain insight into the network structure of the suspensions, with strain sweep and frequency sweep curves shown in **Fig. 4.9A** and **4.9B**, respectively. A large linear viscoelastic region was observed from the strain sweep curves of the extracellular fractions, both showing a critical strain above 50%. In addition, predominant elastic behavior was observed, since values for the storage modulus (G') exceeded those of the loss modulus (G'') in this region. This elastic behavior was more pronounced for EPS compared to EPMS. In contrast, viscous behavior was observed for wsCWPS, with a constant loss modulus and $G' < G''$ over the whole range of shear strains explored.

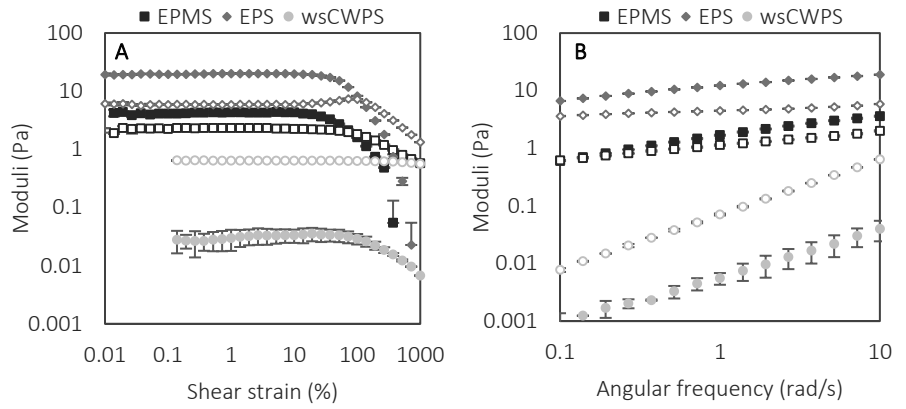

Fig. 4.9 Strain sweep curves **(A)** and frequency sweep curves **(B)** showing storage moduli (G', filled symbols) and loss moduli ($G"$, empty symbols) for suspensions (2% w/w) of different fractions from *Porphyridium cruentum* (EPMS: extracellular polymeric substances; EPS: extracellular polysaccharides; wsCWPS: water soluble cell wall polysaccharides). Strain sweeps were performed at a constant angular frequency of 10 rad/s. Frequency sweeps were determined at a constant shear strain of 2%, within the linear viscoelastic region. Only data points with reliable torque values (> 0.1 µN m) are shown.

To determine the frequency dependence of the moduli, data of the frequency sweeps were fitted by a power law model:

$$G' = a \cdot \omega^c \qquad \textbf{(Eq. 4.1)}$$

$$G" = b \cdot \omega^d \qquad \textbf{(Eq. 4.2)}$$

with ω the angular frequency (rad/s), and a, b, c, and d model parameters. Parameters a and b provide insight into the strength of the network, whereas parameters c and d describe the gel behavior (Larson, 1999). The estimated model parameters for the different fractions are presented in **Table 4.2**. Limited gel behavior was observed for the EPMS suspension. Even though the frequency dependency was rather low (parameter $c < 0.5$), the ratio of $G"/G'$ indicates no dominant elastic behavior, as also observed from similar values for parameters a and b. In contrast, removal of proteins led to a more gel-like structure in EPS, as parameters c and d further decreased. Moreover, the strength of the network largely increased, with parameter a almost ten times higher compared to the EPMS suspension. The network cannot be considered as a true gel, which would be characterized by a clear independence of the angular frequency ($G' \propto G" \propto \omega^0$) and a ratio of $G"/G'$ in the order of 10^{-2}. Instead, the EPS suspension showed a behavior of a weak gel, describing systems falling between covalently crosslinked materials and entanglement networks. In a weak gel, polymer chains are typically physically crosslinked into networks, but the crosslinks are of small finite energy and/or finite lifetime (Kavanagh and Ross-

Murphy, 1998; Lizarraga et al., 2006). In contrast to the structured EPS suspension, wsCWPS presented typical behavior of a viscoelastic fluid, with $G' \propto \omega^2$ and $G'' \propto \omega^1$. Moreover, the value of parameter a was even approaching 0, implying that no elastic behavior was exhibited by this suspension (Lizarraga et al., 2006). This corresponds to the observed flow behavior of an ideal Newtonian viscous fluid (**Fig. 4.8**). In other words, no physical crosslinks or entanglements of wsCWPS polymers occurred in the 2% w/w suspension, indicating the limited potential of this fraction as a thickening or gelling agent.

Table 4.2 Parameters a, b, c, and d (± standard error) of the power law models ($G' = a \cdot \omega^c$ and $G'' = b \cdot \omega^d$) fitted to the storage modulus (G') and loss modulus (G'') as a function of the angular frequency (ω). Suspensions of different fractions isolated from *Porphyridium cruentum* were prepared at a concentration of 2% w/w (EPMS: extracellular polymeric substances; EPS: extracellular polysaccharides; wsCWPS: water soluble cell wall polysaccharides). The estimated values of the model parameters were compared statistically by use of 95% confidence intervals. All values were significantly different.

	a	b	c	d
EPMS	1.63 ± 0.02	1.12 ± 0.01	0.36 ± 0.01	0.24 ± 0.01
EPS	11.93 ± 0.07	4.52 ± 0.02	0.21 ± 0.01	0.10 ± 0.01
wsCWPS	0.0004 ± 0.0003	0.06 ± 0.01	1.64 ± 0.15	1.00 ± 0.01

Finally, attempts were made to improve the rheological properties, since several hydrocolloids require cations or heating-cooling cycles to induce gelation. In fact, the three main mechanisms proposed for gelation of hydrocolloids are ionotropic gelation (typically cation-mediated gelation), cold-set gelation, and heat-set gelation. The latter mechanism consists of heating a hydrocolloid dispersion to induce gelation, typically by unfolding or expansion of starch and proteins into an arranged network, but is also known for some polysaccharide systems such as konjac glucomannan and methyl cellulose. In contrast, cold-set gelation requires cooling of a warm hydrocolloid dispersion to form inter-chain helices, resulting in a stable three-dimensional network. Typical examples of such hydrocolloids are agar and gelatin (Saha and Bhattacharya, 2010). Temperature sweeps of EPS and wsCWPS suspensions are presented in **Fig. 4.10**, showing the storage and loss moduli during heating, holding, and cooling phases. Given that no drastic changes in gelling behavior were observed during the heating-cooling cycles, it was concluded that cold-set gelation and heat-set gelation mechanisms were not prominent in solutions of these cell wall fractions of *Porphyridium cruentum*.

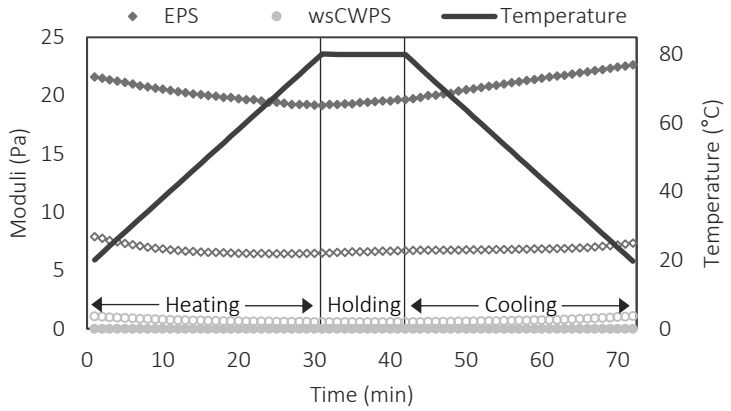

Fig. 4.10 Temperature sweeps of suspensions (2% w/w) of different fractions of *Porphyridium cruentum* (EPS: extracellular polysaccharides; wsCWPS: water soluble cell wall polysaccharides). Temperature was increased from 20 to 80 °C (2 °C/min), kept constant at 80 °C for 10 min, and cooled from 80 to 20 °C (2 °C/min). Storage modulus (G', filled symbols) and loss modulus (G'', empty symbols) were determined at a constant angular frequency of 10 rad/s and a constant shear strain of 5%, within the linear viscoelastic region.

To investigate possible gelation through a cation mediated gelation mechanism, suspensions were prepared in presence of different cations (Na^+, K^+ and Ca^{2+}). This was based on the fact that distinct hydrocolloids such as carrageenans, alginates, and pectins require different cations for successful gelation (Imeson, 1997, 2011; Saha and Bhattacharya, 2010). In the current study, no increases in viscosity or viscoelastic moduli were observed for any of the fractions in presence of different cations, either with or without heating-cooling cycles (data not shown). Eteshola et al. (1998) even reported a decreased viscosity in presence of NaCl, KCl or $CaCl_2$, however, highly concentrated electrolyte solutions were used in that study. Liberman et al. (2016) reported that the addition of Zn^{2+} only led to screening of negative charges of the polysaccharides, resulting in a slight viscosity increase, but did not lead to any network formation. The authors concluded that a low concentration of Zn^{2+} (250 ppm) was sufficient to screen most of these charges, while further addition of ions did not affect the viscosity (Liberman et al., 2016). In the current study, intrinsic cations were present in high amounts in all cell wall fractions (**Fig. 4.4**), implying that additional cations probably did not play a role in the screening of electrostatic repulsions of negatively charged carboxylic groups or sulfate groups of the polysaccharide chains, as no changes in viscosity were observed. Removal of intrinsic cations in combination with additional rheological measurements of suspensions at different pH values could be performed to confirm this hypothesis.

4.4 CONCLUSIONS

Different cell wall fractions, including two extracellular fractions and two cell wall bound fractions, were obtained from the red microalga *Porphyridium cruentum*. EPS were characterized by a population of high molecular weight polymers with high intrinsic viscosities. Even though wsCWPS exhibited the same monosaccharide composition as the extracellular fractions, the sugar residues in the former were probably differently organized into polysaccharide chains, resulting in polymers with lower molecular weights and lower intrinsic viscosities. These differences in polysaccharide characteristics resulted in distinct rheological properties. Whereas polysaccharide solutions of EPS displayed high viscosities and a weak gel structure, wsCWPS suspensions exhibited Newtonian flow behavior. As a consequence, wsCWPS of *Porphyridium* sp. showed limited potential as a thickening agent for food applications, in contrast to the EPS fractions.

Even though the applied extraction procedures resulted in excessive co-extraction of proteins and minerals, with a polysaccharide content below 50% for most fractions, substantial viscosities were observed for EPS suspensions. As predicted by the high intrinsic viscosity of these polysaccharides, comparable or even higher than those of commercially used hydrocolloids, purified EPS might be a sustainable source of new thickening or gelling agents for food applications. However, purification of the cell wall fractions will be of critical importance to maximally exploit their functionality.

PART III

MICROALGAL BIOMASS AS STRUCTURING AGENT

CHAPTER 5

Rheological characterization of microalgal suspensions upon processing

5.1 INTRODUCTION

In contrast to the use of microalgal polysaccharides as food hydrocolloids, the incorporation of the whole microalgal biomass is proposed as a more attractive and more sustainable approach for introduction of microalgal polymers in food products. As a matter of fact, beside enrichment of food with structural biopolymers, several nutrients and health-beneficial components are also introduced, improving the nutritional value of the food product. In addition, the use of exhaustive extraction protocols, polluting solvents, and generated waste streams are avoided. However, the rheological properties of microalgal biomasses (in aqueous model systems or in real food matrices) have been very limitedly studied, as reviewed in Chapter 1.

With the aim of using microalgal biomass as a functional ingredient in food applications, fundamental knowledge is also required about their rheological behavior upon processing. In this context, mechanical and thermal processing represent the most conventional food processing operations. Whereas mechanical processing is often applied for functionalization of food products, e.g. reducing oil droplet size in milk products or creating desired structural properties of vegetable based products, thermal processing is a conventional preservation technique in food processing to create shelf-stable food products (Lopez-Sanchez et al., 2011; Simpson, 2009). To ensure the shelf life stability of the food products, both safety and quality

This chapter is based on the following paper:
Bernaerts T.M.M., Panozzo A., Doumen V., Foubert I., Gheysen L., Goiris K., Moldenaers P., Hendrickx M.E., Van Loey A.M. (2017)
Microalgal biomass as a (multi)functional ingredient in food products: Rheological properties of microalgal suspensions as affected by mechanical and thermal processing.
Algal Research, 25, 452-463.
[2017 Impact Factor = 3.745; Ranked 38/161 (Q1) in Biotechnology and Applied Microbiology]

should be guaranteed, targeting pathogenic and spoilage microorganisms, respectively. The presence and/or growth of these microorganisms is determined by the intrinsic properties of the product, such as pH. Generally, low-acid foods (pH > 4.5) require a sterilization process, targeting a 12 log reduction of the spore forming microorganism *Clostridium botulinum*. Acid foods (pH < 4.5) on the contrary are preserved by a less intense pasteurization process, usually targeting the spoilage organism *Alicyclobacillus acidoterrestris* (Simpson, 2009). As a consequence, these differences in intensity of thermal processing might result in distinct rheological characteristics. However, to the best of our knowledge, the impact of mechanical and thermal processing on the rheological properties of microalgal biomass suspensions has not been studied before.

Therefore, the objective of this chapter is to characterize the rheological behavior of several commercially interesting microalgae species in aqueous suspensions. On the one hand, acid food systems such as fruit juices and acidified food products were simulated by adjusting the pH of the suspensions to 4. On the other hand, suspensions at pH 6 were included to mimic low-acid to neutral food systems, such as vegetable based foods and dairy products. Both viscoelastic behavior (under small deformations) and flow behavior (under larger deformations) were studied. In addition, the effect of HPH and thermal processing on the rheological properties and particle characteristics of the microalgal suspensions was investigated. The intensity of the thermal treatments was based on industrial thermal processes used in the food industry. As such, the understanding of the rheological behavior before and after processing will provide the scientific knowledge base for the selection of appropriate microalgae species for food applications.

5.2 MATERIALS AND METHODS

5.2.1 Microalgal biomass

Seven microalgae species were investigated in the current chapter (*Arthrospira platensis*, *Chlorella vulgaris*, *Nannochloropsis* sp., *Odontella aurita*, *Phaeodactylum tricornutum*, *Porphyridium cruentum*, and *Schizochytrium* sp.), for which the same batch of biomass has been used as those in Chapter 2.

5.2.2 Preparation and processing of microalgal aqueous suspensions

A schematic overview of the preparation and processing of the microalgal aqueous suspensions is presented in Fig. 5.1.

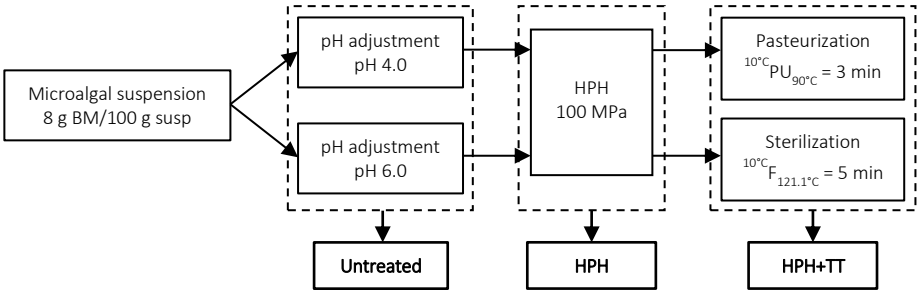

Fig. 5.1 Schematic overview of the preparation and processing of microalgal aqueous suspensions. Boxes with 'Untreated', 'HPH', and 'HPH+TT' indicate the moment of collecting respective samples (HPH: high pressure homogenization; TT: thermal treatment).

5.2.2.1 Preparation of microalgal aqueous suspensions

Dry microalgal biomasses were suspended overnight in demineralized water by gentle stirring and the pH of the suspension was adjusted to pH 4 or 6 using HCl. Demineralized water was subsequently added to obtain a final concentration of 8 g biomass per 100 g suspension (8% w/w). The systems were then mixed for 10 min at 3500 rpm (except for *Porphyridium cruentum* 10 min at 5500 rpm) with a lab mixer (Silverson L5M-A, East Longmeadow, MA, USA) to obtain a homogeneous suspension. The obtained suspensions at respective pH were considered as untreated suspensions. All suspensions were prepared in duplicate.

5.2.2.2 Mechanical treatment

Microalgal suspensions were mechanically treated by HPH (Panda 2K, Gea Niro Soavi, Parma, Italy) at 100 MPa for a single pass. The inlet of the homogenizer was thermostated at 4 °C using a cryostat (Haake, Karlsruhe, Germany) and homogenized samples were collected in an ice water bath.

5.2.2.3 Thermal treatment

Homogenized suspensions were thermally treated by either a pasteurization (suspensions at pH 4) or a sterilization process (suspensions at pH 6). Thermal treatments were performed in a pilot-scale water-cascading retort (Barriquand Steriflow, Paris, France). Glass jars (95 mm height, 45 mm diameter) were filled with 80 mL of suspension and closed with metal lids. Temperature profiles were recorded both in the retort and in the coldest point of the jar using type T thermocouples and registered by the Ellab Valsuite Plus software (Ellab, Hillerød, Denmark).

The intensity of the thermal treatments was chosen based on industrially relevant thermal processing for shelf-stable food products. Suspensions at pH 4, simulating

acid food matrices, were pasteurized at 90 °C to obtain a process value of $^{10\,°C}PU_{90\,°C}$ = 3 min. For suspensions at pH 6, representing low-acid food products, a sterilization process at 121 °C was selected with a process value of $^{10\,°C}F_{121.1\,°C}$ = 5 min. Temperature profiles of pasteurization and sterilization processes are presented in Fig. 5.2 for *Nannochloropsis* sp. (showing the fastest heat transfer) and *Porphyridium cruentum* (showing the slowest heat transfer). Before starting the heating phase, each sample was equilibrated to 40 °C to avoid extensive temperature gradients in the jars. Due to differences in heat transfer characteristics of the investigated microalgae species, the length of the thermal processes (including equilibration, heating phase, holding phase, and cooling phase) varied from 44 to 84 min for the pasteurization process, and between 70 and 94 min for the sterilization process.

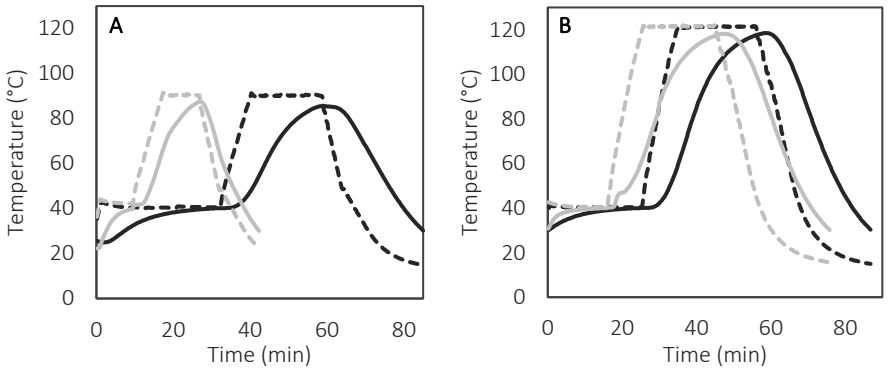

Fig. 5.2 Temperature profile of a **(A)** pasteurization and **(B)** sterilization process for *Nannochloropsis* sp. (gray) and *Porphyridium cruentum* (black). Dashed lines represent the temperature profile within the retort, while solid lines represent the temperature profile as measured in the sample.

5.2.3 Rheological measurements

5.2.3.1 Rheological characterization of microalgal suspensions

Prior to rheological analyses, stability of the suspensions against creaming or sedimentation was checked for 30 min, i.e. the longest time of a rheological measurement, by use of a Turbiscan MA 2000 (Formulaction, L'Union, France). None of the suspensions showed significant creaming or sedimentation within this time frame.

The rheological properties of the microalgal suspensions were then analyzed with a stress-controlled rheometer (MCR 302, Anton Paar, Graz, Austria) at 25 °C. The concentric cylinder Couette (CC27, diameter 26.6 mm and measuring height 40.0 mm) was used as measuring system. A standardized volume of 22 mL suspension was loaded into the cup (diameter 28.9 mm) for each measurement. To avoid effects of loading on the structure, samples were presheared for 30 s at a shear rate of 20 s^{-1} followed by 120 s of rest, i.e. shear rate of 0 s^{-1}, before each measurement. A minimum torque limit was fixed at 0.1 µN m to ensure reliability of the obtained data.

The viscoelastic behavior of the suspensions was studied by oscillatory shear measurements. First, the linear viscoelastic region was determined by performing a strain sweep test at a constant angular frequency of 10 rad/s and a logarithmically increasing shear strain from 0.01 to 1000%. A constant shear strain of 1% within the linear viscoelastic region was then selected for the frequency sweep, with the exception of untreated suspensions of *Odontella aurita* for which a constant shear strain of 0.139% was used. The frequency sweep test was performed to determine the frequency dependence of storage and loss moduli, by decreasing the angular frequency logarithmically from 100 to 0.1 rad/s.

The flow behavior of the suspensions was studied by steady-shear measurements, with logarithmically increasing shear rate from 0.1 to 100 s^{-1}. During this test, 50 measuring points were recorded and each shear rate was applied for 10 s.

All measurements were performed in duplicate. A fresh sample was loaded into the cup for each measurement.

5.2.3.2 Viscosity measurements of the serum phase

Microalgal suspensions were centrifuged for 30 min at 10000g and 25 °C (J2-HS centrifuge, Beckman, CA, USA) in order to separate particles from the continuous phase. The supernatant was collected and denoted as serum phase. The absence of large particles was validated by analyzing particle size distributions (data not shown).

Viscosity of the serum phase was measured with a stress-controlled rheometer (MCR 302, Anton Paar, Graz, Austria) using the double wall Couette geometry (DG26.7, internal radius 12.3 mm, external radius 13.3 mm, and measuring height 40 mm). A standardized volume of 6.5 mL serum was loaded into the cup (internal diameter 23.8 mm, external diameter 27.6 mm) for each measurement. Shear rate was increased logarithmically from 0.1 to 100 s^{-1} and each shear rate was applied for 10 s. Preshear conditions as described in section 5.2.3.1 were used.

5.2.4 Characterization of the microstructure

5.2.4.1 Particle size distribution

Particle size distribution was analyzed by laser diffraction (Beckman Coulter LS 13 320, Miami, FL, USA). Sample was added to a stirring tank filled with deionized water and was pumped through the measuring cell at 30% pump speed, where particles were scattered by the laser light (wavelength of main illumination source: 750 nm; wavelengths of halogen light for polarization intensity differential scattering: 450 nm, 600 nm, 900 nm). Volumetric particle size distributions were calculated with the Fraunhofer optical model by use of instrument software. All measurements were carried out in duplicate.

5.2.4.2 Differential interference contrast microscopy

The microstructure of the samples was visualized by differential interference contrast (DIC) microscopy, using an Olympus BX-51 light microscope equipped with a XC-50 digital camera (Olympus, Optical Co.Ltd., Tokyo, Japan) and visualized using Cell^F software. An objective of 100× was used and at least ten images were obtained for each sample.

5.2.5 Statistical analysis

All treatments of the microalgal suspensions were performed in duplicate and for each individual sample, analyses were done in duplicate. As a result, the obtained data are presented as the mean of four measurements ± standard error. The flow curves of the untreated suspensions were fitted to rheological models using linear and non-linear regression procedures with SAS statistical software (SAS 9.4, Cary, NC, USA). The estimated model parameters of different samples were statistically compared by using 95% confidence intervals. Differences in mean values for viscosity of mechanically and/or thermally treated suspensions were statistically analyzed using one-way ANOVA combined with Tukey's test for multiple comparison ($P < 0.05$) with JMP statistical software (JMP Pro 12, Cary, NC, USA).

5.3 RESULTS AND DISCUSSION

5.3.1 Rheological characterization of untreated suspensions

The rheological behavior of microalgal suspensions was characterized on two levels. On the one hand, small amplitude oscillatory measurements were performed to study the linear viscoelastic behavior of the suspensions. In this case, small deformations were applied to gain insight into the network structure, without disturbing the structural properties of the system. By applying deformations within the linear

viscoelastic region, the original structure of the suspensions could be characterized. On the other hand, the flow behavior was studied under larger deformations. This non-linear flow behavior can be related to food operations, including unit operations like mixing and pumping, as well as chewing and swallowing during consumption of a food product (Steffe, 1996).

5.3.1.1 Linear viscoelastic behavior

Small amplitude oscillatory measurements were performed to gain insight into the network structure of the microalgal suspensions. First, a strain sweep test was executed to determine the linear viscoelastic region. Strain sweep curves of *Arthrospira platensis*, *Chlorella vulgaris*, *Odontella aurita*, and *Porphyridium cruentum* are presented in **Fig. 5.3**, while no reliable torque values (> 0.1 µN m) were observed for the other microalgae species. In these graphs, a zone of linear viscoelasticity could be observed as a plateau at low shear strains, with storage modulus (G') and loss modulus (G'') independent of the shear strain. In this linear viscoelastic region, suspensions of *Chlorella vulgaris*, *Odontella aurita*, and *Porphyridium cruentum* at both pH values showed $G' > G''$, indicating predominantly elastic behavior. In contrast, untreated suspensions of *Arthrospira platensis* at pH 6 displayed predominantly viscous behavior ($G' < G''$). Further increase of the shear strain led to a decrease of both G' and G'' for Arthr*ospira platensis*, *Chlorella vulgaris*, and *Odontella aurita*, showing that at these deformations the network structure was destroyed, typical for polymeric systems. In contrast, *Porphyridium cruentum* showed an increase in G'' together with a decrease of G' at the end of the linear viscoelastic region, characterized as typical suspension behavior.

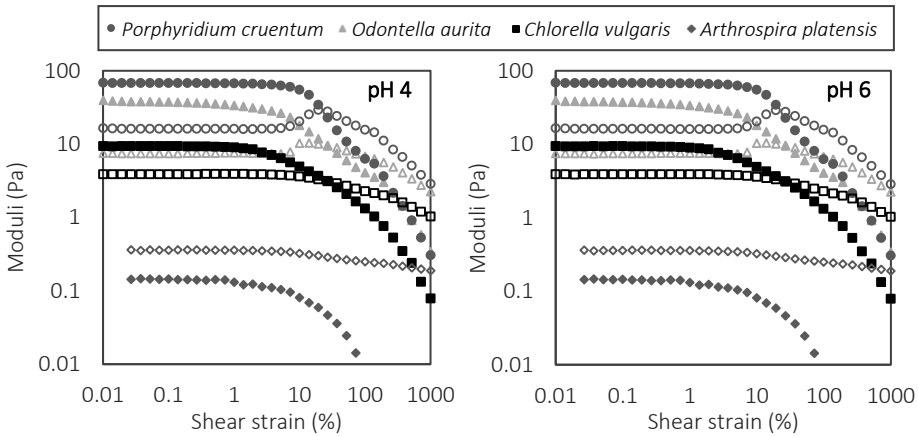

Fig. 5.3 Strain sweeps at a constant angular frequency of 10 rad/s of untreated suspensions at pH 4 and pH 6, showing storage modulus (G', filled symbols) and loss modulus (G'', empty symbols) as a function of shear strain.

Frequency sweep curves of *Chlorella vulgaris*, *Porphyridium cruentum*, and *Odontella aurita* suspensions at both pH values are presented in **Fig. 5.4**. These suspensions showed an elastic-like behavior with $G' > G''$ over the complete range of angular frequencies. Since the other microalgae species did not display reliable torque values over the whole range of angular frequencies, they will not be further discussed in this paragraph.

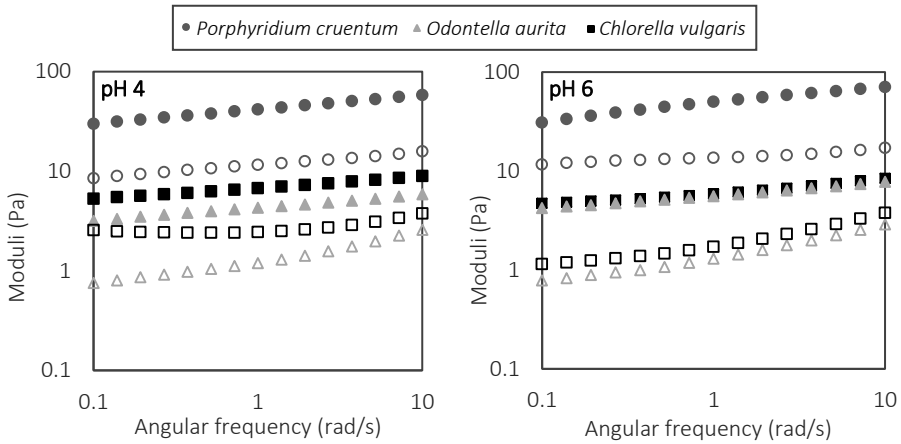

Fig. 5.4 Frequency sweeps of untreated suspensions at pH 4 and pH 6, showing storage modulus (G', filled symbols) and loss modulus (G'', empty symbols) as a function of the angular frequency.

To determine the frequency dependence of G' and G'', data of the frequency sweep were fitted by a power law model (**Eq. 4.1** and **Eq. 4.2**), and estimates for the model parameters are presented in **Table 5.1**. The discussion will mainly focus on the frequency dependence of G', since G'' values are more sensitive to inertia phenomena of the measuring system when analyzing samples with limited structural properties.

All suspensions showed similar values of parameter c and thus a similar frequency dependence of G'. With these values ranging between 0.11 and 0.17 and with $G' > G''$ over the whole range of angular frequencies, the rheological behavior of these suspensions coincides with that of weak gels. Indeed, whereas viscoelastic fluids exhibit high frequency dependence with $G' \propto \omega^2$ and $G'' \propto \omega^1$ at low angular frequencies, parameters c < 0.5 indicate the transition towards solid-like behavior (Kavanagh and Ross-Murphy, 1998; Larson, 1999). According to Kavanagh and Ross-Murphy (1998), a weak gel consists of chains which are physically crosslinked into networks, but the crosslinks are of small finite energy and/or of finite lifetime. Next to possible covalent crosslinks, non-covalent crosslinks might also be present in these microalgal suspensions. It is clear that none of these microalgal suspensions can be described as a true gel of covalently crosslinked networks, which would show a clear

independence of the angular frequency with $G' \propto G'' \propto \omega^0$. The ratio of G''/G' at low angular frequency (ω = 0.1 rad/s) was between 0.19 and 0.49, comparable to that of weak gels (order of 10^{-1}) (Lizarraga et al., 2006).

Table 5.1 Parameters a, b, c, and d (± standard error) of the power law models ($G' = a \cdot \omega^c$ and $G'' = b \cdot \omega^d$) fitted to the storage modulus (G') and loss modulus (G'') as a function of the angular frequency (ω) of the untreated suspensions of *Porphyridium cruentum*, *Odontella aurita*, and *Chlorella vulgaris*.

		a	b	c	d
Porphyridium cruentum	pH 4	41.64 ± 1.31	11.53 ± 0.26	0.15 ± 0.02	0.13 ± 0.02
	pH 6	48.62 ± 0.20	13.73 ± 0.05	0.17 ± 0.01	0.08 ± 0.01
Odontella aurita	pH 4	4.28 ± 0.15	1.25 ± 0.03	0.13 ± 0.02	0.29 ± 0.01
	pH 6	5.61 ± 0.31	1.35 ± 0.05	0.13 ± 0.04	0.31 ± 0.02
Chlorella vulgaris	pH 4	6.77 ± 0.18	2.68 ± 0.06	0.11 ± 0.02	0.09 ± 0.02
	pH 6	6.00 ± 0.04	1.82 ± 0.02	0.13 ± 0.01	0.29 ± 0.01

Higher values of parameters a and b were obtained for *Porphyridium cruentum* than for *Odontella aurita* and *Chlorella vulgaris*. This indicates that a stronger network structure is formed in *Porphyridium cruentum* suspensions, presumably attributed to the presence of sulfated EPS, which have been shown to form weak gel structures in Chapter 4. Values of parameters a and b for *Odontella aurita* suspensions were of the same order of magnitude as *Chlorella vulgaris*. While suspensions of *Porphyridium cruentum* and *Odontella aurita* at pH 6 showed higher values of parameter a compared to pH 4 (and thus a stiffer network structure), the opposite was found for *Chlorella vulgaris*. This might indicate the importance of ionic crosslinks between particles in network formation in these microalgal suspensions.

5.3.1.2 Flow behavior

The flow behavior of the different microalgal suspensions is presented in Fig. 5.5. With both axes in logarithmic scale, deviations from the Newtonian behavior can be easily observed. While *Nannochloropsis* sp. was the only microalga exhibiting Newtonian flow behavior, all other microalgae displayed shear-thinning behavior, as their viscosity decreased with increasing shear rate. Since microalgal suspensions are dispersions of deformable cells and cell debris in a liquid phase containing polymeric substances (e.g. EPS) and dissolved salts, non-Newtonian flow behavior could be expected (Wileman et al., 2012). In addition, *Porphyridium cruentum* suspensions were obviously the most viscous over the whole range of shear rates, followed by suspensions of *Chlorella vulgaris* and *Odontella aurita*.

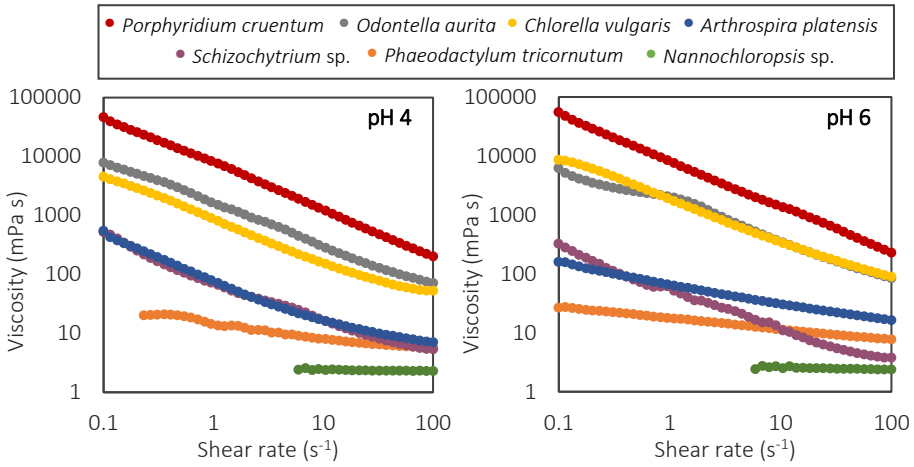

Fig. 5.5 Viscosity curves of untreated suspensions at pH 4 and pH 6 showing viscosity as a function of shear rate for seven microalgae species. Only data points with reliable torque values (> 0.1 µN m) are shown.

To describe the rheological characteristics of the untreated suspensions quantitatively, flow curves were fitted to rheological models. Newtonian, Power Law, and Herschel-Bulkley models are frequently used to describe Newtonian or shear-thinning flow behavior, as presented in **Eq. 5.1**, **Eq. 5.2**, and **Eq. 5.3**, respectively:

$$\sigma = \mu \cdot \dot{\gamma} \qquad \textbf{(Eq. 5.1)}$$

$$\sigma = K \cdot \dot{\gamma}^{n} \qquad \textbf{(Eq. 5.2)}$$

$$\sigma = \sigma_0 + K \cdot \dot{\gamma}^{n} \qquad \textbf{(Eq. 5.3)}$$

with σ the shear stress (Pa), $\dot{\gamma}$ the shear rate (s^{-1}), μ the dynamic viscosity (Pa s), K the consistency coefficient (Pa s^n), n the flow behavior index (-), and σ_0 the dynamic yield stress (Pa). The former two models can be considered as special cases of the Herschel-Bulkley model, with yield stress $\sigma_0 = 0$ and flow behavior index $n = 1$ or $n < 1$ for Newtonian and Power Law model, respectively (Steffe, 1996). To select the appropriate model for each suspension, shear stress was plotted logarithmically as a function of logarithmically increasing shear rate. Since no constant values of log (σ) were reached at low shear rates and thus no clear yield stress was observed, all shear-thinning suspensions were fitted to the Power Law model. The used models and their parameter estimates are presented in **Table 5.2**.

As also observed visually from **Fig. 5.5**, *Nannochloropsis* sp. was the only microalga species presenting Newtonian flow behavior at the examined concentration. Its dynamic viscosity (i.e. consistency coefficient parameter in the Newtonian model)

was low at both pH 4 and 6, approaching the viscosity of pure water (1 mPa s). Hence, it can be inferred that no interactions between particles and only limited solubilization of cell components occurred in *Nannochloropsis* sp. suspensions, presumably related to their rigid uncharged cell wall and the absence of EPS. Newtonian behavior for *Nannochloropsis* sp. was also reported in previous studies, and the critical concentration was actually found to be between 15.8% and 17.7% (Schneider et al., 2016; Wileman et al., 2012). All other microalgal suspensions showed shear-thinning behavior with a flow behavior index $n < 1$. This confirms the observations in the few previous studies on the flow behavior of microalgal suspensions, for *Arthrospira platensis* and *Chlorella* sp. (Chen et al., 2018; Torzillo et al., 1993; Wileman et al., 2012). The smaller the value of n, the larger the deviation from Newtonian behavior. In this regard, the investigated microalgae showed a large variation in rheological properties with n ranging from 0.86 to 0.20. The smallest estimates of n were found for suspensions of *Chlorella vulgaris*, *Odontella aurita*, and especially *Porphyridium cruentum*, the viscosity thus showing the highest dependency on the applied shear rate. Even though the rheological properties of biomass suspensions of *Porphyridium* sp. have not been published before, the explicit shear-thinning behavior observed in the current study is not surprising knowing the rheological characteristics of the EPS as investigated in Chapter 4. No consistent effect of pH on the flow behavior index n was observed among the different microalgal suspensions. Whereas *Chlorella vulgaris* showed smaller values of n for suspensions at pH 6 compared to pH 4, the opposite was observed for *Arthrospira platensis* and *Porphyridium cruentum* suspensions. In contrast, no effect of pH on n was observed for the other microalgae species.

Table 5.2 Consistency coefficient (K) and flow behavior index (n) (± standard error) of the untreated suspensions estimated by Newtonian (N) or Power Law (PL) model. Goodness of fit of linear and non-linear regression is presented as R^2_{adj}. The estimated values of each parameter were compared statistically by use of 95% confidence intervals. Significant differences are indicated with different letters.

		Model	Consistency coefficient (mPa s^n)	Flow behavior index (-)	R^2_{adj}
Nannochloropsis sp.	pH 4	N	2.30 ± 0.01 **(*)**	1 **(**)**	0.99
	pH 6	N	2.40 ± 0.01 **(*)**	1 **(**)**	0.99
Phaeodactylum tricornutum	pH 4	PL	10.86 ± 0.80 **j**	0.86 ± 0.02 **a**	0.98
	pH 6	PL	16.40 ± 1.61 **i**	0.83 ± 0.02 **a**	0.96
Arthrospira platensis	pH 4	PL	50.83 ± 3.23 **gh**	0.55 ± 0.02 **c**	0.96
	pH 6	PL	58.17 ± 0.36 **f**	0.72 ± 0.01 **b**	0.99
Schizochytrium sp.	pH 4	PL	63.30 ± 5.39 **fg**	0.43 ± 0.02 **d**	0.89
	pH 6	PL	45.21 ± 1.89 **h**	0.43 ± 0.01 **d**	0.97
Chlorella vulgaris	pH 4	PL	675.96 ± 21.66 **e**	0.41 ± 0.01 **d**	0.98
	pH 6	PL	1666.04 ± 22.36 **c**	0.35 ± 0.01 **e**	0.99
Odontella aurita	pH 4	PL	1393.29 ± 47.95 **d**	0.32 ± 0.01 **e**	0.97
	pH 6	PL	1687.11 ± 53.22 **c**	0.34 ± 0.01 **e**	0.98
Porphyridium cruentum	pH 4	PL	7735.59 ± 76.79 **b**	0.20 ± 0.01 **g**	0.99
	pH 6	PL	8227.23 ± 55.84 **a**	0.23 ± 0.01 **f**	0.99

(*) Represented as the dynamic viscosity (mPa s) in the Newtonian model

(**) Flow behavior index fixed at 1 by the Newtonian model

Considering the values of the consistency coefficient (K), the microalgae species can be divided into two groups. Untreated suspensions of *Nannochloropsis* sp., *Phaeodactylum tricornutum*, *Schizochytrium* sp., and *Arthrospira platensis* presented only limited consistency at both pH values. In contrast, estimated values for K were about 10 to 100 times higher for suspensions of *Chlorella vulgaris*, *Odontella aurita*, and *Porphyridium cruentum*. Though, care should be taken when comparing the estimated values for K. In fact, these values are expressed in mPa s^n. Due to large variations in non-Newtonian behavior among the examined microalgae species, large differences were found in n which resulted in slightly different units of the consistency coefficient between different microalgae species. Nevertheless, the obtained shear stress at any shear rate can be described as a combination of an elastic and a hydrodynamic component (Zhu et al., 2009). When considering K as the hydrodynamic contribution to the shear stress at $\dot{\gamma}$ = 1 s^{-1}, parameter K is expressed in mPa, irrespective of the used (non-)linear regression model. The larger K, the larger the required shear stress to obtain a certain shear rate and thus the more consistent the fluid, leading to the same conclusions. Next to differences in flow behavior between the investigated microalgae species, significant differences were observed between suspensions at pH 4 and pH 6 for each microalga species. Higher values of K

were obtained for suspensions at pH 6 (with the exception of *Schizochytrium* sp.), suggesting the presence of ionic interactions between particles or polymers in the microalgal suspensions.

Although the Herschel-Bulkley model was not selected to fit the data, for some microalgae species a plateau of constant log (σ) values might be present at lower shear rates than the experimentally tested 0.1 s^{-1}. Extrapolation of the curve in the log (σ) – log ($\dot{\gamma}$) plot would result in estimated yield stresses around 4 Pa for *Porphyridium cruentum* at both pH values and well below 1 Pa for *Chlorella vulgaris* and *Odontella aurita* suspensions. Nevertheless, since these are low yield stress values, their contribution will be very limited in food products.

5.3.2 Effect of mechanical and thermal processing on the rheological properties of microalgal suspensions

A fixed processing sequence was applied in this chapter, consisting of HPH followed by a pasteurization process (suspensions at pH 4) or a sterilization process (suspensions at pH 6). As a consequence, the intensity of the thermal treatment in this study was always linked to the pH of the suspensions, an important fact to keep in mind during the interpretation of the obtained results.

5.3.2.1 Effect of processing on the linear viscoelastic behavior

To study the viscoelastic behavior of the processed suspensions, strain sweep and frequency sweep measurements were performed. A shear strain of 1% was found to be in the linear viscoelastic region for all treated suspensions. In order to provide a clear presentation of all data, the linear viscoelastic properties of different samples are compared as the storage modulus at a certain angular frequency (ω = 10 rad/s), as presented in Fig. 5.6. Since frequency sweep measurements were performed at a constant shear strain within the linear viscoelastic region and with G' showing a limited dependence of ω, this approach was assumed to give an adequate representation of the results. It was validated that no major differences were observed when comparing storage moduli at a lower angular frequency (ω = 1 rad/s) (data not shown).

Oscillatory measurements on *Phaeodactylum tricornutum* and *Schizochytrium* sp. suspensions indicated that no network structure was created in suspensions of these two microalgae species, neither before nor after processing. Furthermore, no detectable storage modulus was observed for untreated and HPH-treated suspensions of *Nannochloropsis* sp., while the combination of HPH and sterilization at pH 6 resulted in a measurable storage modulus. Nevertheless, compared to

(un)processed suspensions of other microalgae species, this increase in storage modulus was rather limited.

For the other microalgae species, different effects of processing were observed. Whereas HPH and/or thermal processing of *Arthrospira platensis* and *Chlorella vulgaris* suspensions resulted in an increase of G', the opposite was observed for suspensions of *Porphyridium cruentum* and *Odontella aurita*. The impact of HPH was pH-dependent in case of *Arthrospira platensis* and *Chlorella vulgaris*, since significant increases in G' were only observed at pH 4. Furthermore, the intensity of the thermal process seemed of major importance, since no significant changes were observed after a pasteurization process, while drastic increases were observed after a sterilization process. Hence, a stiff network structure was created by this intense thermal treatment, probably due to denaturation and gelation of the large amount of proteins in *Arthrospira platensis* and *Chlorella vulgaris*.

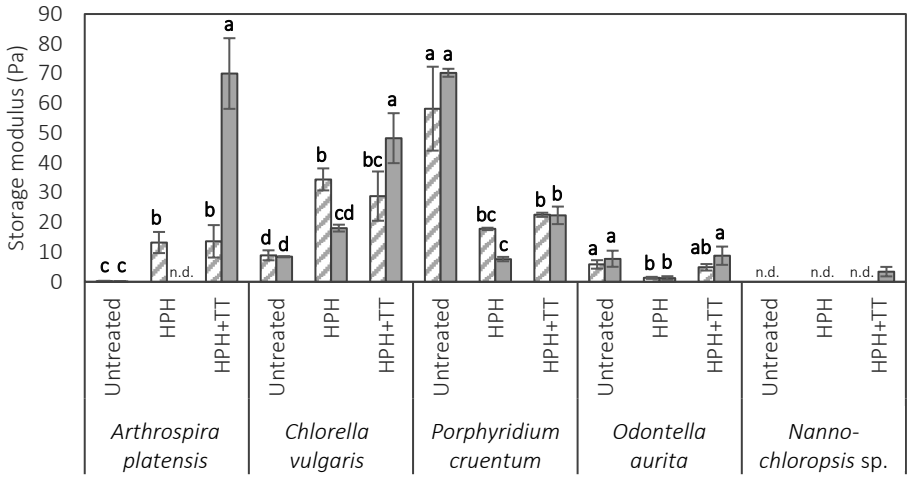

Fig. 5.6 Effect of processing on the storage modulus at ω = 10 rad/s (± standard error) of untreated microalgal aqueous suspensions (Untreated) and suspensions treated by high pressure homogenization (HPH) and a combination of high pressure homogenization and thermal treatment (HPH+TT). Suspensions at pH 4 are represented by dashed bars, suspensions at pH 6 by filled bars. The data obtained were compared statistically (one-way ANOVA). Significant differences (Tukey test, $P < 0.05$) within one microalga species are indicated with different letters. Data below the reliable torque limit (0.1 µN m) are indicated as not detected (n.d.).

In contrast, HPH resulted in a significant decrease of storage modulus for suspensions of *Porphyridium cruentum* and *Odontella aurita* at both pH values. Hence, the network structure that was present in the untreated suspensions was destroyed by the mechanical treatment under the investigated conditions. Ramus and Kenney

(1989) actually reported a loss in bulk rheological properties of microalgal EPS when applying shear stress, presumably by disrupting interactions between different polymers. Furthermore, Yap et al. (2016) showed HPH causing breakage of cell aggregate networks in microalgal slurries, resulting in reduced rheological properties. During subsequent thermal processing, the network structure was somewhat recovered depending on the intensity of the thermal treatment (in combination with pH). However, although a significant increase in G' was observed after sterilization at pH 6 compared to the HPH-treated suspension, no significant differences were found in G' between the pasteurized and sterilized suspensions. It is obvious that the slight regeneration of the network structure after thermal treatment did not restore to the initial value of G' for *Porphyridium cruentum* suspensions.

5.3.2.2 Effect of processing on the flow behavior

The flow behavior of the processed suspensions was studied under larger deformations. Results are presented in Fig. 5.7 as the viscosity at a certain shear rate ($\dot{\gamma}$ = 10.5 s^{-1}) for each suspension. Comparing viscosity values at a lower shear rate ($\dot{\gamma}$ = 1.1 s^{-1}) led to the same conclusions (data not shown).

Suspensions of *Nannochloropsis* sp., *Schizochytrium* sp., and *Phaeodactylum tricornutum* presented low viscosities in comparison with the other microalgae species. In case of *Nannochloropsis* sp., only the sterilization treatment at pH 6 caused a significant viscosity increase. Since the same was observed for the linear viscoelastic behavior (section 5.3.2.1), it can be concluded that the sterilization process mainly influenced the particle characteristics resulting in an increase of both G' and η. Although no significant differences were found between untreated suspensions and suspensions after HPH and/or pasteurization, it must be noted that both mechanical and thermal treatments changed the flow behavior of *Nannochloropsis* sp. suspensions from Newtonian to shear-thinning behavior (not shown). No clear effects of processing were noticed for suspensions of *Schizochytrium* sp. and *Phaeodactylum tricornutum*.

For the other microalgae species, conclusions were consistent with those discussed in section 5.3.2.1. Whereas HPH and/or thermal processing (mainly sterilization) resulted in an increased viscosity of suspensions of *Arthrospira platensis* and *Chlorella vulgaris*, a decreased viscosity was observed after HPH in case of *Porphyridium cruentum* and *Odontella aurita*. Hence, the network structure formed by particle interactions throughout processing had a major contribution to the viscosity and flow characteristics of the microalgal suspensions. However, comparison of viscoelastic properties and flow properties indicates the importance of the continuous phase for some suspensions. Whereas untreated suspensions of *Chlorella vulgaris* at pH 4 and

pH 6 showed a similar value of G', a significantly higher viscosity was observed for the suspension at pH 6. In other words, while the contribution of the network structure to the rheological properties was similar for both suspensions, the viscosity values suggest that additional structure build-up is brought by the liquid serum phase. The same reasoning stands for HPH-treated suspensions of *Chlorella vulgaris*, since a larger viscosity was obtained at pH 6 while a lower G' was observed compared to pH 4.

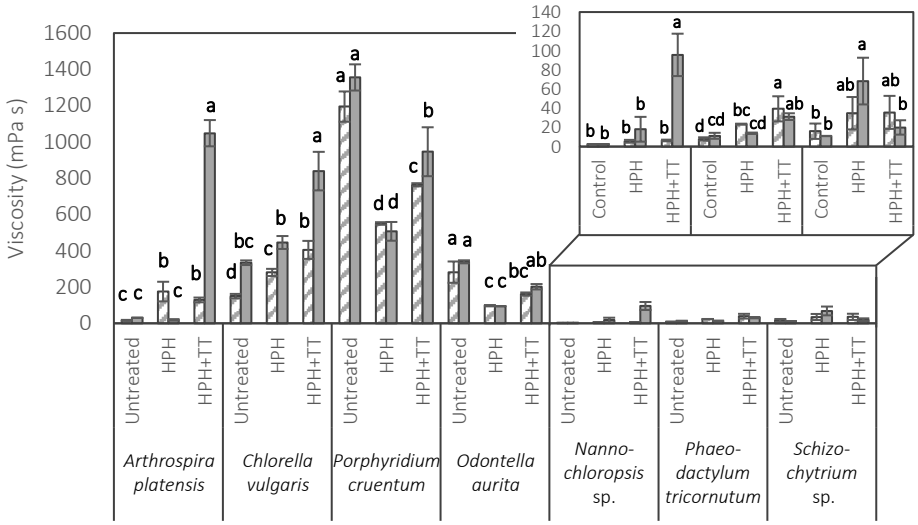

Fig. 5.7 Effect of processing on the viscosity at $\dot{\gamma}$ = 10.5 s^{-1} (± standard error) of untreated microalgal aqueous suspensions (Untreated) and suspensions treated by high pressure homogenization (HPH) and a combination of high pressure homogenization and thermal treatment (HPH+TT). Suspensions at pH 4 are represented by dashed bars, suspensions at pH 6 by filled bars. The data obtained were compared statistically (one-way ANOVA). Significant differences (Tukey test, $P < 0.05$) within one microalga species are indicated with different letters.

The contribution of the serum phase to the overall viscosity of the suspensions was further investigated by determining the viscosity of the separated serum phase. Indeed, for diluted suspensions comprising rigid particles, Einstein's relation (**Eq. 5.4**) shows that the viscosity is determined both by the properties of the dispersed particles and by the characteristics of the continuous serum phase:

$$\eta = \eta_s \cdot (1 + [\eta] \cdot \varphi) \qquad \textbf{(Eq. 5.4)}$$

with η the viscosity of the suspension (Pa s), η_s the viscosity of the suspending medium i.e. the serum phase (Pa s), $[\eta]$ the intrinsic viscosity (dL/g), and φ the phase volume of the suspended particles (g/dL) (Larson, 1999). To study the contribution of

the suspending medium to the overall viscosity of the suspension, steady-shear experiments were performed on the separated serum phase. Due to the high lipid content of *Schizochytrium* sp., no perfect separation of serum and particle phase could be achieved by the applied centrifugation conditions for this microalga species.

The flow curves of the serum phase of the untreated suspensions are presented in Fig. 5.8. Both graphs clearly show the non-Newtonian behavior of the serum phase of *Porphyridium cruentum* suspensions, while all other serum phases behaved as Newtonian fluids. The flow curves of the serum phase of *Porphyridium cruentum* suspensions were fitted by the power law model (Eq. 5.2). Low estimated values of the flow behavior index n (0.38 ± 0.01 and 0.32 ± 0.01 for pH 4 and pH 6, respectively) indicate the strong shear-thinning behavior. Since no (or limited) disruption of *Porphyridium cruentum* cells is expected in the untreated biomass suspensions, it is assumed that no substantial amounts of intracellular components have been solubilized into the serum phase, except for some low-molecular weight compounds. Hence, the shear-thinning behavior of the continuous serum phase is probably attributed to solubilized EPMS of *Porphyridium cruentum*, as no cell disruption is required for release of EPMS into the continuous phase. As concluded from Chapter 4, it is hypothesized that the shear-thinning behavior is mainly caused by the polysaccharide interactions in this extracellular polymer fraction, rather than by the presence of protein moieties. Even though rather low concentrations of EPS were observed in *Porphyridium cruentum* biomass in Chapter 2, it is known that EPS of *Porphyridium cruentum* display a low C*, below 0.06% (Patel et al., 2013). However, additional quantification of solubilized EPS in the serum phase would be of interest to validate the aforementioned hypotheses.

In contrast to *Porphyridium cruentum*, the serum phases of the other microalgae species were characterized by Newtonian flow behavior. Despite the fact that EPMS were also observed in *Arthrospira platensis*, *Chlorella vulgaris*, and *Odontella aurita* (Chapter 2), these EPMS did not show a large extent of polymeric interactions in the continuous serum phase. This might be due to a limited solubilization of EPMS into the serum phase, or to a different molecular structure of EPMS in these microalgae species. Even though only limitedly studied in literature, some reports indeed suggest higher values of C* for EPS isolated from cyanobacteria, including *Arthrospira platensis*, and for *Chlorella* sp. (Badel et al., 2011; Navarini et al., 1992; Yalcin et al., 1994). Hence, it is hypothesized that EPMS of these microalgae species have been solubilized into the serum phase (based on the increased absolute viscosity values), but concentrations were too low (below C*) to induce shear-thinning flow behavior. In contrast, serum viscosities of ~1 mPa s were observed for *Nannochloropsis* sp. and *Phaeodactylum tricornutum*, species which did not possess EPMS (Chapter 2). Hence,

no compounds have been solubilized into the serum phase for these microalgae, with the serum viscosity approaching that of pure water.

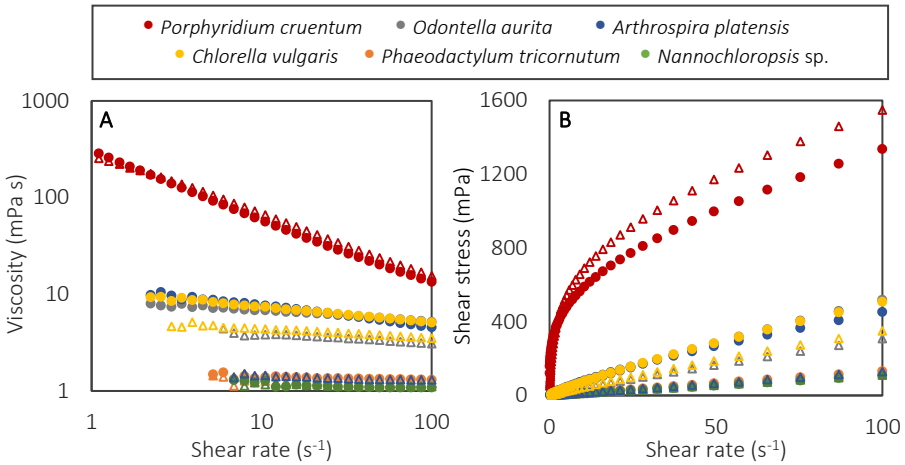

Fig. 5.8 (A) Serum viscosity and **(B)** shear stress as a function of shear rate for untreated suspensions of six microalgae species. Suspensions at pH 6 are presented as solid circles, suspensions at pH 4 as empty triangles.

The impact of processing on the serum viscosity is shown in **Fig. 5.9**, in which the viscosity of *Porphyridium cruentum* at $\dot{\gamma} = 10.5\ s^{-1}$ is compared to the dynamic viscosity of the other microalgal suspensions, which were estimated by fitting the Newtonian model (**Eq. 5.1**). Even at this (rather high) shear rate, the serum viscosity of all *Porphyridium cruentum* suspensions was more than ten times higher than those of the other microalgae species, before and after processing. Furthermore, the destructive impact of HPH and the regeneration by thermal processing as observed for the biomass suspensions is also seen for the serum phase viscosity, probably related to destruction and regeneration of solubilized EPS networks. In contrast, serum phases of *Nannochloropsis* sp. and *Phaeodactylum tricornutum* showed a constant viscosity of approximately 1 mPa s before and after processing, indicating that no viscosity-increasing components were present in the serum phase of these microalgae species. Whereas untreated suspensions of *Arthrospira platensis*, *Chlorella vulgaris*, and *Odontella aurita* showed a higher serum viscosity, their viscosity was decreased after HPH. As cell disruption took place during HPH, more polymers were available for formation of aggregates. It is hypothesized that EPMS also took part in these aggregate formation, therefore resulting in a decreased serum viscosity, as EPMS were transferred from the serum phase (as solubilized polymers) towards the particle phase (as part of created aggregates). However, this hypothesis should be validated by determination of EPMS in the serum phase of untreated and HPH-treated suspensions.

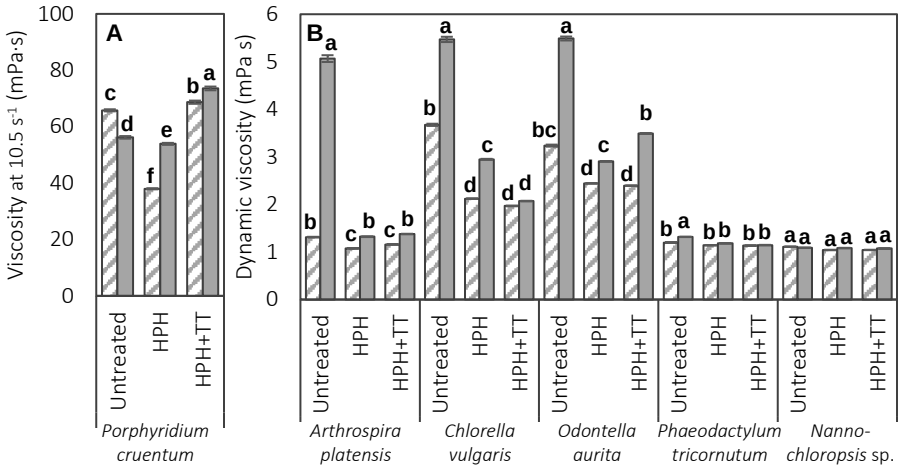

Fig. 5.9 (A) Serum viscosity (η_s) at $\dot{\gamma}$ = 10.5 s^{-1} (± standard error) and **(B)** serum viscosity (μ_s) estimated by the Newtonian model (± standard error) of untreated microalgal aqueous suspensions (Untreated) and suspensions treated by high pressure homogenization (HPH) and a combination of high pressure homogenization and thermal treatment (HPH+TT). Suspensions at pH 4 are represented by dashed bars, suspensions at pH 6 by filled bars. The viscosity values at $\dot{\gamma}$ = 10.5 s^{-1} were analyzed statistically by one-way ANOVA followed by Tukey test ($P < 0.05$). Dynamic viscosity values estimated by the Newtonian model were compared statistically by use of 95% confidence intervals. Significant differences are indicated with different letters within each microalga species.

5.3.3 Relation between the rheological properties and microstructural characteristics of particles and serum phase during processing

The effect of mechanical and/or thermal processing on the microstructure is shown in **Fig. 5.10** and **Fig. 5.11**, representing volumetric particle size distributions and DIC micrographs, respectively. As different effects of processing on the rheological characteristics were observed in the previous paragraph, the effect on the microstructure was likewise depending on the microalgal species and on the pH.

The particle size of *Arthrospira platensis* was mainly affected by processing in suspensions at pH 6, while minimal changes were observed for suspensions at pH 4 (**Fig. 5.10A**). At pH 6, HPH resulted in complete cell disruption, resulting in a narrow particle size distribution below 1 µm, which could be expected based on its fragile cell wall (Safi et al., 2014a). The subsequent sterilization process led to aggregation into larger particles up to 100 µm, as also observed in **Fig. 5.11**. This phenomenon is assumed to be aggregation of denatured proteins, especially since a high protein content was observed for the biomass of *Arthrospira platensis* (**Chapter 2**). Since the contribution of the serum viscosity was very limited, the large increase in rheological

parameters G' and η after sterilization of *Arthrospira platensis* suspensions can be attributed to the formation of these aggregates. Similar observations were made for suspensions of *Odontella aurita* (Fig. 5.10B). HPH resulted in a decreased particle size by the complete disruption of the microalgal cells, since particle sizes were observed below 50 µm, which is the average length of an intact cell of *Odontella aurita* (Wiltshire and Dürselen, 2004). This was also visually confirmed by the micrographs presented in Fig. 5.11. Thermal treatment resulted in an increased particle size due to the formation of aggregates. For this microalga species, no effect of pH was observed, neither on rheological characteristics nor on particle size distribution.

Whereas HPH under the applied conditions proved a successful technique for cell disruption of the aforementioned microalgae, cells of *Nannochloropsis* sp. showed to be more resistant to these pressure conditions, as no differences in particle size distribution were observed before and after HPH (Fig. 5.10C) and intact cells were visualized in the micrographs after HPH (Fig. 5.11). This is in agreement with the study of Spiden et al. (2013b), who reported that still 80% of *Nannochloropsis* sp. cells were intact after HPH for 1 pass at 90 – 102 MPa based on cell count analyses. The low degree of cell disruption is presumably related to the rigidity of the algaenan-containing cell wall (Safi et al., 2014a; Spiden et al., 2013b). An increased particle size was however observed after thermal processing, especially for sterilized suspensions at pH 6, resulting from aggregates of intact cells that seem to be embedded in solubilized cell material. Agglomeration of cell debris after a thermal treatment of microalgal biomass has been previously reported in literature without a preceding HPH treatment (Spiden et al., 2015). Since no changes in serum viscosity were observed for *Nannochloropsis* sp. suspensions, it can be concluded that the increase in rheological parameters G' and η after sterilization was caused by the formation of these larger aggregates.

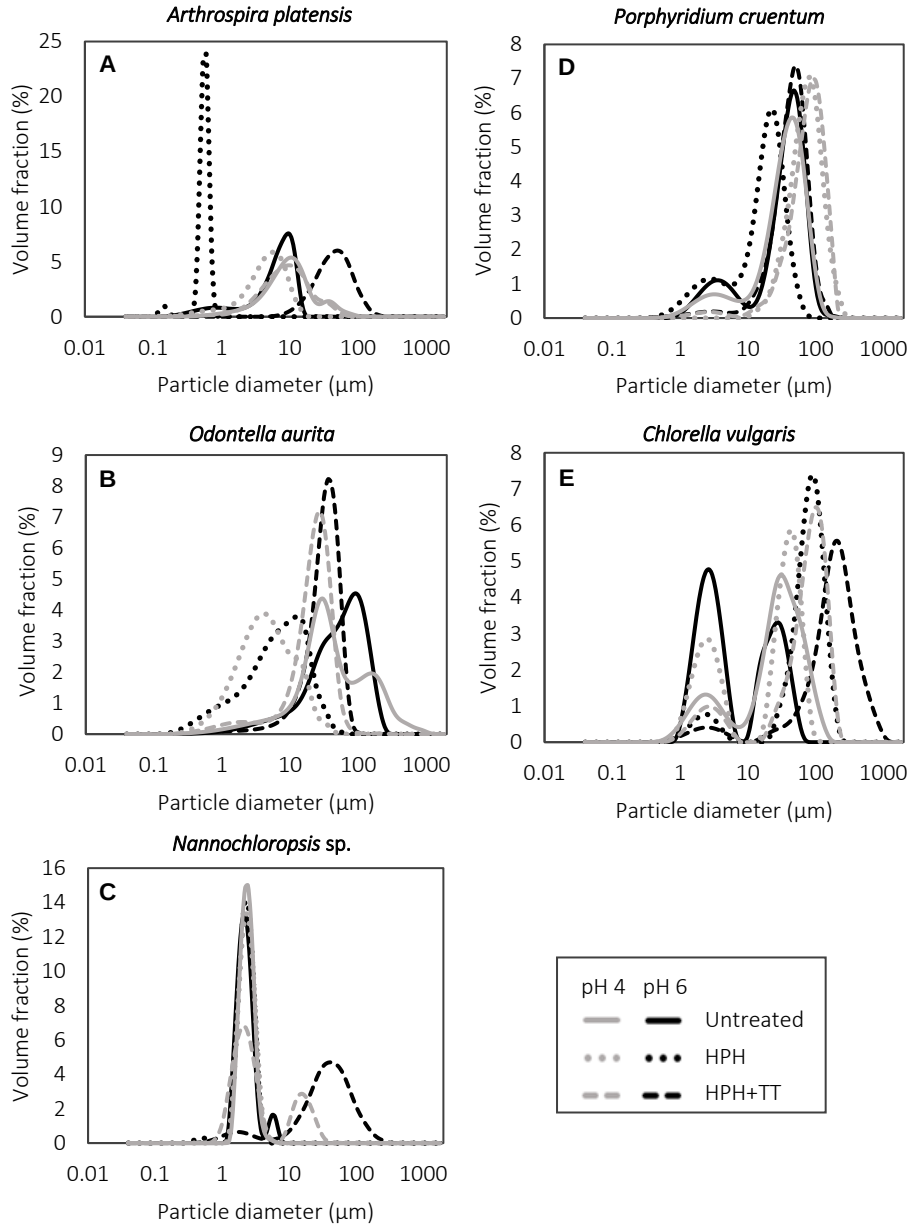

Fig. 5.10 Volumetric particle size distribution of untreated suspensions and suspensions treated by high pressure homogenization (HPH) and a combination of high pressure homogenization and thermal treatment (HPH+TT).

While HPH and thermal processing largely affected the rheological properties of *Porphyridium cruentum* suspensions, only small changes in particle size of this microalga species were observed (Fig. 5.10D). Bimodal particle size distributions were observed in the untreated suspensions at both pH values, in which one peak (1 – 10 µm) accounts for single cells and the other peak (10 – 100 µm) for clusters of intact cells, as observed visually in the micrographs (Fig. 5.11). EPMS in *Porphyridium cruentum* probably act as a glue between intact cells, in that way enhancing cell clustering. In fact, the clusters might be stabilized by screening of electrostatic repulsions between the negatively charged polysaccharides, either by the presence of cations (Liberman et al., 2016) or by the positively charged amino groups of the protein moieties (Eteshola et al., 1998). Subsequent HPH resulted in a decreased particle size for suspensions at pH 6, while larger particles were formed in homogenized suspensions at pH 4. It was observed from microscopic images that the degree of cell disruption seemed to be pH dependent, since more intact cells were found in HPH-treated suspensions at pH 4 compared to pH 6 (data not shown). Moreover, differences in aggregate formation between pH 4 and pH 6 suggest the presence of pH-dependent interactions between above-mentioned components, which is not surprising based on the multiple negative charges observed in the cell wall related polysaccharides (Chapter 4). Whereas pasteurization at pH 4 did not lead to significant changes in particle size, the sterilization process at pH 6 resulted in an increased size of the particles. However, these aggregates were still smaller compared to the particles in the pasteurized suspension. The larger suspension viscosity of the sterilized sample of *Porphyridium cruentum* can thus not only be ascribed to the size of the particles, but also to the contribution of other particle properties and the somewhat higher viscosity of the serum phase.

Similar to *Porphyridium cruentum*, bimodal particle size distributions were observed for untreated suspensions of *Chlorella vulgaris* (Fig. 5.10E). Larger aggregates of intact cells suggest the presence of a gel of EPS in this microalga species. Even though EPS are produced by *Chlorella* sp., as observed in Chapter 3 and as previously reported by other authors (Kaplan et al., 1987; Yalcin et al., 1994), Morineau-Thomas et al. (2002) did not observe a cell envelope in this microalga. When suspensions of *Chlorella vulgaris* were treated by HPH, larger aggregates were formed, especially at pH 6. From the micrographs it was observed that the aggregates were made of both intact cells and released cell material, indicating that partial cell disruption had taken place.

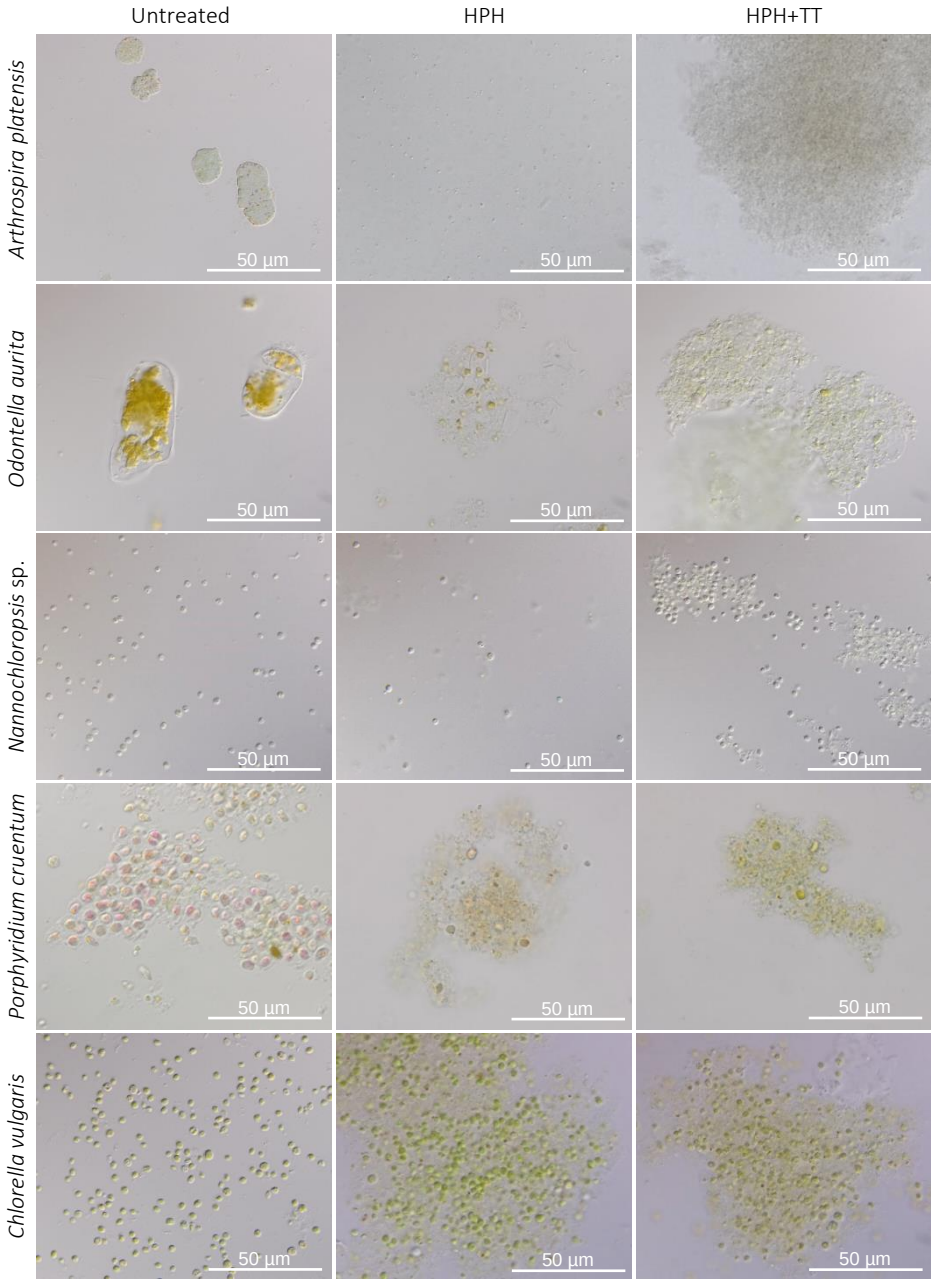

Fig. 5.11 Microscopic images of untreated microalgal suspensions (Untreated) and suspensions treated by high pressure homogenization (HPH) and a combination of high pressure homogenization and thermal treatment (HPH+TT). All micrographs represent suspensions at pH 6, implying that samples of HPH+TT were sterilized.

This observation corresponds to previous studies, in which HPH under similar conditions (1 pass at ~100 MPa) resulted in disruption of 25 – 50% of *Chlorella* sp. cells (Spiden et al., 2013b; Yap et al., 2014). Subsequent thermal processing resulted in an increased particle size, especially for sterilized suspensions at pH 6. As *Chlorella vulgaris* biomass contained 39.4% proteins (Chapter 2), it is very likely that the increased particle size can be ascribed to aggregation of denatured proteins, among others. It is actually hypothesized that suspended metabolites are also involved in the formation of these aggregates, leading to less viscosity-increasing components in the serum phase, as reflected by the lower serum viscosity after processing.

5.4 CONCLUSIONS

This chapter compared the rheological properties of seven microalgae species in aqueous suspensions. Rheological characteristics were largely dependent on the microalga species, presumably resulting from the diverse biopolymer composition of the different species, as observed in Chapter 2. Furthermore, it was observed that rheological properties of the untreated suspensions were pH dependent, since larger consistency coefficient values were observed for suspensions at pH 6 compared to pH 4. This is not surprising, since the interactions of several biopolymers (including cell wall related polysaccharides and proteins) are influenced by environmental conditions such as pH.

The obtained results also proved that rheological properties of microalgal suspensions were altered during mechanical and/or thermal processing. Differences in cell rupture by HPH were observed between the investigated microalgae species, which can be related to size and rigidity of the cells as well as to the cell wall composition (Chapter 3). The effect of subsequent thermal processing on the microstructure and rheological properties was affected by the preceding mechanical treatment, as thermal processing was shown to enhance interactions between released cell material. In addition, it was observed that a sterilization process also led to solubilization of components of intact cells, as was the case for *Nannochloropsis* sp. suspensions. Therefore, applying different sequences of mechanical and thermal processing might provide interesting additional information in tailoring the structural properties of microalgal suspensions, as will be discussed in Chapter 6.

This chapter allows the selection of microalgae species towards desired applications. For instance, biomass of *Nannochloropsis* sp., *Phaeodactylum tricornutum*, and *Schizochytrium* sp. could be of interest for enriching food products in ω3-LC-PUFA, without disturbing the structural properties of the food matrix, as desired in fluid food systems such as fruit juices and smoothies. On the other hand, biomass of *Porphyridium cruentum* showed large structuring potential and could thus be used as

a multifunctional food ingredient, providing improved nutritional value as well as thickening effects to the food product. Similarly, biomasses of *Chlorella vulgaris* and *Arthrospira platensis* may find applications as a multifunctional ingredient in mechanically and/or thermally processed food products, such as vegetable based soups and several dairy products.

CHAPTER 6

Impact of different processing sequences on the rheological properties of *Porphyridium cruentum* and *Chlorella vulgaris*

6.1 INTRODUCTION

Previous chapter showed a large diversity in the rheological properties of microalgal suspensions, with and without processing. Upon a fixed processing sequence of HPH at 100 MPa followed by a thermal treatment, three microalgae (*Arthrospira platensis*, *Chlorella vulgaris*, and *Porphyridium cruentum*) showed large potential as multifunctional ingredients. However, while the structural properties of *Porphyridium cruentum* were yet observed in the untreated suspensions due to the presence of EPS interactions, mechanical and thermal processing was required for structural build-up of the other two microalgal biomasses. Hence, *Porphyridium cruentum* and *Chlorella vulgaris* were selected in the current chapter representing both types of rheological behavior upon processing.

Aside from the fixed processing sequence applied in the previous chapter, the use of different sequences of mechanical and thermal processing at various intensities might provide additional information, allowing a complete view on the use of processing to tailor the rheological properties of these microalgal suspensions. Changing the sequence of mechanical and thermal processing has actually proven successful for plant-based dispersions, such as vegetable based purees. Whereas the largest rheological properties for carrot and broccoli were obtained by blending followed by

This chapter is based on the following paper:
Bernaerts T.M.M., Panozzo A., Verhaegen K.A.F., Gheysen L., Foubert I., Moldenaers P., Hendrickx M.E., Van Loey A.M. (2018)
Impact of different sequences of mechanical and thermal processing on the rheological properties of Porphyridium cruentum and Chlorella vulgaris as functional food ingredients.
Food & Function, 9(4), 2433-2446.
[2017 Impact Factor = 3.289; Ranked 20/133 (Q1) in Food Science & Technology]

thermal treatment, the combination of thermal treatment and subsequent HPH was the most effective strategy for tomato puree. These differences in rheological behavior were attributed to microstructural changes of the plant material, including size and morphology of the particles as well as the disruption of the polysaccharidic cell wall (Lopez-Sanchez et al., 2011). However, prediction of rheological and microstructural changes upon processing might be even more challenging for microalgal suspensions, due to their higher diversity in terms of biomass composition and cell wall characteristics compared to most plant materials (Chapter 2 and 3).

The aim of this chapter is to investigate the impact of different sequences of HPH and thermal processing on the structural properties of *Porphyridium cruentum* and *Chlorella vulgaris*. Combination of these results with data of Chapter 5 will provide an extended scientific knowledge base, allowing an appropriate selection of processing treatments for the use of *Porphyridium cruentum* and *Chlorella vulgaris* biomasses as multifunctional ingredients in food products.

6.2 MATERIALS AND METHODS

6.2.1 Microalgal biomass

Lyophilized biomass of *Porphyridium cruentum* was obtained from Necton Phytobloom (Olhão, Portugal). Biomass of *Chlorella vulgaris* was obtained as a spray-dried powder from Allmicroalgae Natural Products (Lisbon, Portugal). The biomasses were stored in closed containers at -80 °C until use.

6.2.2 Characterization of the biomass composition

Since different batches of microalgal biomass were used in this chapter compared to Chapters 2, 3, and 5, the biomass composition was determined for these new batches. All analyses were performed in triplicate, as described in Chapter 2. As seen from Table 6.1, the biomass composition of the new batches is very similar to the previously used batches, both for *Porphyridium cruentum* and for *Chlorella vulgaris*.

Table 6.1 Biomass composition of different batches of *Porphyridium cruentum* and *Chlorella vulgaris* used in different chapters of this doctoral thesis, expressed as percentage of dry matter (%) ± standard error (n = 3). (SPS: storage polysaccharides; CWPS: cell wall bound polysaccharides; EPS: extracellular polysaccharides).

	Porphyridium cruentum		*Chlorella vulgaris*	
	Chapters 2, 3, 5	Chapters 4, 6	Chapters 2, 3, 5	Chapter 6
Lipids	11.5 ± 1.0	12.6 ± 0.7	6.6 ± 1.5	8.2 ± 0.5
Proteins	28.2 ± 1.2	28.0 ± 0.6	39.4 ± 0.3	45.7 ± 0.8
SPS	2.1 ± 0.1	4.4 ± 0.1	1.8 ± 0.1	2.1 ± 0.2
CWPS	9.6 ± 0.3	14.0 ± 0.5	9.3 ± 0.7	11.5 ± 0.2
EPS	2.6 ± 0.2	2.7 ± 0.1	0.5 ± 0.1	0.5 ± 0.1
Ash	17.9 ± 0.6	22.3 ± 0.8	6.7 ± 0.1	7.6 ± 0.3

6.2.3 Preparation and processing of microalgal aqueous suspensions

Microalgal suspensions were prepared similarly as described in Chapter 5, however a different sequence of mechanical and thermal processing was applied. A schematic overview of the preparation and processing of the suspensions in the current study is presented in Fig. 6.1.

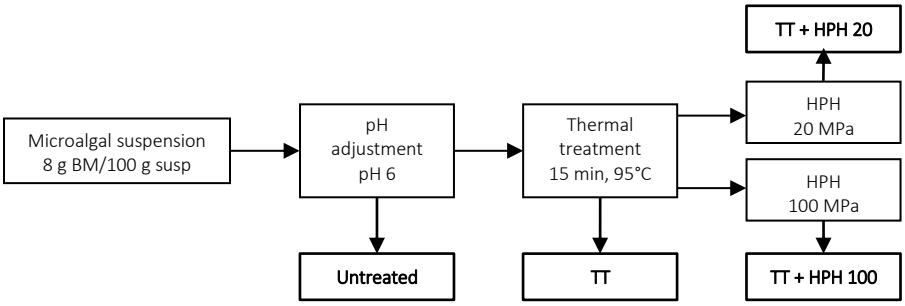

Fig. 6.1 Schematic overview of the preparation and processing of microalgal aqueous suspensions. Boxes with 'Untreated', 'TT', 'TT+HPH 20', and 'TT+HPH 100' indicate the moment of collecting respective samples. (HPH: high pressure homogenization; TT: thermal treatment)

6.2.3.1 Preparation of microalgal aqueous suspensions

Dry biomass was suspended overnight in demineralized water and pH was adjusted to 6 using HCl. Demineralized water was then added to obtain a final concentration of 8 g dry biomass per 100 g suspension (8% w/w), taking into account the moisture content of the biomass powders. A homogenous suspension was created by mixing for 10 min at 6000 rpm with a lab mixer (Silverson, L5M-A, East Longmeadow, MA, USA). The suspensions were prepared in duplicate.

6.2.3.2 Thermal and mechanical treatments

To perform thermal treatments, suspensions were vacuum packed in plastic bags (PET/LDPE, Daklapack), incubated for 15 min in a water bath at 95 °C, and subsequently cooled in an ice water bath. Thermally treated suspensions were then mechanically treated using HPH (Panda 2K, Gea Niro Soavi, Parma, Italy), at either 20 MPa or 100 MPa for a single pass.

6.2.4 Separation of the serum phase

The serum phase was isolated by centrifugation of the microalgal suspensions at 25 °C. Whereas suspensions of *Chlorella vulgaris* were centrifuged for 30 min at 10000g (J2-HS centrifuge, Beckman Coulter, Fullerton, CA, USA), sera of the more viscous suspensions of *Porphyridium cruentum* were obtained by ultracentrifugation for 60 min at 165000g (Optima XPN-80, Beckman Coulter, Fullerton, CA, USA).

6.2.5 Rheological measurements

Rheological analyses were performed as described in **Chapter 5**, with minor modifications. Preshear conditions were extended, using 30 s at 20 s^{-1} followed by 300 s of rest. It was verified by time sweep tests that this resting time was sufficient to ensure a complete recovery of the structure for all samples. Frequency sweep tests were performed to characterize the viscoelastic behavior, using a constant shear strain of 1%. This shear strain was confirmed to be within the linear viscoelastic region for all suspensions by strain sweep tests at a constant angular frequency of 10 rad/s. The flow behavior was studied using steady-shear measurements, in which 40 measuring points were recorded with each shear rate applied for 20 s. All other parameters were exactly the same as described in **Chapter 5**. All rheological measurements were performed in duplicate.

6.2.6 Characterization of the microstructure

The microstructure was characterized as described in **Chapter 5**, by particle size measurements using laser diffraction and by DIC microscopy. In addition, microscopic staining was used to identify specific biopolymers. Coomassie brilliant blue was used to visualize proteins, by adding 200 µL of Bradford reagent (Sigma-Aldrich) to 0.5 mL of sample. Binding with proteins yielded a blue color, which was visualized by DIC microscopy. Acidic polysaccharides were stained by adding 10 µL of 2% acridine orange solution to 1 mL of sample. The sample was visualized under epifluorescence microscopy using an excitation filter between 460 and 495 nm (X-Cite® 120Q, EXFO Europe, Hants, United Kingdom).

6.2.7 Statistical analysis

The microalgal suspensions were processed in duplicate and for each individual sample rheological analyses were performed in duplicate. As a result, these data are presented as the mean of four measurements ± standard error.

Differences between storage modulus, loss modulus, and phase angle of (un)processed suspensions obtained from strain sweep measurements were statistically analyzed using one-way ANOVA combined with Tukey's test for multiple comparison ($P < 0.05$) with JMP statistical software (JMP Pro 13, Cary, NC, USA). Frequency sweep and flow curves were fitted to rheological models using non-linear regression procedures with SAS statistical software (SAS 9.4, Cary, NC, USA). The estimated model parameters of different samples were statistically compared by use of 95% confidence intervals.

6.3 RESULTS AND DISCUSSION

6.3.1 Effect of processing on the rheological characteristics

6.3.1.1 Linear viscoelastic behavior: strain sweep

The linear viscoelastic behavior was studied using strain sweep and frequency sweep tests. The former measurement is typically performed to determine the linear viscoelastic region. In addition, results obtained from strain sweep tests provide information on the network structure of the sample. The obtained strain sweep curves are presented in **Fig. 6.2A** and **6.2B**. The linear viscoelastic region could be clearly observed for all suspensions as a plateau at low shear strains, with storage modulus (G') and loss modulus (G") independent of the shear strain. In **Fig. 6.2C** and **6.2D**, both moduli are presented for the suspensions at a constant shear strain of 1%, within this linear viscoelastic region. Whereas the absolute value of G' provides information on the stiffness of the structure, the viscoelastic behavior is determined by the ratio of both moduli, which is presented in **Fig. 6.2C** and **6.2D** as the phase angle $\delta = \tan^{-1}\left(G^{"}/G'\right)$.

All (un)processed suspensions of *Porphyridium cruentum* presented values of $\delta < 45°$, thus displaying predominantly elastic behavior. As previously observed in **Chapter 5**, untreated suspensions of *Porphyridium cruentum* presented substantial gelling properties, confirmed by the large storage modulus (113 Pa) and a phase angle of 12.6°. Even though the concentration of EPS was not very high (**Table 6.1**), a strong network structure was observed, probably resulting from their unique molecular structure (**Chapter 4**).

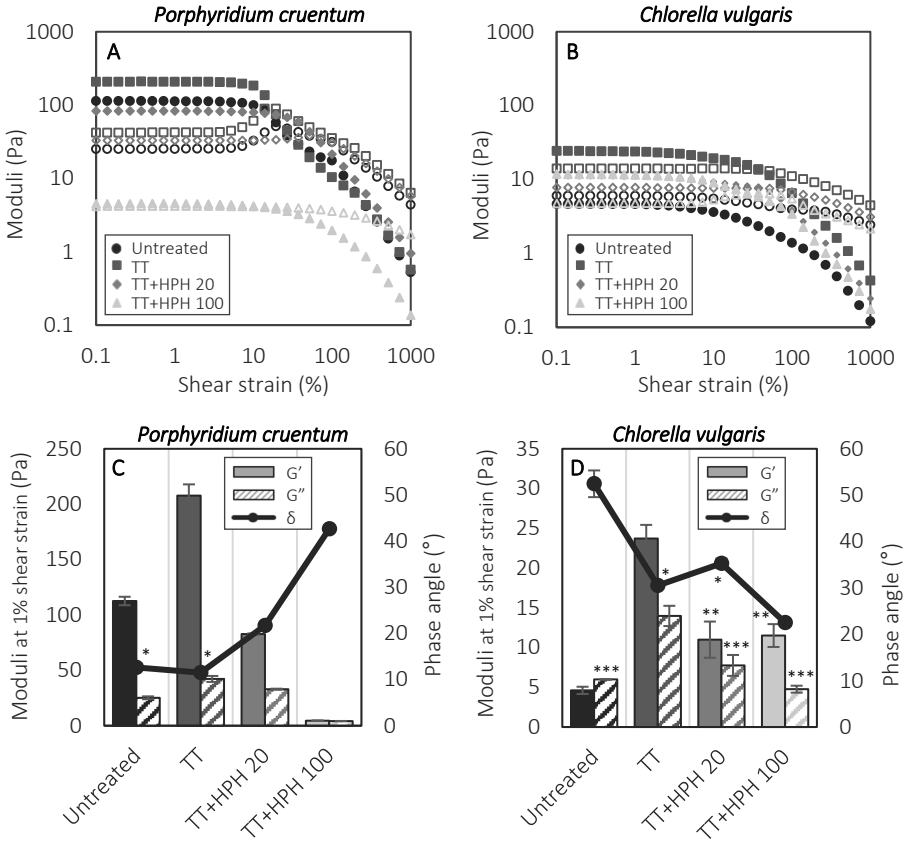

Fig. 6.2 Strain sweep results at a constant angular frequency of 10 rad/s for (un)processed suspensions of *Porphyridium cruentum* and *Chlorella vulgaris*. **A,B**: Storage modulus (G', filled symbols) and loss modulus (G'', empty symbols) as a function of the shear strain. **C,D**: Storage modulus (G', full bars) and loss modulus (G'', dashed bars) at a shear strain of 1% are presented on the left axis, while the phase angle (δ, black line) is presented on the right axis. Standard errors are indicated by error bars (n = 4). The data obtained were compared statistically (one-way ANOVA). Data points of a certain parameter that are indicated with the same number of asterisks are not significantly different (Tukey test, $P < 0.05$).

Thermal treatment of *Porphyridium cruentum* suspensions resulted in an increased gel stiffness, as the value of G' was almost doubled. Interestingly, the gelling behavior was not influenced, since no significant differences were observed between the phase angle of the untreated and thermally treated suspensions. With a storage modulus of 208 Pa and a phase angle of 11.5°, the thermally treated suspension of *Porphyridium cruentum* can be considered as a strong gel structure. The use of HPH resulted in a drastic decrease of the network structure, given the large reduction of the storage modulus and the increased phase angle. However, the extent to which the structure

was destroyed was depending on the applied homogenization pressure. While a lower pressure of 20 MPa resulted in a partial breakdown, the network structure was completely destroyed after HPH at 100 MPa. In fact, the latter suspension presented similar values of G' and $G"$, resulting in a phase angle of approximately 45°. In other words, the elastic behavior was no longer predominant and the suspension cannot be considered as a structured system. As a consequence, although the use of HPH was detrimental to the network structure in *Porphyridium cruentum* suspensions, the effect was remarkably stronger when a higher homogenization pressure of 100 MPa was applied.

Different behavior was observed for suspensions of *Chlorella vulgaris* (Fig. 6.2D). Untreated suspensions presented viscoelastic behavior, characterized by a slightly higher viscous behavior since $G' < G"$ and $\delta > 45°$. In addition, the storage modulus was approximately 20 times lower than for untreated suspensions of *Porphyridium cruentum*, confirming the distinct rheological behavior of these two microalgae species. However, processing of *Chlorella vulgaris* suspensions can be applied to enhance the viscoelastic properties, which was already shown in Chapter 5. In fact, the thermal treatment resulted in a more structured system, with a storage modulus of 24 Pa and a phase angle of 30.5°. Similar to *Porphyridium cruentum*, subsequent HPH resulted in a loss of the gel stiffness. However, no significant differences were observed in G' values between HPH at 20 MPa and 100 MPa. Interestingly, the homogenization pressure influenced the gel behavior, since the elastic properties became more predominant over the viscous properties after HPH at 100 MPa. In other words, even though HPH at 100 MPa resulted in a loss of gel strength, interactions in these suspensions were more characterized by those of an elastic solid than a viscous fluid compared to thermally treated suspensions of *Chlorella vulgaris*.

6.3.1.2 Linear viscoelastic behavior: frequency sweep

The network structure was further characterized by frequency sweep measurements, to study the dependence of G' and $G"$ on the angular frequency. The obtained frequency sweep curves are presented in Fig. 6.3A and 6.3B for *Porphyridium cruentum* and *Chlorella vulgaris*, respectively. In addition, data of the frequency sweeps were fitted by a power law model (Eq. 4.1 and Eq. 4.2). Parameters a and b provide insight into the strength of the network, while parameters c and d are related to the viscoelastic behavior (Larson, 1999). The obtained estimates for parameters a, b and c are presented in Fig. 6.3C and 6.3D. Since values of parameter d are typically more sensitive to inertia phenomena of the measuring system, they will not be discussed in this chapter.

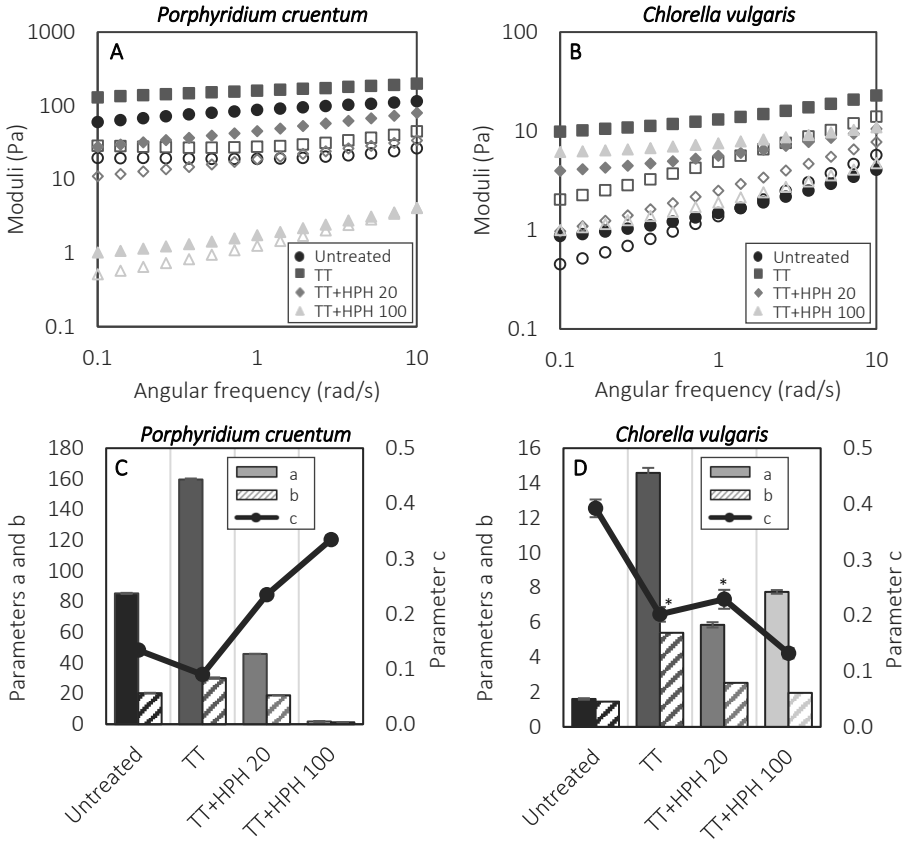

Fig. 6.3 Frequency sweep results at a constant shear strain of 1% for (un)processed suspensions of *Porphyridium cruentum* and *Chlorella vulgaris*. **A,B**: Storage modulus (G', filled symbols) and loss modulus ($G"$, empty symbols) as a function of the angular frequency. **C,D**: Power law models ($G' = a \cdot \omega^c$ and $G" = b \cdot \omega^d$) were fitted to the storage modulus (G') and loss modulus ($G"$) as a function of the angular frequency (ω). Parameters a (full bars) and b (dashed bars) are presented on the left axis, while parameter c is presented on the right axis. Standard errors are indicated by error bars (n = 4). The estimated values of the model parameters were compared statistically by use of 95% confidence intervals. Data points indicated with an asterisk are not significantly different.

The presentation of the network strength (parameters a and b) and the gel behavior (parameter c) in **Fig. 6.3C** and **6.3D** corresponds well with the data obtained from the strain sweep (**Fig. 6.2C** and **6.2D**) and similar conclusions can be drawn as discussed in previous paragraph. Generally, most suspensions of *Porphyridium cruentum* and *Chlorella vulgaris* displayed weak gel behavior, characterized by predominant elastic behavior ($a > b$), a low frequency dependency ($c < 0.5$), and a ratio of $G"/G'$ in the order of 10^{-1} (Kavanagh and Ross-Murphy, 1998; Lizarraga et al., 2006). Thermal processing was for both microalgae species the most effective approach to create

gelling properties in the biomass suspensions. In fact, whereas the strain sweep data suggested that thermal processing only affected the gel stiffness of *Porphyridium cruentum* suspensions (Fig. 6.2A), modelling of the frequency sweep curves also revealed a significant increase in gelling behavior (decrease of parameter c). Subsequent HPH resulted in decreased gelling properties in suspensions of both microalgae species, but different effects of homogenization pressure were observed. Whereas a higher pressure of 100 MPa caused a more drastic breakdown of the *Porphyridium cruentum* network structure compared to 20 MPa, the opposite was observed in *Chlorella vulgaris* suspensions. Finally, *Porphyridium cruentum* showed larger potential for use as a gelling agent than *Chlorella vulgaris*, with its network in the thermally treated suspensions about 10 times stronger than in *Chlorella vulgaris* suspensions.

6.3.1.3 Flow behavior

The viscosity curves of the (un)processed suspensions of *Porphyridium cruentum* and *Chlorella vulgaris* are presented in Fig. 6.4A and 6.4B, respectively. All suspensions presented shear-thinning flow behavior, as their viscosity decreased when shear rate was increased. This non-Newtonian flow behavior was also observed in Chapter 5 for these two microalgae species, indicating the presence of interactions between microalgal cells and/or polymers. To describe the flow behavior quantitatively, flow curves of (un)processed suspensions were fitted to a power law model (Eq. 5.2). No apparent yield stress was included in the model, since no constant values of log (σ) were observed at low shear rates in a log (σ) – log ($\dot{\gamma}$) plot. The parameter estimates of K and n are presented in Fig. 6.4C and 6.4D, respectively.

First, it was observed that values for the consistency coefficient were higher for all *Porphyridium cruentum* suspensions than for *Chlorella vulgaris*. Hence, next to its potential as a gelling agent, *Porphyridium cruentum* biomass is also a more promising source as a thickening agent than *Chlorella vulgaris*. Furthermore, an increased consistency coefficient was observed after thermal processing of *Porphyridium cruentum* suspensions. Thus, the increased network structure upon thermal processing (Fig. 6.3C) was also contributing to the viscosity of the suspension. Interestingly, no significant change in shear-thinning behavior was observed after thermal processing, with a flow behavior index of 0.23. It should be noted that very low values of n were obtained for *Porphyridium cruentum* suspensions, indicating that the increase of the shear stress was very limited at higher shear rates. Even though no yield stress parameter was included in our model, these findings suggest that a yield stress could be present in these suspensions. Extrapolation to lower shear rates would result in estimated yield stresses below 10 Pa for *Porphyridium cruentum* suspensions that were untreated, thermally processed, and treated by the

combination of thermal treatment and HPH at 20 MPa. Moreover, an increased consistency coefficient and shear-thinning behavior was observed after subsequent HPH at 20 MPa, even though a decreased network structure was found in the previous paragraph. Hence, the high viscosity in this suspension cannot be ascribed to the formation of an organized network structure. Instead, the increased viscosity could result from non-specific entanglement of disordered polymers or an increased water-binding capacity of biopolymers released by HPH (Saha and Bhattacharya, 2010; Santiago et al., 2017). However, when a higher homogenization pressure of 100 MPa was applied, the consistency coefficient was drastically reduced. In addition, the flow behavior index largely increased, indicating a loss of interactions between polymers and/or particles that would provide resistance to the flow. According to Ramus and Kenney (1989), shear forces reduce the viscosity of microalgal EPS, by breaking weak interactions between copolymers. The present results suggest that this phenomenon is only occurring at higher shear forces, since no loss in viscosity was observed after HPH at 20 MPa.

Thermal processing was also effective in increasing the viscosity of *Chlorella vulgaris* suspensions. A higher consistency coefficient and a lower flow behavior index indicate the presence of stronger interactions in thermally treated suspensions. Subsequent HPH at both pressure levels resulted in a decreased consistency coefficient and a slightly reduced shear-thinning behavior, however still higher than that of the untreated suspension. These results suggest that interactions which were formed during the thermal treatment, were partially destroyed by the mechanical process. Although interactions were occurring in the suspension that was thermally treated followed by HPH at 100 MPa (**Fig. 6.3D**), combination with the flow behavior illustrates that these interactions were rather weak, since they gave low resistance to higher shear stresses.

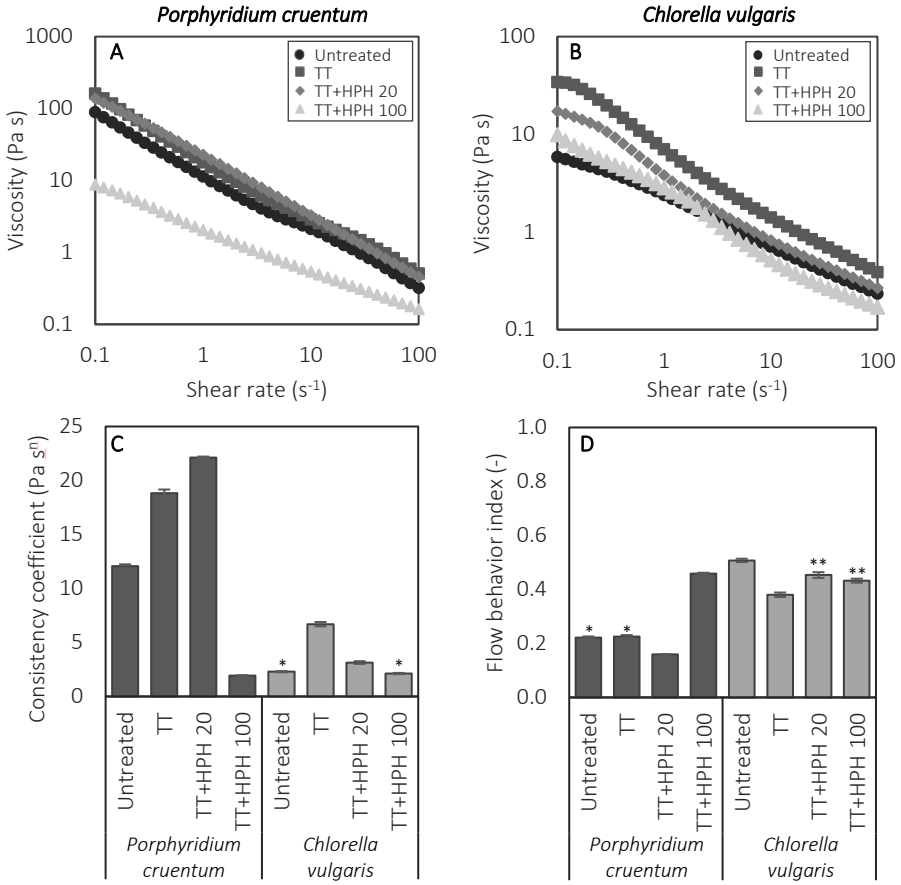

Fig. 6.4 Viscosity curves for (un)processed suspensions of *Porphyridium cruentum* **(A)** and *Chlorella vulgaris* **(B)**. A power law model ($\sigma = K \cdot \dot{\gamma}^n$) was fitted to the shear stress (σ) as a function of the shear rate ($\dot{\gamma}$), resulting in a consistency coefficient K and the flow behavior index n, plotted in **(C)** and **(D)**, respectively. Standard errors are indicated by error bars (n = 4). The estimated values of the model parameters were compared statistically by use of 95% confidence intervals. Data points of one microalga species that are indicated with a different number of asterisks are not significantly different.

As the rheological properties of suspensions are not only influenced by particle properties, such as size and shape, but also by the continuous phase (as described by Einstein's relation, **Eq. 5.4**), the contribution of the continuous phase to the overall viscosity of the suspensions was investigated by determining the flow behavior of the separated serum phase (**Fig. 6.5A** and **6.5B**). The flow curves were fitted to the power law model (**Eq. 5.2**) and the estimated parameters are shown in **Fig. 6.5C** and **6.5D**.

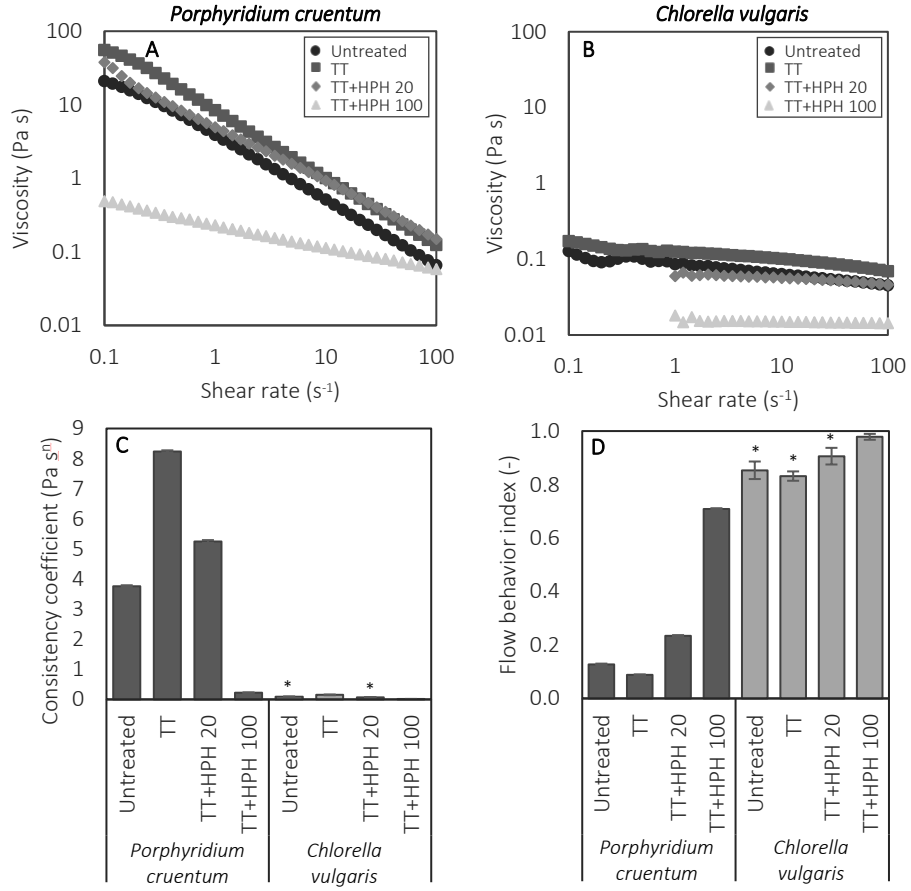

Fig. 6.5 Viscosity curves for the sera separated from (un)processed suspensions of *Porphyridium cruentum* **(A)** and *Chlorella vulgaris* **(B)**. A power law model ($\sigma = K \cdot \dot{\gamma}^n$) was fitted to the shear stress (σ) as a function of the shear rate ($\dot{\gamma}$), resulting in a consistency coefficient K and the flow behavior index n, plotted in **(C)** and **(D)**, respectively. Standard errors are indicated by error bars (n = 4). The estimated values of the model parameters were compared statistically by use of 95% confidence intervals. Data points indicated with an asterisk are not significantly different.

Low consistency coefficients were observed for all sera of *Chlorella vulgaris*, indicating that the solubilization of components into the continuous phase was limited. In addition, these sera presented little deviation from the Newtonian flow behavior, since flow indices of 0.83 – 0.98 were observed. In contrast, the serum phases of *Porphyridium cruentum* suspensions presented high consistency coefficients in combination with low flow behavior indices. Thermal processing resulted in a large increase of the consistency coefficient, in accordance with the suspension viscosity (Fig. 6.4). However, subsequent HPH at 20 MPa led to a decreased consistency and shear-thinning behavior. The high suspension viscosity can thus not be fully ascribed to solubilized polymers in the continuous phase. A drastic loss of viscosity and shear-thinning behavior was observed after HPH at 100 MPa, indicating that these high shear forces resulted in a reduced network formation between solubilized polymers in the continuous phase.

6.3.2 Effect of processing on the microstructure

In order to relate the rheological properties to changes in microstructural properties, the microstructure of the suspensions was studied by determining volumetric particle size distributions (Fig. 6.6) and visualized by microscopic images (Fig. 6.7). For both microalgae, the untreated suspensions were characterized by a bimodal particle size distribution, with one peak (1 – 10 µm) accounting for individual cells and the other peak (10 – 100 µm) for clusters of intact cells. This was previously observed in Chapter 5 and confirmed by microscopic images in the current chapter. These observations demonstrate the presence of intercellular polymer interactions, probably related to the EPS in both microalgae. However, the more elastic behavior of untreated *Porphyridium cruentum* suspensions suggests that interactions are stronger in this microalga compared to those in *Chlorella vulgaris*.

Thermal processing resulted in the formation of larger particles, with a diameter up to 200 µm. A large decrease in the volume fraction of individual cells indicates that more individual cells were introduced in cell clusters by the thermal treatment for both microalgae species. Whereas the clusters in the untreated suspensions were exclusively composed of intact cells, microscopic images suggest that the aggregates in the thermally treated suspensions also contained free cell material, especially for *Chlorella vulgaris*.

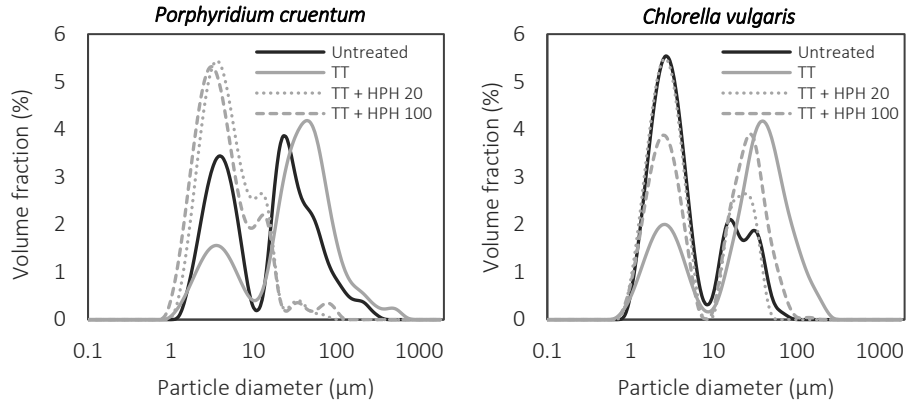

Fig. 6.6 Volumetric particle size distribution of suspensions of *Porphyridium cruentum* and *Chlorella vulgaris*. Untreated suspensions (Untreated), suspensions treated by a thermal treatment (TT) and a combination of a thermal treatment and high pressure homogenization at 20 MPa (TT+HPH 20) or 100 MPa (TT+HPH 100) are presented.

To identify the nature of this material, microscopic staining was performed with specific dyes (Fig. 6.8). Coomassie brilliant blue was used to localize proteins, yielding a blue color (465 nm) (Sedmak and Grossberg, 1977), whereas anionic polysaccharides were stained by acridine orange. In fact, acridine orange is a general dye which is also able to stain other anionic polymers such as DNA and shows two emission bands, resulting in a green (532 nm) or an orange-red color (650 nm) (Falcone et al., 2002). Proteins were only observed inside the cells of *Porphyridium cruentum*, visualized as blue colored material, with the exception of a few protein groups in the surrounding cell envelope. Staining with acridine orange clearly demonstrated the presence of anionic polysaccharides between the cells, as observed from the bright orange color of the filamentous structures surrounding the cells. The orange color indicates the highly acidic characteristics of these polysaccharides (Falcone et al., 2002), attributed to substantial amounts of glucuronic acid residues and sulfate groups in these polysaccharides (Chapter 4). These observations suggest that EPS play an important role as a glue between cells to create large aggregates, resulting in enhanced rheological properties of *Porphyridium cruentum* suspensions. In contrast, free material in aggregates of thermally treated suspensions of *Chlorella vulgaris* was clearly stained by the coomassie brilliant blue dye. In addition, acridine orange staining resulted in small spherical structures emitting green light. These observations suggest that proteins were solubilized during the thermal treatment and contributed to the formation of larger aggregates. Both protein and carbohydrate solubilization by thermal processing have been previously reported for microalgae (Gonzalez-Fernandez et al., 2012; Passos et al., 2014).

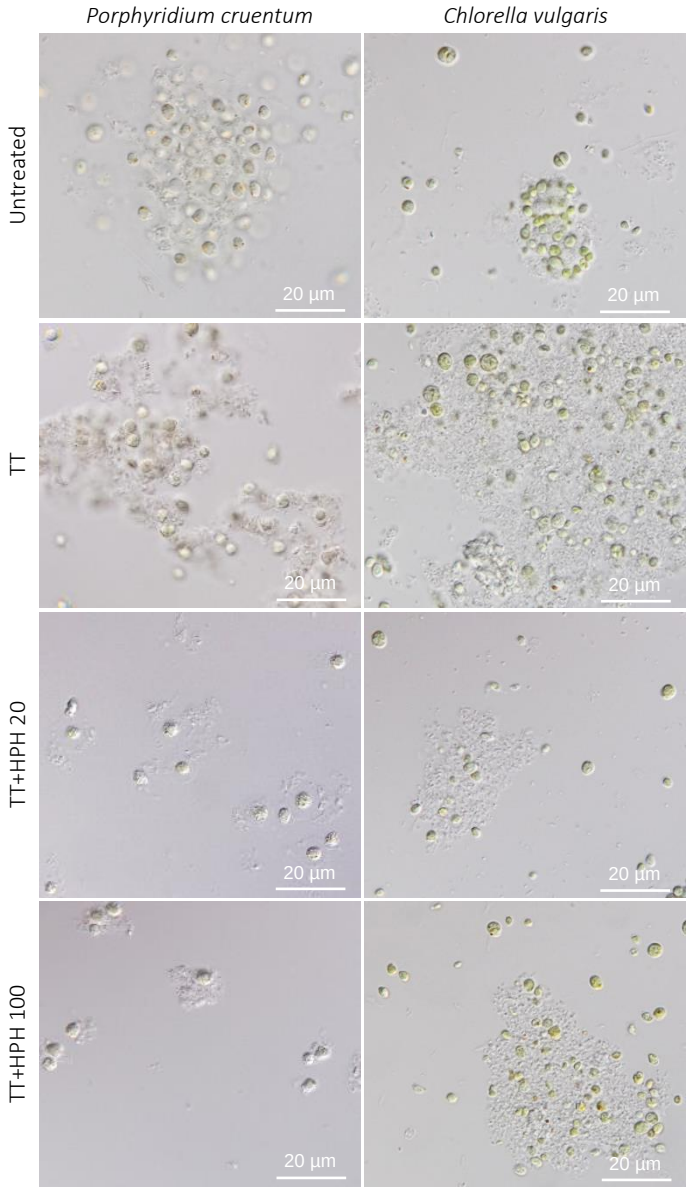

Fig. 6.7 Microscopic images of untreated suspensions (Untreated), suspensions treated by a thermal treatment (TT) and by a combination of a thermal treatment and high pressure homogenization at 20 MPa (TT+HPH 20) or 100 MPa (TT+HPH 100).

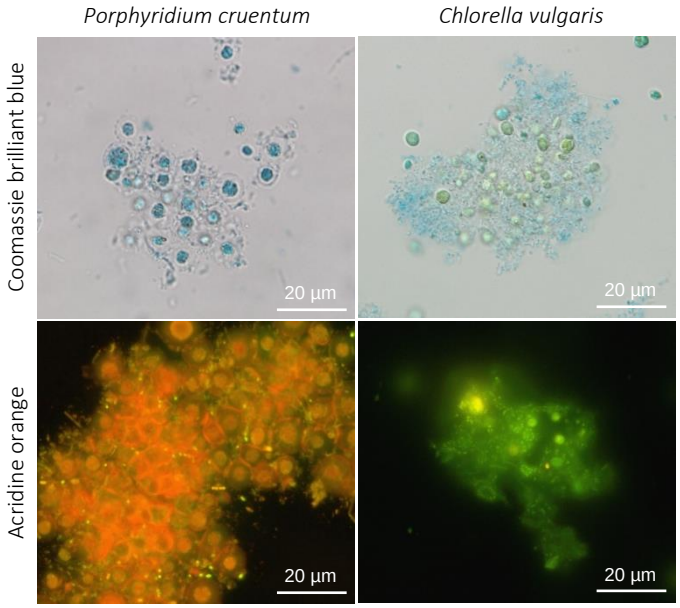

Fig. 6.8 Microscopic images of thermally treated suspensions (TT) that were stained with coomassie brilliant blue and acridine orange.

The use of HPH after thermal processing resulted in a decreased particle size for both microalgae species (**Fig. 6.6**). In *Porphyridium cruentum* suspensions, the final particle size was between 1 and 30 µm, irrespective of the homogenization pressure. Moreover, microscopic images showed similar microstructures in the homogenized samples (**Fig. 6.7**). As a consequence, the differences in rheological properties between HPH at 20 MPa and 100 MPa can be completely ascribed to the changes in serum viscosity. On the other hand, the effect of HPH on the particle size in *Chlorella vulgaris* suspensions was dependent on the pressure level. Surprisingly, HPH at 20 MPa resulted in a larger fraction of individual cells (1 – 10 µm) and somewhat smaller cell clusters (10 – 50 µm) compared to HPH at 100 MPa, which was also observed in the microscopic images. At higher homogenization pressures, larger shear forces occur which would intuitively facilitate the disruption of aggregates. However, it is hypothesized that HPH at 100 MPa did not only break aggregates, but also resulted in disruption of individual cells. As a consequence, more intracellular material was released, which contributed to the formation of aggregates and therefore resulted in larger particles compared to the suspension homogenized at 20 MPa. These microstructural findings support the observed changes in rheological behavior. In fact, the combination of thermal processing with HPH at 100 MPa resulted in a more elastic behavior, characterized by the lowest parameter c (**Fig. 6.3**), probably resulting from the composition and size of these aggregates. Interestingly, the processing sequence of thermal treatment followed by HPH resulted in a large

fraction of individual cells, regardless of the homogenization pressure. However, when HPH was directly applied on untreated suspensions of *Porphyridium cruentum* or *Chlorella vulgaris*, previous data showed a substantial degree of cell disruption (Chapter 5). It can therefore be concluded that a thermal pretreatment of microalgal suspensions influences the effect of HPH on cell disruption. Spiden et al. (2015) also reported a reduced degree of cell disruption for *Chlorella* sp. when thermally pretreated for 10 min at 90 °C. However, scanning electron microscopy (SEM) images revealed that the thermal treatment caused solidification of the protoplast, which remained intact after subsequent HPH (Spiden et al., 2015). Hence, the use of SEM imaging might be an interesting tool to investigate whether intact cells or solidified protoplasts were present in our processed suspensions. Nevertheless, it can still be concluded that the use of the thermal pretreatment hindered the release of intracellular material during HPH and therefore resulted in distinct rheological properties compared to HPH of untreated suspensions.

6.3.3 Comparison of different processing sequences

To quantify the effect of different processing sequences of mechanical and thermal treatments on the rheological properties, the data obtained in this chapter were compared with those of Chapter 5. This comparison was done for viscosity values at a specific shear rate of 10 s^{-1} and is presented in Fig. 6.9. Comparison of the linear viscoelastic behavior of these suspensions, as the storage modulus at an angular frequency of 10 rad/s, yielded similar conclusions (not shown). Since slightly different viscosities were observed for untreated suspensions due to batch variability, all data were normalized according to their untreated suspensions. In addition, a hypothesized schematic overview of the observed microstructural changes due to different processing sequences is shown in Fig. 6.10. Depending on the type, the intensity, and the sequence of processing steps, different biopolymers are affected resulting in distinct microstructures. For instance, the occurrence of protein denaturation or interactions between solubilized EPS in the serum phase largely influenced the microstructural and rheological properties.

It should be noted that different intensities of thermal processing were used in the two chapters. In Chapter 5, a sterilization process was applied for suspensions at pH 6 as a preservation step to create shelf-stable products, equivalent to 5 min at 121.1 °C. In the present chapter, a thermal treatment with a lower intensity was applied as a functionalization process, i.e. 15 min at 95 °C. Nevertheless, thermal processing always resulted in an increased viscosity of suspensions of *Porphyridium cruentum* and *Chlorella vulgaris*, irrespective of the intensity of the thermal treatment. In contrast, HPH mostly decreased the viscosity of the suspensions, with large influence of the homogenization pressure. However, due to distinct biomass profiles of the two

microalgae species, differences were observed in rheological behavior and microstructural changes upon processing between *Porphyridium cruentum* and *Chlorella vulgaris*.

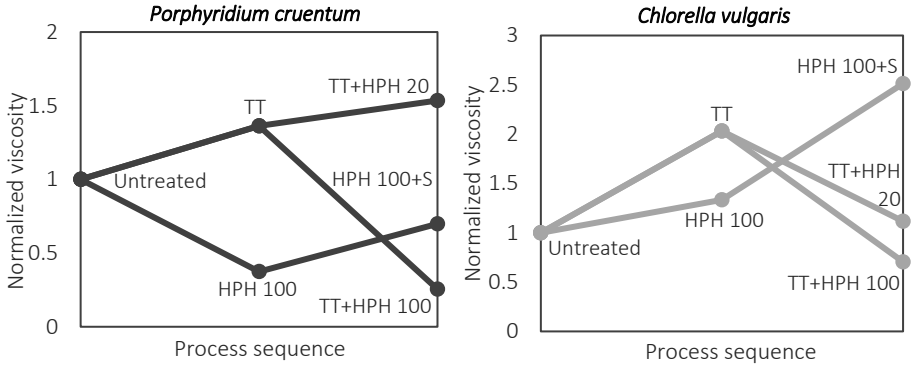

Fig. 6.9 Comparison of different sequences of mechanical and thermal processing of microalgal suspensions of *Porphyridium cruentum* and *Chlorella vulgaris*. The normalized viscosity at a shear rate of 10 s^{-1} is presented for untreated suspensions (Untreated), suspensions treated by a thermal treatment (TT) and a combination of a thermal treatment and high pressure homogenization at 20 MPa (TT+HPH 20) or 100 MPa (TT+HPH 100). In addition, data obtained in **Chapter 5** were included, presenting suspensions treated by high pressure homogenization at 100 MPa (HPH 100) and by a combination of high pressure homogenization and sterilization with a process value of $^{10\,°C}F_{121.1\,°C}$ = 5 min (HPH 100+S).

Untreated suspensions of *Porphyridium cruentum* presented a high viscosity, which was ascribed to their EPS causing intercellular interactions, resulting in large and stable cell clusters. Moreover, solubilization of these EPS into the continuous phase provided pronounced shear-thinning flow behavior to the serum phase. Whereas thermal processing strengthened these interactions, the use of HPH led to a drastic reduction of the viscosity due to its high shear forces. Even though the combination of thermal processing and HPH at 20 MPa resulted in the highest suspension viscosity, the mechanism behind it could not be revealed by the particle and serum characteristics. However, a drastic decrease in gel strength was observed for this suspension (**Fig. 6.3**), implying that the advantages of this processing sequence might be limited to specific applications. Therefore, it can be concluded that a thermal treatment is the most effective strategy to obtain a high viscosity in *Porphyridium cruentum* suspensions.

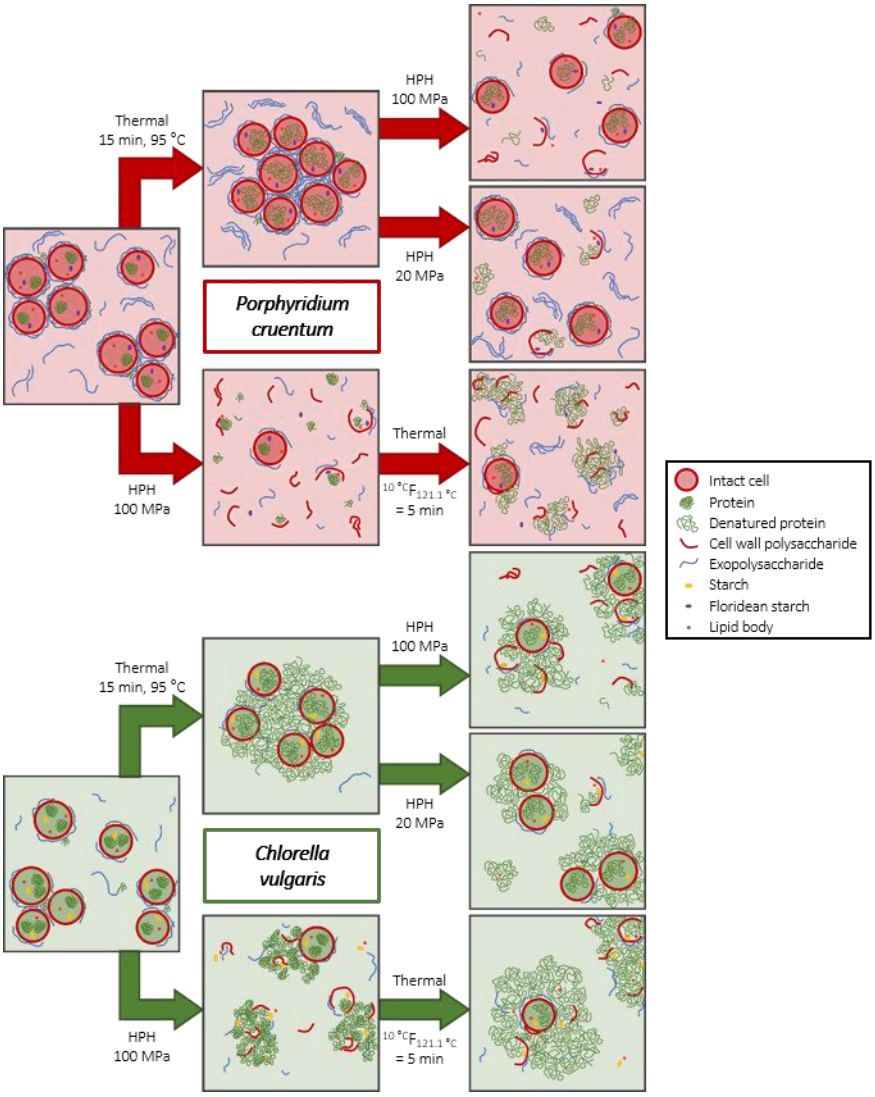

Fig. 6.10 Hypothesized schematic representation of the observed microstructural changes due to different processing sequences for suspensions of *Porphyridium cruentum* and *Chlorella vulgaris*, as applied in the current chapter and in Chapter 5. (HPH: high pressure homogenization)

In contrast, HPH of untreated *Chlorella vulgaris* suspensions resulted in a slight increase of the viscosity. As the untreated suspensions displayed only limited structural properties, disruption of the cells by HPH to release intracellular material provided structural build-up in this suspension. In fact, given the minimal contribution of the serum phase in all *Chlorella vulgaris* suspensions, the particle phase is determining the rheological behavior for this microalga. Applying thermal processing

resulted in improved rheological properties, mainly ascribed to protein denaturation and solubilization. Although a combination of HPH with sterilization led to the largest increase in viscosity, the same linear viscoelastic properties were observed when suspensions were immediately thermally treated (data not shown). As a consequence, these two treatments are both considered as the most effective processing strategies to obtain enhanced rheological properties of *Chlorella vulgaris* suspensions.

Interestingly, even though different processing strategies could be used to obtain certain gelling or thickening properties, the microstructure is affected differently (as shown in Fig. 6.10). When HPH is included as a first processing step, a substantial degree of cell disruption is achieved, which might be desired in many applications. For instance, nutrient bioaccessibility might possibly be improved by a cell disruption step, removing the cell wall as a barrier for releasing nutrients in the gastrointestinal tract, which will be studied in Chapter 8. In contrast, the use of direct thermal processing did not lead to disruption of the cells, but only resulted in solubilization of some intracellular components. Applying HPH on thermally pretreated suspensions resulted for both microalgae in a lower degree of cell disruption compared to HPH on untreated suspensions. Hence, taking into account the microstructural changes might be an important factor in the selection of the most suitable processing strategy for specific food applications, in order to design high-quality food products (both in terms of structural properties and nutritional characteristics).

6.4 CONCLUSIONS

The current chapter investigated the rheological properties of aqueous suspensions of *Porphyridium cruentum* and *Chlorella vulgaris*, two microalgae species that showed large potential as multifunctional ingredients in Chapter 5. It was demonstrated that different sequences of mechanical and thermal processing resulted in distinct rheological properties. In general, HPH resulted in a reduction of the rheological properties, whereas thermal treatment was an effective processing step to achieve structure build-up. However, combination of HPH with a subsequent sterilization process also proved successful for *Chlorella vulgaris* suspensions. Protein denaturation and solubilization were regarded as the main mechanisms influencing the rheological properties of *Chlorella vulgaris* suspensions, with only minimal contribution of the serum viscosity. In contrast, a large serum viscosity for all (un)processed suspensions of *Porphyridium cruentum* revealed the importance of the EPS, providing substantial contribution to the rheological properties.

The results of this chapter also demonstrate the importance of the microstructural changes upon processing. Even though HPH did not result in structure build-up, it

might still be a necessary processing step for disruption of microalgal cells, for instance to possibly enhance the bioaccessibility of intracellular compounds as will be studied in Chapter 8. For suspensions of *Chlorella vulgaris*, HPH could be combined with a subsequent sterilization process to improve the rheological properties, since this sequence resulted in equal gelling and thickening properties as a thermal treatment alone. In contrast, no effective processing strategy was found for *Porphyridium cruentum* suspensions when HPH was included. As a consequence, optimization of cell disruption treatments in relation to the rheological properties might be desired. The use of a lower homogenization pressure could possibly result in an optimal balance between a substantial degree of cell disruption and a minimal destruction of the network structure.

PART IV

IMPLICATIONS FOR NUTRIENT BIOACCESSIBILITY

CHAPTER 7

Effect of (ultra) high pressure homogenization on cell disruption of *Nannochloropsis* sp.

7.1 INTRODUCTION

The enormous diversity in cell wall composition of different microalgae species leads to a high variability in resistance to cell disruption. In fact, whereas some microalgal cells are easily ruptured by mild processes, such as the fragile cells of *Arthrospira* sp. and *Isochrysis* sp. (Safi et al., 2014a; Zhu and Lee, 1997), other microalgae species are known to have very rigid cells. *Nannochloropsis* sp. belongs to the latter category, and is actually known as one of the most resistant microalgae species (Alhattab et al., 2019). *Nannochloropsis* sp. belongs to the Eustigmatophyta, and is characterized by spherical cells with a diameter between 2 and 5 µm (Fawley and Fawley, 2007). Its cell wall is composed of an inner cell wall layer of cellulosic polymers (representing 75% of the cell wall) and an outer cell wall layer of algaenans. The latter are characterized as highly resistant long-chain aliphatic hydrocarbons cross-linked by ether bonds, and are most likely responsible for the strong resistance of the *Nannochloropsis* sp. cell wall against mechanical rupture (Scholz et al., 2014).

Microalgal cell disruption is required for various applications, for instance to improve lipid extractability with non-halogenated solvents (Alhattab et al., 2019; Günerken et al., 2015; Halim et al., 2012). In addition, it is hypothesized that disruption of microalgal cells would enhance the digestibility and nutrient bioaccessibility, since it is assumed that the cell wall is not degraded by the digestive enzymes in the gastrointestinal tract up to the small intestine (Cavonius et al., 2016; Gille et al., 2016). In this context, there is a need for efficient cell disruption techniques. HPH is one of the most promising cell disruption techniques, mainly due to its scalability, its

This chapter is based on the following paper:
Bernaerts T.M.M., Gheysen L., Foubert I., Hendrickx M.E., Van Loey A.M.
Evaluating microalgal cell disruption upon ultra high pressure homogenization.
Algal Research, submitted.

applicability on highly concentrated algal slurries, and its effectiveness for disruption of rigid cell walled microalgae species (Lee et al., 2017). To date, most studies on HPH for microalgal disruption have been performed with homogenization pressures up to 100 – 150 MPa, requiring multiple homogenization passes for rigid microalgae (Günerken et al., 2015). Higher homogenization pressures might actually be applied (up to 300 MPa), designated as UHPH, probably resulting in a more efficient disruption process by reducing the number of homogenization passes. However, little evidence has been found in literature in this range of ultra high homogenization pressures.

The aim of this chapter is to investigate the potential of (U)HPH on the disruption of *Nannochloropsis* sp. cells. To understand the impact of (U)HPH on the extent of cell disruption, four techniques for evaluation of cell rupture will be combined, including turbidity measurement, scanning electron microscopy (SEM), lipid extractability with different solvents, and microscopy using the viability stain SYTOX green. The combination of these four analytical methods will provide comprehensive insights into the disruption process of *Nannochloropsis* sp. cells upon (U)HPH.

7.2 MATERIALS AND METHODS

7.2.1 Microalgal biomass

Lyophilized biomass of *Nannochloropsis* sp. was purchased from Proviron Industries nv (Hemiksem, Belgium) and stored in closed containers at -80 °C until use. The microalgae were cultivated as described by Fret et al. (2017), with slight modifications. In short, the microalgae were cultivated in ProviAPT flat panel photobioreactors illuminated with LED-lighting in a semi-continuous mode. About one third of the culture was harvested daily and substituted by fresh culture medium. The microalgae were harvested by centrifugation and lyophilized.

Spray-dried biomass of *Chlorella vulgaris* obtained from Allmicroalgae Natural Products (Lisbon, Portugal) was used for SEM imaging, for comparing the disruption process to *Nannochloropsis* sp. biomass.

7.2.2 (Ultra) high pressure homogenization

Microalgal biomass was suspended overnight in demineralized water in a concentration of 0.1% (w/w). Additional suspensions were prepared in a concentration of 0.025% (w/w) for evaluation of turbidity according to Spiden et al. (2013a). All suspensions were treated by (U)HPH using a pressure cell homogenizer (Stansted Fluid Power SPCH-10, Harlow, United Kingdom), operating at 100 MPa or 250 MPa. The suspensions were at room temperature when fed into the homogenizer

and the pressure cell was cooled using a cryostat at 4 °C to minimize temperature increases. However, this could not prevent sample heating at the highest pressures, as temperatures up to ~70 °C were measured immediately after UHPH at 250 MPa. The homogenized samples were collected and immediately cooled to room temperature in an ice water bath between different passes and before conducting analyses. Part of the homogenized suspensions were lyophilized (Christ Alpha 2-4 LSCplus, Osterode, Germany) for determination of the hexane:isopropanol (HI) extraction efficiency. All other analyses were performed on the freshly homogenized suspensions, within the same day of the (U)HPH treatment. Suspensions at each concentration were prepared in twofold and were (U)HPH treated independently from its duplicate.

7.2.3 Evaluation of degree of cell disruption

7.2.3.1 Turbidity measurement

Turbidity was determined according to Spiden et al. (2013a). The turbidity was determined by measuring the optical density of the samples at 750 nm using a UV-VIS spectrophotometer (Ultrospec 2100 pro, Biochrom, Cambridge, United Kingdom). Turbidity measurements were performed in duplicate.

Turbidity values were normalized to be expressed as relative turbidity, according to Eq. 7.1:

$$RT_i = 1 - \frac{T_i - T_0}{T_9 - T_0} \qquad \text{(Eq. 7.1)}$$

with RT_i the relative turbidity after i passes, T_i the measured transmission for a suspension homogenized for i passes, T_9 the measured transmission for the suspension homogenized by UHPH at 250 MPa for 9 passes (i.e. the maximum transmission), and T_0 the measured transmission for the untreated suspension (corresponding to 0 passes).

7.2.3.2 Scanning electron microscopy

Visualization of cell disruption by SEM was performed as described by Spiden et al. (2015), with minor modifications. Glass coverslips were coated with a 0.1% solution of polyethyleneimine and dried by heating under a flame. Freshly homogenized suspensions were incubated on the glass coverslips for 1 h. Then, the coverslips were immersed in 2.5% glutaraldehyde in phosphate buffered saline (PBS) for 1 h and subsequently rinsed three times in PBS for 10 min. The samples were subsequently dehydrated using increasing concentrations of ethanol, by immersing for 10 min in 10%, 30%, 50%, and 70% ethanol in water. The coverslips were transferred to a

mixture of 70% ethanol and dimethoxymethane (1:1 v/v) for 5 min, followed by immersing in pure dimethoxymethane for 20 min. The coverslips were then dried in a critical point dryer (CPD 030, Balzers, Liechtenstein), by gradually replacing the solvent with liquid CO_2 (8 °C, 50 bar). Subsequently, the liquid CO_2 was brought to the gaseous phase by trespassing the critical point of CO_2 (45 °C, 100 bar). The dried coverslips were then mounted onto aluminum stubs with double-sided carbon tabs and coated with gold using a sputter coater (SPI-Module, SPI Supplies, West-Chester, PA, USA). Finally, images were obtained with a scanning electron microscope (JSM-6360, Jeol, Tokyo, Japan) using a spot size of 15 kV.

7.2.3.3 Hexane:isopropanol extraction efficiency

The HI extraction efficiency was determined as the ratio of the extraction yield with hexane:isopropanol (3:2 v/v) compared to the extraction yield with chloroform:methanol (1:1 v/v). The latter solvent mixture is known to extract the total amount of lipids, whereas HI does not easily penetrate intact rigid microalgal cells, resulting in a lower extraction yield (Balduyck et al., 2017; Ryckebosch et al., 2014b).

The HI extraction was performed in duplicate as described by Balduyck et al. (2017). Hereto, 6 mL of hexane:isopropanol (3:2 v/v) was added to 100 mg of microalgal biomass and the mixtures were vortexed for 30 s. The samples were centrifuged (10 min, 750g, 25°C) and the solvent layer was transferred to a weighed flask. In total, these extraction steps were performed 4 times. All solvent layers were combined, the solvent was removed by rotary evaporation, and lipids were quantified gravimetrically. The CM extraction was performed in triplicate, exactly as described in section 2.2.3.

7.2.3.4 Fluorescence microscopy using a viability stain

The viability of the cells was investigated by a dual-fluorescence procedure of Sato et al. (2004), using the fluorescent dye SYTOX green. In short, 0.5 µL of SYTOX green stock solution (supplied as a 5 mM stock solution in DMSO, ThermoFisher Scientific) was added to 1 mL cell suspension, and the mixture was incubated for at least 5 min in the dark. The samples were visualized by epifluorescence microscopy, using an Olympus BX-51 light microscope equipped with a XC-50 digital camera (Olympus, Optical Co.Ltd., Tokyo, Japan), and an excitation filter between 460 and 495 nm (X-Cite® 120Q, EXFO Europe, Hants, United Kingdom).

The fraction of cells stained with SYTOX green was quantified using ImageJ 1.52k software. To identify stained cells (i.e. green-colored cells), the color threshold was adjusted using L*a*b* values ($0 \leq L^* \leq 255$; $0 \leq a^* \leq 110$; $0 \leq b^* \leq 255$). The identified cells were automatically counted by software's 'Find maxima' tool, using a noise

tolerance of 20 and excluding edge maxima. Cells with intact membranes (i.e. red-colored cells) were identified with different color thresholds ($0 \leq L^* \leq 255$; $140 \leq a^* \leq 255$; $0 \leq b^* \leq 255$) and counted using a noise tolerance of 15 and excluding edge maxima. The fraction of cells with damaged membranes (x) was finally calculated using **Eq. 7.2**:

$$x(\%) = \frac{N_g}{N_g + N_r} \times 100 \quad \textbf{(Eq. 7.2)}$$

with N_g the number of green-colored cells (i.e. with damaged membranes, stained by SYTOX green) and N_r the number of red-colored cells (i.e. with intact membranes, colored by autofluorescence). For each sample 20 microscopic images were analyzed, and only images displaying more than 10 cells were used.

7.3 RESULTS AND DISCUSSION

7.3.1 Turbidity

Although measuring turbidity is an indirect quantification technique, it has been proposed as a fast and reproducible analysis to monitor cell disruption of *Nannochloropsis* sp., only giving slight underestimation of the degree of cell disruption compared to cell counting (Spiden et al., 2013b). The observed changes in turbidity upon (U)HPH are presented in **Fig. 7.1**. A decrease in turbidity as a function of homogenization passes was in agreement with studies of Spiden et al. (2013a, 2013b), corresponding to a reduction in the effective solid biomass concentration and the subsequent light scattering. A similar decay was observed for HPH at 100 MPa as in the study of Spiden et al. (2013b), and the relative turbidity of 0.33 ± 0.03 obtained after 9 passes coincides well with cell count data obtained by Spiden et al. (2013b). The same relative turbidity (0.32 ± 0.08) was however obtained after a single pass when applying a higher homogenization pressure of 250 MPa. As a matter of fact, these observations correspond well with the predictions of the exponential decay model for *Nannochloropsis* sp. constructed by Spiden et al. (2013b). It might however still be an underestimation of the disruption degree, as Montalescot et al. (2015) even reported > 95% of *Nannochloropsis oculata* cells to be disrupted after 1 pass at 250 MPa based on cell counting. Moreover, the current study shows that a plateau value seems to be reached after 2 passes at 250 MPa, indicating that further UHPH caused little changes in turbidity. Hence, increasing the homogenization pressure obviously reduces the number of passes required to obtain a certain degree of cell disruption.

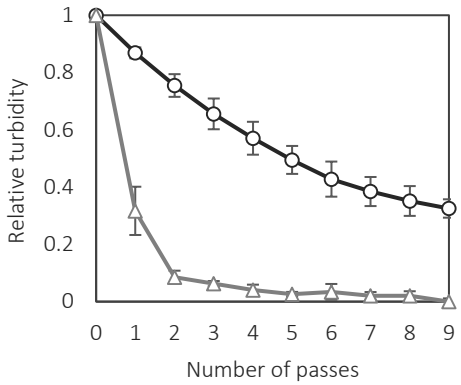

Fig. 7.1 Relative turbidity of *Nannochloropsis* sp. suspensions as a function of passes of (ultra) high pressure homogenization at 100 MPa (circles) and 250 MPa (triangles). Turbidity values were normalized to the value for untreated suspensions (0 passes). Error bars represent the standard error from duplicate sample preparation and duplicate measurements (n = 4).

It is worth noting that the applicability of a processing treatment (e.g. combination of passes and pressure level of (U)HPH) and/or quantification parameter (e.g. indirect versus direct technique) is largely depending on the depicted definition of cell disruption. In fact, cell disruption generally covers the whole range from damaged cells to completely fragmented cell compounds, as clearly illustrated by Spiden et al. (2013a). In case of turbidity, the indirect nature of this evaluation technique might complicate the interpretation of the results obtained, since turbidity values are also affected by further fragmentation of released intracellular components, even after complete cell breakage. Therefore, turbidity curves were combined with SEM images in the present study.

7.3.2 Scanning electron microscopy

Intact cells of *Nannochloropsis* sp. can be described as spherical cells with a smooth cell surface and a diameter of approximately 2 µm (Fawley and Fawley, 2007), corresponding to the visual observations in **Fig. 7.2**.

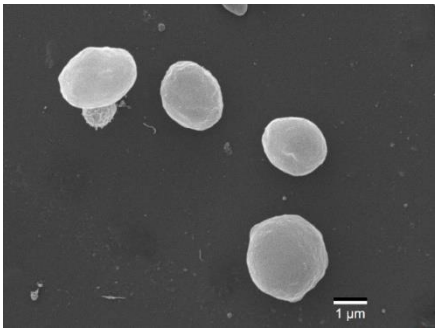

Fig. 7.2 Representative scanning electron microscopy images of untreated *Nannochloropsis* sp. cells.

The impact of (U)HPH on the microstructure of *Nannochloropsis* sp. suspensions can be seen in Fig. 7.3, from SEM images after a different number of passes at different pressure levels (100 MPa and 250 MPa). To assess the effect of cell disruption in SEM images, intact cells were distinguished from damaged ones based on the smoothness of their cell surface. Hence, a single pass of HPH at 100 MPa resulted in the disruption of some microalgal cells, while the majority of the cells seemed unaffected. This corresponds to the turbidity curves (Fig. 7.1), indicating that less than 20% of the cells were disrupted under these HPH conditions. A low degree of cell disruption at 100 MPa was also observed in Chapter 5, irrespective of the pH of the *Nannochloropsis* sp. suspensions. The more passes of HPH at 100 MPa were applied, the lesser the number of undamaged cells were observed, and the larger the aggregates of released compounds. Applying a higher pressure of 250 MPa obviously enhanced cell disruption, since aggregated material was observed together with a minority of undamaged cells, even after a single pass. Whereas intact cells were only sporadically encountered after 2 passes of UHPH at 250 MPa, no intact cells were observed after 4 passes at 250 MPa. Hence, the latter UHPH conditions evidently lead to complete cell disruption, generating large aggregates of released cell material in which interactions seem to occur between proteins (globular structures) and cell wall fragments (smooth layers), amongst others. The visual appearance of the aggregates observed after 4 passes of UHPH at 250 MPa suggests a larger extent of network formation compared to milder homogenization conditions (i.e. lower number of passes and/or lower pressure level), probably related to the temperature increases occurring during UHPH at 250 MPa (up to ~70 °C).

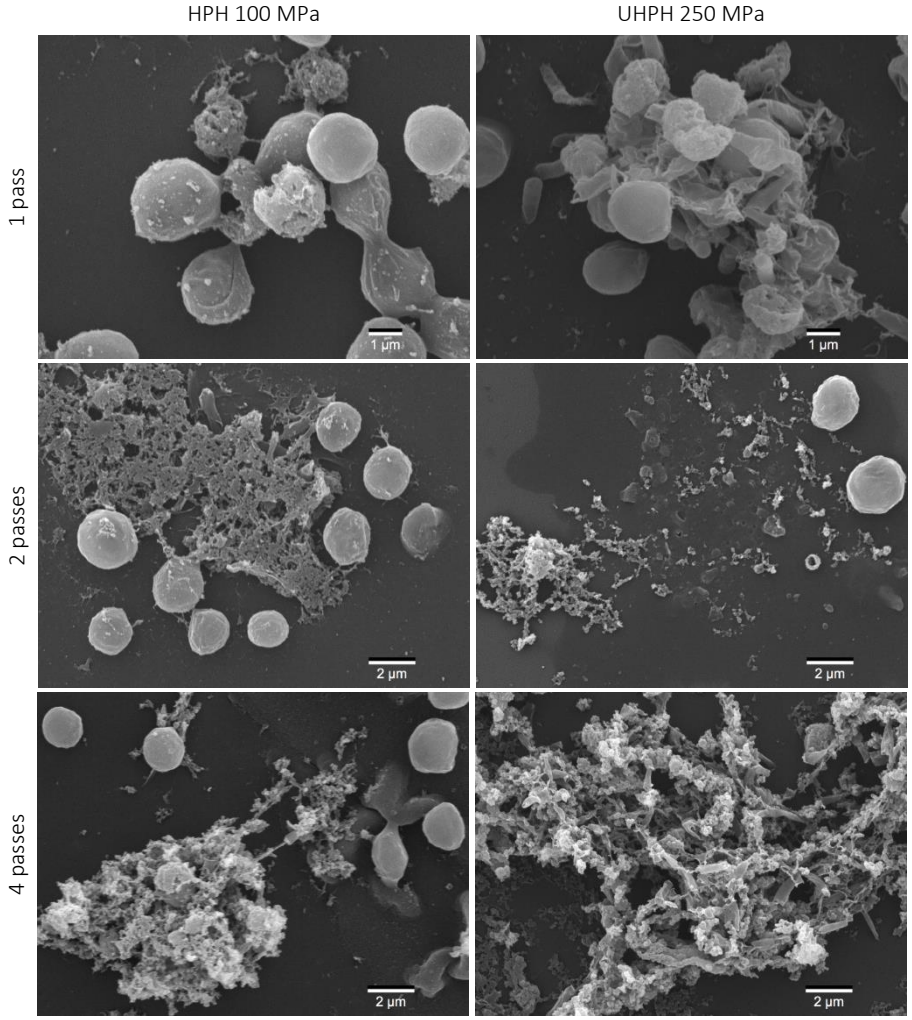

Fig. 7.3 Representative scanning electron microscopy images of *Nannochloropsis* sp. suspensions after different passes of high pressure homogenization (HPH 100 MPa) and ultra high pressure homogenization (UHPH 250 MPa).

The SEM images illustrated that *Nannochloropsis* sp. cells rather experienced cell damaging by (U)HPH than disintegration of the cell wall. This was evidenced by the fact that (U)HPH mainly resulted in sphere-like structures with a roughened surface, and no cells were encountered with a partially broken cell wall layer under any of the (U)HPH conditions. In contrast, when applying a single pass of HPH at 100 MPa on *Chlorella vulgaris* suspensions, breakage of the cell wall was clearly observed together with the release of intracellular material, as shown in **Fig. 7.4**. Similar cell breakage has been previously visualized for *Chlorella* sp. by Yap et al. (2014) after HPH at

75 MPa. The difference in cell disruption mechanism between the two microalgae species is probably related to the composition of the cell wall, suggesting a higher rigidity and lower flexibility of the algaenan-based cell wall of *Nannochloropsis* sp. compared to *Chlorella vulgaris*.

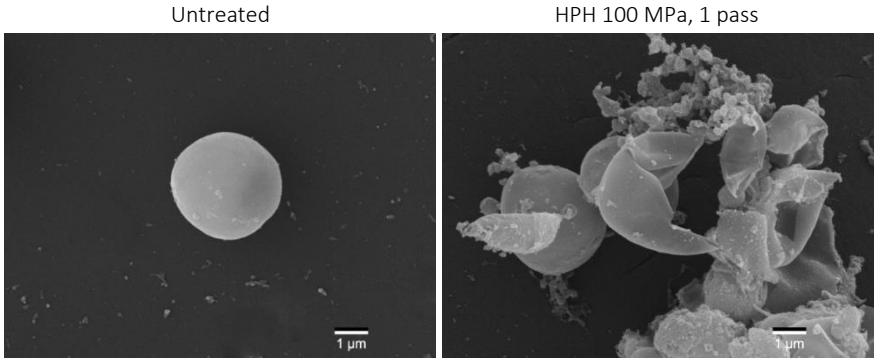

Fig. 7.4 Representative scanning electron microscopy images of *Chlorella vulgaris* cells before and after a single pass of high pressure homogenization (HPH) at 100 MPa.

Even though SEM imaging proves useful to get more insight into the impact of (U)HPH treatments on the microstructure, the use of this technique for evaluation of the cell disruption degree has some drawbacks. First, assessment of the cell integrity is solely based on the visual appearance of the cells, and an irregular cell surface might also be induced by experimental defects such as the collapse during (incorrect) drying of the sample. Secondly, SEM imaging is a non-quantitative technique, complicating the interpretation at intermediate levels of cell disruption. Hence, combination of SEM imaging with a quantitative technique for evaluation of cell disruption is recommended.

7.3.3 Hexane:isopropanol extraction efficiency

Comparison of lipid extraction yields obtained by different solvents has recently been suggested as a quantitative measure for the degree of cell disruption (Balduyck et al., 2017, 2018; Lemahieu et al., 2016). This is based on the fact that the non-halogenated solvent mixture HI is not able to penetrate through intact cells, whereas the halogenated solvent mixture CM has been demonstrated to extract the total amount of lipids regardless of the cell integrity (Balduyck et al., 2017; Ryckebosch et al., 2012, 2014b). The HI extraction efficiency, given as the ratio of HI extraction yield to CM extraction yield, is shown in **Fig. 7.5** for the (U)HPH-treated *Nannochloropsis* sp. suspensions. HI extraction efficiency as a function of the number of homogenization passes follows a similar trend as observed in the turbidity curves (**Fig. 7.1**). In addition, the use of a higher homogenization pressure requires a reduced number of passes to

obtain complete lipid extraction, since the plateau value seems to be reached after 2 passes for UHPH at 250 MPa, similarly as concluded from the turbidity curves. However, a less pronounced difference between the different pressures was observed from the HI extraction efficiency as compared to turbidity values. Moreover, suspensions homogenized at these different pressure levels tend to reach the same plateau value close to 100%, implying extraction of the total lipid content regardless of the homogenization pressure. A possible explanation for the discrepancy between turbidity and HI extraction efficiency might be the fact that absolute turbidity values were largely influenced by heating of the sample at ultra high pressures (due to heat-induced reactions resulting in distinct light scattering properties of the sample), while HI extraction efficiency is assumed to be less affected by short-time temperature increases (except for possible microstructural changes facilitating lipid extraction). In addition, it is likely that partial disruption of a microalgal cell might be sufficient for extraction of the lipids with HI, whereas turbidity measurements are sensitive to further fragmentation of the cell material.

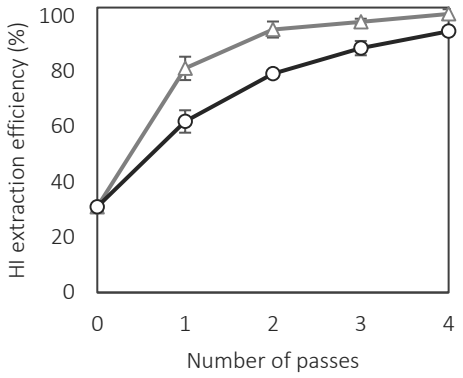

Fig. 7.5 Hexane:isopropanol (HI) extraction efficiency of *Nannochloropsis* sp. suspensions as a function of passes of (ultra) high pressure homogenization at 100 MPa (circles) and 250 MPa (triangles). HI extraction efficiency is defined as the ratio between the extraction yield with hexane:isopropanol (3:2 v/v) and the extraction yield with chloroform:methanol (1:1 v/v). Error bars represent the standard error from duplicate sample preparation and duplicate measurements (n = 4).

It is worth noting that a HI extraction efficiency of 31.0 ± 1.3% was observed for the untreated *Nannochloropsis* sp. biomass, even though the cells appeared to be intact from the SEM image based on their smooth cell surface (Fig. 7.2). HI extraction efficiencies between 17.3% and ~45% have actually been reported for untreated *Nannochloropsis* sp. biomasses in previous studies (Balduyck et al., 2017, 2018; Lemahieu et al., 2016). Since the dry biomass was suspended in demineralized water

in the current study, membrane permeabilization might have occurred due to osmotic stress, possibly resulting in a higher extraction yield with HI. However, Balduyck et al. (2018) reported an even higher HI extraction efficiency (~45%) for microalgal paste of *Nannochloropsis* sp., suggesting that the enhanced lipid extractability possibly results from the cultivation and/or harvesting to obtain the concentrated algal paste, rather than from resuspending dried biomass in demineralized water. Nevertheless, based on the SEM images, the HI extractability for the untreated suspension could not be related to any microstructural characteristics of the surface cell wall layer.

7.3.4 SYTOX green staining

In order to investigate the integrity of the cell membrane before and after (U)HPH, a dual-fluorescence microscopy method with SYTOX green fluorescent dye was used. SYTOX green is a nucleic acid stain which can only penetrate damaged cell membranes, thereby functioning as a viability stain (Sato et al., 2004). This is illustrated in Fig. 7.6, representing a micrograph of the untreated *Nannochloropsis* sp. suspension. Cells with intact membranes can be observed as red colored cells, resulting from autofluorescence, whereas cells with damaged membranes are recognized by the green fluorescence color of the SYTOX green dye that was able to penetrate into the cells. It is clearly shown that before applying any (U)HPH treatment, about one third of the *Nannochloropsis* sp. cells showed damaged cell membranes. This microscopic observation corresponds well with the HI extraction efficiency of the untreated suspension (31.0 ± 1.3%), suggesting that the integrity of the cell membrane might be the limiting factor for lipid extraction with the HI solvent mixture.

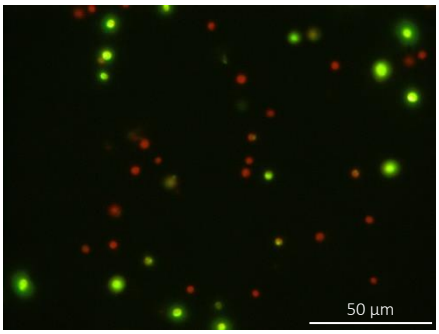

Fig. 7.6 Representative microscopic image of untreated *Nannochloropsis* sp. cells stained with SYTOX green. Cells with intact cell membranes (only red colored autofluorescence) can be distinguished from cells with damaged cell membranes (green fluorescence due to penetration of the SYTOX green dye).

Microscopic images of (U)HPH-treated suspensions stained with SYTOX green are shown in Fig. 7.7. When applying HPH at 100 MPa for multiple passes, the fraction of cells with intact membranes was noticeably reduced, with almost no intact cell membranes observed after 4 passes. This corresponds well with the HI extraction efficiency, as the plateau value for total lipid extraction seemed to be reached under these conditions (Fig. 7.5). Even though one might conclude that intact cells are still present after 4 passes of HPH at 100 MPa based on their visual appearance in SEM images, it is shown in Fig. 7.7 that these remaining cells are damaged in terms of membrane integrity. This observation raises concerns about the use of cell counting as the reference method for evaluating microalgal cell disruption, as our results clearly show that the visual appearance of spherical smooth cells under light microscopy does not predict the integrity of the cell membrane, therefore presumably underestimating the degree of cell disruption in terms of membrane integrity. After UHPH at 250 MPa, cells with intact membranes were less abundant, in agreement with the higher HI extraction efficiency of UHPH-treated suspensions. Furthermore, the presence of large aggregates can be observed from the micrographs. The different size and shapes of fluorescent spots after 3 and 4 passes of UHPH at 250 MPa suggests the staining of nucleic acids that have been released from the cells. This is also evidenced by a higher background fluorescence, indicating more nucleic acids being released into the aqueous phase of the *Nannochloropsis* sp. suspensions. Hence, UHPH at 250 MPa has a larger impact on *Nannochloropsis* sp. cells than HPH at 100 MPa, not only in terms of disintegrating the cell membrane and/or cell wall, but also by further fragmenting cell debris as concluded from the higher release of nucleic acids into the aqueous medium. It should be noted that the temperature increase during UHPH at 250 MPa might also have contributed to damaging the cell membranes. For instance, González-Fernández et al. (2012b) reported an enhanced SYTOX green staining of thermally pretreated cells of *Scenedesmus* sp. at 70 °C and 80 °C.

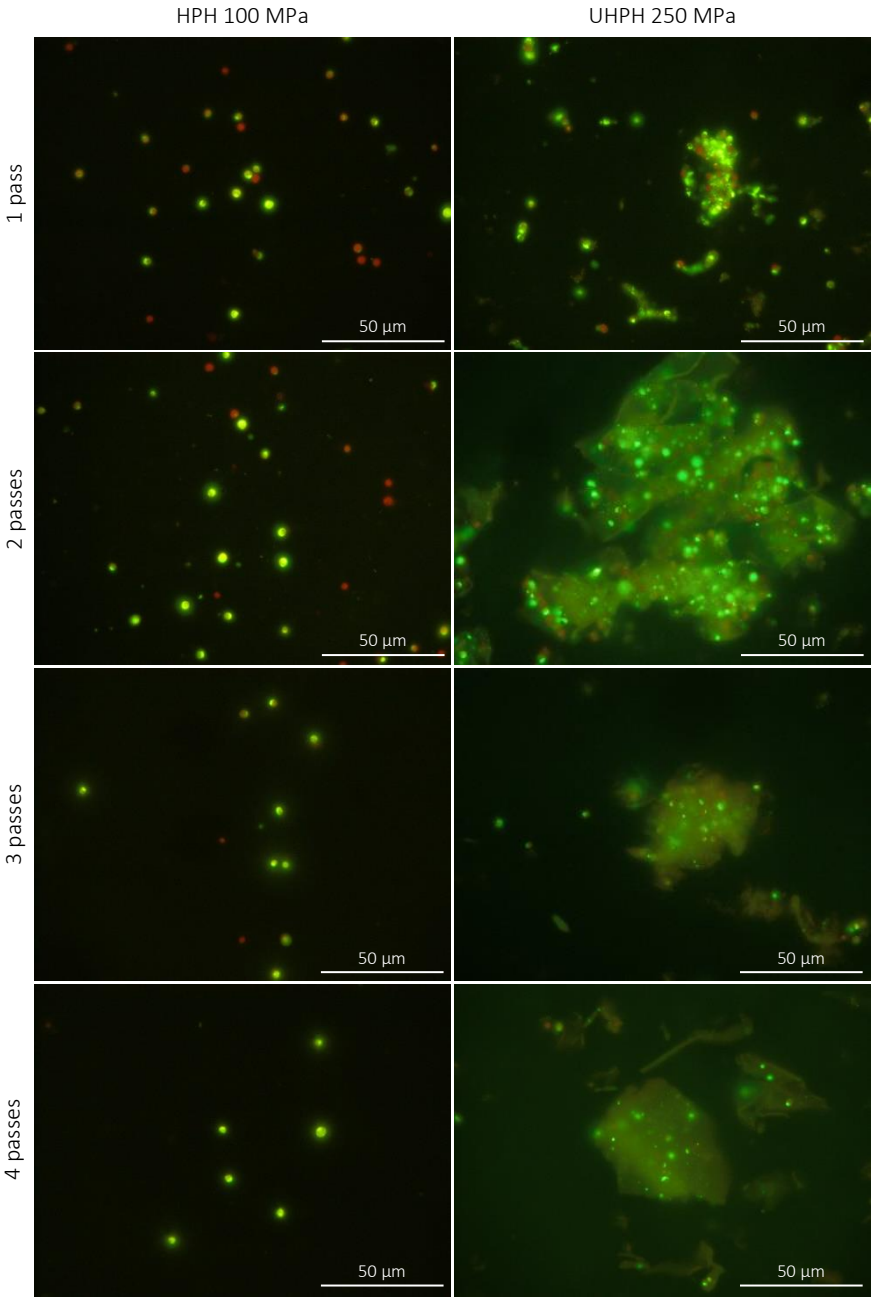

Fig. 7.7 Representative microscopic images of *Nannochloropsis* sp. cells after different passes of high pressure homogenization (HPH 100 MPa) and ultra high pressure homogenization (UHPH 250 MPa) stained with SYTOX green. Cells with intact cell membranes (only red colored autofluorescence) can be distinguished from cells with damaged cell membranes (green fluorescence due to penetration of the SYTOX green dye).

The fraction of cells stained with SYTOX green was quantified using image analysis, and compared to HI extraction efficiency in Fig. 7.8. The proportions of cells with damaged cell membranes estimated by these two techniques clearly coincide at all disruption stages, confirming the hypothesis that lipid extractability by different solvent mixtures is related to the integrity of the cell membrane. Hence, both methods are considered reliable techniques for quantitative evaluation of the membrane integrity of microalgal cells, which might be relevant for screening microalgae species and/or processing conditions based on membrane disruption degrees as desired for specific applications. Even though the dual-fluorescence method with SYTOX green is the least time-consuming method, it should be noted that this technique is not applicable when substantial aggregate formation occurs. This is observed from the micrographs of UHPH-treated *Nannochloropsis* sp. suspensions in Fig. 7.7, in which cellular structures cannot be accurately identified due to the extensive disintegration and aggregate formation. In contrast, HI extraction efficiency can be performed regardless of the extent of cellular disintegration.

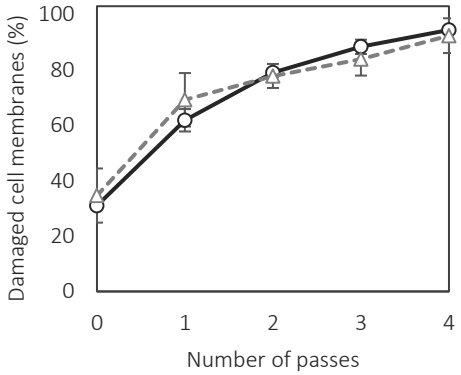

Fig. 7.8 Fraction of *Nannochloropsis* sp. cells with damaged cell membranes as a function of passes of high pressure homogenization at 100 MPa, determined by image analysis of microscopic images stained with SYTOX green (triangles, n = 20) and by hexane:isopropanol extraction efficiency (circles, n = 4).

Even though SYTOX green staining is directly related to the integrity of the cell membrane, it is worth noting that no conclusive information is gained on the integrity of the cell wall by use of this viability stain. In fact, it is generally assumed that membrane-impermeable fluorescent probes can passively diffuse through cell walls (Lebaron et al., 1998). Contrary to this general statement, a limited staining in *Nannochloropsis* sp. has been observed for some microscopic dyes such as Nile Red, attributed to a reduced penetration of the dye due to the cell wall structure and/or cell wall thickness (Balduyck et al., 2015; Rumin et al., 2015). In case of SYTOX green, a limited penetration has only been reported once for *Nannochloropsis* sp. (Veldhuis

et al., 1997), while other authors have successfully used this dye for this microalga, without reporting any penetration issues (Halim et al., 2019; Jeong et al., 2017). Moreover, SYTOX green penetration was studied for PEF-treated cells of *Chlamydomonas reinhardtii* and *Scenedesmus* sp., i.e. for cells with electroporated membranes without distorted cell walls, showing successful staining with SYTOX green (Bodénès et al., 2019; Lai et al., 2014). Hence, it is concluded that SYTOX green is a successful dye for nucleic acids in microalgal cells with damaged membranes, regardless of the cell wall integrity. Nevertheless, it should be kept in mind that changes in cell wall integrity might have occurred during (U)HPH (even for cells displaying a smooth surface in SEM images), which could not be investigated by use of SYTOX green staining.

7.4 CONCLUSIONS

The impact of (U)HPH on the disruption of the rigid *Nannochloropsis* sp. cells was investigated in this chapter. It was obvious that a higher homogenization pressure drastically reduced the number of passes required to obtain a certain degree of cell disruption. However, heating of the sample was inevitable at 250 MPa, which might not only lead to a different microstructure, but also to degradation of heat-labile compounds. Furthermore, it was shown that (U)HPH not only affected the cell wall, but also the membrane integrity. While cells would be considered intact based on the smoothness of the cell surface in SEM images, epifluorescence microscopy with the viability stain SYTOX green revealed the damaged membranes of several cells after (U)HPH, which was confirmed by an improved lipid extractability with HI. Hence, an accurate definition of cell disruption (i.e. membrane damaging vs. destruction of the cell wall) for a specific application is crucial in order to select appropriate (U)HPH conditions.

CHAPTER 8

The role of cell integrity in the lipid digestibility and *in vitro* bioaccessibility of carotenoids and ω3-LC-PUFA in *Nannochloropsis* sp.

8.1 INTRODUCTION

It was shown in previous chapters that the application of microalgal biomass in processed food products can be an effective and sustainable strategy to enrich food products with various nutrients and health-beneficial components, in combination with possible structuring benefits. Various processing strategies have been proposed to maximize the structuring potential of some microalgae, resulting in different microstructural properties as shown in Chapter 6, which might potentially lead to a distinct nutrient digestibility and bioaccessibility of health-beneficial components. It is actually hypothesized that the microalgal cell wall (except for cell walls rich in glycoproteins) is not degraded by the digestive enzymes present in the mouth, stomach, and/or small intestine. Hence, since absorption of nutritional compounds generally occurs in the small intestine, an intact cell wall might act as a physical barrier limiting the digestibility of intracellular nutrients as well as the bioaccessibility of health-beneficial components (Cavonius et al., 2016; Gille et al., 2016). Even though there are some indicative reports on the impact of processing to enhance the *in vitro* bioaccessibility of carotenoids in microalgae, results are contradicting and were not related to the microstructure of the processed microalgae (Chapter 1).

Therefore, the aim of this chapter is to investigate the role of the *Nannochloropsis* sp. cell integrity in the lipid digestibility and *in vitro* bioaccessibility of carotenoids and

This chapter is based on the following paper:
Bernaerts T.M.M., Verstreken H., Dejonghe C., Gheysen L., Foubert I., Grauwet T., Van Loey A.M.
The role of cell integrity in the lipid digestibility and in vitro bioaccessibility of ω3-LC-PUFA and carotenoids in Nannochloropsis sp.
In preparation.

ω3-LC-PUFA. *Nannochloropsis* sp. is known for its very rigid cell wall (Chapter 3), among the most resistant ones against mechanical and/or ultrasonic treatments (Montalescot et al., 2015; Spiden et al., 2013b). Nevertheless, strategies to obtain samples with disrupted cells have been identified in Chapter 7, by use of (U)HPH. Even though UHPH proved more efficient in disrupting *Nannochloropsis* sp. cells than HPH, the heating of the sample due to the ultra high pressures limits its applicability when studying heat-sensitive compounds such as carotenoids and ω3-LC-PUFA. In addition, the use of UHPH resulted in the formation of dense networks, possibly restricting the enzyme accessibility and/or the mobility of some health-beneficial components (e.g. structurally bound carotenoids) for migration to mixed micelles. Therefore, the use of HPH at 100 MPa for multiple passes was selected to obtain (nearly) full disruption of *Nannochloropsis* sp. cells, without drastic losses of carotenoids and ω3-LC-PUFA.

8.2 MATERIALS AND METHODS

8.2.1 Microalgal biomass

Lyophilized biomass of *Nannochloropsis* sp. was purchased from Proviron Industries nv (Hemiksem, Belgium) and stored in closed containers at -80 °C until use. The experiments were performed with the same batch used in Chapter 7. In addition, a different batch of *Nannochloropsis* sp. biomass with higher membrane permeability was provided by Proviron Industries nv for comparison of lipid digestibility and bioaccessibility (as discussed in section 8.3.5).

8.2.2 Production of different *Nannochloropsis* sp. samples

8.2.2.1 High pressure homogenization of biomass suspensions

Nannochloropsis sp. biomass was suspended in demineralized water for 1 h in a concentration of 10% w/w. The suspension was subsequently treated using HPH at 100 MPa for 4 passes (Panda 2K, Gea Niro Soavi, Parma, Italy), since these conditions were proven to result in disruption of the majority of *Nannochloropsis* sp. cells (Chapter 7). The inlet of the homogenizer was thermostated at 4 °C using a cryostat, and homogenized suspensions were cooled to room temperature in an ice water bath after each pass of HPH. Finally, the homogenized suspensions were lyophilized (Christ Alpha 2-4 LSCplus, Osterode, Germany) and stored in closed containers at -80 °C. The degree of cell disruption was estimated by determining the HI extraction efficiency and by use of the viability stain SYTOX green, as described in sections 7.2.3.3 and 7.2.3.4.

8.2.2.2 Extraction of Nannochloropsis sp. oil

Nannochloropsis sp. oil was extracted with hexane:isopropanol (3:2 v/v) as described by Gheysen et al. (2019b). In short, 1.5 L of hexane:isopropanol (3:2 v/v) was added to 100 g biomass and stirred for 90 min. The solvent was removed by vacuum filtration and the residual biomass was re-extracted using the same extraction procedure. Both extracts were combined, and the solvent was removed by rotary evaporation to obtain *Nannochloropsis* sp. oil.

8.2.3 *In vitro* digestion of *Nannochloropsis* sp. samples

A static *in vitro* digestion was performed based on the international consensus method of Minekus et al. (2014), in which a gastric and a small intestinal phase were simulated. Since *Nannochloropsis* sp. does not contain starch as SPS but chrysolaminarin (as shown in Chapter 2), no oral phase was simulated. *In vitro* digestion experiments were conducted under subdued light conditions.

8.2.3.1 Enzymes, bile salts, and simulated digestion fluids

Prior to the *in vitro* digestion procedure, enzymatic activities were determined in quadruplicate using the protocols described by Minekus et al. (2014). Pepsin from porcine gastric mucosa (Sigma-Aldrich) had a protease activity of 2959.2 U/mg according to the certificate of analysis of the supplier. Pancreatin 80/60/3 was kindly donated by Nordmark Arzneimittel GmbH & Co. KG (Uetersen, Germany), and displayed lipase activity of 151 ± 6 U/mg, trypsin activity of 1.9 ± 0.2 U/mg, chymotrypsin activity of 5.9 ± 0.7 U/mg, and amylase activity of 111 ± 13 U/mg. For lipase from porcine pancreas (Type II, Sigma-Aldrich), a lipase activity of 57.4 ± 2.5 U/mg was determined. Trypsin from porcine pancreas (Type IX-S, Sigma-Aldrich) and α-chymotrypsin from bovine pancreas (Type II, Sigma-Aldrich) had enzyme activities of 262.4 U/mg and 34.8 U/mg, respectively, according to the certificate of analysis of the supplier.

Porcine bile extract was purchased from Sigma-Aldrich. The concentration of bile salts was determined in quadruplicate using a commercial kit (Total Bile Acid Assay Kit, Diazyme) as proposed by Minekus et al. (2014). A bile salt concentration of 1.10 ± 0.13 mmol/g was found.

Simulated gastric fluid (SGF) and simulated intestinal fluid (SIF) were prepared exactly as recommended by Minekus et al. (2014).

8.2.3.2 Preparation of biomass suspensions and o/w-emulsions

Microalgal suspensions were prepared by suspending intact or disrupted biomass of *Nannochloropsis* sp. in ultrapure water (organic free, 18 MΩ cm resistance) in a concentration of 8% w/w, followed by stirring for exactly 30 min protected from light.

A 5% o/w-emulsion was prepared from the extracted *Nannochloropsis* sp. oil. Therefore, 12.5 g oil and 1.25 g Tween80 emulsifier were combined, and the total weight was adjusted to 250 g with ultrapure water (organic free, 18 MΩ cm resistance). The emulsion was mixed for 10 min at 9000 rpm with a lab mixer (Silverson L5M-A, East Longmeadow, MA, USA) and subsequently stabilized by HPH for 1 pass at 100 MPa (Panda 2K, Gea Niro Soavi, Parma, Italy). The o/w-emulsion was prepared the day before the *in vitro* digestion procedure, and was stored overnight at 4 °C protected from light.

8.2.3.3 In vitro digestion procedure

The *in vitro* digestion procedure was performed in dark brown falcon tubes, each containing 10 mL of suspension or 5 mL of o/w-emulsion (combined with 5 mL of ultrapure water) in order to standardize the lipid content to approximately 250 mg per tube. The exact weight of the suspension or o/w-emulsion was noted. Since a kinetic approach was used in the simulated intestinal phase (7.5, 15, 30, 45, 60, 90, and 120 min), a separate tube was prepared for each time moment. For additional experiments, endpoint determinations (i.e. 120 min) were performed in duplicate.

To simulate the gastric phase, following solutions were added to the samples: 7.5 mL of SGF, 5 µL of 0.3 M calcium chloride, 1.6 mL of pepsin solution (to obtain 2000 U/mL in the final chyme) containing 18.76 mg/mL pyrogallol as oxygen scavenger, 250 µL of 2 M HCl (to adjust the pH to 3), and 645 µL of ultrapure water (to achieve a total volume of 20 mL). The tubes were flushed with N_2 for 20 s and subsequently incubated for 2 h at 37 °C using end-over-end rotation.

Afterwards, the small intestinal phase was simulated by adding 11 mL of SIF, 40 µL of 0.3 M calcium chloride, 5 mL of pancreatic solution (containing pancreatin as well as additional lipase, trypsin, and/or α-chymotrypsin to obtain a lipase activity of 550 or 2000 U/mL, a trypsin activity of 100 U/mL, and a chymotrypsin activity of 25 U/mL in the final digest; and containing 14 mg/mL α-tocopherol as antioxidant), 2.5 mL of bile solution (to obtain 10 mM in the final digest), 400 µL of 0.1 M NaOH (to adjust the pH to 7), and 1.06 mL of ultrapure water (to achieve a total volume of 40 mL). The intestinal fluids were tempered at 37 °C before addition to the samples, in order to minimize temperature differences in the incubated samples. The tubes were flushed with N_2 for 10 s and subsequently incubated at 37 °C using end-over-end rotation. In

case a kinetic approach was used in the simulated intestinal phase, tubes were removed from the incubator at different time moments during the intestinal phase (7.5, 15, 30, 45, 60, 90, and 120 min).

Enzymes were inactivated by performing a heat shock. Therefore, digests were transferred to glass pyrex tubes and incubated in a water bath at 86.5 °C for 14 min, followed by cooling in an ice water bath. Part of the digest was ultracentrifuged (68 min, 165000g, 4 °C) (Optima XPN-80, Beckman Coulter, Fullerton, CA, USA), resulting in an aqueous phase, i.e. the micellar phase, and an insoluble pellet. The micellar phase was filtered through a 0.2 µm syringe filter (Chromafil® PET-20/25, Macherey-Nagel, Duren, Germany). All samples (i.e. suspension or o/w-emulsion, digest, micellar phase, and pellet) were finally lyophilized protected from light and analyzed in terms of lipid composition and carotenoid content.

8.2.4 Analyses

8.2.4.1 Determination of fatty acid profile and ω3-LC-PUFA content

The fatty acid profile was determined as described by Ryckebosch et al. (2012), with minor modifications. Total lipids were extracted from the lyophilized fractions using the CM extraction as described in section 2.2.3, with tridecanoic acid (C13:0) as an internal standard. Methylation of the fatty acids was performed by dissolving 5 mg of extracted lipids in 1 mL toluene, and addition of 2 mL of 1% sulfuric acid in methanol. The mixture was incubated overnight at 50 °C. Afterwards, 5 mL of 5% aqueous NaCl solution was added and the fatty acid methyl esters (FAME) were subsequently extracted with hexane. The hexane phase was finally diluted to 500 ng/µL for chromatographic analysis, using gas chromatography with cold-on-column injection and flame ionization detection (GC-FID) (Trace GC Ultra, Thermo Scientific, Interscience, Louvain-la-Neuve, Belgium). Samples were eluted on an EC Wax column of length 30 m, internal diameter 0.32 mm, and film 0.25 µm (Grace, Lokeren, Belgium), using the following time-temperature program: 70 – 180 °C (10 °C/min), 180 – 235 °C (4 °C/min), 235 °C (4.75 min). Peaks were identified by comparing retention times with those of FAME standards (Nu-Chek Prep. Inc., Elysian, USA) and peak areas were quantified with Chromcard 2.5 software.

8.2.4.2 Determination of free fatty acid content

The free fatty acid (FFA) content was determined according to Kangani et al. (2008) with slight modifications. After dissolving 10 mg of extracted lipids in 1 mL of dichloromethane, 10 µL of diisopropylethylamine and 30 µL of diethylamine were added, and the solution was cooled to 0 °C. Afterwards, 40 µL of bis(2-methoxyethyl)aminosulfur trifluoride was added dropwise and the solution was kept

at 0 °C for 5 min, before bringing the mixture to room temperature. Then, 2 mL water and 4 mL hexane were added, the samples were vortexed for 1 min, and centrifuged (10 min, 750g, 25 °C). The upper organic layer, containing the FFA derivatives, was analyzed with GC-FID. The following time-temperature program was used: 100 – 160 °C (20 °C/min), 160 – 240 °C (4 °C/min), 240 °C (27 min). Peak areas were quantified with Chromcard 2.5 software and the sum of the peak areas was compared to the peak area of the internal standard to calculate the total FFA content.

8.2.4.3 Quantification of carotenoids

The carotenoid content was determined according to Gheysen et al. (2019b). Lyophilized sample (25 mg) was dissolved in 5 mL acetone:methanol (7:3 v/v) and mixed with glass beads for 30 s. The mixture was centrifuged (10 min, 750g, 25 °C) and the supernatant was collected. The extraction steps were performed 3 more times, and all solvent layers were combined. The extracts were then filtered (PVDF syringe filters, 4 mm, 0.2 µm) and analyzed using HPLC coupled to a diode array detector (DAD) at 436 nm (Alliance Waters, Zellik, Belgium). A Nova Pak C18 column 60A (4 µm, 3.9 mm × 150 mm) was used at 30 °C, and samples were kept at 10 °C. Samples were eluted at 0.7 mL/min using three mobile phases: (A) methanol:ammonium acetate buffer (80:20 v/v, pH 7.2, 0.5 M), (B) acetonitrile:ultrapure water (90:10 v/v), and (C) ethyl acetate, in the following gradient program:

0 – 3 min: linear gradient from 100% A to 100% B
3 – 14 min: linear gradient to 50% B and 50% C
14 – 16 min: linear gradient to 50% A and 50% C
16 – 22.5 min: linear gradient to 20% A and 80% C
22.5 – 26 min: isocratic at 20% A and 80% C
26 – 30 min: linear gradient to 100% C
30 – 32 min: linear gradient to 80% A and 20% C
32 – 33 min: linear gradient to 100% A

Mixtures of the commercial carotenoid standards violaxanthin, antheraxanthin, zeaxanthin, and β-carotene (DHI, Horsholm, Denmark) were used as external standards for identification and quantification with Empower 2 software.

8.2.5 Definition of lipid digestibility, bioaccessibility, and micellar incorporation

Lipid digestibility represents the extent to which esterified fatty acids (in the form of triacylglycerols, phospholipids, and/or glycolipids) are hydrolyzed to monoacylglycerols (MAG), lyso-phospholipids, lyso-glycolipids, and FFA. In the current

work, lipid digestibility is estimated by analyzing the release of FFA as a percentage of the total fatty acids, which were analyzed as FAME.

Bioaccessibility of a component was calculated using **Eq. 8.1**:

$$Bioaccessibility\ (\%) = \frac{c_{mic} \cdot V_{mic}}{c_{susp} \cdot V_{susp}} \times 100 \qquad \textbf{(Eq. 8.1)}$$

with c_{mic} the concentration of the component in the micellar phase, V_{mic} the volume of micellar phase present in the total digest, c_{susp} the concentration of the component in the undigested suspensions or o/w-emulsion, and V_{susp} the volume of suspension or o/w-emulsion present in the total digest.

Micellar incorporation of a component was calculated using **Eq. 8.2**:

$$Micellar\ incorporation\ (\%) = \frac{c_{mic} \cdot V_{mic}}{c_{dig} \cdot V_{dig}} \times 100 \qquad \textbf{(Eq. 8.2)}$$

with c_{dig} the concentration of the component in the digest and V_{dig} the total volume of digest.

8.3 RESULTS AND DISCUSSION

8.3.1 Characterization of the different *Nannochloropsis* sp. samples

The aim of the HPH treatment of *Nannochloropsis* sp. biomass was to generate a sample with a large degree of cell disruption, in contrast to the untreated biomass. The degree of cell disruption was estimated by determining the HI extraction efficiency in analogy with **Chapter 7**. An extraction efficiency of 31.0 ± 1.5% was obtained for the untreated biomass. HPH for 4 passes at 100 MPa drastically increased the HI extraction efficiency up to 92.6 ± 0.5%, indicating that the majority of the cells displayed a ruptured cell membrane and/or cell wall, allowing the extraction of the lipids with a non-halogenated solvent mixture. Similar to the microscopic observations in **Chapter 7**, DIC microscopy clearly showed the presence of released intracellular material together with a minority of intact *Nannochloropsis* sp. cells (images not shown). Hence, as expected from the previous chapter, the applied HPH conditions were successful for creating *Nannochloropsis* sp. samples with different degree of cell disruption.

The different *Nannochloropsis* sp. samples were also characterized in terms of lipid composition, FFA content, and carotenoid composition (**Table 8.1**). Untreated biomass was characterized by similar amounts of saturated fatty acids (C14:0 and C16:0), monounsaturated fatty acids (C16:1 and C18:1), and polyunsaturated fatty acids (C18:2 and C20:5), in agreement with Gheysen et al. (2018). *Nannochloropsis* sp.

only contained eicosapentaenoic acid (EPA, C20:5) as a source of ω3-LC-PUFA, representing 34.4 ± 1.6 mg/g biomass, in line with previous reports (Gheysen et al., 2018, 2019b; Ryckebosch et al., 2014b). It was shown that the fatty acid profile was unaffected by the sample preparation. While HPH-treated biomass presented the same amounts of the aforementioned fatty acids, a non-selective enrichment of the fatty acids was observed in the extracted oil, representing the fatty acids in the same ratios as for the untreated biomass. In contrast, the FFA content drastically increased, not only during the HPH treatment, but also during the oil extraction. It is known that lipolysis in *Nannochloropsis* sp. is induced by HPH, with a higher FFA formation when multiple homogenization passes are applied (Balduyck et al., 2018). The major formation of FFA is caused by enzymatic lipolysis, due to the presence of endogenous lipases and carboxylesterases, as it was shown that lipolytic reactions in *Tisochrysis lutea* can be inhibited by a (mild) heat treatment (Balduyck et al., 2017, 2019). FFA formation after HPH and oil extraction has also been observed by Gheysen et al. (2019b), reporting similar amounts of FFA in HPH-treated biomass and extracted oil of *Nannochloropsis*. The observed differences in FFA content might have implications for the *in vitro* lipid digestibility, since fewer lipids in the HPH-treated biomass and the extracted oil need to be digested, as part of the lipid hydrolysis already occurred during the sample preparation. In fact, whereas only 2.3 ± 0.1% of the fatty acids were available as FFA in the untreated biomass (determined as the ratio of FFA to FAME), FFA represented 18.6 ± 0.3% and 18.9 ± 0.8% of the total fatty acids in HPH-treated biomass and extracted oil, respectively.

The carotenoid profile of *Nannochloropsis* sp. biomass was characterized by the presence of three xanthophylls (violaxanthin, antheraxanthin, and zeaxanthin) and β-carotene, in agreement with Gheysen et al. (2018, 2019b). Carotenoids were degraded during the HPH treatment, in particular violaxanthin and antheraxanthin. Moreover, it is well known that violaxanthin and antheraxanthin can be converted into zeaxanthin via de-epoxidation reactions, also referred to as the violaxanthin cycle or the xanthophyll cycle (Mulders et al., 2014). During the oil extraction, the carotenoid profile was changed, as violaxanthin and antheraxanthin were not enriched in the oil, in contrast to zeaxanthin and β-carotene. Apart from possible de-epoxidation reactions of the violaxanthin cycle, this change in carotenoid profile could also be explained by different affinities of the carotenoids for the extraction solvent HI based on their polarity. Similar changes in carotenoid content and profile after HPH and oil extraction have been observed by Gheysen et al. (2019b) for *Nannochloropsis* sp. samples. Hence, it should be kept in mind that the differences in FFA and carotenoid content might also contribute to possible changes in *in vitro* lipid digestibility and bioaccessibility, next to differences in cell integrity of the different *Nannochloropsis* sp. samples.

Table 8.1 Characterization of the different *Nannochloropsis* sp. samples in terms of lipid content, fatty acid profile (analyzed as fatty acid methyl esters, FAME), free fatty acids (FFA), and carotenoids (n = 3).

	Untreated	HPH	Oil
Lipids (g/100 g)			
Lipids	28.4 ± 0.5	28.6 ± 0.3	
FAME	15.0 ± 0.6	14.3 ± 0.4	46.4 ± 0.1
FFA	0.35 ± 0.01	2.65 ± 0.04	8.76 ± 0.37
Fatty acids (mg/g)			
C14:0	5.7 ± 0.1	5.6 ± 0.1	22.9 ± 0.1
C16:0	31.0 ± 0.8	31.2 ± 0.8	83.5 ± 0.2
C16:1	40.0 ± 1.5	39.7 ± 1.1	139.3 ± 0.3
C18:1	2.7 ± 0.1	3.2 ± 0.1	7.7 ± 0.1
C18:2	3.4 ± 0.1	3.8 ± 0.1	10.0 ± 0.1
C20:5 ω3	34.4 ± 1.6	37.9 ± 1.0	139.9 ± 0.5
Carotenoids (mg/g)			
Violaxanthin	4.25 ± 0.21	1.93 ± 0.06	2.50 ± 0.34
Antheraxanthin	1.87 ± 0.10	1.36 ± 0.02	1.74 ± 0.34
Zeaxanthin	0.42 ± 0.04	0.35 ± 0.01	1.93 ± 0.24
β-carotene	2.87 ± 0.20	2.50 ± 0.06	10.07 ± 1.70

8.3.2 Effect of HPH on *in vitro* lipid digestibility and bioaccessibility of carotenoids and ω3-LC-PUFA

8.3.2.1 Effect of HPH on lipid digestibility

The release of FFA during the simulated small intestinal phase was determined as an estimation of the lipid digestibility. First, it should be noted that the release of FFA does not provide full information on the lipid digestibility. In fact, hydrolysis of triacylglycerols by pancreatic lipase is generally limited to the formation of two FFA and sn2-MAG due to the stereoselectivity of the enzyme. Although isomerization of sn2-MAG to sn1-MAG can occur in the small intestine, thus creating new substrate for the enzyme to hydrolyze it to FFA and glycerol, this isomerization is thought to be limited (< 25%) due to the fast absorption of sn2-MAG by the enterocytes (Phan and Tso, 2001). Moreover, as the main digestive enzyme for phospholipids in pancreatin is the stereoselective phospholipase A_2, which is hydrolyzing the sn2-acyl chain resulting in a sn1-lyso-phospholipid and a FFA, only one out of two fatty acids is released from the phospholipids (Ratnayake and Galli, 2009). The same reasoning applies to digestion of glycolipids by pancreatic lipase-related protein 2, generating only one FFA (released from the sn-1 position) and a sn2-lyso-glycolipid (Amara et al., 2009). Hence, complete lipid digestion will not be reflected by values of 100% released FFA. In fact, based on the lipid class composition reported for *Nannochloropsis* sp. biomass and HI oil extracts (Ryckebosch et al., 2013, 2014a,

2014b), and taking into account the amount of released FFA upon digestion for each lipid class, it is suggested that values between 55% and 65% released FFA correspond to complete lipid digestion of *Nannochloropsis* sp. samples.

Differences in lipid digestibility were observed between the untreated and HPH-treated *Nannochloropsis* sp. suspensions, regardless of the enzymatic activity of the pancreatic lipase (**Fig. 8.1**). Whereas 36 – 40% of the fatty acids were hydrolyzed in the untreated suspension at the end of the small intestinal phase (i.e. after 120 min), a FFA release of 56 – 62% was determined for the HPH-treated suspensions. Since the latter coincides with the estimated values for complete lipid hydrolysis, it is hypothesized that the improved digestibility is related to the disrupted cell wall and/or cell membrane layer in the HPH-treated sample, or in other words, the absence of physical barriers limiting the contact of the pancreatic lipase with its substrate. Surprisingly, the lipid digestibility in the untreated sample is rather high. In fact, Cavonius et al. (2016) reported no FFA release after *in vitro* digestion of intact *Nannochloropsis oculata* biomass. A possible explanation could be the difference in downstream processing of the microalgal biomass, which possibly resulted in a distinct integrity of the cells. While the *Nannochloropsis* sp. biomass in the current study was lyophilized before *in vitro* digestion, resulting in ~30% damaged cell membranes even in absence of HPH (**Chapter 7**), the microalgae in the other study were supplied as a frozen wet paste. Even though the authors did not investigate the integrity of the cells, it is plausible that the absence of lipid hydrolysis was related to the intactness of the cells. Furthermore, Cavonius et al. (2016) also reported an increased FFA release after digestion of the disrupted sample generated by ball milling, however reaching lower values (34%) than for the HPH-treated sample in the current work (56 – 62%). The incomplete lipid digestion in that study might be attributed to an incomplete cell disruption by ball milling (not reported by the authors) or to the large abundance of ions in the microalgal sample. In fact, *Nannochloropsis* sp. samples were supplied in seawater, presumably affecting the enzymatic activity of the pancreatic lipase due to the disordered ionic strength of the medium. Besides, the higher FFA release upon digestion in the current work might also result from the larger amount of FFA in the starting sample before digestion. In fact, while 18.6 ± 0.3% of the total fatty acids were available as FFA in the HPH-treated sample, Cavonius et al. (2016) reported the FFA content in the ball-milled sample before digestion to be limited to 2 – 3% of the total fatty acids.

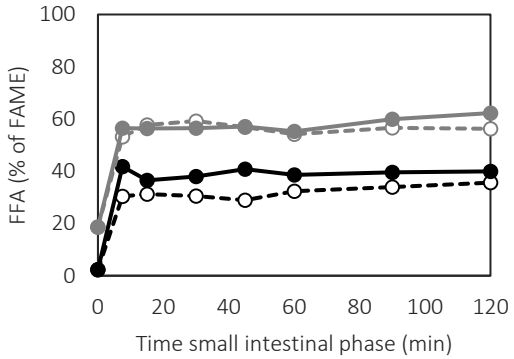

Fig. 8.1 Estimation of lipid digestibility during the small intestinal phase. Free fatty acid (FFA) content is presented as a percentage of the total fatty acid content (FAME) for untreated (black) and HPH-treated (gray) *Nannochloropsis* sp. suspensions digested with 550 U/mL (dashed lines) or 2000 U/mL (solid lines) pancreatic lipase.

The effect of pancreatic lipase activity in the simulated small intestinal phase was investigated to obtain a better understanding of the lipid digestibility of the microalgal biomasses. Even though a lipase activity of 2000 U/mL is recommended in the consensus method of Minekus et al. (2014), the actual pancreatic lipase activity *in vivo* is still under discussion. In fact, activity measurements of human pancreatic lipase by several authors covered a range of 80 to 7000 U/mL. This large diversity was mainly attributed to the fact that the secretion of pancreatic lipase in the human body is adapted based on the lipid content of the ingested meal, in order to ensure efficient intestinal lipid digestion (Armand, 2007). The fixed enzyme activity of 2000 U/mL in the consensus method of Minekus et al. (2014) might therefore not be representative for the activity of pancreatic lipase in the human body. Many authors actually propose a different approach, in which the lipase activity is optimized (usually to lower lipase activities) to study differences in lipid digestibility kinetics among different samples (Lin et al., 2014; Mutsokoti et al., 2017). In this context, a pancreatic lipase activity of 550 U/mL has previously been used for *in vitro* digestion of an ω3-LC-PUFA-rich emulsion by Lin and Wright (2018). In the current work, little or no differences in lipid digestibility were observed between *Nannochloropsis* sp. samples digested with 550 or 2000 U/mL pancreatic lipase. Furthermore, the final value of FFA release was already reached after 7.5 min incubation in the small intestinal phase, regardless of the lipase activity. This was observed for both the untreated and the HPH-treated *Nannochloropsis* sp. suspensions, suggesting that the intact cell wall and/or cell membrane acts as a physical barrier obstructing the transport of the pancreatic enzyme towards the intracellular space, rather than slowing it down.

8.3.2.2 Effect of HPH on bioaccessibility of carotenoids and ω3-LC-PUFA

The bioaccessibility of lipophilic compounds is related to the lipid digestion, since lipid digestion products (FFA and MAG) are crucial for the formation of mixed micelles. This is observed in **Fig. 8.2**, in which *in vitro* bioaccessibility kinetics as a function of the time in the small intestinal phase follows a similar trend as lipid digestion kinetics. A fast incorporation of carotenoids and EPA into mixed micelles is observed, with the plateau value generally being reached after 7.5 min. This is in agreement with previous studies, showing similar rate constant values of FFA release and their incorporation into mixed micelles in o/w-emulsions, confirming the immediate incorporation of FFA into mixed micelles (Mutsokoti et al., 2017). Only for untreated cells digested with 550 U/mL pancreatic lipase, a short delay can be observed, reaching the final bioaccessibility values after 15 min.

Analogous to the lipid digestibility, higher bioaccessibility values were observed for HPH-treated suspensions compared to untreated suspensions. Absolute values for carotenoid bioaccessibility of untreated *Nannochloropsis* sp. biomass were actually low after 120 min of small intestinal phase, between 1.6% and 6.0%. Low *in vitro* bioaccessibility values have been previously reported for carotenoids in unprocessed biomass of other microalgae species. In fact, untreated *Chlorella* sp. biomass showed bioaccessibility values of 0 – 2.6% and 1.7% for β-carotene and zeaxanthin, respectively (Cha et al., 2012; Gille et al., 2016). Higher values were observed for β-carotene bioaccessibility in *Chlamydomonas reinhardtii* and *Phaeodactylum tricornutum*, being 10% and 29%, respectively (Gille et al., 2019). However, the latter two microalgae species are characterized by a less rigid cell wall, in contrast to *Chlorella* sp. and *Nannochloropsis* sp. Furthermore, approximately 13% of the initial amount of EPA in the untreated biomass was incorporated into mixed micelles, similar as observed by Bonfanti et al. (2018) for *Isochrysis galbana* biomass.

The effect of HPH on the bioaccessibility of carotenoids and EPA was obvious, resulting in final bioaccessibility values up to three times higher than for untreated biomass suspensions (7.8 – 15.6% for carotenoids and 26.5 – 28.9% for EPA). The enhanced bioaccessibility is in agreement with studies of Cha et al. (2012) and Gille et al. (2016), reporting increases in carotenoid bioaccessibility up to 18% after cell disruption of *Chlorella* sp. by sonication and microfluidization. This suggests that the observed increases in bioaccessibility and lipid digestibility are presumably related to the cell integrity, and only partially to differences in initial FFA content of the different *Nannochloropsis* sp. samples. A similar impact of processing on the carotenoid bioaccessibility was previously observed for vegetable based systems. In fact, while bioaccessibility values of 5 – 11% were found for β-carotene in raw carrot slices, up

to a threefold increase was observed after thermal processing and/or HPH, related to changes in cell wall polysaccharides (Knockaert et al., 2012; Lemmens et al., 2009).

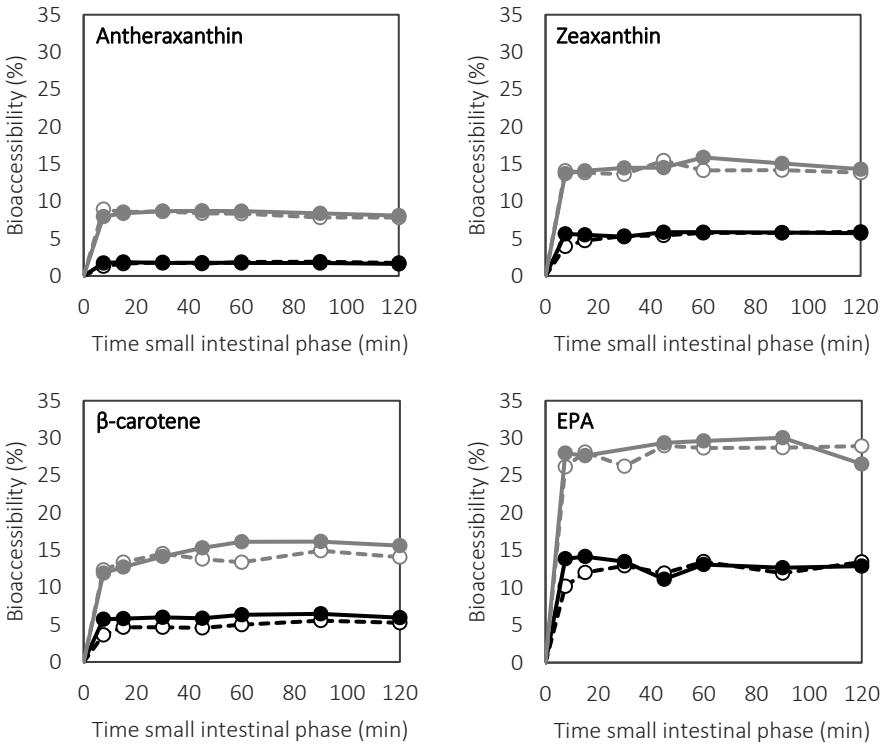

Fig. 8.2 *In vitro* bioaccessibility of antheraxanthin, zeaxanthin, β-carotene, and eicosapentaenoic acid (EPA) during the small intestinal phase, for untreated (black) and HPH-treated (gray) *Nannochloropsis* sp. suspensions digested with 550 U/mL (dashed lines) or 2000 U/mL (solid lines) pancreatic lipase. No violaxanthin was detected in the micellar phase.

A remarkable observation in **Fig. 8.2** is the lower bioaccessibility of antheraxanthin compared to zeaxanthin and β-carotene. As a matter of fact, due to the higher hydrophilicity of xanthophylls compared to carotenes, the highest bioaccessibility was expected for antheraxanthin and zeaxanthin, since more hydrophobic carotenoids such as β-carotene require higher amounts of FFA for incorporation into mixed micelles (Salvia-Trujillo et al., 2017; Yonekura and Nagao, 2007). In order to gain better understanding of the carotenoid bioaccessibility, the stability of the carotenoids during the simulated *in vitro* digestion was studied. **Fig. 8.3** presents the carotenoid stability after the gastric and the small intestinal phase, expressed as the ratio between the carotenoid content in the digest and the carotenoid content in the initial suspension. Whereas β-carotene was almost completely stable during the *in vitro* digestion protocol, a lower stability was observed for the xanthophylls, with only

36 – 38% of antheraxanthin and 67 – 76% of zeaxanthin recovered in the digest. Moreover, violaxanthin was present in substantial amounts in the *Nannochloropsis* sp. biomasses, but was fully degraded during the *in vitro* digestion procedure. A low stability of xanthophylls upon *in vitro* digestion has previously been reported for leafy vegetables, with only ~25% of zeaxanthin recovered in lettuce and < 5% of violaxanthin in spinach (Courraud et al., 2013; Granado-Lorencio et al., 2007). The larger degradation of violaxanthin followed by antheraxanthin and zeaxanthin coincides with possible de-epoxidation reactions occurring in the violaxanthin cycle (Mulders et al., 2014; Stahl and Sies, 2003). In contrast to the instability of the xanthophylls, **Fig. 8.3** shows that no degradation of EPA occurred during simulation of gastric and small intestinal phase.

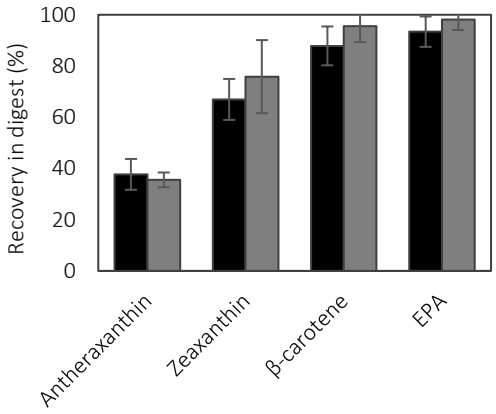

Fig. 8.3 Recovery of carotenoids and eicosapentaenoic acid (EPA) in the digest (%) for untreated (black) and HPH-treated (gray) *Nannochloropsis* sp. suspensions digested with 550 U/mL pancreatic lipase (n = 2). No violaxanthin was detected in the digest.

An additional experiment was performed to investigate whether the carotenoid instability was attributed to experimental artefacts instead of the physiological conditions of the simulated gastrointestinal tract. In fact, to inactivate the digestive enzymes, the digested samples were transferred to pyrex tubes (in presence of oxygen) and treated by a heat shock for 14 min at 86.5 °C, which was expected to partially influence the carotenoid stability. Therefore, a heat shock was performed on samples in which digestive enzymes were replaced by simulated digestion fluids, and without preceding incubation at 37 °C. As can be seen in **Fig. 8.4**, part of the carotenoid degradation could be attributed to the heat shock, resulting in ~30% loss of antheraxanthin and ~15% loss of zeaxanthin. In this context, the use of enzyme inhibitors for quenching the enzymatic conversions of the digestive enzymes would be a valuable alternative for future research, to avoid excessive carotenoid degradation.

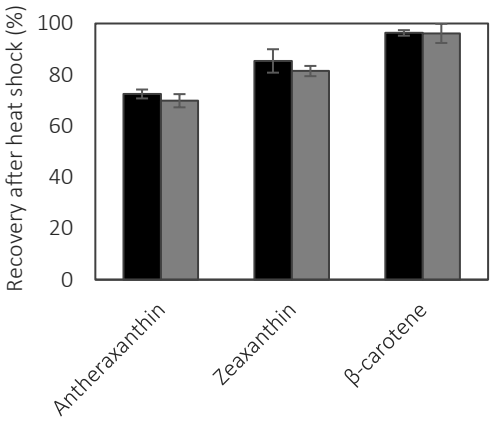

Fig. 8.4 Stability of carotenoids after a heat shock (14 min, 86.5 °C) for untreated (black) and HPH-treated (gray) *Nannochloropsis* sp. (n = 2).

Since part of the carotenoid degradation was attributed to the experimental procedure, the bioaccessibility values in **Fig. 8.2** are not representative for simulation of *in vivo* bioaccessibility. Therefore, the data obtained are presented in **Fig. 8.5** in terms of micellar incorporation, i.e. the fraction of compounds in the digest that has been incorporated into mixed micelles, after 120 min of small intestinal phase. According to the differences in hydrophobicity, a slightly higher micellar incorporation is observed for the xanthophylls compared to β-carotene (except for antheraxanthin in the untreated biomass). However, regardless of the cell integrity, values for micellar incorporation of carotenoids are rather low, being 4.5 – 8.7% for untreated suspensions and 15.5 – 22.4% for HPH-treated suspensions. On the one hand, these low values could possibly be attributed to the location of the carotenoids in the microalgal cells. While primary carotenoids are functionally and structurally bound to the photosynthetic apparatus, only secondary carotenoids are located in oil droplets, either in the stroma of the chloroplast or in the cytosol (Mulders et al., 2014). Hence, primary carotenoids need to overcome an additional barrier before being incorporated into mixed micelles, since they need to be transported through the aqueous phase, while secondary carotenoids are yet in contact with the lipid phase and/or lipid digestion products. On the other hand, the presence of other macromolecules originating from the microalgal biomass (e.g. proteins, polysaccharides) might obstruct the transport of carotenoids into mixed micelles. To validate the aforementioned hypotheses, oil was extracted from *Nannochloropsis* sp. and subjected to the *in vitro* digestion protocol. As such, all carotenoids were located in the lipid phase, and the presence of other macromolecules was avoided. These results will be discussed in the next section.

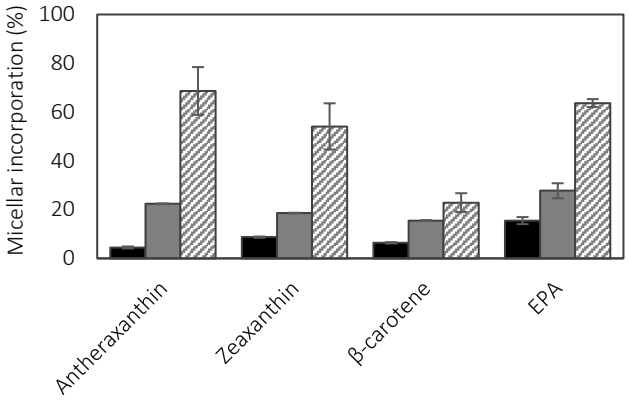

Fig. 8.5 Incorporation of carotenoids and eicosapentaenoic acid (EPA) in micelles (%) after 120 min of small intestinal phase for untreated (black) and HPH-treated (gray) *Nannochloropsis* sp. suspensions, and for o/w-emulsions (dashed) digested with 550 U/mL pancreatic lipase (n = 2).

8.3.3 *In vitro* lipid digestibility and bioaccessibility of carotenoids and ω3-LC-PUFA in o/w-emulsions

The micellar incorporation of carotenoids and EPA in the digested o/w-emulsions is also presented in Fig. 8.5, in comparison with the untreated and HPH-treated biomass suspensions. Significantly higher proportions of carotenoids and EPA were incorporated into mixed micelles for digested o/w-emulsions, being 68.6 ± 9.8% of antheraxanthin, 54.1 ± 9.5% of zeaxanthin, and 63.7 ± 1.7% of EPA. Hence, the absence of other macromolecules and/or the location of carotenoids in the lipid phase have obviously favored the micellar incorporation. Nevertheless, despite the nearly complete lipid digestion (62.3 ± 1.3% FFA), a large fraction of the carotenoids and EPA was not incorporated into the mixed micelles. An increase of the bile salt concentration could possibly improve their micellar incorporation, as studied in section 8.3.4. Surprisingly, only a marginal increase was observed for β-carotene, with only 22.9 ± 3.9% incorporated into mixed micelles in the digested o/w-emulsions. Apart from the higher hydrophobicity of β-carotene compared to the xanthophylls, it is unclear which factors could have influenced their micellar incorporation to cause such drastic differences among the different carotenoids. A similar observation was however made by Gille et al. (2018), who reported a substantial micellar incorporation of the xanthophyll lutein in ball-milled *Chlorella vulgaris* biomass (up to 32%), while only traces of β-carotene were detected in the mixed micelles. Nevertheless, in spite of its low relative incorporation in comparison with antheraxanthin and zeaxanthin, similar absolute amounts of β-carotene were

observed in the mixed micelles in the current study, since its original concentration in the extracted oil was 4 to 5 times higher than for the other carotenoids (Table 8.1).

8.3.4 Effect of bile salt concentration on lipid digestibility and bioaccessibility of carotenoids and ω3-LC-PUFA

One limitation of the static *in vitro* digestion protocol is the use of a fixed bile salt concentration in the simulated small intestinal phase. In fact, secretion of bile salts occurs gradually in the human body, and the levels of secreted bile salts are in response to the amount of lipid digestion products formed in the small intestine (Coleman, 1987). As a consequence, the fixed bile salt concentration used in the static *in vitro* digestion method might possibly influence the lipid digestibility and/or carotenoid bioaccessibility. It is actually known that high bile salt concentrations can possibly lead to a reduced activity or even inactivation of pancreatic lipase enzymes (Bauer et al., 2005). However, it was validated that the different bile salt concentrations used in the current work (up to 20 mM) did not affect the lipid digestibility, as seen in Fig. 8.6.

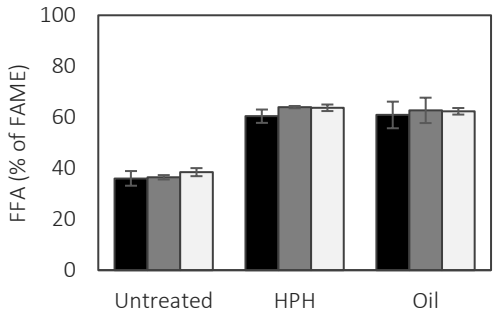

Fig. 8.6 Estimation of lipid digestibility after 120 min of small intestinal phase as a function of the bile salt concentration, for the different *Nannochloropsis* sp. samples digested with 550 U/mL pancreatic lipase. Free fatty acid (FFA) content is presented as a percentage of the total fatty acid content (FAME) for bile salt concentrations of 10 mM (black), 15 mM (gray), and 20 mM (white) (n = 2).

From a bioaccessibility point of view, it was hypothesized that the low values of micellar incorporation of *Nannochloropsis* sp. samples observed in section 8.3.2.2 might be related to the fixed bile salt concentration of 10 mM. This could be the case if carotenoids were present in excess, i.e. when all bile salts were consumed in the formation of mixed micelles and the generated micelles were all saturated with carotenoids, resulting in an underestimation of the *in vivo* micellar incorporation of carotenoids. Fig. 8.7 shows the effect of bile salt concentration on the micellar incorporation of carotenoids and EPA for the different *Nannochloropsis* sp. samples.

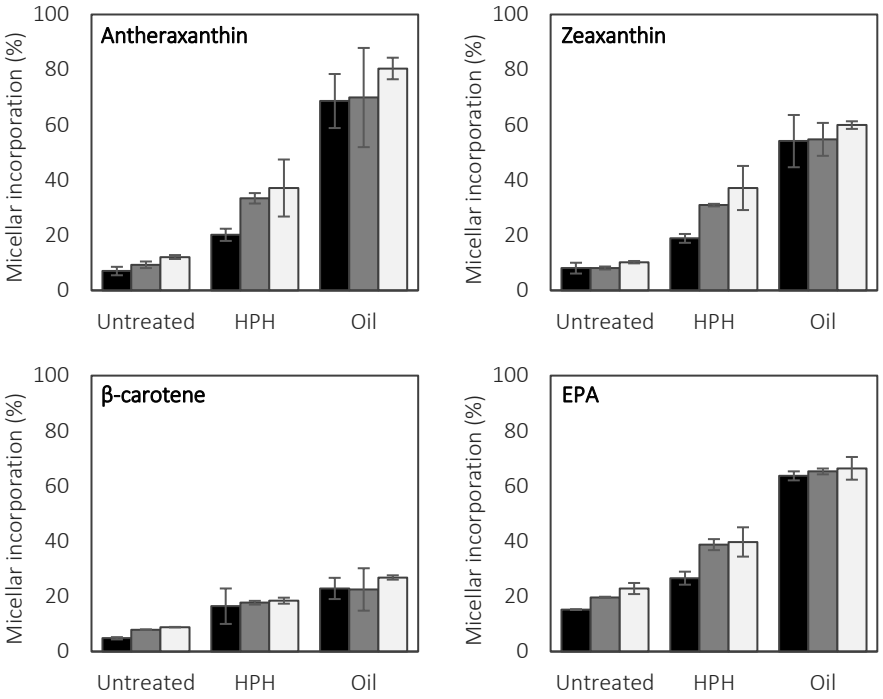

Fig. 8.7 Incorporation of carotenoids and eicosapentaenoic acid (EPA) in micelles (%) after 120 min of small intestinal phase for the different *Nannochloropsis* sp. samples digested with 550 U/mL pancreatic lipase, in presence of bile salt concentrations of 10 mM (black), 15 mM (gray), and 20 mM (white) (n = 2).

Whereas an increasing trend was observed for *Nannochloropsis* sp. biomass suspensions, bile salt concentration did not influence the micellar incorporation of carotenoids and EPA in o/w-emulsions. This could be explained by the lower amount of carotenoids present during digestion of the latter, as a lower sample amount was used for o/w-emulsions (5 mL) compared to biomass suspensions (10 mL) in order to standardize the amount of lipids for the digestion procedure. Hence, it is plausible that an excess of carotenoids was present in the digested biomass suspensions at a bile salt concentration of 10 mM, while this was not the case for the digested o/w-emulsions. Elevating the bile salt concentration to 15 or 20 mM resulted in an increase of the micellar incorporation for the biomass suspensions by a factor 1.5 to 2. Nevertheless, values for micellar incorporation in the digested biomass suspensions were still limited and significantly lower than for the o/w-emulsions, being 7.9 – 22.8% for untreated biomass and 17.7 – 39.7% for HPH-treated biomass.

8.3.5 Comparing lipid digestibility and bioaccessibility of carotenoids and ω3-LC-PUFA in different batches of *Nannochloropsis* sp. biomass

Even though the use of HPH was proven effective in increasing the lipid digestibility and bioaccessibility of carotenoids and EPA, it should be noted that the effect is depending on the integrity of the initial *Nannochloropsis* sp. biomass. This was evidenced by comparing previous results with those obtained for a batch of *Nannochloropsis* sp. biomass with a higher membrane permeability, but with similar lipid content and fatty acid profile. As shown in Fig. 8.8, the HI extraction efficiency of untreated biomass of the latter batch was almost twice as high as for the previous batch, being 55.7 ± 4.9% versus 31.0 ± 1.5%. This observation corresponds to the micrographs presented in Fig. 8.9, in which the viability stain SYTOX green was used to visualize the integrity of the cell membrane, showing a damaged cell membrane for more than half of the *Nannochloropsis* sp. cells for the batch with higher membrane permeability (in absence of HPH). Similar to the results of section 8.3.1, a nearly complete lipid extraction with HI was obtained after HPH for 4 passes at 100 MPa (94.2 ± 0.9%), indicating almost full cell disruption in this HPH-treated sample.

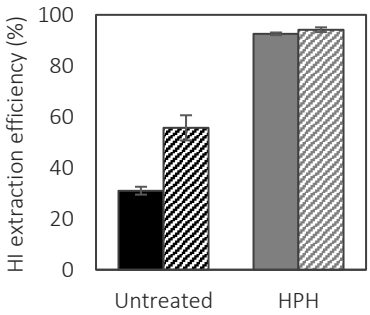

Fig. 8.8 Hexane:isopropanol (HI) extraction efficiency of different batches of *Nannochloropsis* sp. biomass, for suspensions of untreated biomass (Untreated) and biomass that was high pressure homogenized for 4 passes at 100 MPa (HPH). The batch used for all previous experiments is presented by full bars, while a batch with higher membrane permeability is presented by dashed bars (n = 3).

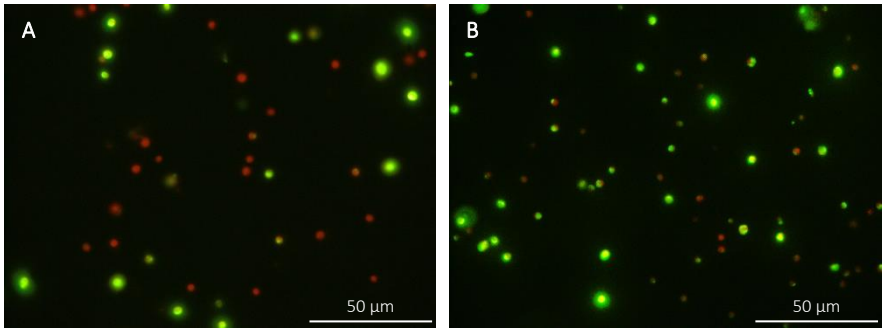

Fig. 8.9 Representative microscopic images of different batches of *Nannochloropsis* sp. biomass stained with SYTOX green: **(A)** the batch used for all previous experiments and **(B)** a batch with higher membrane permeability. Cells with intact cell membranes (only red colored autofluorescence) can be distinguished from cells with damaged cell membranes (green fluorescence due to penetration of the SYTOX green dye).

The lipid digestibility was clearly depending on the integrity of the *Nannochloropsis* sp. cells, as observed from comparing the FFA release of the untreated suspensions of the different *Nannochloropsis* sp. biomasses (**Fig. 8.10**). Even in absence of HPH, the batch with higher membrane permeability presented a FFA release of 56.2 ± 2.3%. Hence, it is obvious that a damaged cell membrane (and/or damaged cell wall) promotes the penetration of pancreatic lipase in order to get in contact with its substrate. An increased lipid digestibility was still observed after HPH treatment, resulting in a final FFA release of 70.8 ± 2.5% corresponding to a full lipid hydrolysis. Although the HPH-treated biomasses of the different batches displayed the same HI extraction efficiency (**Fig. 8.8**), it is unclear why a difference of 8.6% in FFA release was observed after *in vitro* digestion. In fact, beside similar cell integrity, no difference in initial FFA content was observed between the different HPH-treated batches (18.6 ± 0.3% versus 19.2 ± 1.6% of total fatty acids).

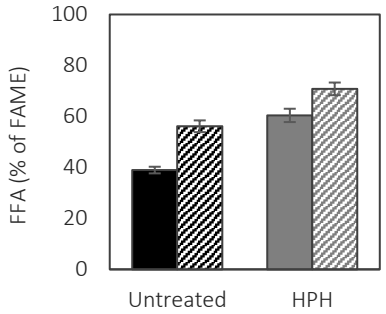

Fig. 8.10 Estimation of lipid digestibility after 120 min of small intestinal phase for different batches of *Nannochloropsis* sp. biomass, i.e. the batch used for all previous experiments (full bars) and a batch with higher membrane permeability (dashed bars). Digestion was performed with 2000 U/mL pancreatic lipase, for suspensions of untreated biomass (Untreated) and biomass that was high pressure homogenized for 4 passes at 100 MPa (HPH). Free fatty acid (FFA) content is presented as a percentage of the total fatty acid content (FAME) (n = 2).

Differences in lipid digestibility between the two *Nannochloropsis* sp. batches were also reflected in the bioaccessibility of carotenoids and EPA, as shown in **Fig. 8.11**. First, it should be noted that antheraxanthin was fully degraded during the *in vitro* digestion procedure of the latter batch, implying that no antheraxanthin was available for incorporation into mixed micelles. Higher values were observed for the micellar incorporation of zeaxanthin and β-carotene. In fact, digestion of the untreated biomass with higher membrane permeability resulted in a similar or even higher micellar incorporation as for the HPH-treated biomass of the previous batch (24.7 ± 2.7% for zeaxanthin and 15.1 ± 1.1% for β-carotene). The same observation was made for the micellar incorporation of EPA, being 36.4 ± 3.8% in the untreated biomass. Hence, validation of the membrane and/or cell wall integrity of *Nannochloropsis* sp. biomass is of critical importance in estimating the bioaccessibility of carotenoids and ω3-LC-PUFA. In fact, HPH only limitedly affected the micellar incorporation of the batch with high membrane permeability, in contrast to the previous batch. This can possibly explain the variability in literature data on the effect of processing to enhance the bioaccessibility of carotenoids, as discussed in **Chapter 1**. Indeed, improved bioaccessibility upon processing was mainly observed for rigid cell walled microalgae species such as *Chlorella* sp. (Cha et al., 2011, 2012; Gille et al., 2016), while the impact of processing was rather limited for microalgae species with a more fragile cell wall such as *Chlamydomonas reinhardtii* and *Phaeodactylum tricornutum* (Gille et al., 2016, 2019).

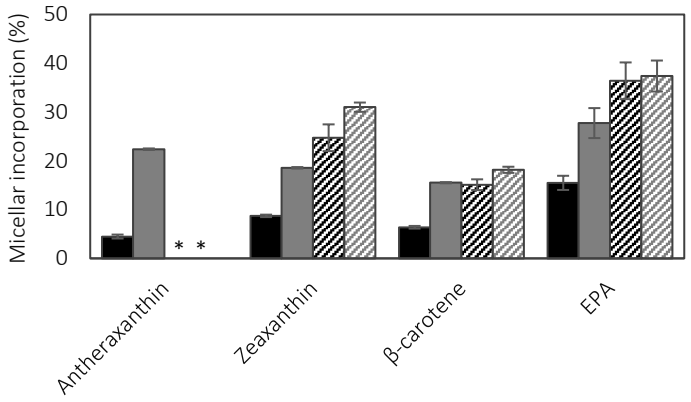

Fig. 8.11 Incorporation of carotenoids and eicosapentaenoic acid (EPA) in micelles (%) after 120 min of small intestinal phase for different batches of *Nannochloropsis* sp. biomass digested with 2000 U/mL pancreatic lipase, i.e. the batch used for all previous experiments (full bars) and a batch with higher membrane permeability (dashed bars), for untreated (black) and HPH-treated (gray) *Nannochloropsis* sp. suspensions (n = 2).
* no antheraxanthin was detected in the digest or micellar phase for the batch with higher membrane permeability

8.4 CONCLUSIONS

This chapter proved the importance of the microstructure of *Nannochloropsis* sp. cells in the lipid digestibility and *in vitro* bioaccessibility of carotenoids and ω3-LC-PUFA. While an incomplete lipid digestion and low bioaccessibility values of carotenoids and ω3-LC-PUFA were observed for untreated *Nannochloropsis* sp. biomass, cell disruption drastically improved the lipid digestibility and bioaccessibility. However, it was shown that the efficiency of cell disruption for enhancing lipid digestibility and bioaccessibility was largely depending on the cell integrity of the initial *Nannochloropsis* sp. biomass. In fact, similar values for lipid digestibility and bioaccessibility were observed for biomass with a high membrane permeability (characterized by a HI extraction efficiency of 55.7 ± 4.9%), even in absence of a cell disruption treatment. Moreover, the incorporation of carotenoids was also impeded by the location of the carotenoids and/or the presence of other macromolecules in the microalgal biomass, since micellar incorporation of carotenoids was substantially promoted in *Nannochloropsis* sp. o/w-emulsions compared to biomass suspensions. Hence, targeted processing of microalgae in the presence of lipids might be an interesting strategy for transferring carotenoids to the lipid bulk phase, possibly enhancing their micellar incorporation upon digestion, as previously shown for carotenoids in different fruit and vegetable matrices (Lemmens et al., 2014; Mutsokoti et al., 2015).

Even though the use of a static *in vitro* digestion model provides useful insights into the lipid digestibility and bioaccessibility of lipophilic compounds in microalgae, it should be noted that there are some limitations. First, the enzymatic activity of the pancreatic lipase used in the static *in vitro* digestion protocol might not be representative for lipid digestion in the human body, since it was shown in healthy humans that pancreatic lipase is secreted in response to the lipid content of the ingested diet (Armand, 2007). Nevertheless, since no differences were observed in lipid digestibility and carotenoid bioaccessibility between *in vitro* digestion with a low (550 U/mL) and a higher (2000 U/mL) pancreatic lipase activity, it is inferred that the results obtained in this study are representative for human digestion. Secondly, secretion of bile salts into the small intestine occurs gradually *in vivo* and is also regulated by the amount of lipid digestion products (Coleman, 1987), in contrast to the fixed bile salt concentration in the *in vitro* protocol. As such, the *in vitro* bioaccessibility of carotenoids and ω3-LC-PUFA might be underestimating *in vivo* bioaccessibility if insufficient bile salts are present in the *in vitro* model for incorporation of the lipid digestion products. This was the case in the current study, since the *in vitro* bioaccessibility of carotenoids and ω3-LC-PUFA in *Nannochloropsis* sp. biomass suspensions improved as a function of bile salt concentration (although the observed increases were rather small). Even though it can be concluded that the data obtained are representative for human digestion of *Nannochloropsis* sp., future experiments using a dynamic *in vitro* digestion model are recommended for validation of these results.

GENERAL CONCLUSIONS

General conclusions and future perspectives

Microalgae are without any doubt a promising source of functional food ingredients, due to their chemical composition rich in (essential) nutrients and health-beneficial components, as extensively reviewed by many authors. In contrast, their potential as structuring ingredients in food is very limitedly investigated, as evidenced by compilation of the literature data in Chapter 1. Not only this potential application has received little attention, a lack of fundamental knowledge on the molecular structure of microalgal structural biopolymers as well as on their functionality was demonstrated in the literature review. Hence, this doctoral thesis aimed to fill the research gaps that were identified in this context, in order to allow a thorough evaluation of the potential of microalgae and their structural biopolymers as structuring ingredients in food. This was established by focusing on three different aspects of this application: (i) the potential of cell wall related polysaccharides extracted from microalgae as thickening or gelling agents, (ii) the potential of microalgal biomass as a structuring ingredient as influenced by food processing operations, and (iii) possible implications of the use of microalgal biomass on the bioaccessibility of nutrients and health-beneficial components.

Molecular structure of extracted cell wall related polysaccharides in relation to their rheological properties

In spite of several attempts in literature to characterize the molecular structure of cell wall related polysaccharides of microalgae, these polymers are still poorly understood. It is generally acknowledged that microalgal cell walls are characterized by a high complexity and a high diversity, even within a genus, a species, or a strain. This was confirmed by the data obtained in Chapter 3, displaying variable monosaccharide and uronic acid profiles among different microalgae species, with at least five monosaccharides present in each microalgal cell wall. Generally, no analogies were observed between different microalgae, even for taxonomically related microalgae species classified within the same phylum or class. In addition, cell wall related polysaccharides of the investigated microalgae displayed little similarities with conventional thickening or gelling agents, even with those of (taxonomically related) macroalgae. Hence, based on the molecular composition of the extracted cell wall related polysaccharides, no predictions could be done about their potential as food hydrocolloids.

Despite differences in molecular composition compared to conventional thickening agents, promising rheological properties were observed for extracellular polysaccharides (EPS) of *Porphyridium cruentum* in Chapter 4. Their potential as thickening agent was obvious from their intrinsic viscosities, being higher than those

of most commercial thickening agents. In contrast to the EPS, cell wall bound polysaccharides of *Porphyridium cruentum* presented rather low intrinsic viscosity values, even though the same monosaccharide composition was observed. It was actually shown that the monosaccharides and uronic acids were organized into a different molecular structure, resulting in polymers with a lower molecular weight and thus a lower intrinsic viscosity. Hence, not only the monosaccharide profile, but also the molecular organization is of major importance in anticipating possible functionalities of the polysaccharides. Furthermore, major challenges are to be faced in the functionalization of *Porphyridium cruentum* EPS, particularly in terms of extraction and purification of the polysaccharides. It was actually shown that the excessive co-extraction of proteins and minerals resulted in a decreased functionality.

Based on the obtained results, the potential of microalgal polysaccharides as food hydrocolloids seems to be limited to specific cell wall fractions of certain microalgae species. In addition, the question arises whether microalgal polysaccharides will be able to compete with conventional polysaccharides from plants or macroalgae. As a matter of fact, the high production costs of microalgae and complex regulatory issues (e.g. European novel food regulation) are currently limiting the industrial exploitation of microalgal polysaccharides. Hence, due to the availability of alternative thickening and gelling agents for food applications, it is suggested that the potential use of microalgal polysaccharides as food hydrocolloids should not be the main strategy for introducing structural biopolymers of microalgae into food products.

Rheological and microstructural properties of microalgal biomass suspensions in relation to food processing operations

The incorporation of the whole microalgal biomass is considered a more effective and more sustainable strategy to introduce structural biopolymers of microalgae in food, since nutritional and health-beneficial components are also included, and extraction protocols and generated waste streams are avoided. However, it was shown in Chapter 5 that the structuring capacity of intact microalgal biomass was rather low. Deviation from Newtonian flow behavior was actually only observed for EPS-producing microalgae, with biomass suspensions of *Porphyridium cruentum* yielding the highest viscosities. The latter were attributed to the formation of large particles, consisting of intact cells aggregated through EPS interactions, as well as to an increased viscosity of the serum phase. Hence, the thickening properties of *Porphyridium cruentum* EPS as observed in previous chapters are efficiently exposed in the more complex biomass suspensions.

A major breakthrough of this research part was the ability to use mechanical and thermal processing for functionalization of the biomass suspensions in terms of

rheological and microstructural properties. Even though various responses to the processing techniques were observed among the different microalgae species, the majority of the microalgal suspensions exhibited enhanced rheological properties after processing. High pressure homogenization (HPH) generally induced cell disruption, which resulted in the release of intracellular compounds, as such promoting structural interactions of the released polymers. Improved rheological properties were mainly generated after a subsequent thermal treatment as heat-induced reactions occurred, especially when more intense sterilization processes were applied. Even though the major viscosity increases and related microstructural changes after thermal processing were attributed to protein denaturation reactions (as obvious for the protein-rich biomasses of *Chlorella vulgaris* and *Arthrospira platensis*), other heat-induced reactions such as enhanced polysaccharide interactions were not excluded.

A well-considered selection of a specific processing strategy is however of crucial importance to maximally exploit the structuring potential of microalgal biomasses, as proven in Chapter 6. Whereas a combination of HPH with subsequent sterilization was effective in enhancing rheological properties of *Chlorella vulgaris* suspensions, examination of various process sequences on the rheological properties of *Porphyridium cruentum* suspensions clearly revealed the destructive nature of HPH for this microalga. In contrast, a thermal treatment at moderate intensity proved successful in doubling the viscosity and gel strength of the latter microalga, notwithstanding the high values that were already obtained for the untreated suspensions. The different behavior of the two microalgae upon processing was related to different microstructural changes, mainly attributed to differences in abundant polymers, being proteins and EPS in *Chlorella vulgaris* and *Porphyridium cruentum*, respectively. Hence, the biomass composition might possibly provide a first indication of the structuring potential upon processing, although other factors such as cell rigidity should also be considered.

In order to further explore the potential of microalgal biomass as structuring food ingredients, these promising results on the functionalization of rheological properties by mechanical and thermal processing should be extended in the near future, by considering other types of food processing operations and by optimizing process conditions (such as pressure levels and time-temperature combinations for HPH and thermal processing, respectively). Furthermore, it should be investigated whether this functionalization, e.g. cell disruption and improvement of the rheological properties, can be performed to the same extent in a complex food matrix. The latter strategy would actually be preferred over a preceding functionalization of microalgal slurries that would later on be added to the food products, especially since the obtained

functionalities might get lost during inevitable drying steps of the microalgal suspensions.

It should also be noted that some microalgae species did not display substantial viscosities, even in presence of mechanical and thermal processing. This was the case for *Nannochloropsis* sp., *Phaeodactylum tricornutum*, and *Schizochytrium* sp., and was mainly attributed to a low extent of cell disruption and/or low levels of structural biopolymers present in the biomass. Although these microalgae cannot be used as structuring food ingredients, they may find applications for nutritional enrichment of food products without disturbing the structural properties of the food matrix. As such, they are actually applicable in all types of food products, while they will be of preference for enrichment of low-viscous foods such as fruit juices and dairy beverages.

Bioaccessibility of carotenoids and ω3-LC-PUFA of *Nannochloropsis* sp. in relation to cell integrity

While the use of the whole microalgal biomass in food products has been identified as the most promising strategy to introduce structural biopolymers in food, there might be implications for the digestibility and bioaccessibility of intracellular compounds upon consumption, especially for rigid cell walled microalgae such as *Nannochloropsis*. It was hypothesized that cell disruption would enhance the bioaccessibility of microalgal components, based on some indicative reports available in literature. However, achieving cell disruption for resistant microalgae as well as precisely evaluating the degree of cell disruption are known to be very challenging. The use of ultra high pressure homogenization (UHPH) proved successful in obtaining full cell disruption of *Nannochloropsis* sp. (Chapter 7), but resulted in inevitable heating of the sample. Therefore, HPH might be preferred to avoid excessive degradation of heat-labile components, even though a larger number of homogenization passes was required to realize (almost) complete cell disruption. However, a comparative study investigating the effect of HPH and UHPH on the quality of *Nannochloropsis* sp. is required, for instance focusing on the free fatty acid formation in the context of lipid oxidation. Furthermore, the use of various evaluation techniques highlighted the different impact of HPH and UHPH on the cell integrity. In fact, whereas a clear disruption of the cell wall was observed under intense homogenization conditions, moderate conditions resulted in cells with a (visually) intact cell wall but a damaged cell membrane. Hence, a clear definition of cell disruption and/or cell integrity is of major importance in evaluating the impact of processing techniques.

The role of the cell integrity in the lipid digestibility and bioaccessibility of carotenoids and ω3-LC-PUFA was investigated in Chapter 8, by performing *in vitro* digestion experiments on untreated and disrupted *Nannochloropsis* sp. cells. Even though a drastic increase in lipid digestibility and bioaccessibility of carotenoids and ω3-LC-PUFA was observed after cell disruption, it was shown to be dependent on the cell integrity of the untreated *Nannochloropsis* sp. biomass. In fact, it is still unclear whether lipid digestibility is mainly determined by the integrity of the cell membrane or the intactness of the cell wall layer. In this context, digestion experiments of microalgae treated with pulsed electric fields (PEF) will be highly relevant to provide a decisive answer on the role of cell wall and/or membrane integrity in the bioaccessibility of carotenoids and ω3-LC-PUFA, as PEF generally induces membrane permeabilization without distorting the microalgal cell wall. If the integrity of the cell membrane plays the major role, it could actually imply that less harsh disruption treatments could be sufficient for improvement of the nutritional value in terms of digestibility and bioaccessibility. Moreover, this might also suggest that substantial values of digestibility and bioaccessibility might be seen in microalgae with fragile cell walls, for which disrupted membranes can be easily generated (e.g. through an osmotic shock), possibly eliminating the need for (intense) cell disruption treatments.

Despite the extensive removal of both cell membrane and cell wall barriers in the disrupted biomass, the bioaccessibility of carotenoids and ω3-LC-PUFA was still drastically lower than for extracted *Nannochloropsis* sp. oil, indicating that the location of the carotenoids and/or the presence of other macromolecules in the biomass obstructs the micellar incorporation of carotenoids. In this context, processing of microalgae in the presence of added lipids might be worth investigating, as it has previously been proven successful in enhancing the carotenoid bioaccessibility in vegetable based matrices.

General future outlook

This doctoral thesis demonstrated the potential of different strategies to use microalgae and their structural biopolymers as functional ingredients in food applications. Due to the complexity in terms of molecular structure and extractability of microalgal cell wall related polysaccharides, it was concluded that their potential use as food hydrocolloids should not be the main strategy for introducing microalgal biopolymers into food products. In contrast, promising results were shown when using the whole biomass as structuring ingredients, especially photoautotrophic microalgae rich in structural biopolymers such as proteins and EPS, at least when specific sequences of food processing operations are applied. Food processing steps, in particular those resulting in microalgal cell disruption, were also proven successful in enhancing lipid digestibility and *in vitro* bioaccessibility of carotenoids and ω3-LC-

PUFA in *Nannochloropsis* sp. biomass. Hence, it is suggested that targeted processing can be applied to create healthy and sustainable food products enriched with microalgae displaying desired rheological properties. Nevertheless, this application is obviously still in its infancy and several challenges need to be overcome, including economic and regulatory issues as well as food quality aspects.

One of the major issues is the high production cost of (photoautotrophic) microalgae on a commercial scale, although literature data on production costs of microalgae are rather inconsistent. In fact, production costs range from €4 to €300/kg dry biomass (Acién et al., 2017; Acién Fernández et al., 2013; Norsker et al., 2011; Wijffels and Barbosa, 2010). Hence, the use of (photoautotrophic) microalgae as food ingredients will lead to considerable costs of the enriched food product. Drastic decreases of production costs are however predicted by several scientific studies, below €1/kg dry biomass (Norsker et al., 2011; Ruiz et al., 2016). It is obvious that future research on optimization of microalgae production will be of crucial importance to ensure the economic feasibility of this application.

Apart from economic challenges, complex regulatory issues are considered another major factor hampering the commercialization of microalgae as food ingredients, in particular the European novel food regulation. In fact, regulation was considered as important as developments in science and technology in the breakthrough of microalgae based products on the European market, based on a survey with experts (Vigani et al., 2015). Currently, four of the investigated microalgae are yet approved (*Arthrospira platensis*, *Chlorella vulgaris*, and *Tetraselmis chuii*) or authorized by notification (*Odontella aurita*) under the European novel food regulation, and some applications are ongoing (European Commission, 2016, 2017, 2019a, 2019b).

The addition of whole microalgal biomass will obviously influence other quality parameters of the food products, such as color and aroma. The abundance of pigments in photoautotrophic microalgal biomasses will drastically alter the color of the enriched food products, even at low incorporation concentrations. In addition, several microalgae species have a characteristic flavor, and a well-considered selection of microalga species and food product is obviously required to guarantee consumer acceptance. Small sensorial trials during this PhD research (data not shown) revealed promising combinations of specific microalgae and different vegetable matrices upon processing, based on consumer acceptance in terms of color and aroma. Furthermore, according to experts, consumer attitude is considered the least important factor in hampering the breakthrough of microalgae based products on the European market (Vigani et al., 2015).

In spite of the aforementioned challenges, microalgae are a promising ingredient in the design of healthy and sustainable food products with desired rheological properties. In case of low-viscosity biomasses (including *Nannochloropsis* sp., *Phaeodactylum tricornutum*, and *Schizochytrium* sp.), it is anticipated that their addition to food products in concentrations up to 8% will not drastically affect the rheological properties of the enriched food product. However, future research should investigate the physical stability upon storage, as phase separation phenomena could possibly occur during long-term storage. In addition, the nutritional value upon processing and storage should be studied for these enriched food systems. In this context, recent studies have actually shown a higher oxidative stability of photoautotrophic microalgae compared to the heterotrophic *Schizochytrium* sp. (Gheysen et al., 2018, 2019a). Furthermore, since a positive effect of cell disruption on the *in vitro* bioaccessibility of carotenoids and ω3-LC-PUFA was shown for *Nannochloropsis* sp. in this doctoral thesis, this should be further investigated for the less-rigid cell walled species *Schizochytrium* sp. and *Phaeodactylum tricornutum*.

In contrast, the use of microalgal biomasses with pronounced structuring capacity (in particular *Porphyridium cruentum*, *Chlorella vulgaris*, and *Arthrospira platensis*) requires further optimization of processing conditions to maximally exploit their structuring potential. As this doctoral research proved thermal processing to be an essential processing step in obtaining an increased viscosity and gel strength, thermal processing conditions should be optimized to exploit the structuring potential without compromising the nutritional value of the microalgae. Nevertheless, it was recently shown that a pasteurization process did not result in excessive degradation of ω3-LC-PUFA in photoautotrophic microalgae, showing promising results in the context of food applications (Gheysen et al., 2018). Furthermore, the question arises whether functionalization of microalgal biomass, i.e. cell disruption and/or improvement of the rheological properties, will occur to the same extent when performed in a complex food matrix. In that case, the aforementioned microalgae can be used as multifunctional food ingredients, by combining nutritional and structural enrichment of the food products.

List of references

Abd El-Razik M.M., Mohamed A.G. (2013). *Utilization of acid casein curd enriched with Chlorella vulgaris biomass as substitute of egg in mayonnaise production*. World Applied Sciences Journal, 26, 917–925.

Abd El Baky H.H., El Baroty G.S., Ibrahem E.A. (2015). *Functional characters evaluation of biscuits sublimated with pure phycocyanin isolated from Spirulina and Spirulina biomass*. Nutricion Hospitalaria, 32, 231–241.

Abdullahi A.S., Underwood G.J.C., Gretz M.R. (2006). *Extracellular matrix assembly in diatoms (Bacillariophyceae). V. Environmental effects on polysaccharide synthesis in the model diatom, Phaeodactylum tricornutum*. Journal of Phycology, 42, 363–378.

Aburto N.J., Ziolkovska A., Hooper L., Elliott P., Cappuccio F.P., Meerpohl J.J. (2013). *Effect of lower sodium intake on health: systematic review and meta-analyses*. British Medical Journal, 346, f1326.

Acién F.G., Molina E., Fernández-Sevilla J.M., Barbosa M., Gouveia L., Sepúlveda C., Bazaes J., Arbib Z. (2017). *Economics of microalgae production*, in: Microalgae-Based Biofuels and Bioproducts. Woodhead Publishing, pp. 485–503.

Acién Fernández F.G., Fernández Sevilla J.M., Molina Grima E. (2013). *Photobioreactors for the production of microalgae*. Reviews in Environmental Science and Biotechnology, 12, 131–151.

Agustini T.W., Ma'ruf W.F., Widayat, Wibowo B.A., Hadiyanto. (2017). *Study on the effect of different concentration of Spirulina platensis paste added into dried noodle to its quality characteristics*. IOP Conf. Series: Earth and Environmental Science, 55, 012068.

Alhattab M., Kermanshahi-Pour A., Brooks M.S. (2019). *Microalgae disruption techniques for product recovery: influence of cell wall composition*. Journal of Applied Phycology, 31, 61–88.

Allard B., Templier J. (2000). *Comparison of neutral lipid profile of various trilaminar outer cell wall (TLS)-containing microalgae with emphasis on algaenan occurrence*. Phytochemistry, 54, 369–380.

Amara S., Lafont D., Fiorentino B., Boullanger P., Carrière F., De Caro A. (2009). *Continuous measurement of galactolipid hydrolysis by pancreatic lipolytic enzymes using the pH-stat technique and a medium chain monogalactosyl diglyceride as substrate*. Biochimica et Biophysica Acta, 1791, 983–990.

Arad S., Friedman O., Rotem A. (1988). *Effect of nitrogen on polysaccharide production in a Porphyridium sp.* Applied and Environmental Microbiology, 54, 2411–2414.

Arad S., Levy-Ontman O. (2010). *Red microalgal cell-wall polysaccharides: Biotechnological aspects*. Current Opinion in Biotechnology, 21, 358–364.

Arad S., Rapoport L., Moshkovich A., van Moppes D., Karpasas M., Golan R., Golan Y. (2006). *Superior biolubricant from a species of red microalga*. Langmuir, 22, 7313–7317.

Arad S., Yaron A. (1992). *Natural pigments from red microalgae for use in foods and cosmetics*. Trends in Food Science and Technology, 3, 92–97.

Armand M. (2007). *Lipases and lipolysis in the human digestive tract: where do we stand?*

Current Opinion in Clinical Nutrition and Metabolic Care, 10, 156–164.

Arnold A.A., Genard B., Zito F., Tremblay R., Warschawski D.E., Marcotte I. (2015). *Identification of lipid and saccharide constituents of whole microalgal cells by 13C solid-state NMR*. Biochimica et Biophysica Acta, 1848, 369–377.

Arora M., Anil A.C., Delany J., Rajarajan N., Emami K., Mesbahi E. (2012). *Carbohydrate degrading bacteria closely associated with Tetraselmis indica: influence on algal growth*. Aquatic Biology, 15, 61–71.

Baba Hamed S., Baba Hamed M.B., Kassouar S., Abi Ayad S.E. (2016). *Physicochemical analysis of cellulose from microalgae Nannochloropsis gaditana*. African Journal of Biotechnology, 15, 1201–1207.

Babuskin S., Krishnan K.R., Babu P.A.S., Sivarajan M., Sukumar M. (2014). *Functional foods enriched with marine microalga Nannochloropsis oculata as a source of omega-3 fatty acids*. Food Technology and Biotechnology, 52, 292–299.

Babuskin S., Radhakrishnan K., Azhagu Saravana Babu P., Sukumar M., Fayidh M.A., Sabina K., Archana G., Sivarajan M. (2015). *Effects of rosemary extracts on oxidative stability of chikkis fortified with microalgae biomass*. Journal of Food Science and Technology, 52, 3784–3793.

Badel S., Callet F., Laroche C., Gardarin C., Petit E., El Alaoui H., Bernardi T., Michaud P. (2011). *A new tool to detect high viscous exopolymers from microalgae*. Journal of Industrial Microbiology and Biotechnology, 38, 319–326.

Bahnweg G., Jackle I. (1986). *A new approach to taxonomy of the Thraustochytriales and Labyrinthulales*, in: The Biology of Marine Fungi. CUP Archive, pp. 131–140.

Balduyck L., Bruneel C., Goiris K., Dejonghe C., Foubert I. (2018). *Influence of high pressure homogenization on free fatty acid formation in Nannochloropsis sp.* European Journal of Lipid Science and Technology, 120, 1–6.

Balduyck L., Dejonghe C., Goos P., Jooken E., Muylaert K., Foubert I. (2019). *Inhibition of lipolytic reactions during wet storage of T-Isochrysis lutea biomass by heat treatment*. Algal Research, 38, 101388.

Balduyck L., Stock T., Bijttebier S., Bruneel C., Jacobs G., Voorspoels S., Muylaert K., Foubert I. (2017). *Integrity of the microalgal cell plays a major role in the lipolytic stability during wet storage*. Algal Research, 25, 516–524.

Balduyck L., Veryser C., Goiris K., Bruneel C., Muylaert K., Foubert I. (2015). *Optimization of a Nile Red method for rapid lipid determination in autotrophic, marine microalgae is species dependent*. Journal of Microbiological Methods, 118, 152–158.

Barkallah M., Dammak M., Louati I., Hentati F., Hadrich B., Mechichi T., Ayadi M.A., Fendri I., Attia H., Abdelkafi S. (2017). *Effect of Spirulina platensis fortification on physicochemical, textural, antioxidant and sensory properties of yogurt during fermentation and storage*. LWT - Food Science and Technology, 84, 323–330.

Batista A.P., Gouveia L., Bandarra N.M., Franco J.M., Raymundo A. (2013). *Comparison of microalgal biomass profiles as novel functional ingredient for food products*. Algal Research, 2, 164–173.

Batista A.P., Niccolai A., Fradinho P., Fragoso S., Bursic I., Rodolfi L., Biondi N., Tredici M.R., Sousa I., Raymundo A. (2017). *Microalgae biomass as an alternative ingredient in*

cookies: Sensory, physical and chemical properties, antioxidant activity and in vitro digestibility. Algal Research, 26, 161–171.

Batista A.P., Nunes M.C., Fradinho P., Gouveia L., Sousa I., Raymundo A., Franco J.M. (2012). *Novel foods with microalgal ingredients - Effect of gel setting conditions on the linear viscoelasticity of Spirulina and Haematococcus gels*. Journal of Food Engineering, 110, 182–189.

Batista A.P., Nunes M.C., Raymundo A., Gouveia L., Sousa I., Cordobés F., Guerrero A., Franco J.M. (2011). *Microalgae biomass interaction in biopolymer gelled systems*. Food Hydrocolloids, 25, 817–825.

Baudelet P., Ricochon G., Linder M., Muniglia L. (2017). *A new insight into cell walls of Chlorophyta*. Algal Research, 25, 333–371.

Bauer E., Jakob S., Mosenthin R. (2005). *Principles of physiology of lipid digestion*. Asian-Australian Journal of Animal Sciences, 18, 282–295.

Beattie A., Hirst E.L., Percival E. (1961). *Studies on the metabolism of the Chrysophyceae. Comparative structural investigations on leucosin (chrysolaminarin) separated from diatoms and laminarin from the brown algae*. The Biochemical journal, 79, 531–537.

Becker B., Lommerse J.P.M., Melkonian M., Kamerling J.P., Vliegenthart J.F.G. (1995). *The structure of an acidic trisaccharide component from a cell wall polysaccharide preparation of the green alga Tetraselmis striata Butcher*. Carbohydrate Research, 267, 313–321.

Becker B., Melkonian M., Kamerling J.P. (1998). *The cell wall (theca) of Tetraselmis striata (Chlorophyta): Macromolecular composition and structural elements of the complex polysaccharides*. Journal of Phycology, 34, 779–787.

Becker E.W. (2007). *Micro-algae as a source of protein*. Biotechnology Advances, 25, 207–210.

Becker E.W. (2004). *Microalgae in Human and Animal Nutrition*, in: Handbook of Microalgal Culture: Biotechnology and Applied Phycology. pp. 312–351.

Beckett S.T. (2012). Physico-chemical aspects of food processing. Springer.

Beheshtipour H., Mortazavian A.M., Haratian P., Khosravi-Darani K. (2012). *Effects of Chlorella vulgaris and Arthrospira platensis addition on viability of probiotic bacteria in yogurt and its biochemical properties*. European Food Research and Technology, 235, 719–728.

BeMiller J.N., Whistler R.L. (2009). Starch: Chemistry and technology, 3rd ed. Academic Press.

Ben-Amotz A., Avron M. (1992). Dunaliella: Physiology, Biochemistry, and Biotechnology. CRC Press.

Bernaerts T.M.M., Gheysen L., Kyomugasho C., Jamsazzadeh Kermani Z., Vandionant S., Foubert I., Hendrickx M.E., Van Loey A.M. (2018a). *Comparison of microalgal biomasses as functional food ingredients: Focus on the composition of cell wall related polysaccharides*. Algal Research, 32, 150–161.

Bernaerts T.M.M., Kyomugasho C., Van Looveren N., Gheysen L., Foubert I., Hendrickx M.E., Van Loey A.M. (2018b). *Molecular and rheological characterization of different cell wall fractions of Porphyridium cruentum*. Carbohydrate Polymers, 195, 542–550.

Bernaerts T.M.M., Panozzo A., Verhaegen K.A.F., Gheysen L., Foubert I., Moldenaers P., Hendrickx M.E., Van Loey A.M. (2018c). *Impact of different sequences of mechanical and thermal processing on the rheological properties of Porphyridium cruentum and Chlorella vulgaris as functional food ingredients*. Food & Function, 9, 2433–2446.

Bertocchi C., Navarini L., Cesàro A., Anastasio M. (1990). *Polysaccharides from cyanobacteria*. Carbohydrate Polymers, 12, 127–153.

Bhatnagar M., Pareek S., Ganguly J., Bhatnagar A. (2012). *Rheology and composition of a multi-utility exopolymer from a desert borne cyanobacterium Anabaena variabilis*. Journal of Applied Phycology, 24, 1387–1394.

Bisalputra T., Weier W.E. (1963). *The cell wall of Scenedesmus quadricauda*. American Journal of Botany, 50, 1011–1019.

Blumenkrantz N., Asboe-Hansen G. (1973). *New method for quantitative determination of uronic acids*. Analytical Biochemistry, 54, 484–489.

Blumreisinger M., Meindl D., Loos E. (1983). *Cell wall composition of chlorococcal algae*. Phytochemistry, 22, 1603–1604.

Bodénès P., Bensalem S., Français O., Pareau D., Le Pioufle B., Lopes F. (2019). *Inducing reversible or irreversible pores in Chlamydomonas reinhardtii with electroporation: Impact of treatment parameters*. Algal Research, 37, 124–132.

Bolanho B.C., Egea M.B., Jácome A.L.M., Campos I., de Carvalho J.C.M., Danesi E.D.G. (2014). *Antioxidant and nutritional potential of cookies enriched with Spirulina platensis and sources of fibre*. Journal of Food and Nutrition Research, 53, 171–179.

Bold H.C., Wynne M.J. (1985). Introduction to the algae: Structure and reproduction. Prentice-Hall.

Bonfanti C., Cardoso C., Afonso C., Matos J., Garcia T., Tanni S., Bandarra N.M. (2018). *Potential of microalga Isochrysis galbana: Bioactivity and bioaccessibility*. Algal Research, 29, 242–248.

Borowitzka M., Beardall J., Raven J.A. (2016). The physiology of microalgae. Springer.

Brányiková I., Maršálková B., Doucha J., Brányik T., Bišová K., Zachleder V., Vítová M. (2011). *Microalgae-novel highly efficient starch producers*. Biotechnology and Bioengineering, 108, 766–776.

Brody M., Vatter A.E. (1959). *Observations on cellular structures of Porphyridium cruentum*. The Journal of Biophysical and Biochemical Cytology, 5, 289–294.

Brown M.R. (1991). *The amino-acid and sugar composition of 16 species of microalgae used in mariculture*. Journal of Experimental Marine Biology and Ecology, 145, 79–99.

Buchmann L., Bloch R., Mathys A. (2018). *Comprehensive pulsed electric field (PEF) system analysis for microalgae processing*. Bioresource Technology, 265, 268–274.

Buléon A., Colonna P., Planchot V., Ball S. (1998). *Starch granules: structure and biosynthesis*. International Journal of Biological Macromolecules, 23, 85–112.

Buono S., Langellotti A.L., Martello A., Rinna F., Fogliano V. (2014). *Functional ingredients from microalgae*. Food & Function, 5, 1669–1685.

Burczyk J., Dworzanski J. (1988). *Comparison of sporopollenin-like algal resistant polymer from*

cell wall of Botryococcus, Scenedesmus and Lycopodium clavatum by GC-pyrolysis. Phytochemistry, 27, 2151–2153.

Cagney N., Zhang T., Bransgrove R., Allen M.J., Balabani S. (2017). *Effects of cell motility and morphology on the rheology of algae suspensions*. Journal of Applied Phycology, 29, 1145–1157.

Calder P.C. (1991). *Glycogen structure and biogenesis*. International journal of biochemistry, 23, 1335–1352.

Camara F., Amaro M.A., Barbera R., Clemente G. (2005). *Bioaccessibility of minerals in school meals: Comparison between dialysis and solubility methods*. Food Chemistry, 92, 481–489.

Carbonell-Capella J.M., Buniowska M., Barba F.J., Esteve M.J., Frígola A. (2014). *Analytical methods for determining bioavailability and bioaccessibility of bioactive compounds from fruits and vegetables: A review*. Comprehensive Reviews in Food Science and Food Safety, 13, 155–171.

Carullo D., Abera B.D., Casazza A.A., Donsì F., Perego P., Ferrari G., Pataro G. (2018). *Effect of pulsed electric fields and high pressure homogenization on the aqueous extraction of intracellular compounds from the microalgae Chlorella vulgaris*. Algal Research, 31, 60–69.

Castillejo N., Martínez-Hernández G.B., Goffi V., Gómez P.A., Aguayo E., Artés F., Artés-Hernández F. (2018). *Natural vitamin B12 and fucose supplementation of green smoothies with edible algae and related quality changes during their shelf life*. Journal of the Science of Food and Agriculture, 98, 2411–2421.

Cavonius L.R., Albers E., Undeland I. (2016). *In vitro bioaccessibility of proteins and lipids of pH-shift processed Nannochloropsis oculata microalga*. Food & Function, 7, 2016–2024.

Cesàro A., Liut G., Bertocchi C., Navarini L., Urbani R. (1990). *Physicochemical properties of the exocellular polysaccharide from Cyanospira capsulata*. International Journal of Biological Macromolecules, 12, 79–84.

Cha K.H., Koo S.Y., Song D., Pan C. (2012). *Effect of microfluidization on bioaccessibility of carotenoids from Chlorella ellipsoidea during simulated digestion*. Journal of Agricultural and Food Chemistry, 60, 9437–9442.

Cha K.H., Lee J.Y., Song D., Kim S.M., Lee D., Jeon J., Pan C. (2011). *Effect of microfluidization on in vitro micellization and intestinal cell uptake of lutein from Chlorella vulgaris*. Journal of Agricultural and Food Chemistry, 59, 8670–8674.

Chacón-Lee T.L., González-Mariño G.E. (2010). *Microalgae for "healthy" foods – Possibilities and challenges*. Comprehensive Reviews in Food Science and Food Safety, 9, 655–675.

Chen B., Li F., Liu N., Ge F., Xiao H., Yang Y. (2015). *Role of extracellular polymeric substances from Chlorella vulgaris in the removal of ammonium and orthophosphate under the stress of cadmium*. Bioresource Technology, 190, 299–306.

Chen C., Zhao X., Yen H., Ho S., Cheng C., Lee D., Bai F., Chang J. (2013). *Microalgae-based carbohydrates for biofuel production*. Biochemical Engineering Journal, 78, 1–10.

Chen H., Fu Q., Liao Q., Zhang H., Huang Y., Xia A., Zhu X. (2018). *Rheological properties of microalgae slurry for application in hydrothermal pretreatment systems*. Bioresource Technology, 249, 599–604.

Chen W., Zhou P., Zhang M., Zhu Y., Wang X., Luo X., Bao Z., Yu L. (2016). *Transcriptome analysis reveals that up-regulation of the fatty acid synthase gene promotes the accumulation of docosahexaenoic acid in Schizochytrium sp. S056 when glycerol is used*. Algal Research, 15, 83–92.

Cheng Y., Labavitch J.M., Vandergheynst J.S. (2015). *Elevated CO2 concentration impacts cell wall polysaccharide composition of green microalgae of the genus Chlorella*. Letters in Applied Microbiology, 60, 1–7.

Cheng Y., Zheng Y., Labavitch J.M., Vandergheynst J.S. (2011). *The impact of cell wall carbohydrate composition on the chitosan flocculation of Chlorella*. Process Biochemistry, 46, 1927–1933.

Cho S., Choi W., Oh S., Lee C., Seo Y., Kim J., Song C., Kim G., Lee S., Kang D., Lee H. (2012). *Enhancement of lipid extraction from marine microalga, Scenedesmus associated with high-pressure homogenization process*. Journal of Biomedicine and Biotechnology,.

Chronakis I.S. (2001). *Gelation of edible blue-green algae protein isolate (Spirulina platensis strain Pacifica): Thermal transitions, rheological properties, and molecular forces involved*. Journal of Agricultural and Food Chemistry, 49, 888–898.

Ciferri O. (1983). *Spirulina, the edible microorganism*. Microbiological reviews, 47, 551–578.

Coleman R. (1987). *Biochemistry of bile secretion*. Biochemical Journal, 244, 249–261.

Courraud J., Berger J., Cristol J., Avallone S. (2013). *Stability and bioaccessibility of different forms of carotenoids and vitamin A during in vitro digestion*. Food Chemistry, 136, 871–877.

Damiani M.C., Popovich C.A., Constenla D., Leonardi P.I. (2010). *Lipid analysis in Haematococcus pluvialis to assess its potential use as a biodiesel feedstock*. Bioresource Technology, 101, 3801–3807.

Darley W.M., Porter D., Fuller M.S. (1973). *Cell wall composition and synthesis via Golgi-directed scale formation in the marine eucaryote, Schiozchytrium aggregatum, with a note on Thraustochytrium sp.* Archives of Microbiology, 90, 89–106.

de Jesus Raposo M.F., de Morais A.M.M.B., de Morais R.M.S.C. (2015). *Bioactivity and Applications of Polysaccharides from Marine Microalgae*, in: Polysaccharides. Springer, pp. 1683–1727.

de Jesus Raposo M.F., de Morais A.M.M.B., de Morais R.M.S.C. (2014). *Influence of sulphate on the composition and antibacterial and antiviral properties of the exopolysaccharide from Porphyridium cruentum*. Life Sciences, 101, 56–63.

de Leeuw J.W., Versteegh G.J.M., van Bergen P.F. (2006). *Biomacromolecules of algae and plants and their fossil analogues*. Plant Ecology, 182, 209–233.

De Marco E.R., Steffolani M.E., Martínez C.S., León A.E. (2014). *Effects of spirulina biomass on the technological and nutritional quality of bread wheat pasta*. LWT - Food Science and Technology, 58, 102–108.

De Marco E.R., Steffolani M.E., Martínez M., León A.E. (2018). *The use of Nannochloropsis sp. as a source of omega-3 fatty acids in dry pasta: chemical, technological and sensory evaluation*. International Journal of Food Science and Technology, 53, 499–507.

De Philippis R., Sili C., Paperi R., Vincenzini M. (2001). *Exopolysaccharide-producing*

cyanobacteria and their possible exploitation: A review. Journal of Applied Phycology, 13, 293–299.

De Philippis R., Sili C., Vincenzini M. (1992). *Glycogen and poly-β-hydroxybutyrate synthesis in Spirulina maxima*. Journal of General Microbiology, 138, 1623–1628.

De Philippis R., Vincenzini M. (1998). *Exocellular polysaccharides from cyanobacteria and their possible applications*. FEMS Microbiology Reviews, 22, 151–175.

De Ruiter G.A., Schols H.A., Voragen A.G.J., Rombouts F.M. (1992). *Carbohydrate analysis of water-soluble uronic acid containing polysaccharides with high-performance anion-exchange chromatography using methanolysis combined with TFA hydrolysis is superior to four other methods*. Analytical Biochemistry, 207, 176–185.

de Souza M.F., Santos Pereira D., Pereira Freitas S., da Silva Bon E.P., Almenara Rodrigues M. (2017). *Neutral sugars determination in Chlorella: Use of a one-step dilute sulfuric acid hydrolysis with reduced sample size followed by HPAEC analysis*. Algal Research, 24, 130–137.

Delattre C., Pierre G., Laroche C., Michaud P. (2016). *Production, extraction and characterization of microalgal and cyanobacterial exopolysaccharides*. Biotechnology Advances, 34, 1159–1179.

Depraetere O., Pierre G., Noppe W., Vandamme D., Foubert I., Michaud P., Muylaert K. (2015). *Influence of culture medium recycling on the performance of Arthrospira platensis cultures*. Algal Research, 10, 48–54.

Deruyck B., Thi Nguyen K.H., Decaestecker E., Muylaert K. (2019). *Modeling the impact of rotifer contamination on microalgal production in open pond, photobioreactor and thin layer cultivation systems*. Algal Research, 38, 101398.

Desbois A.P., Walton M., Smith V.J. (2010). *Differential antibacterial activities of fusiform and oval morphotypes of Phaeodactylum tricornutum (Bacillariophyceae)*. Journal of the Marine Biological Association of the United Kingdom, 90, 769–774.

Dodgson K.S., Price R.G. (1962). *A note on the determination of the ester sulphate content of sulphated polysaccharides*. Biochemical Journal, 84, 106–110.

Dubois M.K., Gilles K.A., Hamilton J.K., Rebers P.A., Smith F. (1956). *Colorimetric method for determination of sugars and related substances*. Analytical Chemistry, 28, 350–356.

Dvir I., Chayoth R., Sod-Moriah U., Shany S., Nyska A., Stark A.H., Madar Z., Arad S.M. (2000). *Soluble polysaccharide and biomass of red microalga Porphyridium sp. alter intestinal morphology and reduce serum cholesterol in rats*. British Journal of Nutrition, 84, 469–476.

Eboibi B.E., Lewis D.M., Ashman P.J., Chinnasamy S. (2015). *Influence of process conditions on pretreatment of microalgae for protein extraction and production of biocrude during hydrothermal liquefaction of pretreated Tetraselmis sp.* RSC Advances, 5, 20193–20207.

El-Baz F.K., Abdo S.M., Hussein A.M.S. (2017). *Microalgae Dunaliella salina for use as food supplement to improve pasta quality*. International Journal of Pharmaceutical Sciences Review and Research, 46, 45–51.

Eteshola E., Gottlieb M., Arad S. (1996). *Dilute solution viscosity of red microalga exopolysaccharide*. Chemical Engineering Science, 51, 1487–1494.

Eteshola E., Karpasas M., Arad S., Gottlieb M. (1998). *Red microalga exopolysaccharides: 2. Study of the rheology, morphology and thermal gelation of aqueous preparations*. Acta Polymerica, 49, 549–556.

European Commission. (2019a). Novel food catalogue: Chlorella vulgaris [WWW Document]. URL http://ec.europa.eu/food/safety/novel_food/catalogue/search/public/index.cfm# (accessed 1.22.19).

European Commission. (2019b). Novel food catalogue: Arthrospira platensis [WWW Document]. URL http://ec.europa.eu/food/safety/novel_food/catalogue/search/public/index.cfm# (accessed 1.22.19).

European Commission. (2017). *Applications under Regulation (EC) N ° 258 / 97 of the European Parliament and of the Council*.

European Commission. (2016). *Notifications pursuant to article 5 of regulation (EC) N° 258/97 of the European Parliament and of the Council*.

Faeth J.L., Valdez P.J., Savage P.E. (2013). *Fast hydrothermal liquefaction of Nannochloropsis sp. to produce biocrude*. Energy & Fuels, 27, 1391–1398.

Falcone R.D., Correa N.M., Biasutti M.A., Silber J.J. (2002). *Acid-base and aggregation processes of acridine orange base in n-heptane/AOT/water reverse micelles*. Langmuir, 18, 2039–2047.

Fawley K.P., Fawley M.W. (2007). *Observations on the diversity and ecology of freshwater Nannochloropsis (Eustigmatophyceae), with descriptions of new taxa*. Protist, 158, 325–336.

Fernández-Reiriz M.J., Perez-Camacho A., Ferreiro M.J., Blanco J., Planas M., Campos M.J., Labarta U. (1989). *Biomass production and variation in the biochemical profile (total protein, carbohydrates, RNA, lipids and fatty acids) of seven species of marine microalgae*. Aquaculture, 83, 17–37.

Filali Mouhim R., Cornet J.-F., Fontaine T., Fournet B., Dubertret G. (1993). *Production, isolation and preliminary characterization of the exopolysaccharide of the cyanobacterium Spirulina platensis*. Biotechnology Letters, 15, 567–572.

Firoozmand H., Rousseau D. (2014). *Tailoring the morphology and rheology of phase-separated biopolymer gels using microbial cells as structure modifiers*. Food Hydrocolloids, 42, 204–214.

Ford C.W., Percival E. (1965). *Carbohydrates of Phaeodactylum tricornutum. Part II.* A Sulphated Glucuronomannan*. Journal of the Chemical Society, 7042–7046.

Fradique M., Batista A.P., Nunes M.C., Gouveia L., Bandarra N.M., Raymundo A. (2013). *Isochrysis galbana and Diacronema vlkianum biomass incorporation in pasta products as PUFA's source*. LWT - Food Science and Technology, 50, 312–319.

Fradique M., Batista A.P., Nunes M.C., Gouveia L., Bandarra N.M., Raymundo A. (2010). *Incorporation of Chlorella vulgaris and Spirulina maxima biomass in pasta products. Part 1: Preparation and evaluation*. Journal of the Science of Food and Agriculture, 90, 1656–1664.

Francius G., Tesson B., Dague E., Martin-Jézéquel V., Dufrêne Y.F. (2008). *Nanostructure and nanomechanics of live Phaeodactylum tricornutum morphotypes*. Environmental

Microbiology, 10, 1344–1356.

Fret J., Roef L., Blust R., Diels L., Tavernier S., Vyverman W., Michiels M. (2017). *Reuse of rejuvenated media during laboratory and pilot scale cultivation of Nannochloropsis sp.* Algal Research, 27, 265–273.

García-Segovia P., Pagán-Moreno M.J., Lara I.F., Martínez-Monzó J. (2017). *Effect of microalgae incorporation on physicochemical and textural properties in wheat bread formulation*. Food Science and Technology International, 23, 437–447.

Gelin F., Volkman J.K., Largeau C., Derenne S., Sinninghe Damsté J.S., De Leeuw J.W. (1999). *Distribution of aliphatic, nonhydrolyzable biopolymers in marine microalgae*. Organic Geochemistry, 30, 147–159.

Geresh S., Adin I., Yarmolinsky E., Karpasas M. (2002). *Characterization of the extracellular polysaccharide of Porphyridium sp.: Molecular weight determination and rheological properties*. Carbohydrate Polymers, 50, 183–189.

Geresh S., Arad S. (1991). *The extracellular polysaccharides of the red microalgae: Chemistry and rheology*. Bioresource Technology, 38, 195–201.

Geresh S., Arad S., Levy-Ontman O., Zhang W., Tekoah Y., Glaser R. (2009). *Isolation and characterization of poly- and oligosaccharides from the red microalga Porphyridium sp.* Carbohydrate Research, 344, 343–349.

Geresh S., Lupescu N., Arad S. (1992). *Fractionation and partial characterization of the sulphated polysaccharide of Porphyridium*. Phytochemistry, 31, 4181–4186.

Gerken H.G., Donohoe B., Knoshaug E.P. (2013). *Enzymatic cell wall degradation of Chlorella vulgaris and other microalgae for biofuels production*. Planta, 237, 239–253.

Gheysen L., Bernaerts T., Bruneel C., Goiris K., Van Durme J., Van Loey A., De Cooman L., Foubert I. (2018). *Impact of processing on n-3 LC-PUFA in model systems enriched with microalgae*. Food Chemistry, 268, 441–450.

Gheysen L., Demets R., Devaere J., Bernaerts T., Goos P., Van Loey A., De Cooman L., Foubert I. (2019a). *Impact of microalgal species on the oxidative stability of n-3 LC-PUFA enriched tomato puree*. Algal Research, 40, 101502.

Gheysen L., Lagae N., Devaere J., Goiris K., Goos P., Bernaerts T., Van Loey A., De Cooman L., Foubert I. (2019b). *Impact of Nannochloropsis sp. dosage form on the oxidative stability of n-3 LC-PUFA enriched tomato purees*. Food Chemistry, 279, 389–400.

Gille A., Hollenbach R., Trautmann A., Posten C., Briviba K. (2019). *Effect of sonication on bioaccessibility and cellular uptake of carotenoids from preparations of photoautotrophic Phaeodactylum tricornutum*. Food Research International, 118, 40–48.

Gille A., Neumann U., Louis S., Bischoff S.C., Briviba K. (2018). *Microalgae as a potential source of carotenoids: Comparative results of an in vitro digestion method and a feeding experiment with C57BL/6J mice*. Journal of Functional Foods, 49, 285–294.

Gille A., Trautmann A., Posten C., Briviba K. (2016). *Bioaccessibility of carotenoids from Chlorella vulgaris and Chlamydomonas reinhardtii*. International Journal of Food Sciences and Nutrition, 67, 507–513.

Ginzberg A., Korin E., Arad S. (2008). *Effect of drying on the biological activities of a red*

microalgal polysaccharide. Biotechnology and Bioengineering, 99, 411–420.

Gloaguen V., Ruiz G., Morvan H., Mouradi-Givernaud A., Maes E., Krausz P., Strecker G. (2004). *The extracellular polysaccharide of Porphyridium sp.: An NMR study of lithium-resistant oligosaccharidic fragments*. Carbohydrate Research, 339, 97–103.

González-Fernández C., Ballesteros M. (2012). *Linking microalgae and cyanobacteria culture conditions and key-enzymes for carbohydrate accumulation*. Biotechnology Advances, 30, 1655–1661.

Gonzalez-Fernandez C., Sialve B., Bernet N., Steyer J.P. (2012). *Impact of microalgae characteristics on their conversion to biofuel. Part II: Focus on biomethane production*. Biofuels, Bioproducts & Biorefining, 6, 205–218.

González-Fernández C., Sialve B., Bernet N., Steyer J.P. (2012a). *Thermal pretreatment to improve methane production of Scenedesmus biomass*. Biomass and Bioenergy, 40, 105–111.

González-Fernández C., Sialve B., Bernet N., Steyer J.P. (2012b). *Comparison of ultrasound and thermal pretreatment of Scenedesmus biomass on methane production*. Bioresource Technology, 110, 610–616.

González López C. V, Cerón García M. d C., Acién Fernández F.G., Bustos C.S., Chisti Y., Fernández Sevilla J.M. (2010). *Protein measurements of microalgal and cyanobacterial biomass*. Bioresource Technology, 101, 7587–7591.

Gouveia L., Batista A.P., Miranda A., Empis J., Raymundo A. (2007). *Chlorella vulgaris biomass used as colouring source in traditional butter cookies*. Innovative Food Science and Emerging Technologies, 8, 433–436.

Gouveia L., Batista A.P., Raymundo A., Bandarra N. (2008a). *Spirulina maxima and Diacronema vlkianum microalgae in vegetable gelled desserts*. Nutrition & Food Science, 38, 492–501.

Gouveia L., Coutinho C., Mendonça E., Batista A.P., Sousa I., Bandarra N.M., Raymundo A. (2008b). *Functional biscuits with PUFA-ω3 from Isochrysis galbana*. Journal of the Science of Food and Agriculture, 88, 891–896.

Gouveia L., Marques A.E., Sousa J.M., Moura P., Bandarra N.M. (2010). *Microalgae – source of natural bioactive molecules as functional ingredients*. Food Science & Technology Bulletin: Functional Foods, 7, 21–37.

Gouveia L., Oliveira A.C. (2009). *Microalgae as a raw material for biofuels production*. Journal of Industrial Microbiology and Biotechnology, 36, 269–274.

Gouveia L., Raymundo A., Batista A.P., Sousa I., Empis J. (2006). *Chlorella vulgaris and Haematococcus pluvialis biomass as colouring and antioxidant in food emulsions*. European Food Research and Technology, 222, 362–367.

Graça C., Fradinho P., Sousa I., Raymundo A. (2018). *Impact of Chlorella vulgaris on the rheology of wheat flour dough and bread texture*. LWT - Food Science and Technology, 89, 466–474.

Granado-Lorencio F., Herrero-Barbudo C., Acién-Fernández G., Molina-Grima E., Fernández-Sevilla J.M., Pérez-Sacristán B., Blanco-Navarro I. (2009). *In vitro bioaccesibility of lutein and zeaxanthin from the microalgae Scenedesmus almeriensis*. Food Chemistry, 114, 747–752.

Granado-Lorencio F., Olmedilla-Alonso B., Herrero-Barbudo C., Pérez-Sacristán B., Blanco-Navarro I., Blázquez-García S. (2007). *Comparative in vitro bioaccessibility of carotenoids from relevant contributors to carotenoid intake*. Journal of Agricultural and Food Chemistry, 55, 6387–6394.

Granum E., Myklestad S.M. (2002). *A simple combined method for determination of β-1,3-glucan and cell wall polysaccharides in diatoms*. Hydrobiologia, 477, 155–161.

Grobbelaar J.U. (2004). *Algal Nutrition - Mineral Nutrition*, in: Handbook of Microalgal Culture: Biotechnology and Applied Phycology. John Wiley & Sons, pp. 97–115.

Gügi B., Le Costaouec T., Burel C., Lerouge P., Helbert W., Bardor M. (2015). *Diatom-specific oligosaccharide and polysaccharide structures help to unravel biosynthetic capabilities in diatoms*. Marine Drugs, 13, 5993–6018.

Guihéneuf F., Fouqueray M., Mimouni V., Ulmann L., Jacquette B., Tremblin G. (2010). *Effect of UV stress on the fatty acid and lipid class composition in two marine microalgae Pavlova lutheri (Pavlovophyceae) and Odontella aurita (Bacillariophyceae)*. Journal of Applied Phycology, 22, 629–638.

Guil-Guerrero J.L., Navarro-Juárez R., López-Martínez J.C., Campra-Madrid P., Rebolloso-Fuentes M.M. (2004). *Functional properties of the biomass of three microalgal species*. Journal of Food Engineering, 65, 511–517.

Guldas M., Irkin R. (2010). *Influence of Spirulina platensis powder on the microflora of yoghurt and acidophilus milk*. Mljekarstvo, 60, 237–243.

Günerken E., D'Hondt E., Eppink M.H.M., Garcia-Gonzalez L., Elst K., Wijffels R.H. (2015). *Cell disruption for microalgae biorefineries*. Biotechnology Advances, 33, 243–260.

Guzman-Murillo M.A., Ascencio F. (2000). *Anti-adhesive activity of sulphated exopolysaccharides of microalgae on attachment of red sore disease-associated bacteria and Helicobacter pylori to tissue culture cells*. Letters in Applied Microbiology, 30, 473–478.

Guzmán-Murillo M.A., López-Bolaños C.C., Ledesma-Verdejo T., Roldan-Libenson G., Cadena-Roa M.A., Ascencio F. (2007). *Effects of fertilizer-based culture media on the production of exocellular polysaccharides and cellular superoxide dismutase by Phaeodactylum tricornutum (Bohlin)*. Journal of Applied Phycology, 19, 33–41.

Guzmán S., Gato A., Lamela M., Freire-Garabal M., Calleja J.M. (2003). *Anti-inflammatory and immunomodulatory activities of polysaccharide from Chlorella stigmatophora and Phaeodactylum tricornutum*. Phytotherapy Research, 17, 665–670.

Halaj M., Chválová B., Cepák V., Lukavský J., Capek P. (2018). *Searching for microalgal species producing extracellular biopolymers*. Chemical Papers, 72, 2673–2678.

Halim R., Danquah M.K., Webley P.A. (2012). *Extraction of oil from microalgae for biodiesel production: A review*. Biotechnology Advances, 30, 709–732.

Halim R., Hill D.R.A., Hanssen E., Webley P.A., Blackburn S., Grossman A.R., Posten C., Martin G.J.O. (2019). *Towards sustainable microalgal biomass processing: anaerobic induction of autolytic cell-wall self-ingestion in lipid-rich Nannochloropsis slurries*. Green Chemistry, accepted f.

Han P., Sun Y., Wu X., Yuan Y., Dai Y., Jia S. (2014). *Emulsifying, flocculating, and physicochemical properties of exopolysaccharide produced by cyanobacterium Nostoc*

flagelliforme. Applied Biochemistry and Biotechnology, 172, 36–49.

Hanlon A.R.M., Bellinger B., Haynes K., Xiao G., Hofmann T.A., Gretz M.R., Ball A.S., Osborn A.M., Underwood G.J.C. (2006). *Dynamics of extracellular polymeric substance (EPS) production and loss in an estuarine, diatom-dominated, microalgal biofilm over a tidal emersion-immersion period*. Limnology and Oceanography, 51, 79–93.

Harding S.E. (2005). *Analysis of polysaccharides by ultracentrifugation. Size, conformation and interactions in solution*. Advances in Polymer Science, 186, 211–254.

Heaney-Kieras J., Chapman D.J. (1976). *Structural studies on the extracellular polysaccharide of the red alga Porphyridium cruentum*. Carbohydrate Research, 52, 169–177.

Henderson R.K., Baker A., Parsons S.A., Jefferson B. (2008). *Characterisation of algogenic organic matter extracted from cyanobacteria, green algae and diatoms*. Water Research, 42, 3435–3445.

Heo Y.M., Lee H., Lee C., Kang J., Ahn J., Lee Y.M., Kang K., Choi Y., Kim J. (2017). *An integrative process for obtaining lipids and glucose from Chlorella vulgaris biomass with a single treatment of cell disruption*. Algal Research, 27, 286–294.

Ho S., Chen C., Chang J. (2012). *Effect of light intensity and nitrogen starvation on CO2fixation and lipid/carbohydrate production of an indigenous microalga Scenedesmus obliquus CNW-N*. Bioresource Technology, 113, 244–252.

Honda D., Yokochi T., Nakahara T., Raghukumar S., Nakagiri A., Schaumann K., Higashihara T. (1999). *Molecular phylogeny of Labyrinthulids and Thraustochytrids based on the sequencing of 18S ribosomal RNA gene*. Journal of Eukaryotic Microbiology, 46, 637–647.

Hu H., Gao K. (2003). *Optimization of growth and fatty acid composition of a unicellular marine picoplankton, Nannochloropsis sp., with enriched carbon sources*. Biotechnology Letters, 25, 421–425.

Hu J., Nagarajan D., Zhang Q., Chang J.-S., Lee D.-J. (2018). *Heterotrophic cultivation of microalgae for pigment production: A review*. Biotechnology Advances, 36, 54–67.

Hu Q. (2004). *Environmental effects on cell composition*, in: Handbook of Microalgal Culture: Biotechnology and Applied Phycology. John Wiley & Sons, pp. 83–95.

Huerlimann R., de Nys R., Heimann K. (2010). *Growth, lipid content, productivity, and fatty acid composition of tropical microalgae for scale-up production*. Biotechnology and Bioengineering, 107, 245–257.

Imeson A. (2011). Food stabilisers, thickeners and gelling agents. John Wiley & Sons.

Imeson A. (1997). Thickening and gelling agents for food, 2nd ed. Springer.

Jamsazzadeh Kermani Z., Shpigelman A., Bernaerts T.M.M., Van Loey A.M., Hendrickx M.E. (2015). *The effect of exogenous enzymes and mechanical treatment on mango purée: Effect on the molecular properties of pectic substances*. Food Hydrocolloids, 50, 193–202.

Jamsazzadeh Kermani Z., Shpigelman A., Kyomugasho C., Van Buggenhout S., Ramezani M., Van Loey A.M., Hendrickx M.E. (2014). *The impact of extraction with a chelating agent under acidic conditions on the cell wall polymers of mango peel*. Food chemistry, 161, 199–207.

Jeong S.W., Nam S.W., Hwangbo K., Jeong W.J., Jeong B., Chang Y.K., Park Y. (2017). *Transcriptional regulation of cellulose biosynthesis during the early phase of nitrogen deprivation in Nannochloropsis salina*. Nature Scientific Reports, 7, 5264–5274.

Johnson M.B., Wen Z. (2009). *Production of biodiesel fuel from the microalga Schizochytrium limacinum by direct transesterification of algal biomass*. Energy & Fuels, 23, 5179–5183.

Joshi S.M.R., Bera M.B., Panesar P.S. (2014). *Extrusion cooking of maize/Spirulina mixture: Factors affecting expanded product characteristics and sensory quality*. Journal of Food Processing and Preservation, 38, 655–664.

Kangani C.O., Kelley D.E., DeLany J.P. (2008). *New method for GC/FID and GC-C-IRMS analysis of plasma free fatty acid concentration and isotopic enrichment*. Journal of Chromatography B, 873, 95–101.

Kapaun E., Loos E., Reisser W. (1992). *Cell wall composition of virus-sensitive symbiotic Chlorella species*. Phytochemistry, 31, 3103–3104.

Kaplan D., Christiaen D., Arad S. (1987). *Chelating properties of extracellular polysaccharides from Chlorella spp.* Applied and Environmental Microbiology, 53, 2953–2956.

Kavanagh G.M., Ross-Murphy S.B. (1998). *Rheological characterisation of polymer gels*. Progress in Polymer Science, 23, 533–562.

Kent M., Welladsen H.M., Mangott A., Li Y. (2015). *Nutritional evaluation of Australian microalgae as potential human health supplements*. PLoS ONE, 10, 1–14.

Kermanshahi-pour A., Sommer T.J., Anastas P.T., Zimmerman J.B. (2014). *Enzymatic and acid hydrolysis of Tetraselmis suecica for polysaccharide characterization*. Bioresource Technology, 173, 415–421.

Khazaei Pool E., Shahidi F., Mortazavi S.A., Azizpour M., Daneshzad E. (2016). *Examination of the effect of Spirulina platensis microalgae on drying kinetics and the color change of kiwifruit pastille*. Journal of Food Measurement and Characterization, 10, 634–642.

Khosravi-Darani K., Gholami Z., Gouveia L. (2017). *Effect of Arthrospira platensis on the shelf life, sensorial and rheological properties of strudel*. Romanian Biotechnological Letters, 22, 12250–12258.

Kim J.H., Kim S.M., Cha K.H., Mok I., Koo S.Y., Pan C., Lee J.K. (2016). *Evaluation of the anti-obesity effect of the microalga Phaeodactylum tricornutum*. Applied Biological Chemistry, 59, 283–290.

Kim S.S., Ly H. V, Kim J., Lee E.Y., Woo H.C. (2015). *Pyrolysis of microalgae residual biomass derived from Dunaliella tertiolecta after lipid extraction and carbohydrate saccharification*. Chemical Engineering Journal, 263, 194–199.

Kishida N., Okimasu S., Kamata T. (1978). *Molecular weight and intrinsic viscosity of konjac gluco-mannan*. Agricultural and Biological Chemistry, 42, 1645–1650.

Knockaert G., Lemmens L., Van Buggenhout S., Hendrickx M., Van Loey A. (2012). *Changes in β-carotene bioaccessibility and concentration during processing of carrot puree*. Food Chemistry, 133, 60–67.

Kodner R.B., Summons R.E., Knoll A.H. (2009). *Phylogenetic investigation of the aliphatic, non-hydrolyzable biopolymer algaenan, with a focus on green algae*. Organic Geochemistry,

40, 854–862.

Kuhnhenn V., Krägel J., Horstmann U., Miller R. (2006). *Surface shear rheological studies of marine phytoplankton cultures - Nitzschia closterium, Thalassiosira rotula, Thalassiosira punctigera and Phaeocystis sp.* Colloids and Surfaces B: Biointerfaces, 47, 29–35.

Kumar D. (2017). *Value addition of green apple ginger smoothie by enrichment with Chlorella vulgaris: Sensory evaluation*. International Journal of Applied Home Science, 4, 800–804.

Kyomugasho C., Willemsen K.L.D.D., Christiaens S., Van Loey A.M., Hendrickx M.E. (2015). *Pectin-interactions and in vitro bioaccessibility of calcium and iron in particulated tomato-based suspensions*. Food Hydrocolloids, 49, 164–175.

Lai Y.S., Parameswaran P., Li A., Baez M., Rittmann B.E. (2014). *Effects of pulsed electric field treatment on enhancing lipid recovery from the microalga, Scenedesmus*. Bioresource Technology, 173, 457–461.

Larson R.G. (1999). The structure and rheology of complex fluids. Oxford University Press.

Le Costaouëc T., Unamunzaga C., Mantecon L., Helbert W. (2017). *New structural insights into the cell-wall polysaccharide of the diatom Phaeodactylum tricornutum*. Algal Research, 26, 172–179.

Lebaron P., Catala P., Parthuisot N. (1998). *Effectiveness of SYTOX green stain for bacterial viability assessment*. Applied and Environmental Microbiology, 64, 2697–2700.

Lee Chang K.J., Nichols C.M., Blackburn S.I., Dunstan G.A., Koutoulis A., Nichols P.D. (2014). *Comparison of Thraustochytrids Aurantiochytrium sp., Schizochytrium sp., Thraustochytrium sp., and Ulkenia sp. for production of biodiesel, long-chain omega-3 oils, and exopolysaccharide*. Marine Biotechnology, 16, 396–411.

Lee J., Hayashi T., Hayashi K., Sankawa U., Maeda M., Nemoto T., Nakanishi H. (1998). *Further purification and structural analysis of calcium spirulan from Spirulina platensis*. Journal of Natural Products, 61, 1101–1104.

Lee S.Y., Cho J.M., Chang Y.K., Oh Y. (2017). *Cell disruption and lipid extraction for microalgal biorefineries: A review*. Bioresource Technology, 244, 1317–1328.

Lee Y. (2004). *Algal Nutrition - Heterotrophic Carbon Nutrition*, in: Handbook of Microalgal Culture: Biotechnology and Applied Phycology. John Wiley & Sons, pp. 116–124.

Lemahieu C., Bruneel C., Dejonghe C., Buyse J., Foubert I. (2016). *The cell wall of autotrophic microalgae influences the enrichment of long chain omega-3 fatty acids in the egg*. Algal Research, 16, 209–215.

Lemes A.C., Takeuchi K.P., de Carvalho J.C.M., Danesi E.D.G. (2012). *Fresh pasta production enriched with Spirulina platensis biomass*. Brazilian Archives of Biology and Technology, 55, 741–750.

Lemmens L., Colle I., Van Buggenhout S., Van Loey A., Hendrickx M. (2014). *Carotenoid bioaccessibility in based food products as affected by product (micro) structural characteristics and the presence of lipids : A review*. Trends in Food Science & Technology, 38, 125–135.

Lemmens L., Van Buggenhout S., Oey I., Van Loey A., Hendrickx M. (2009). *Towards a better understanding of the relationship between the β-carotene in vitro bio-accessibility and*

pectin structural changes: A case study on carrots. Food Research International, 42, 1323–1330.

Liang Y., Sarkany N., Cui Y., Yesuf J., Trushenski J., Blackburn J.W. (2010). *Use of sweet sorghum juice for lipid production by Schizochytrium limacinum SR21*. Bioresource Technology, 101, 3623–3627.

Liberman G.N., Ochbaum G., Arad S., Bitton R. (2016). *The sulfated polysaccharide from a marine red microalga as a platform for the incorporation of zinc ions*. Carbohydrate Polymers, 152, 658–664.

Lin X., Wang Q., Li W., Wright A.J. (2014). *Emulsification of algal oil with soy lecithin improved DHA bioaccessibility but did not change overall in vitro digestibility*. Food and Function, 5, 2913–2921.

Lin X., Wright A.J. (2018). *Pectin and gastric pH interactively affect DHA-rich emulsion in vitro digestion microstructure, digestibility and bioaccessibility*. Food Hydrocolloids, 76, 49–59.

Lizarraga M.S., De Piante Vicin D., González R., Rubiolo A., Santiago L.G. (2006). *Rheological behaviour of whey protein concentrate and lambda-carrageenan aqueous mixtures*. Food Hydrocolloids, 20, 740–748.

Lombardi A.T., Hidalgo T.M.R., Vieira A.A.H. (2005). *Copper complexing properties of dissolved organic materials exuded by the freshwater microalgae Scenedesmus acuminatus (Chlorophyceae)*. Chemosphere, 60, 453–459.

Loos E., Meindl D. (1982). *Composition of the cell wall of Chlorella fusca*. Planta, 156, 270–273.

Lopez-Sanchez P., Nijsse J., Blonk H.C.G., Bialek L., Schumm S., Langton M. (2011). *Effect of mechanical and thermal treatments on the microstructure and rheological properties of carrot, broccoli and tomato dispersions*. Journal of the Science of Food and Agriculture, 91, 207–217.

Lourenço S.O., Barbarino E., Lavín P.L., Lanfer Marquez U.M., Aidar E. (2004). *Distribution of intracellular nitrogen in marine microalgae: Calculation of new nitrogen-to-protein conversion factors*. European Journal of Phycology, 39, 17–32.

Lucas B.F., de Morais M.G., Santos T.D., Costa J.A. V. (2018). *Spirulina for snack enrichment: Nutritional, physical and sensory evaluations*. LWT - Food Science and Technology, 90, 270–276.

Lucas B.F., de Morais M.G., Santos T.D., Costa J.A. V. (2017). *Effect of Spirulina addition on the physicochemical and structural properties of extruded snacks*. Food Science and Technology, 37, 16–23.

Malik P., Kempanna C., Paul A. (2013). *Quality characteristics of ice cream enriched with Spirulina powder*. International Journal of Food and Nutritional Sciences, 2, 44–50.

Marcati A., Ursu A. V, Laroche C., Soanen N., Marchal L., Jubeau S., Djelveh G., Michaud P. (2014). *Extraction and fractionation of polysaccharides and B-phycoerythrin from the microalga Porphyridium cruentum by membrane technology*. Algal Research, 5, 258–263.

Markou G., Angelidaki I., Georgakakis D. (2012). *Microalgal carbohydrates: an overview of the factors influencing carbohydrates production, and of main bioconversion technologies*

for production of biofuels. Applied Microbiology and Biotechnology, 96, 631–645.

Massoud R., Khosravi-Darani K., Nakhsaz F., Varga L. (2016). *Evaluation of physicochemical, microbiological and sensory properties of croissants fortified with Arthrospira platensis (Spirulina)*. Czech Journal of Food Sciences, 34, 350–355.

Matos Â.P., Feller R., Moecke E.H.S., de Oliveira J. V, Junior A.F., Derner R.B., Sant'Anna E.S. (2016). *Chemical characterization of six microalgae with potential utility for food application*. Journal of the American Oil Chemists' Society, 93, 963–972.

Matos J., Cardoso C., Bandarra N.M., Afonso C. (2017). *Microalgae as healthy ingredients for functional food: A review*. Food & Function, 8, 2672–2685.

Mazinani S., Fadaei V., Khosravi-Darani K. (2016). *Impact of Spirulina platensis on physicochemical properties and viability of Lactobacillus acidophilus of probiotic UF feta cheese*. Journal of Food Processing and Preservation, 40, 1318–1324.

McBride R.C., Smith V.H., Carney L.T., Lane T.W. (2016). *Crop protection in open ponds*, in: Microalgal Production for Biomass and High-Value Products. CRC Press, pp. 165–182.

McCleary B. V, Solah V., Gibson T.S. (1994). *Quantitative measurement of total starch in cereal flours and products*. Journal of Cereal Science, 20, 51–58.

McCracken D.A., Cain J.R. (1981). *Amylose in floridean starch*. New Phytologist, 88, 67–71.

McFeeters R.F., Armstrong S.A. (1984). *Measurement of pectin methylation in plant cell walls*. Analytical Biochemistry, 139, 212–217.

Melis A. (2009). *Solar energy conversion efficiencies in photosynthesis: Minimizing the chlorophyll antennae to maximize efficiency*. Plant Science, 177, 272–280.

Milke L.M., Bricelj V.M., Ross N.W. (2011). *Changes in enzymatic activity during early development of bay scallops argopecten irradians and sea scallops Pacopecten magellanicus*. Aquatic Biology, 14, 207–216.

Minekus M., Alminger M., Alvito P., Ballance S., Bohn T., Bourlieu C., Carrière F., Boutrou R., Corredig M., Dupont D., Dufour C., Egger L., Golding M., Karakaya S., Kirkhus B., Le Feunteun S., Lesmes U., MacIerzanka A., MacKie A., Marze S., McClements D.J., Ménard O., Recio I., Santos C.N., Singh R.P., Vegarud G.E., Wickham M.S.J., Weitschies W., Brodkorb A. (2014). *A standardised static in vitro digestion method suitable for food - an international consensus*. Food and Function, 5, 1113–1124.

Mishra A., Jha B. (2009). *Isolation and characterization of extracellular polymeric substances from micro-algae Dunaliella salina under salt stress*. Bioresource Technology, 100, 3382–3386.

Mishra A., Kavita K., Jha B. (2011). *Characterization of extracellular polymeric substances produced by micro-algae Dunaliella salina*. Carbohydrate Polymers, 83, 852–857.

Mocanu G., Botez E., Nistor O. V, Andronoiu D.G., Vlăsceanu G. (2013). *Influence of Spirulina platensis biomass over some starter culture of lactic bacteria*. Journal of Agroalimentary Processes and Technologies, 19, 474–479.

Mofasser Hossain A.K.M., Brennan M.A., Mason S.L., Guo X., Zeng X.A., Brennan C.S. (2017). *The effect of astaxanthin-rich microalgae "Haematococcus pluvialis" and wholemeal flours incorporation in improving the physical and functional properties of cookies*. Foods, 6, 57–67.

Mohamed A.G., Abo-El-Khair B.E., Shalaby S.M. (2013). *Quality of novel healthy processed cheese analogue enhanced with marine microalgae Chlorella vulgaris biomass*. World Applied Sciences Journal, 23, 914–925.

Montalescot V., Rinaldi T., Touchard R., Jubeau S., Frappart M., Jaouen P., Bourseau P., Marchal L. (2015). *Optimization of bead milling parameters for the cell disruption of microalgae: Process modeling and application to Porphyridium cruentum and Nannochloropsis oculata*. Bioresource Technology, 196, 339–346.

Montsant A., Zarka A., Boussiba S. (2001). *Presence of a nonhydrolyzable biopolymer in the cell wall of vegetative cells and astaxanthin-rich cysts of Haematococcus pluvialis (chlorophyceae)*. Marine Biotechnology, 3, 515–521.

Morales-Sánchez D., Martinez-Rodriguez O.A., Kyndt J., Martinez A. (2015). *Heterotrophic growth of microalgae: metabolic aspects*. World journal of microbiology & biotechnology, 31, 1–9.

Moreno J., Vargas M.A., Madiedo J.M., Muñoz J., Rivas J., Guerrero M.G. (2000). *Chemical and rheological properties of an extracellular polysaccharide produced by the cyanobacterium Anabaena sp. ATCC 33047*. Biotechnology and Bioengineering, 67, 283–290.

Morineau-Thomas O., Jaouen P., Legentilhomme P. (2002). *The role of exopolysaccharides in fouling phenomenon during ultrafiltration of microalgae (Chlorella sp. and Porphyridium purpureum): Advantage of a swirling decaying flow*. Bioprocess and Biosystems Engineering, 25, 35–42.

Morita E., Kumon Y., Nakahara T., Kagiwada S., Noguchi T. (2006). *Docosahexaenoic acid production and lipid-body formation in Schizochytrium limacinum SR21*. Marine Biotechnology, 8, 319–327.

Mulders K.J.M., Lamers P.P., Martens D.E., Wijffels R.H. (2014). *Phototrophic pigment production with microalgae: Biological constraints and opportunities*. Journal of Phycology, 50, 229–242.

Mussgnug J.H., Klassen V., Schlüter A., Kruse O. (2010). *Microalgae as substrates for fermentative biogas production in a combined biorefinery concept*. Journal of Biotechnology, 150, 51–56.

Mutsokoti L., Panozzo A., Musabe E.T., Van Loey A., Hendrickx M. (2015). *Carotenoid transfer to oil upon high pressure homogenisation of tomato and carrot based matrices*. Journal of Functional Foods, 19, 775–785.

Mutsokoti L., Panozzo A., Pallares Pallares A., Jaiswal S., Van Loey A., Grauwet T., Hendrickx M. (2017). *Carotenoid bioaccessibility and the relation to lipid digestion: A kinetic study*. Food Chemistry, 232, 124–134.

Myklestad S.M. (1988). *Production, chemical structure, metabolism, and biological function of the (1 → 3)-linked, β-D-glucans in diatoms*. Biological Oceanography, 6, 313–326.

Navacchi M.F.P., de Carvalho J.C.M., Takeuchi K.P., Danesi E.D.G. (2012). *Development of cassava cake enriched with its own bran and Spirulina platensis*. Acta Scientiarum. Technology, 34, 465–472.

Navarini L., Bertocchi C., Cesàro A., Lapasin R., Crescenzi V. (1990). *Rheology of aqueous solutions of an extracellular polysaccharide from Cyanospira capsulata*. Carbohydrate

Polymers, 12, 169–187.

Navarini L., Cesàro A., Ross-Murphy S.B. (1992). *Viscoelastic properties of aqueous solutions of an exocellular polysaccharide from cyanobacteria*. Carbohydrate Polymers, 18, 265–272.

Nguyen H.H., Shpigelman A., Van Buggenhout S., Moelants K., Haest H., Buysschaert O., Hendrickx M., Van Loey A. (2016). *The evolution of quality characteristics of mango piece after pasteurization and during shelf life in a mango juice drink*. European Food Research and Technology, 242, 703–712.

Nichols C.A.M., Guezennec J., Bowman J.P. (2005). *Bacterial exopolysaccharides from extreme marine environments with special consideration of the Southern Ocean, sea ice, and deep-sea hydrothermal vents: A review*. Marine Biotechnology, 7, 253–271.

Norsker N.H., Barbosa M.J., Vermuë M.H., Wijffels R.H. (2011). *Microalgal production - A close look at the economics*. Biotechnology Advances, 29, 24–27.

Nuño K., Villarruel-López A., Puebla-Pérez A.M., Romero-Velarde E., Puebla-Mora A.G., Ascencio F. (2013). *Effects of the marine microalgae Isochrysis galbana and Nannochloropsis oculata in diabetic rats*. Journal of Functional Foods, 5, 106–115.

Ogbonda K.H., Aminigo R.E., Abu G.O. (2007). *Influence of temperature and pH on biomass production and protein biosynthesis in a putative Spirulina sp.* Bioresource Technology, 98, 2207–2211.

Ometto F., Quiroga G., Pšenička P., Whitton R., Jefferson B., Villa R. (2014). *Impacts of microalgae pre-treatments for improved anaerobic digestion: Thermal treatment, thermal hydrolysis, ultrasound and enzymatic hydrolysis*. Water Research, 65, 350–361.

Onacik-Gür S., Zbikowska A., Majewska B. (2018). *Effect of Spirulina (Spirulina platensis) addition on textural and quality properties of cookies*. Italian Journal of Food Science, 30, 1–12.

Ördög V., Stirk W.A., Bálint P., Aremu A.O., Okem A., Lovász C., Molnár Z., van Staden J. (2016). *Effect of temperature and nitrogen concentration on lipid productivity and fatty acid composition in three Chlorella strains*. Algal Research, 16, 141–149.

Pagnussatt F.A., Spier F., Bertolin T.E., Costa J.A. V, Gutkoski L.C. (2014). *Technological and nutritional assessment of dry pasta with oatmeal and the microalga Spirulina platensis*. Brazilian Journal of Food Technology, 17, 296–304.

Palabiyik I., Durmaz Y., Öner B., Toker O.S., Coksari G., Konar N., Tamtürk F. (2018). *Using spray-dried microalgae as a natural coloring agent in chewing gum: effects on color, sensory, and textural properties*. Journal of Applied Phycology, 30, 1031–1039.

Pales Espinosa E., Perrigault M., Ward J.E., Shumway S.E., Allam B. (2010). *Microalgal cell surface carbohydrates as recognition sites for particle sorting in suspension-feeding bivalves*. Biological Bulletin, 218, 75–86.

Parages M.L., Rico R.M., Abdala-Díaz R.T., Chabrillón M., Sotiroudis T.G., Jiménez C. (2012). *Acidic polysaccharides of Arthrospira (Spirulina) platensis induce the synthesis of TNF-α in RAW macrophages*. Journal of Applied Phycology, 24, 1537–1546.

Parikh A., Madamwar D. (2006). *Partial characterization of extracellular polysaccharides from cyanobacteria*. Bioresource Technology, 97, 1822–1827.

Passos F., Uggetti E., Carrère H., Ferrer I. (2014). *Pretreatment of microalgae to improve biogas production: A review*. Bioresource Technology, 172, 403–412.

Patel A.K., Laroche C., Marcati A., Ursu A. V, Jubeau S., Marchal L., Petit E., Djelveh G., Michaud P. (2013). *Separation and fractionation of exopolysaccharides from Porphyridium cruentum*. Bioresource Technology, 145, 345–350.

Percival E. (1979). *The polysaccharides of green, red and brown seaweeds: Their basic structure, biosynthesis and function*. British Phycological Journal, 14, 103–117.

Percival E., Foyle R.A.J. (1979). *The extracellular polysaccharides of Porphyridium cruentum and Porphyridium aerugineum*. Carbohydrate Research, 72, 165–176.

Perez-Garcia O., Escalante F.M.E., De-Bashan L.E., Bashan Y. (2011). *Heterotrophic cultures of microalgae: Metabolism and potential products*. Water Research, 45, 11–36.

Phan C.T., Tso P. (2001). *Intestinal lipid absorption and transport*. Frontiers in Bioscience, 6, 299–319.

Pieper S., Unterieser I., Mann F., Mischnick P. (2012). *A new arabinomannan from the cell wall of the chlorococcal algae Chlorella vulgaris*. Carbohydrate Research, 352, 166–176.

Pignolet O., Jubeau S., Vaca-Garcia C., Michaud P. (2013). *Highly valuable microalgae: biochemical and topological aspects*. Journal of Industrial Microbiology and Biotechnology, 40, 781–796.

Plaza M., Herrero M., Cifuentes A., Ibáñez E. (2009). *Innovative natural functional ingredients from microalgae*. Journal of Agricultural and Food Chemistry, 57, 7159–7170.

Pleissner D., Eriksen N.T. (2012). *Effects of phosphorous, nitrogen, and carbon limitation on biomass composition in batch and continuous flow cultures of the heterotrophic dinoflagellate Crypthecodinium cohnii*. Biotechnology and Bioengineering, 109, 2005–2016.

Ponis E., Probert I., Véron B., Mathieu M., Robert R. (2006). *New microalgae for the Pacific oyster Crassostrea gigas larvae*. Aquaculture, 253, 618–627.

Pulz O., Gross W. (2004). *Valuable products from biotechnology of microalgae*. Applied Microbiology and Biotechnology, 65, 635–648.

Qu L., Ren L.-J., Li J., Sun G.-N., Sun L.-N., Ji X.-J., Nie Z.-K., Huang H. (2013). *Biomass composition, lipid characterization, and metabolic profile analysis of the fed-batch fermentation process of two different docosahexanoic acid producing Schizochytrium sp. strains*. Applied Biochemistry and Biotechnology, 171, 1865–1876.

Rabelo S.F., Lemes A.C., Takeuchi K.P., Frata M.T., de Carvalho J.C.M., Danesi E.D.G. (2013). *Development of cassava doughnuts enriched with Spirulina platensis biomass*. Brazilian Journal of Food Technology, 16, 42–51.

Ramus J., Kenney B.E. (1989). *Shear degradation as a probe of microalgal exopolymer structure and rheological properties*. Biotechnology and Bioengineering, 34, 1203–1208.

Rao M.A. (2013). Rheology of fluid, semisolid, and solid foods: Principles and applications. Springer.

Rao M.A. (2010). Rheology of fluid and semisolid foods: Principles and applications. Springer.

Ratnayake W.N.M., Galli C. (2009). *Fat and fatty acid terminology, methods of analysis and fat digestion and metabolism: A background review paper*. Annals of Nutrition and Metabolism, 55, 8–43.

Raven J.A., Beardall J. (2003). *Carbohydrate metabolism and respiration in algae*, in: Photosynthesis in Algae. Springer, pp. 205–224.

Raymundo A., Gouveia L., Batista A.P., Empis J., Sousa I. (2005). *Fat mimetic capacity of Chlorella vulgaris biomass in oil-in-water food emulsions stabilized by pea protein*. Food Research International, 38, 961–965.

Rebolloso-Fuentes M.M., Navarro-Pérez A., García-Camacho F., Ramos-Miras J.J., Guil-Guerrero J.L. (2001a). *Biomass nutrient profiles of the microalga Nannochloropsis*. Journal of Agricultural and Food Chemistry, 49, 2966–2972.

Rebolloso-Fuentes M.M., Navarro-Pérez A., Ramos-Miras J.J., Guil-Guerrero J.L. (2001b). *Biomass nutrient profiles of the microalga Phaeodactylum tricornutum*. Journal of Food Biochemistry, 25, 57–76.

Rebolloso Fuentes M.M., Acién Fernández G.G., Sánchez Pérez J.A., Guil Guerrero J.L. (2000). *Biomass nutrient profiles of the microalga Porphyridium cruentum*. Food Chemistry, 70, 345–353.

Rego D., Costa L., Pereira M.T., Redondo L.M. (2015). *Cell membrane permeabilization studies of Chlorella sp. by pulsed electric fields*. IEEE Transactions on Plasma Science, 43, 3483–3488.

Rochefort W.E., Middleman S. (1987). *Rheology of xanthan gum: Salt, temperature, and strain effects in oscillatory and steady shear experiments*. Journal of Rheology, 31, 337–369.

Rodolfi L., Zittelli G.C., Bassi N., Padovani G., Biondi N., Bonini G., Tredici M.R. (2009). *Microalgae for oil: Strain selection, induction of lipid synthesis and outdoor mass cultivation in a low-cost photobioreactor*. Biotechnology and Bioengineering, 102, 100–112.

Rousseau S., Kyomugasho C., Celus M., Hendrickx M.E.G., Grauwet T. (2019). *Barriers impairing mineral bioaccessibility and bioavailability in plant-based foods and the perspectives for food processing*. Critical Reviews in Food Science and Nutrition, 1–18.

Roussel M., Villay A., Delbac F., Michaud P., Laroche C., Roriz D., El Alaoui H., Diogon M. (2015). *Antimicrosporidian activity of sulphated polysaccharides from algae and their potential to control honeybee nosemosis*. Carbohydrate Polymers, 133, 213–220.

Ruiz J., Olivieri G., De Vree J., Bosma R., Willems P., Reith J.H., Eppink M.H.M., Kleinegris D.M.M., Wijffels R.H., Barbosa M.J. (2016). *Towards industrial products from microalgae*. Energy and Environmental Science, 9, 3036–3043.

Rumin J., Bonnefond H., Saint-Jean B., Rouxel C., Sciandra A., Bernard O., Cadoret J., Bougaran G. (2015). *The use of fluorescent Nile red and BODIPY for lipid measurement in microalgae*. Biotechnology for Biofuels, 8, 42–57.

Ryckebosch E., Bruneel C., Termote-Verhalle R., Goiris K., Muylaert K., Foubert I. (2014a). *Nutritional evaluation of microalgae oils rich in omega-3 long chain polyunsaturated fatty acids as an alternative for fish oil*. Food Chemistry, 160, 393–400.

Ryckebosch E., Bruneel C., Termote-Verhalle R., Lemahieu C., Muylaert K., Van Durme J., Goiris K., Foubert I. (2013). *Stability of omega-3 LC-PUFA-rich photoautotrophic*

microalgal oils compared to commercially available omega-3 LC-PUFA oils. Journal of Agricultural and Food Chemistry, 61, 10145–10155.

Ryckebosch E., Bruneel C., Termote-Verhalle R., Muylaert K., Foubert I. (2014b). *Influence of extraction solvent system on extractability of lipid components from different microalgae species*. Algal Research, 3, 36–43.

Ryckebosch E., Muylaert K., Foubert I. (2012). *Optimization of an analytical procedure for extraction of lipids from microalgae*. Journal of the American Oil Chemists' Society, 89, 189–198.

Safi C., Charton M., Pignolet O., Silvestre F., Vaca-Garcia C., Pontalier P. (2013). *Influence of microalgae cell wall characteristics on protein extractability and determination of nitrogen-to-protein conversion factors*. Journal of Applied Phycology, 25, 523–529.

Safi C., Frances C., Ursu A. V, Laroche C., Pouzet C., Vaca-Garcia C., Pontalier P. (2015). *Understanding the effect of cell disruption methods on the diffusion of Chlorella vulgaris proteins and pigments in the aqueous phase*. Algal Research, 8, 61–68.

Safi C., Ursu A. V, Laroche C., Zebib B., Merah O., Pontalier P., Vaca-Garcia C. (2014a). *Aqueous extraction of proteins from microalgae: Effect of different cell disruption methods*. Algal Research, 3, 61–65.

Safi C., Zebib B., Merah O., Pontalier P., Vaca-Garcia C. (2014b). *Morphology, composition, production, processing and applications of Chlorella vulgaris: A review*. Renewable and Sustainable Energy Reviews, 35, 265–278.

Saha D., Bhattacharya S. (2010). *Hydrocolloids as thickening and gelling agents in food: A critical review*. Journal of Food Science and Technology, 47, 587–597.

Salvia-Trujillo L., Verkempinck S.H.E., Sun L., Van Loey A.M., Grauwet T., Hendrickx M.E. (2017). *Lipid digestion, micelle formation and carotenoid bioaccessibility kinetics: Influence of emulsion droplet size*. Food Chemistry, 229, 653–662.

Sánchez S., Martínez M.E., Espinola F. (2000). *Biomass production and biochemical variability of the marine microalga Isochrysis galbana in relation to culture medium*. Biochemical Engineering Journal, 6, 13–18.

Santiago J., Jamsazzadeh Kermani Z., Xu F., Van Loey A.M., Hendrickx M.E. (2017). *The effect of high pressure homogenization and endogenous pectin-related enzymes on tomato purée consistency and serum pectin structure*. Innovative Food Science and Emerging Technologies, 43, 35–44.

Santos T.D., Bastos de Freitas B.C., Moreira J.B., Zanfonato K., Costa J.A. V. (2016). *Development of powdered food with the addition of Spirulina for food supplementation of the elderly population*. Innovative Food Science and Emerging Technologies, 37, 216–220.

Sato M., Murata Y., Mizusawa M., Iwahashi H., Oka S. (2004). *A simple and rapid dual-fluorescence viability assay for microalgae*. Microbiology and Culture Collections, 20, 53–59.

Schneider N., Fortin T.J., Span R., Gerber M. (2016). *Thermophysical properties of the marine microalgae Nannochloropsis salina*. Fuel Processing Technology, 152, 390–398.

Schneider N., Gerber M. (2014). *Correlation between viscosity, temperature and total solid content of algal biomass*. Bioresource Technology, 170, 293–302.

Scholz M.J., Weiss T.L., Jinkerson R.E., Jing J., Roth R., Goodenough U., Posewitz M.C., Gerken H.G. (2014). *Ultrastructure and composition of the Nannochloropsis gaditana cell wall*. Eukaryotic Cell, 13, 1450–1464.

Schwede S., Rehman Z., Gerber M., Theiss C., Span R. (2013). *Effects of thermal pretreatment on anaerobic digestion of Nannochloropsis salina biomass*. Bioresource Technology, 143, 505–511.

Schwenzfeier A., Helbig A., Wierenga P.A., Gruppen H. (2013a). *Emulsion properties of algae soluble protein isolate from Tetraselmis sp.* Food Hydrocolloids, 30, 258–263.

Schwenzfeier A., Lech F., Wierenga P.A., Eppink M.H.M., Gruppen H. (2013b). *Foam properties of algae soluble protein isolate: Effect of pH and ionic strength*. Food Hydrocolloids, 33, 111–117.

Schwenzfeier A., Wierenga P.A., Gruppen H. (2011). *Isolation and characterization of soluble protein from the green microalgae Tetraselmis sp.* Bioresource Technology, 102, 9121–9127.

Sedmak J.J., Grossberg S.E. (1977). *A rapid, sensitive, and versatile assay for protein using Coomassie Brilliant Blue G250*. Analytical Biochemistry, 79, 544–552.

Selmo M.S., Salas-Mellado M.M. (2014). *Technological quality of bread from rice flour with Spirulina*. International Food Research Journal, 21, 1523–1528.

Sengupta S., Bhowal J. (2017). *Optimization of ingredient and processing parameter for the production of Spirulina platensis incorporated soy yogurt using response surface methodology*. Journal of Microbiology, Biotechnology and Food Sciences, 6, 1081–1085.

Shahbazizadeh S., Khosravi-Darani K., Sohrabvandi S. (2015). *Fortification of Iranian traditional cookies with Spirulina platensis*. Annual Research & Review in Biology, 7, 144–154.

Shalaby S.M., Yasin N.M.N. (2013). *Quality characteristics of croissant stuffed with imitation processed cheese containing microalgae Chlorella vulgaris biomass*. World Journal of Dairy & Food Sciences, 8, 58–66.

Sharoba A.M. (2014). *Nutritional value of Spirulina and its use in the preparation of some complementary baby food formulas*. Journal of Agroalimentary Processes and Technologies, 20, 330–350.

Shi Y., Sheng J., Yang F., Hu Q. (2007). *Purification and identification of polysaccharide derived from Chlorella pyrenoidosa*. Food Chemistry, 103, 101–105.

Shpigelman A., Kyomugasho C., Christiaens S., Van Loey A.M., Hendrickx M.E. (2015). *The effect of high pressure homogenization on pectin: Importance of pectin source and pH*. Food Hydrocolloids, 43, 189–198.

Sila D.N., Doungla E., Smout C., Van Loey A., Hendrickx M. (2006). *Pectin fraction interconversions: Insight into understanding texture evolution of thermally processed carrots*. Journal of Agricultural and Food Chemistry, 54, 8471–8479.

Sila D.N., Van Buggenhout S., Duvetter T., Fraeye I., De Roeck A., Van Loey A., Hendrickx M. (2009). *Pectins in processed fruits and vegetables: Part II - Structure-function relationships*. Comprehensive Reviews in Food Science and Food Safety, 8, 86–104.

Simpson R. (2009). Engineering aspects of thermal food processing. CRC Press LLC.

Singh P., Singh R., Jha A., Rasane P., Gautam A.K. (2015). *Optimization of a process for high fibre and high protein biscuit*. Journal of Food Science and Technology, 52, 1394–1403.

Soanen N., Da Silva E., Gardarin C., Michaud P., Laroche C. (2015). *Improvement of exopolysaccharide production by Porphyridium marinum*. Bioresource Technology, 213, 231–238.

Souliès A., Pruvost J., Legrand J., Castelain C., Burghelea T.I. (2013). *Rheological properties of suspensions of the green microalga Chlorella vulgaris at various volume fractions*. Rheologica Acta, 52, 589–605.

Spiden E.M., Scales P.J., Kentish S.E., Martin G.J.O. (2013a). *Critical analysis of quantitative indicators of cell disruption applied to Saccharomyces cerevisiae processed with an industrial high pressure homogenizer*. Biochemical Engineering Journal, 70, 120–126.

Spiden E.M., Scales P.J., Yap B.H.J., Kentish S.E., Hill D.R.A., Martin G.J.O. (2015). *The effects of acidic and thermal pretreatment on the mechanical rupture of two industrially relevant microalgae: Chlorella sp. and Navicula sp.* Algal Research, 7, 5–10.

Spiden E.M., Yap B.H.J., Hill D.R.A., Kentish S.E., Scales P.J., Martin G.J.O. (2013b). *Quantitative evaluation of the ease of rupture of industrially promising microalgae by high pressure homogenization*. Bioresource Technology, 140, 165–171.

Srikumar T.S. (1993). *The mineral and trace element composition of vegetables, pulses and cereals of southern India*. Food Chemistry, 46, 163–167.

Stahl W., Sies H. (2003). *Antioxidant activity of carotenoids*. Molecular Aspects of Medicine, 24, 345–351.

Steffe J.F. (1996). Rheological methods in food process engineering, 2nd ed. Freeman Press.

Suarez Garcia E., van Leeuwen J., Safi C., Sijtsma L., Eppink M.H.M., Wijffels R.H., van den Berg C. (2018a). *Selective and energy efficient extraction of functional proteins from microalgae for food applications*. Bioresource Technology, 268, 197–203.

Suarez Garcia E., Van Leeuwen J.J.A., Safi C., Sijtsma L., Van Den Broek L.A.M., Eppink M.H.M., Wijffels R.H., Van Den Berg C. (2018b). *Techno-functional properties of crude extracts from the green microalga Tetraselmis suecica*. Journal of Agricultural and Food Chemistry, 66, 7831–7838.

Sun L., Ren L., Zhuang X., Ji X., Yan J., Huang H. (2014). *Differential effects of nutrient limitations on biochemical constituents and docosahexaenoic acid production of Schizochytrium sp.* Bioresource Technology, 159, 199–206.

Sun Y., Wang H., Guo G., Pu Y., Yan B. (2014). *The isolation and antioxidant activity of polysaccharides from the marine microalgae Isochrysis galbana*. Carbohydrate Polymers, 113, 22–31.

Suzuki E., Suzuki R. (2013). *Variation of storage polysaccharides in phototrophic microorganisms*. Journal of Applied Glycoscience, 60, 21–27.

Szmejda K., Duliński R., Byczyński Ł., Karbowski A., Florczak T., Żyła K. (2018). *Analysis of the selected antioxidant compounds in ice cream supplemented with Spirulina (Arthrospira platensis) extract*. Biotechnology and Food Science, 82, 41–48.

Takeda H. (1996). *Cell wall sugars of some Scenedesmus species*. Phytochemistry, 42, 673–675.

Tańska M., Konopka I., Ruszkowska M. (2017). *Sensory, physico-chemical and water sorption properties of corn extrudates enriched with Spirulina*. Plant Foods for Human Nutrition, 72, 250–257.

Tegelaar E.W., de Leeuw J.W., Derenne S., Largeau C. (1989). *A reappraisal of kerogen formation*. Geochimica et Cosmochimica Acta, 53, 3103–3106.

Templeton D.W., Quinn M., Van Wychen S., Hyman D., Laurens L.M.L. (2012). *Separation and quantification of microalgal carbohydrates*. Journal of Chromatography A, 1270, 225–234.

Tesson B., Genet M.J., Fernandez V., Degand S., Rouxhet P.G., Martin-Jézéquel V. (2009). *Surface chemical composition of diatoms*. ChemBioChem, 10, 2011–2024.

Tibbetts S.M., Milley J.E., Lall S.P. (2015). *Chemical composition and nutritional properties of freshwater and marine microalgal biomass cultured in photobioreactors*. Journal of Applied Phycology, 27, 1109–1119.

Toker O.S. (2019). *Porphyridum cruentum as a natural colorant in chewing gum*. Food Science and Technology, In press.

Tokusoglu Ö., Unal M.K. (2003). *Biomass nutrient profiles of three microalgae: Spirulina platensis, Chlorella vulgaris, and Isochrysis galbana*. Journal of Food Science, 68, 1144–1148.

Tomaselli L. (2004). *The Microalgal Cell*, in: Handbook of Microalgal Culture: Biotechnology and Applied Phycology. Blackwell Science Ltd, pp. 3–19.

Torzillo G. (1997). *Tubular Bioreactors*, in: Spirulina Platensis (Arthrospira): Physiology, Cell-Biology and Biotechnology. CRC Press, pp. 101–116.

Torzillo G., Carlozzi P., Pushparaj B., Montaini E., Materassi R. (1993). *A two-plane tubular photobioreactor for outdoor culture of Spirulina*. Biotechnology and Bioengineering, 42, 891–898.

Trabelsi L., M'sakni N.H., Ouada H.B., Bacha H., Roudesli S. (2009). *Partial characterization of extracellular polysaccharides produced by cyanobacterium Arthrospira platensis*. Biotechnology and Bioprocess Engineering, 14, 27–31.

Ursu A., Marcati A., Sayd T., Sante-Lhoutellier V., Djelveh G., Michaud P. (2014). *Extraction, fractionation and functional properties of proteins from the microalgae Chlorella vulgaris*. Bioresource Technology, 157, 134–139.

Van Eykelenburg C., Fuchs A., Schmidt G.H. (1980). *Some theoretical considerations on the in vitro shape of the cross-walls in Spirulina spp.* Journal of Theoretical Biology, 82, 271–282.

Varga L., Szigeti J., Kovács R., Földes T., Buti S. (2002). *Influence of a Spirulina platensis biomass on the microflora of fermented ABT milks during storage (R1)*. Journal of Dairy Science, 85, 1031–1038.

Veldhuis M.J.W., Cucci T.L., Sieracki M.E. (1997). *Cellular DNA content of marine phytoplankton using two new fluorochromes: Taxonomic and ecological implications*. Journal of Phycology, 33, 527–541.

Vieler A., Wu G., Tsai C.-H., Bullard B., Cornish A.J., Harvey C., Reca I.-B., Thornburg C., Achawanantakun R., Buehl C.J., Campbell M.S., Cavalier D., Childs K.L., Clark T.J.,

Deshpande R., Erickson E., Ferguson A.A., Handee W., Kong Q., Li X., Liu B., Lundback S., Peng C., Roston R.L., Sanjaya, Simpson J.P., TerBush A., Warakanont J., Zäuner S., Farre E.M., Hegg E.L., Jiang N., Kuo M.-H., Lu Y., Niyogi K.K., Ohlrogge J., Osteryoung K.W., Shachar-Hill Y., Sears B.B., Sun Y., Takahashi H., Yandell M., Shiu S.-H., Benning C. (2012). *Genome, Functional Gene Annotation, and Nuclear Transformation of the Heterokont Oleaginous Alga Nannochloropsis oceanica CCMP1779*. PLoS Genetics, 8, e1003064.

Vigani M., Parisi C., Rodríguez-Cerezo E., Barbosa M.J., Sijtsma L., Ploeg M., Enzing C. (2015). *Food and feed products from micro-algae: Market opportunities and challenges for the EU*. Trends in Food Science and Technology, 42, 81–92.

Vincenzini M., De Philippis R., Sili C., Materassi R. (1993). *Stability of molecular and rheological properties of the exopolysaccharide produced by Cyanospira capsulata cultivated under different growth conditions*. Journal of Applied Phycology, 5, 539–541.

Vincenzini M., De Philippis R., Sill C., Materassi R. (1990). *A novel exopolysaccharide from a filamentous cyanobacterium: Production, chemical characterization and rheological properties*, in: Novel Biodegradable Microbial Polymers. Springer, pp. 295–310.

Wang G., Wang T. (2012). *Characterization of lipid components in two microalgae for biofuel application*. Journal of the American Oil Chemists' Society, 89, 135–143.

Wang M., He C., Chen S., Wen S., Wu X., Zhang D., Yuan Q., Wei C. (2018). *Microalgal cell disruption via extrusion for the production of intracellular valuables*. Energy, 142, 339–345.

Wang Z.T., Ullrich N., Joo S., Waffenschmidt S., Goodenough U. (2009). *Algal lipid bodies: Stress induction , purification , and biochemical characterization in wild-type and starchless Chlamydomonas reinhardtii*. Eukaryotic Cell, 8, 1856–1868.

Whyte J.N.C. (1987). *Biochemical composition and energy content of six species of phytoplankton used in mariculture of bivalves*. Aquaculture, 60, 231–241.

Wijffels R.H., Barbosa M.J. (2010). *An Outlook on Microalgal Biofuels*. Science, 329, 796–799.

Wild K.J., Steingaß H., Rodehutscord M. (2018). *Variability in nutrient composition and in vitro crude protein digestibility of 16 microalgae products*. Journal of Animal Physiology and Animal Nutrition, 102, 1306–1319.

Wileman A., Ozkan A., Berberoglu H. (2012). *Rheological properties of algae slurries for minimizing harvesting energy requirements in biofuel production*. Bioresource Technology, 104, 432–439.

Willis A., Chiovitti A., Dugdale T.M., Wetherbee R. (2013). *Characterization of the extracellular matrix of Phaeodactylum tricornutum (Bacillariophyceae): Structure, composition, and adhesive characteristics*. Journal of Phycology, 49, 937–949.

Wiltshire K.H., Dürselen C. (2004). *Revision and quality analyses of the Helgoland Reede long-term phytoplankton data archive*. Helgoland Marine Research, 252–268.

Wu N., Li Y., Lan C.Q. (2011). *Production and rheological studies of microalgal extracellular biopolymer from lactose using the green alga Neochloris oleoabundans*. Journal of Polymers and the Environment, 19, 935–942.

Wu Z., Shi X. (2008). *Rheological properties of Chlorella pyrenoidosa culture grown heterotrophically in a fermentor*. Journal of Applied Phycology, 20, 279–282.

Xia S., Gao B., Li A., Xiong J., Ao Z., Zhang C. (2014). *Preliminary characterization, antioxidant properties and production of chrysolaminarin from marine diatom Odontella aurita*. Marine Drugs, 12, 4883–4897.

Xia S., Wan L., Li A., Sang M., Zhang C. (2013). *Effects of nutrients and light intensity on the growth and biochemical composition of a marine microalga Odontella aurita*. Chinese Journal of Oceanology and Limnology, 31, 1163–1173.

Xiao R., Zheng Y. (2016). *Overview of microalgal extracellular polymeric substances (EPS) and their applications*. Biotechnology Advances, 34, 1225–1244.

Yalcin I., Hicsasmaz Z., Boz B., Bozoglu F. (1994). *Characterization of the extracellular polysaccharide from freshwater microalgae Chlorella sp.* LWT - Food Science and Technology, 27, 158–165.

Yang Z., Liu Y., Ge J., Wang W., Chen Y., Montagnes D. (2010). *Aggregate formation and polysaccharide content of Chlorella pyrenoidosa Chick (Chlorophyta) in response to simulated nutrient stress*. Bioresource Technology, 101, 8336–8341.

Yao C., Ai J., Cao X., Xue S., Zhang W. (2012). *Enhancing starch production of a marine green microalga Tetraselmis subcordiformis through nutrient limitation*. Bioresource Technology, 118, 438–444.

Yap B.H.J., Crawford S.A., Dumsday G.J., Scales P.J., Martin G.J.O. (2014). *A mechanistic study of algal cell disruption and its effect on lipid recovery by solvent extraction*. Algal Research, 5, 112–120.

Yap B.H.J., Martin G.J.O., Scales P.J. (2016). *Rheological manipulation of flocculated algal slurries to achieve high solids processing*. Algal Research, 14, 1–8.

Yonekura L., Nagao A. (2007). *Intestinal absorption of dietary carotenoids*. Molecular Nutrition and Food Research, 51, 107–115.

Zhang X., Jiang Z., Chen L., Chou A., Yan H., Zuo Y.Y., Zhang X. (2013). *Influence of cell properties on rheological characterization of microalgae suspensions*. Bioresource Technology, 139, 209–213.

Zhu B., Shi H., Yang G., Lv N., Yang M., Pan K. (2016). *Silencing UDP-glucose pyrophosphorylase gene in Phaeodactylum tricornutum affects carbon allocation*. New Biotechnology, 33, 237–244.

Zhu C.J., Lee Y.K. (1997). *Determination of biomass dry weight of marine microalgae*. Journal of Applied Phycology, 9, 189–194.

Zhu Y., Cardinaels R., Mewis J., Moldenaers P. (2009). *Rheological properties of PDMS/clay nanocomposites and their sensitivity to microstructure*. Rheologica Acta, 48, 1049–1058.

List of publications

Publications as first author in international peer-reviewed journals

Bernaerts T.M.M., Verstreken H., Dejonghe C., Gheysen L., Foubert I., Grauwet T., Van Loey A.M. *The role of cell integrity in the lipid digestibility and in vitro bioaccessibility of carotenoids and ω3-LC-PUFA in Nannochloropsis sp.* In preparation.

Bernaerts T.M.M., Gheysen L., Foubert I., Hendrickx M.E., Van Loey A.M. *Evaluating microalgal cell disruption upon ultra high pressure homogenization*. Algal Research, submitted.

Bernaerts T.M.M., Gheysen L., Foubert I., Hendrickx M.E., Van Loey A.M. *The potential of biopolymers of microalgae as structuring ingredients in food: a review*. Biotechnology Advances, under review.

Bernaerts T.M.M., Kyomugasho C., Van Looveren N., Gheysen L., Foubert I., Hendrickx M.E., Van Loey A.M. (2018). *Molecular and rheological characterization of different cell wall fractions of Porphyridium cruentum*. Carbohydrate Polymers, 195, 542 – 550.

Bernaerts T.M.M., Panozzo A., Verhaegen K.A.F., Gheysen L., Foubert I., Moldenaers P., Hendrickx M.E., Van Loey A.M. (2018). *Impact of different sequences of mechanical and thermal processing on the rheological properties of Porphyridium cruentum and Chlorella vulgaris as functional food ingredients*. Food & Function, 9(4), 2433 – 2446.

Bernaerts T.M.M., Gheysen L., Kyomugasho C., Jamsazzadeh Kermani Z., Vandionant S., Foubert I., Hendrickx M.E., Van Loey A.M. (2018). *Comparison of microalgal biomasses as functional food ingredients: Focus on the composition of cell wall related polysaccharides*. Algal Research, 32, 150 – 161.

Bernaerts T.M.M., Panozzo A., Doumen V., Foubert I., Gheysen L., Goiris K., Moldenaers P., Hendrickx M.E., Van Loey A.M. (2017). *Microalgal biomass as a (multi)functional ingredient in food products: Rheological properties of microalgal suspensions as affected by mechanical and thermal processing*. Algal Research, 25, 452 – 463.

Publications as co-author in international peer-reviewed journals

Gheysen L., Durnez N., Devaere J., **Bernaerts T.**, Van Loey A., De Cooman L., Foubert I. *Impact of vegetable matrix on the oxidative stability of vegetable purees enriched with n-3 LC-PUFA rich microalgae*. In preparation.

Gheysen L., Dejonghe C., **Bernaerts T.**, Van Loey A., De Cooman L., Foubert I. *Measuring primary lipid oxidation in food products enriched with colored microalgae*. Food Analytical Methods, under review.

Gheysen L., Demets R., Devaere J., **Bernaerts T.**, Van Loey A., De Cooman L., Foubert I. *Impact of microalgal species on the oxidative stability of n-3-LC-PUFA enriched tomato puree*. Algal Research, 40, 101502.

Gheysen L., Lagae N., Devaere J., Goiris K., Goos P., **Bernaerts T.**, Van Loey A., De Cooman L., Foubert I. (2019). *Impact of Nannochloropsis sp. dosage form on the oxidative stability of n-3 LC-PUFA enriched tomato purees*. Food Chemistry, 279, 389 – 400.

Gheysen L., **Bernaerts T.**, Bruneel C., Goiris K., Van Durme J., Van Loey A., De Cooman L., Foubert I. (2018). *Impact of processing on n-3 LC-PUFA in model systems enriched with microalgae*. Food Chemistry, 268, 441 – 450.

Active contributions to international conferences

Bernaerts T., Gheysen L., Foubert I., Moldenaers P., Grauwet T., Hendrickx M., Van Loey A. (2019). *Processing of microalgae plays a key role in the design of healthy and sustainable food products with desired rheological properties*. Oral presentation at 13th European PhD Workshop on Food Engineering and Technology, 14 – 15 May 2019, Vienna, Austria.

Bernaerts T., Panozzo A., Gheysen L., Foubert I., Moldenaers P., Hendrickx M., Van Loey A. (2018). *Microalgae as multifunctional food ingredients: different processing sequences to tailor rheological and nutritional properties*. Oral presentation at 32nd EFFoST International Conference, 6 – 8 November 2018, Nantes, France.

At this conference, Tom Bernaerts was awarded the **PhD Student of the Year Award (2nd prize)**, organized by the European Federation of Food Science and Technology (EFFoST) in collaboration with Cargill.

Bernaerts T., Panozzo A., Gheysen L., Foubert I., Moldenaers P., Hendrickx M., Van Loey A. (2018). *Processing of microalgae for use as multifunctional food ingredients*. Poster presentation at 32nd EFFoST International Conference, 6 – 8 November 2018, Nantes, France.

Bernaerts T., Gheysen L., Panozzo A., Doumen V., Foubert I., Goiris K., Moldenaers P., Hendrickx M., Van Loey A. (2017). *Screening of rheological properties of various microalgae species towards their application in processed food products*. Oral presentation at 6th Congress of the International Society of Applied Phycology, 18 – 23 June 2017, Nantes, France.

Tom Bernaerts received the **Young Researchers Fellowship** for this conference, awarded by the International Society for Applied Phycology.

Active contributions to national conferences

Bernaerts T., Panozzo A., Doumen V., Foubert I., Gheysen L., Goiris K., Moldenaers P., Hendrickx M., Van Loey, A. (2017). *Screening of rheological properties of various microalgae species towards their application in food products*. Oral presentation at 21st National Symposium for Applied Biological Sciences, 7 February 2017, Leuven, Belgium.